TOTAL SYNTHESIS OF (–)-IRCINIASTATIN B; DESIGN AND SYNTHESIS OF ANALOGUES

Chihui An

A DISSERTATION

in

Chemistry

Presented to the Faculties of the University of Pennsylvania

in

Partial Fulfillment of the Requirements for the

Degree of Doctor of Philosophy

2013

Supervisor of Dissertation

_____

Amos B. Smith, III

Rhodes-Thompson Professor of Chemistry

Graduate Group Chairperson

_____

Gary A. Molander, Hirschmann-Makineni Professor of Chemistry

Dissertation Committee

Jeffrey D. Winkler, Merriam Professor of Chemistry

Marisa C. Kozlowski, Professor of Chemistry

William D. Dailey, Associate Professor of Chemistry

TOTAL SYNTHESIS OF (–)-IRCINIASTATIN B; DESIGN AND SYNTHESIS OF ANALOGUES

ACKNOWLEDGEMENT

Graduate school has been an arduous yet rewarding journey. I would like to first thank my Ph.D advisor, Professor Amos Smith for his unyielding support and guidance throughout my graduate career. He has provided me with the intellectual freedom in my research project, which has made me become an independent researcher and problem solver. It has been a pleasure to work for him and to work in his laboratory. I would also like to thank my dissertation committee members, Professor Jeffrey Winkler, Professor Marisa Kozlowski and Professor William Dailey for their helpful suggestions during the annual committee meetings.

I would not have completed my dissertation project if it were not for the numerous graduate students and postdoctoral fellows in the Smith group. When I first began research in the Smith group, the postdoctoral fellows and senior graduate students at the time had taught me everything I know about chemistry. I would like to thank Dr. Jeffrey Sperry and Dr. Zhuqing Liu for mentoring me during my first summer at Penn in 2008. After I officially joined the group in May 2009, my labmates in Chem 435, Professor Bill Maio, Dr. Jeffrey Gladding, Dr. Adam Hoye and Yanran Ai were a great pleasure to work with over the years. It is because of these people that made Chem 435 the best lab in the Smith group. I am thankful for Bill for his helpful advice both in the two years we had overlapped as well as his continued guidance even after he had left the Smith group. Adam was a great pleasure to work with. With his help, we successfully devised a modified synthetic strategy that led to the completion of the first total synthesis of (–)-irciniastatin B. Our everyday discussions greatly shaped the way I think about

chemistry today. The Smith group has had many talented students and postdoctoral fellows and among the ones that I am extremely thankful for their help and support are Dr. David Jones, Dr. Alia Orbin, Professor Junha Jeon, Dr. Anne Marie Hogan, Dr. Joel Courter, Dr. Jim Bacci, Dr. Wonsuk Kim, Dr. Onur Atasoylu, Jason Melvin, Brett Williams and Artem Shvartsbart. My coworkers have made the Smith laboratory a great place to work. Special thanks to Jason Melvin who is not only my colleague but also a great friend who did not hesitate to agree to become a reverend upon my request.

I would like to give thanks to the Percec group because I have used many of their resources such as the glove box and MALDI. The people I owe thanks to in the Percec group are Dr. Chris Wilson, Dr Daniella Wilson, Dr. Andrew Hughes and Pawaret Leowanawat.

Special thanks to Dr. George Furst and Dr. Jun Gu for their help with NMR. They have been invaluable in my research efforts in the characterization of the late-stage compounds that I synthesized. Without their help, I would not be able to obtain the excellent quality NMR spectra of the irciniastatins and its analogues. I'd like to thank Judith Currano for all of the excellent library resources available to us and her help with Endnote in writing this dissertation. Dr. Sally Mallory has also been a great mentor to me since I started graduate school. She was a wonderful person to teach for and always supported me even when I was contemplating changing programs in the middle of my graduate studies.

Finally I would like to thank my family for their unyielding support throughout my life. My parents and my sister have always been supportive of all my pursuits and I

know they will continue to support me in my future endeavors. I thank my loving wife, Nga Nguyen for being my best friend and always encouraging me to be my best. Meeting her has been one of the highlights of my graduate career and I know she will always be there to support me in the future.

ABSTRACT

TOTAL SYNTHESIS OF (–)-IRCINIASTATIN B; DESIGN AND SYNTHESIS OF ANALOGUES

Chihui An

Amos B. Smith, III

The dissertation herein presents the first total synthesis of (–)-irciniastatin B in conjunction with the design and synthesis of analogues. Chapter One details the isolation and biological data of two potent cytotoxins (+)-irciniastatin A and (–)-irciniastatin B by Pettit and Crews. Also outlined in Chapter One are selected total syntheses and endgame strategies for (+)-irciniastatin A and reported structure activity relationship studies of the irciniastatin family of natural products.

The synthetic strategy toward the construction of (–)-irciniastatin B is outlined in Chapter Two. A chemoselective deprotection/oxidation sequence was proposed to install the requisite oxidation state at C(11). To this end, a late-stage alcohol from the earlier Smith synthesis of (+)-irciniastatin A was employed. However, protection of the late-stage alcohol as an orthogonal SEM ether resulted in unexpected degradation. A modified protecting group strategy employing robust 3,4-dimethoxybenzyl ethers successfully led to the first total synthesis of (–)-irciniastatin B. This strategy also led to the construction

of (+)-irciniastatin A from (–)-irciniastatin B, confirming the structural relationship of these two secondary metabolites.

The design and synthesis of irciniastatin analogues are detailed in Chapter Three. Our synthetic strategy permits modification at C(11), which has been suggested to be a key structural element for the potent biological activity observed with the irciniastatins. Biological evaluation of C(11)-irciniastatin analogues will aid in the elucidation of the biological mode of action of the irciniastatin family of natural products.

TABLE OF CONTENTS

LIST OF TABLES

Chapter 1

CHAPTER 2

LIST OF FIGURES

CHAPTER 1

LIST OF SCHEMES

CHAPTER 1

CHAPTER 2

CHAPTER 3

LIST OF ABBREVIATIONS

1-Me-AZADO	1-Me-2-azaadamantane *N*-oxyl
Ac	Acetyl
Ac_2O	Acetic anhydride
aq.	Aqueous
$BF_3•OEt_2$	Boron trifluoride diethyl etherate
Bn	Benzyl
Bu	Butyl
Bz	Benzoyl
CSA	Camphorsulfonic acid
DAST	Diethylaminosulfur trifluoride
DBU	1,8-Diazabicyclo[5.4.0]undec-7-ene
DDQ	2,3-Dichloro-5,6-dicyano-*para*-benzoquinone
DET	Diethyltartrate
DIBAL-H	Diisobutylaluminum hydride
DIPT	Diisopropyltartrate
DMAP	4-Dimethylaminopryidine

DMF	*N,N*-Dimethylformamide
DMPU	1,3-Dimethyl-3,4,5,6-tetrahydro-2(1H)-pyrimidinone
DMSO	Dimethyl sulfoxide
dr	diastereomeric ratio
er	Enantiomeric ratio
ESI	Electrospray ionization
Et_2O	Diethyl ether
Et_3N	Triethylamine
EtOAc	Ethyl acetate
FAB	Fast atom bombardment
GI	Growth inhibition
H_2O_2	Hydrogen peroxide
HCl	Hydrochloric Acid
HFIP	Hexafluoroisopropanol
HMBC	Heteronuclear multiple-bond correlation
HSQMBC	Heteronuclear single quantum multiple-bond correlation
HMPA	Hexamethylphosphoramide

HMQC	Heteronuclear multiple-quantum correlation
HRMS	High resolution mass spectrum
IC	Inhibitory concentration
i-Pr	Isopropyl
i-PrMgCl	Isopropylmagnesium chloride
i-Pr_2Net	Diisopropylethylamine
Ipc	Isopinocampheyl
JNK	c-Jun-N-terminal kinase
LC	Lethal concentration
LDA	Lithium diisopropylamide
LiHMDS	Lithium hexamethyldisilazide
LiOH	Lithium Hydroxide
m-CPBA	*meta*-Chloroperoxybenzoic acid
Me	Methyl
MeCN	Acetonitrile
$Me_3O•BF_4$	Trimethyloxonium tetrafluoroborate
MEST	Mouse ear-swelling test

MS	Mass spectroscopy
$NaBH_4$	Sodium Borohydride
NCI	National Cancer Institute
NMR	Nuclear magnetic resonance
NOE	Nuclear Overhauser effect
NOESY	Nuclear Overhauser effect spectroscopy
Nu	Nucleophile
Ph	Phenyl
Piv	Pivaloyl
PMB	*para*-Methoxybenzyl
py	Pyridine
SAR	Structure activity relationship
SEM	2-(Trimethylsilyl)ethoxymethyl
TAS-F	Tris-(dimethylamino)sulfonium difluorotrimethylsilicate
TBAF	Tetrabutylammonium fluoride
TBAI	Tetrabutylammonium iodide
TBS	*tert*-butyldimethylsilyl

TBSOTf	*tert*-butyldimethylsilyl trifluoromethanesulfonate
TEMPO	2,2,6,6-Tetramethylpiperidine-1-oxyl
Teoc	Trimethylsilylethoxycarbonyl
TES	Triethylsilyl
TMEDA	Tetramethylethylenediamine
THF	Tetrahydrofuran
TIPS	Triisopropylsilyl
TLC	Thin-layer chromatography
TMS	Trimethylsilyl
Ts	Tosyl

CHAPTER 1 Introduction

Adapted with permission from An, C.; Jurica, J. A.; Walsh, S. P.; Hoye, T. A.; Smith, A. B. III. "Total Synthesis of (+)-Ircinia stat in A (a.k.a Psymberin) and (–)-Ircinia stat in B" *Journal of Organic Chemistry*. **2013***, 78*, 4278-4296.

1.1 Introduction: Irciniastatin Family

In 2004 two new potent cytotoxins, (+)-irciniastatin A (**1.1**) and (–)-irciniastatin B (**1.2**), isolated from the Indo-Pacific marine sponge *Ircinia ramosa*, were reported by Pettit and coworkers (Figure 1.1).[1] In the same year, a closely related metabolite, (+)-psymberin (**1.1**), was reported independently by Crews and coworkers from marine sponge *Psammocinia.*[2] Analysis of these reports suggests that irciniastatin A (**1.1**), irciniastatin B (**1.2**), and psymberin (**1.1**) possessed the same architectural features, including a highly substituted 2,6-*trans*-tetrahydropyran core, a dihydroisocoumarin, and an *N,O*-aminal.

Figure 1.1. Irciniastatin Family

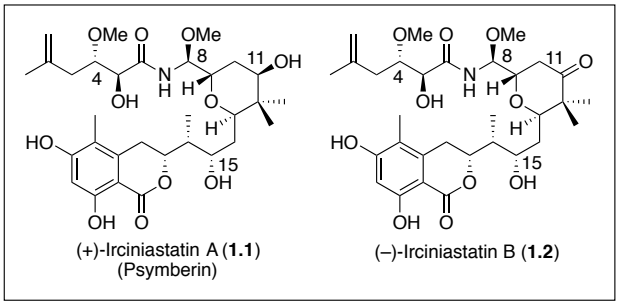

The molecular structures of these natural products are very similar to the members of the pederin family of natural products (Figure 1.2). Pederin was first isolated in 1952[3] and fully characterized in 1965.[4] Currently, there are 36 known members of this family of

natural products, including pederin (**1.3**),[3] theopederin B (**1.4**),[5] and mycalamide A (**1.5**).[6] Similar to the irciniastatins, all members of this family possess potent protein synthesis and tumor growth inhibition properties.[7] In each case, they possess a similar *trans*-tetrahydropyran core and an acid-labile *N,O*-aminal group. Instead of an acyclic acid side chain that is present in the irciniastatins, the members of the pederin family have a cyclic psymberate side chain. The most notable difference is the absence of the dihydroisocoumarin group. Due to their similarities, many structure activity relationship (SAR) studies and biological evaluations were driven by the hypothesis that these two families of natural products possess similar biological mode of actions.

Figure 1.2. Pederin Family

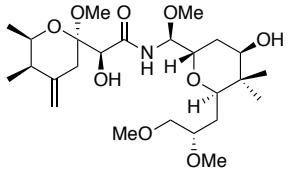

(+)-Pederin (**1.3**)

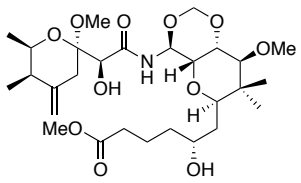

(+)-Theopederin B (**1.4**)

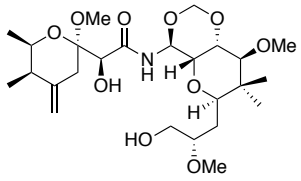

(+)-Mycalamide A (**1.5**)

1.1.1 Characterization of (+)-Irciniastatin A and (–)-Irciniastatin B by the Pettit Laboratory

The Pettit laboratory[1] characterized (+)-irciniastatin A and (–)-irciniastatin B by employing high-resolution mass spectrometry and 2-D NMR techniques. The high-resolution FAB mass spectrum of (+)-irciniastatin A revealed a pseudomolecular ion

peak at *m/z* 610.3228 $[M+H]^+$, which led to a molecular formula of $C_{31}H_{48}NO_{11}$. The combined 1-D and 2-D NMR spectral data permitted structure assignment of (+)-irciniastatin A as **1.6** (Figure 1.3). The relative stereochemical configurations at C(3)-C(4) and C(15)-C(16) however remained undefined. Interestingly, the assigned (*R*) configuration at C(8) is the opposite configuration as that in the pederin family of natural products.

Figure 1.3. Structural Determination of (+)-Irciniastatin A (**1.6**) and (–)-Irciniastatin B (**1.7**) by Pettit and Coworkers

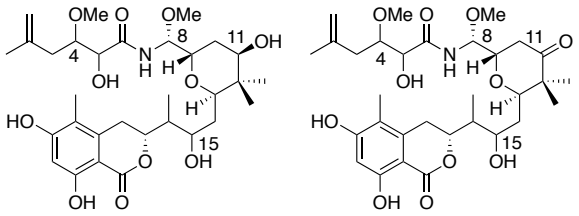

Pettit et al. determined the molecular formula for (–)-irciniastatin B (**1.7**), *via* high-resolution FAB mass spectroscopy to be $C_{31}H_{45}NO_{11}$. Compared to (+)-irciniastatin A (**1.6**), the ^{13}C NMR revealed the absence of a hydroxyl group and the appearance of a ketone signal. HMBC correlations and ^{13}C NMR data indicated that the carbonyl resides at C(11); thus the two cytotoxins differ only at the oxidation state at C(11) (Figure 1.3).

1.1.2 Characterization of (+)-Psymberin by the Crews Laboratory

The molecular ion of (+)-psymberin[2] was characterized *via* ESI-MS/MS analysis of the *m/z* 610 ion that fragmented to give *m/z* 578 and 560. A negative ESIMS ion was observed at *m/z* 608 $[M–H]^-$. The molecular formula of psymberin was therefore assigned as $C_{31}H_{47}NO_{11}$. Combination of 2-D NMR studies revealed the structure of psymberin to

1.8 (Figure 1.4). The absolute stereoconfiguration at C(4) remained undefined, while the C(8) *N,O*-aminal stereocenter was assigned as (*S*), which is opposite of that reported by Pettit,[1] but identical to the pederin family of natural products. Importantly, the C(8)-*(S)* configuration in the pederins proved to be highly important for potent cytotoxicity.[8,9] Crews also determined the relative stereochemical configuration of the C(15)-C(17) stereo-triad *via* NOESY and HSQMBC analysis of coupling constants, which provided additional stereochemical information for the initial analysis by Pettit.[1]

Figure 1.4. Structural Determination of (+)-Psymberin (**1.8**) by Crews and Coworkers

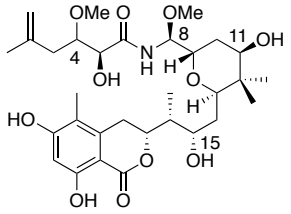

(+)-Psymberin (**1.8**)

Crews postulated that both (+)-irciniastatin A (**1.6**) and (+)-psymberin (**1.8**) might be identical,[2] but unfortunately the NMR spectra of the two congeners were taken in different solvents, thus the exact stereochemical relationship at C(4) and C(8) could not be established. In 2005, De Brabander and colleagues resolved the structural ambiguity with the first total synthesis of (+)-psymberin by construction of all four C(4)-C(8) diastereomers of (+)-psymberin.[10] This effort not only yielded the absolute configuration of (+)-psymberin (**1.1**) (Figure 1.1), but also confirmed that both (+)-irciniastatin A (**1.1**) and (+)-psymberin (**1.1**) possessed identical chemical structures.[10] In this thesis, we will use the names irciniastatin A and B as Pettit was the first to report these natural products.[1]

1.2 Biological Evaluation of (+)-Irciniastatin A (1.1) and (–)-Irciniastatin B (1.2)

1.2.1 Pettit's Biological Studies

Pettit and coworkers tested both (+)-irciniastatin A (**1.1**) and (–)-irciniastatin B (**1.2**) against a series of human cancer cell lines and murine P388 leukemia cell line.[1] They discovered both natural products displayed impressive biological properties (Table 1.1). Interestingly, even though the chemical structures of (+)-irciniastatin A (**1.1**) and (–)-irciniastatin B (**1.2**) differ only in the oxidation state at C(11), the ketone congener (**1.2**) was nearly 10 times more active than the alcohol congener (**1.1**) against human pancreas (BXPC-3), breast (MCF-7), and central nervous system (SF268) cancer cell lines.[1] This significant difference in activity suggested that the C(11) substituent plays an important role in the biological mode of action. Additionally, (+)-ircinaistatin A (**1.1**) possesed modest antifungal and antibacterial activities against *Cryptococcus neoformans* and *Neisseria gonorrhoeae* (16 μg/mL and 64 μg/mL respectively).

Table 1.1. Inhibition of Cancer Cell Line Growth (GI_{50}Table, μg/mL) by (+)-Irciniastatin A (**1.1**) and (–)-Irciniastatin B (**1.2**)

Human cancer cell lines		irciniastatin A	irciniastatin B
pancreas	BXPC-3	0.0038	0.00073
breast	MCF-7	0.0032	0.00050
CNS	SF268	0.0034	0.00066
lung	NCI-H460	<0.0001	0.0012
colon	KM20L2	0.0027	0.0021
prostate	DU-145	0.0024	0.0016
leukemia[a]	P388	0.00413	0.006
normal endothelial	HUVEC	<0.005	ND

[a]Murine.

1.2.2 Crews' Biological Studies

Crews and coworkers evaluated (+)-irciniastatin A (**1.1**) against the NCI 60 human tumor cell panel (Table 1.2).[2] Interestingly, (+)-irciniastatin A (**1.1**) displayed highly differential cytotoxicity (>10,000-fold). Irciniastatin A [(+)-**1.1**] possessed high sensitivity toward several melanoma, breast cancer, and colon cancer cell lines, while leukemia cell lines tested proved to be insensitive, when treated with the cytotoxin. Significantly, this differential biological profile was unprecedented in the pederins, which raised an intriguing possibility that the observed cytotoxicity of the irciniastatins might arise *via* a novel mode of action.

Table 1.2. Differential Sensitivities (LC_{50}) of Different Cancer Cell lines to (+)-Irciniastatin A (**1.1**)

Cancer cell lines	LC_{50} (nM)	Cancer cell lines	LC_{50} (nM)
leukemia		melanoma	
CCRF-CEM	> 25,000	LOX IMVI	> 25,000
HL-60 (TB)	> 25,000	**MALME-3M**	**< 2.5**
K-562	> 25,000	SK-MEL-2	>25,000
MOLT-4	> 25,000	**SK-MEL-5**	**< 2.5**
RPMI-8226	> 25,000	SK-MEL-28	>25,000
SR	> 25,000	UACC-257	> 25,000
		UACC-62	**< 2.5**
breast cancer		colon cancer	
MCF7	> 25,000	HCC-2998	367
HS 578T	> 25,000	**HCT-116**	**< 2.5**
MDA-MB-435	**< 2.5**	HT29	> 25,000
NCI/ADR-RES	> 19,000	SW-620	> 25,000
T-47/D	13,600		

1.2.3 Usui's Biological Studies

In 2010, Usui and coworkers probed the biological mechanism of (+)-irciniastatin A (**1.1**) after completion of a total synthesis.[11,12] They determined (+)-irciniastatin A (**1.1**) was a potent protein translation inhibitor (IC_{50} = 6.7 nM) without affecting DNA and RNA syntheses in human leukemia Jurkat cells. Similar results were obtained when (+)-irciniastatin A (**1.1**) was evaluated against human cervical carcinoma HeLa cells (IC_{50} =

2.6 nM). Additionally, the enantiomer, (–)-irciniastatin A, did not display any inhibition of protein translation (~20% inhibition even at 10 μM) or cytotoxicity (GI_{50} >1000 nM) in HeLa cells.[11,12] This data illustrates that (+)-irciniastatin A (**1.1**) is an enantio-specific inhibitor of protein synthesis.

Usui also reported that the tumor growth inhibition activity of (+)-irciniastatin A (**1.1**) arises from activation of stress-activated protein kinases, such as JNK and p38, that in turn leads to apoptosis.[11] The mechanism of induction of JNK and p38 by (+)-irciniastatin A (**1.1**) was the same for onnamide A and theopederin B (**1.4**), members of the pederin family of natural products.[13]

1.2.4 De Brabander's Biological Studies

De Brabander and coworkers evaluated the cytotoxicity of (+)-irciniastatin A (**1.1**) against a series of cancer cell lines (Table 1.3), again after completion of a total synthesis.[10,14] To their surprise, synthetic (+)-irciniastatin A (**1.1**), constructed in their laboratories, did not reveal the highly differential cytotoxicity[2] as previously reported by Crews and coworkers. All cell lines employed for this study resulted in potent cytotoxicity in the low nanomolar range. They also evaluated (+)-irciniastatin A (**1.1**) for protein translation inhibitory properties and discovered that (+)-irciniastatin A (**1.1**) was 10 times more potent than mycalamide A (**1.5**) (28 nM *vs* 238 nM) in their *in vitro* assays. De Brabander, in collaboration with Roth, also disclosed a forward genetic screen of (+)-irciniastatin A (**1.1**) employing *C. elegans* that demonstrated **1.1** binds to the ribosome to induce cell death. In addition, they demonstrated that (+)-irciniastatin A (**1.1**)

does not possess the same potent vesicant activity as possessed by the pederins, when employing a mouse ear-swelling test (MEST).[7]

Table 1.3. (+)-Irciniastatin A (**1.1**) Biological Evaluations by De Brabander and Coworkers

Cell line	IC_{50} (nM)	GI_{50}(nM)
BJ *normal fibroblast*	10.43	0.14
BJHtert *telomerase immortalized fibroblast*	4.29	0.3
H2126 *non-small cell lung tumor*	0.45	0.13
HCT116 *colon tumor*	0.52	0.40
HT1080 *fibroblast tumor*	0.43	0.24
IGROV1 *ovarian tumor*	2.40	1.03
KM12 *colon tumor*	0.30	0.20
MDA-MB-231 *breast tumor*	0.61	0.23
PC3 *prostate tumor*	1.64	0.53
SKMEL2 *melanoma tumor*	0.71	0.22

1.3 Selected Total Syntheses of (+)-Irciniastatin A (1.1) (Psymberin): Key Disconnections and End Game Strategies

Since the De Brabander seminal total synthesis,[10] there have been six other total syntheses of (+)-irciniastatin A (**1.1**) (psymberin) to date,[10,12,15-19] including one report from our Laboratory.[16] However, at the start of our synthetic endeavor towards (–)-irciniastatin B (**1.2**), there had been no reported total synthesis of **1.2**. Indeed, the total synthesis of (–)-irciniastatin B (**1.2**) was only recently achieved in our laboratory.[20,21] Our successful synthetic strategy to the construction of **1.2** will be outlined in Chapter Two.

This subchapter will outline the various strategies employed in selected total syntheses of (+)-irciniastatin A (**1.1**) (psymberin).

1.3.1 The De Brabander Synthesis of (+)-Irciniastatin A (1.1) (Psymberin) and Structural Confirmation

De Brabander and coworkers set out to construct psymberin to determine the structural relationship between (+)-irciniastatin A and (+)-psymberin.[10,22] At the outset of this endeavor, the relative stereochemical configuration at C(4) was unknown and the configuration at C(8) had conflicting assignments.[1,2] The De Brabander synthetic strategy therefore required access to all four possible C(4)-C(8) diastereomers (Scheme 1.1). Their retrosynthetic strategy first involved a disconnection at the amide leading to acid chloride **1.9** and methoxy-imidate **1.10**. Both stereochemical configurations of the *N,O*-aminal moiety were envisioned to be constructed *via* reduction of the resulting *N*-acyl-methoxy-imidate. The epimeric acid chlorides **1.9** would be constructed from a common intermediate derived from D-mannitol. Methoxy imidate **1.10** in turn would be accessed *via* a substrate controlled aldol reaction between aryl aldehyde **1.11** and ethyl ketone **1.12**.

Scheme 1.1. Retrosynthetic Analysis by De Brabander and Coworkers

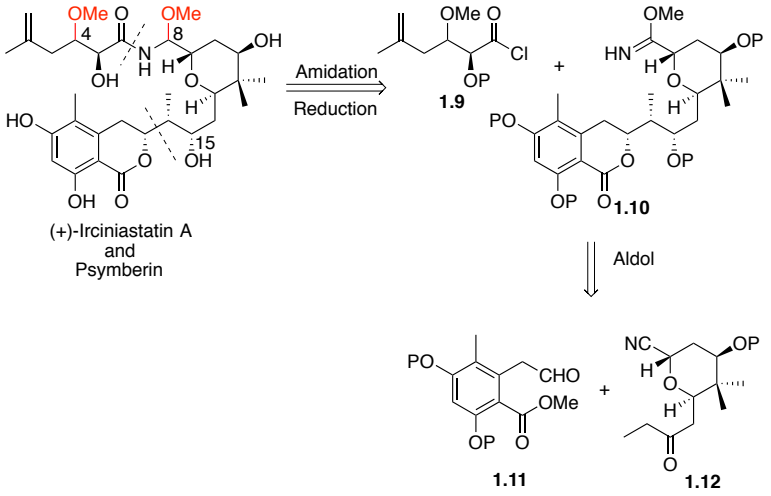

Once ketone **1.12** was elaborated to nitrile **1.13**, the nitrile had to be converted to the methoxy-imidate before the final coupling with the acid side chain (Scheme 1.2). Towards this end, nitrile **1.13** was treated with the Ghaffar-Parkins[23] catalyst **1.14** to effect hydrolysis of the nitrile to the amide. Both 4-methoxybenzyl (PMB) ethers were removed under hydrogenolysis conditions and peracetylated. Amide **1.15** was then treated with $Me_3O{\bullet}BF_4$ and poly(4-vinylpyridine) to furnish methoxy-imidate **1.16**, which was treated with acid chlorides **1.17** and **1.18** to provide the corresponding acyl-methoxy-imidates. Upon reduction and saponification steps, a separable mixture of **1.1** and **1.19** (71:29) from **1.17** and an inseparable mixture **1.20** and **1.21** (75:25) from **1.18** were isolated. Since the spectral data of natural (+)-irciniastatin A (**1.6**) and (+)-psymberin (**1.8**) were taken in different solvents, their exact stereochemical relationship was not resolved at the time of isolation. De Brabander conducted NMR studies on all four diastereomers in both solvents and determined that **1.1** is the correct structure for both irciniastatin A and psymberin. This seminal total synthesis not only established

unamibguously the absolute stereochemical configuration of psymberin but also proved that irciniastatin A and psymberin are identical.

In summary, De Brabander accomplished the total synthesis of (+)-irciniastatin A (**1.1**) with a longest linear sequence of 21 steps from commercially available starting materials in an overall yield of 6.1%.

Scheme 1.2. Total Synthesis of (+)-Irciniastatin A (**1.1**) (Psymberin) and its Structural Confirmation

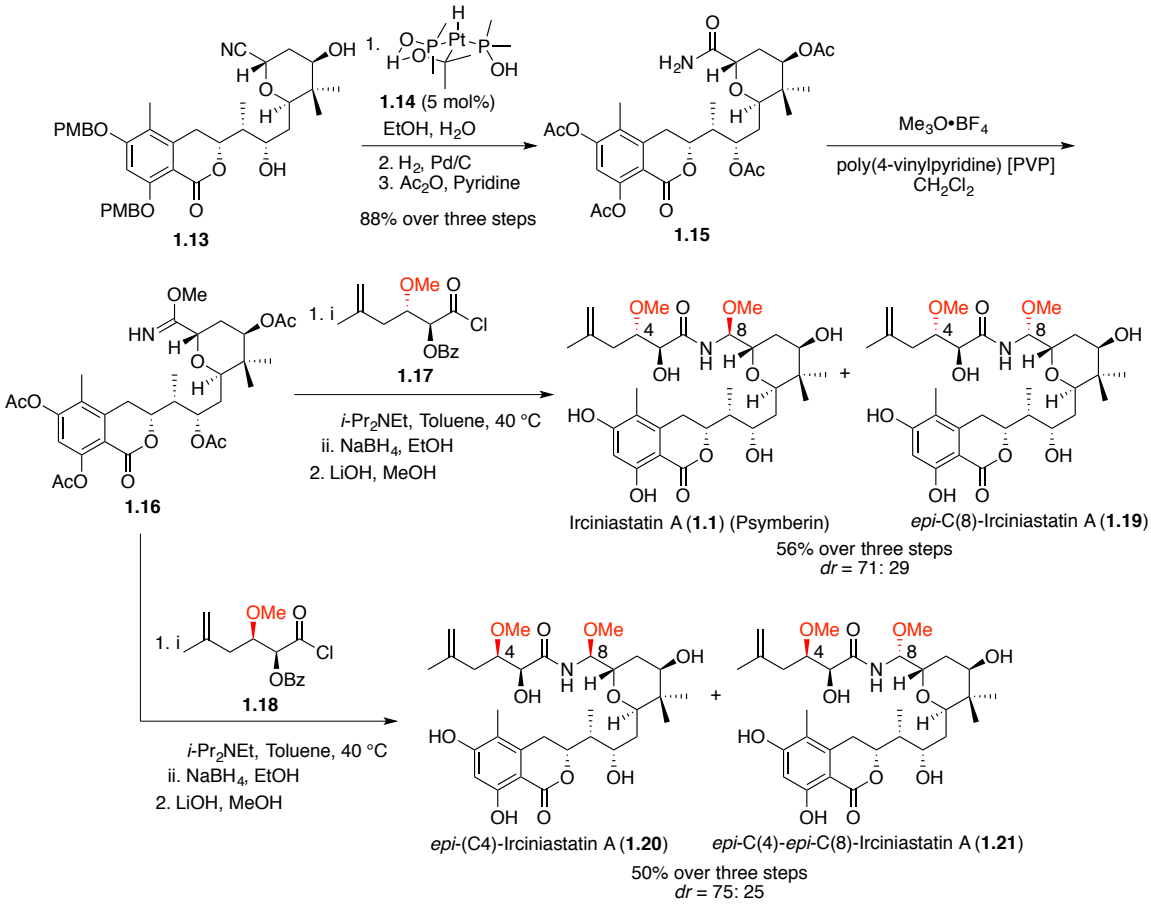

1.3.2 The Schering-Plough Synthesis of (+)-Irciniastatin A (1.1)

In 2007, a group at the Schering-Plough Research Institute achieved the second total synthesis of (+)-irciniastatin A (**1.1**).[15,24] They elected to disconnect the complex

structure at C(9)-O bond to provide enamide **1.22** (Scheme 1.3). The tetrahydropyran core was envisioned to be constructed *via* a novel (diacetoxyiodo)benzene-mediated oxidative cyclization,[25] a method previously developed in their laboratories. Enamide **1.22** would in turn be derived from the unions of amide **1.23**, silyl enol ether **1.24**, and aldehyde **1.25**.

Scheme 1.3. Retrosynthetic Analysis by the Schering-Plough group

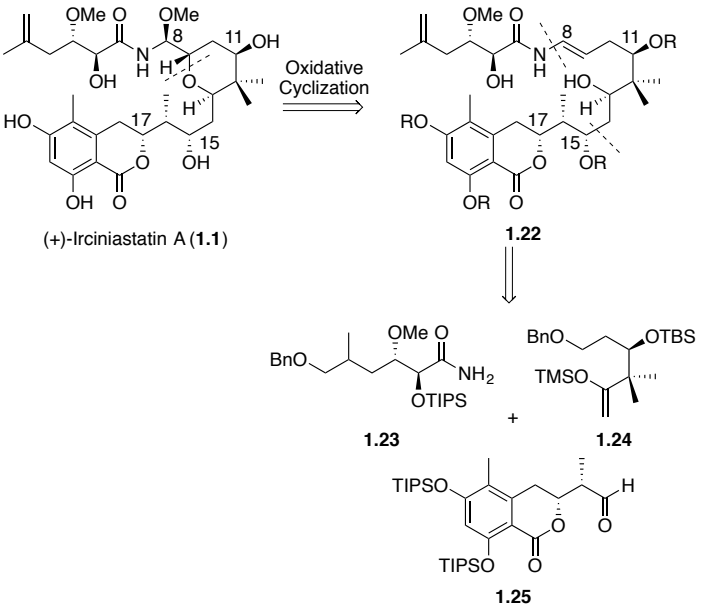

In the forward direction, aldehyde **1.25** was shown to undergo Mukaiyama aldol reaction in good yield (76% as pure isomer, *dr* = 5:1) with silylenol ether **1.24** (Scheme 1.4). The ketone was then subjected to chelation-controlled reduction, mediated by catecholborane[26] to furnish diol **1.26** with excellent diastereoselectivity (*dr* = 15:1). Diol **1.26** was bisacetylated, followed by removal of the benzyl ether, Dess-Martin periodinane oxidation,[27] and Takai olefination[28] to furnish vinyl iodide **1.27**. A Buchwald union[29] between vinyl iodide **1.27** and amide **1.23** completed construction of the full carbon skeleton of the target natural product. Treatment under basic conditions next led

to hydrolysis of both acetate groups and one TIPS ether. The free phenol was selectively acetylated with acetic anhydride. Enamide **1.28** was exposed to $PhI(OAc)_2$ to mediate cyclization, which proceeded in good yield (60% for two major diastereomers, 1:1). The secondary hydroxyl in turn was acetylated, followed by hydrogenolysis to furnish **1.29** and **1.30**. To reveal the terminal olefin, the diastereomers were separated and exposed to *o*-nitrophenylselenocyanate, followed by treatment with H_2O_2.[30] The intermediates were then treated with TBAF at 50 °C to achieve global deprotection to (+)-irciniastatin A (**1.1**) (63% over three steps) and *epi*-C(8)-*epi*-C(9)-irciniastatin A (**1.31**).

In summary, the group at Schering-Plough completed the total synthesis of (+)-irciniastatin A (**1.1**) with a longest linear sequence of 25 steps from commercially available starting materials in an overall yield of 2.5%. The cornerstone of their strategy was the $PhI(OAc)_2$ mediated oxidative cyclization to construct the *trans*-tetrahydropyran core.

Scheme 1.4. Total Synthesis of (+)-Irciniastatin A (**1.1**) by the Schering Plough Group

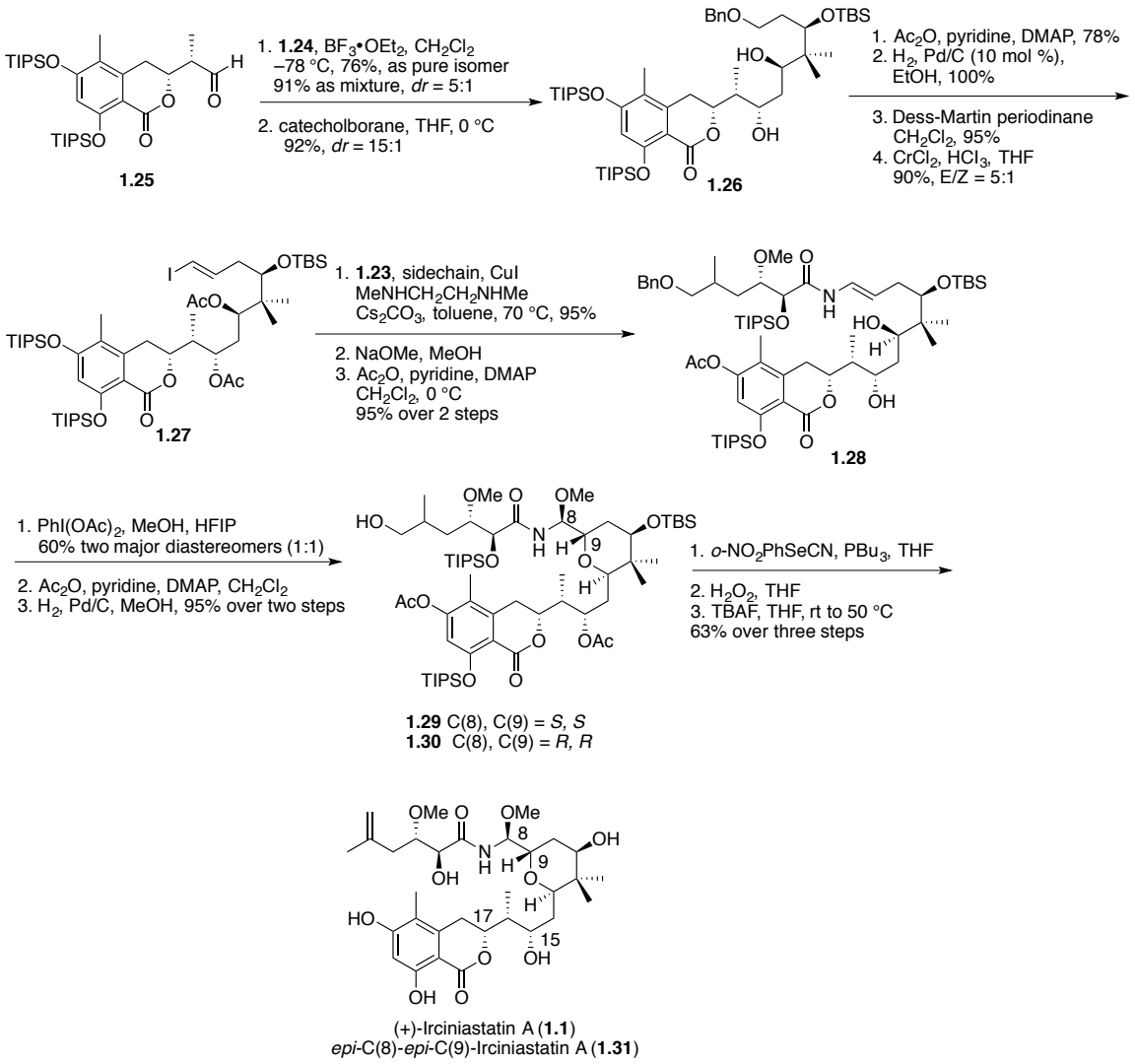

1.3.3 The Crimmins Synthesis of (+)-Irciniastatin A (1.1)

Crimmins and coworkers reported their successful total synthesis of (+)-irciniastatin A (**1.1**) in 2009.[17] Retrosynthetically, they disconnected **1.1** at the amide linkage to furnish acid chloride **1.32** and *N,O*-aminal **1.33** (Scheme 1.5). The *N,O*-aminal moiety was then envisioned to be constructed *via* a Curtius rearrangement[16,31,32] of a carboxylic acid derived from benzyl ether **1.34**. Construction of **1.34** in turn would be

achieved *via* stereoselective addition of silylenol ether **1.35** to the oxocarbenium ion derived from acetate **1.36**.

Scheme 1.5. Retrosynthetic Analysis by Crimmins and Coworkers

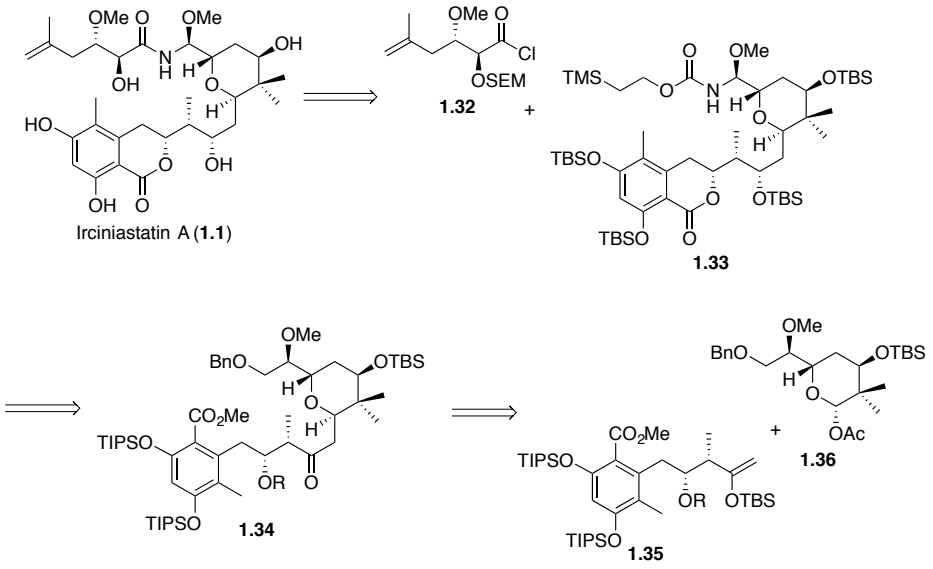

The key union of acetate **1.36**, constructed from 2-deoxy-D-ribose in 9 steps, and silylenol ether **1.35** was achieved *via* a BF_3•OEt_2 mediated coupling to provide ketone **1.34** with excellent diastereoselectivity (*dr* >20:1) (Scheme 1.6). The high level of stereoselectivity can be explained by pseudoaxial addition of **1.35** to the oxocarbenium ion. The oxocarbenium ion adopts conformation **1.37**, which is favored due to through-space stereoelectronic stabilization of the oxocarbenium ion by the axial TBS ether.[33]

Scheme 1.6. Elaboration to Ketone **1.34**

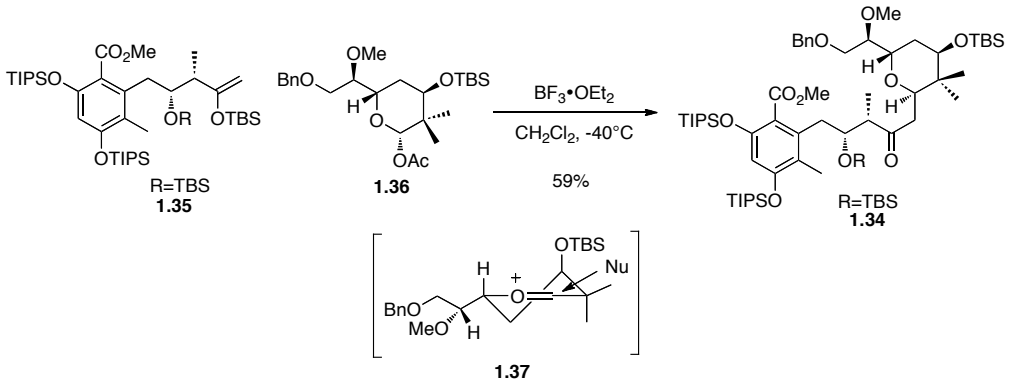

With ketone **1.34** in hand, Crimmins continued the synthesis with elaboration to *N,O*-aminal **1.33** (Scheme 1.7). Stereoselective reduction of **1.34** was achieved *via* Corey-Bakshi-Shibata protocol[34] employing the (*R*)-CBS reagent to provide alcohol **1.38** as a single diastereomer. The secondary TBS ether was then hydrolyzed with concomitant lactonization to furnish **1.39**. The alcohols were next reprotected as TBS ethers and the benzyl ether was removed under hydrogenolysis conditions. Alcohol **1.40** was then oxidized to the corresponding acid, which underwent a Curtius rearrangement[16,31,32] to install the *N,O*-aminal moiety, furnishing **1.33** in 76% yield with complete retention of stereochemical configuration. The union of **1.33** with acid chloride **1.32** proved challenging; however, Crimmins discovered that employing *i*-PrMgCl as the base successfully provided amide **1.42** in an excellent 87% yield. The final global deprotection was then achieved with TAS-F[35,36] in DMF to furnish (+)-irciniastatin A (**1.1**) in 94% yield.

Scheme 1.7. Completion of (+)-Irciniastatin A (**1.1**) by Crimmins and Coworkers

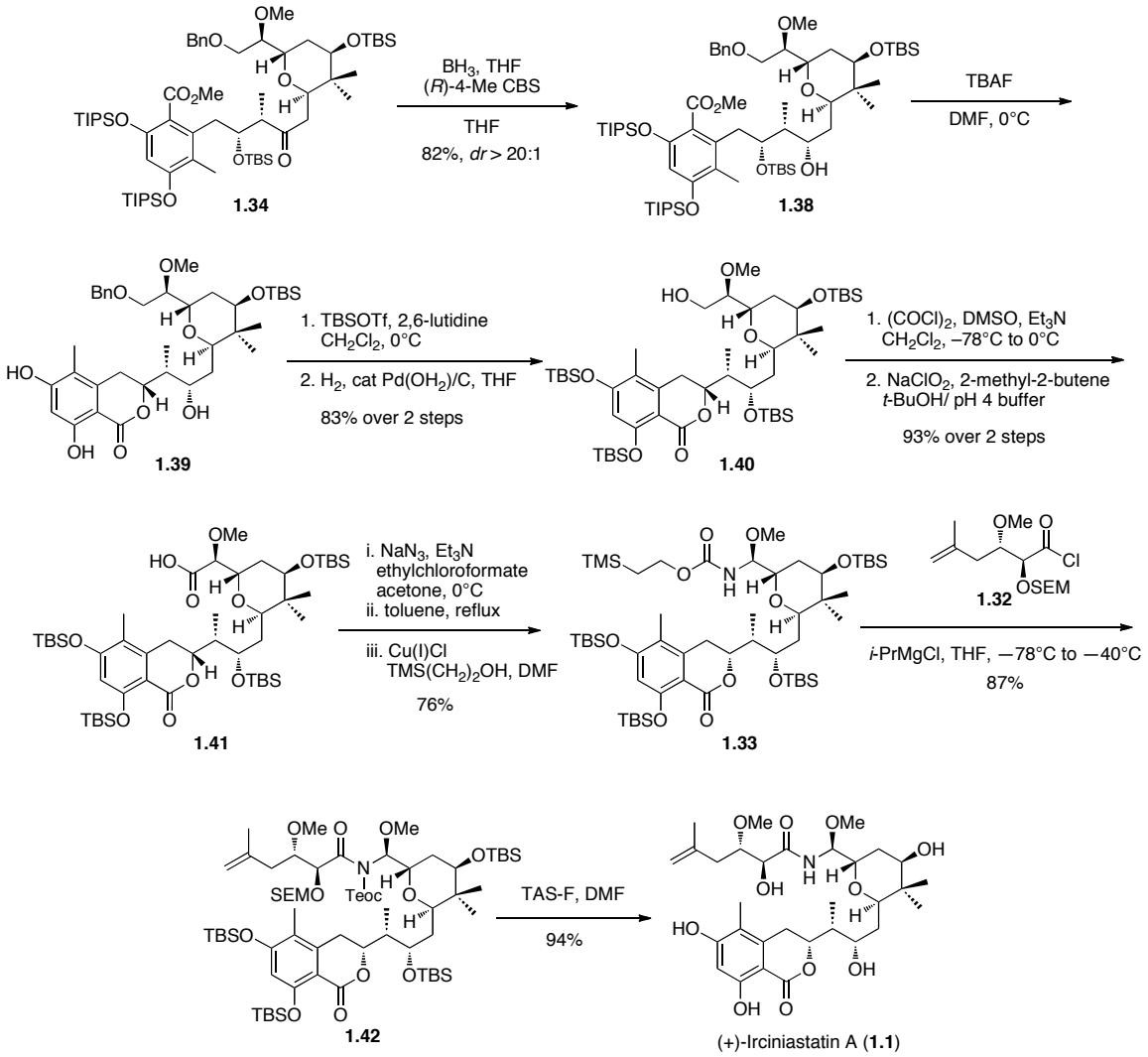

In summary, Crimmins and coworkers achieved the total synthesis of (+)-irciniastatin A (**1.1**) with a longest linear sequence of 19 steps from commercially available materials, with a 6% overall yield. Highlights in the synthetic sequence include the stereoselective silylenol ether-oxocarbenium ion union, Curtius rearrangement to install the *N,O*-aminal, and a late-stage union of *N,O*-aminal **1.33** with acid chloride **1.32**.

1.3.4 The Floreancig Synthesis of (+)-Irciniastatin A (1.1)

Floreancig and coworkers[18] set out to construct (+)-irciniastatin A (**1.1**) *via* a multicomponent sequence that includes nitrile hydrozirconation,[37] acylation,[38] and nucleophilic addition (Scheme 1.8). The Floreancig group had applied this strategy toward the construction of several amide scaffolds.[39,40] This sequence was envisioned to begin with hydrozirconation of nitrile **1.45**, followed by acylation with acid chloride **1.44**. The resulting *N*-acyl-imine **1.43** would then be trapped by methanol to furnish the complete carbon skeleton of (+)-irciniastatin A (**1.1**).

Scheme 1.8. Retrosynthetic Analysis by Floreancig and Coworkers

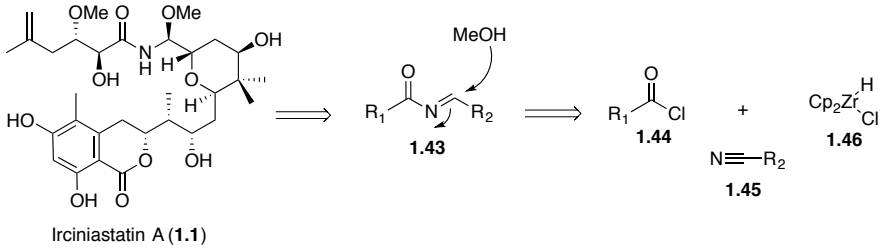

Irciniastatin A (**1.1**)

The proposed multicomponent coupling proved to be a challenge (Table 1.4). Nitrile **1.48** was treated with Cp_2ZrHCl, then acylated with acid chloride **1.47** followed by addition of MeOH to result in a mixture of diastereomeric *N,O*-aminals, with a 1:3 ratio, where the undesired isomer predominated (Table 1.4, entry 1). Addition of $Mg(ClO_4)_2$ enhanced the selectivity of the desired isomer to 3:1, but only proceeded in a very low overall yield (Table 1.4, entry 2). Floreancig and coworkers reasoned that a bulkier and less reactive source of methanol would improve selectivity and yield. Indeed, addition of 2 eq of $Mg(ClO_4)_2$ and $(MeO)_3CH$ resulted in a 3:1 mixture, albeit again with low overall yield (~20%) (Table 1.4, entry 3). In order to improve further the efficiency

of the transformation, $Zn(OTf)_2$ was employed as the Lewis acid, which in this case resulted in lower stereoselectivity (~1.5:1), but higher yield (Table 1.4, entry 4). The crude mixture was subsequently treated with TBAF to result in hydrolysis of the silyl ethers, lactonization and loss of the benzoate to provide (+)-irciniastatin A (**1.1**) in 27% yield and *epi*-C(8)-irciniastatin A in 12% yield. Removal of the benzoate group was rationalized by the production of Bu_4NOH during the removal of the silyl ethers.

Table 1.4. Hydrozirconation/Acylation Sequence to the Construction of (+)-Irciniastatin A (**1.1**)

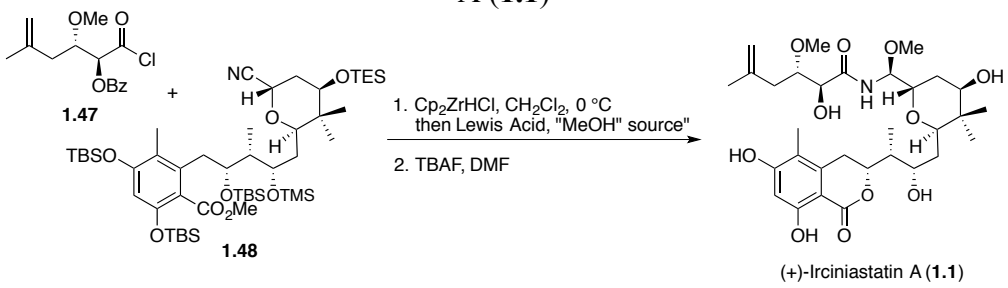

Entry	Lewis Acid	"MeOH" source	Yield	dr
1	None	MeOH	"Less Efficient"	1:3
2	$Mg(ClO_4)_2$	MeOH	"Less Efficient"	3:1
3	$Mg(ClO_4)_2$	$(MeO)_3CH$	~20% single step	3:1
4	$Zn(OTf)_2$	$(MeO)_3CH$	27% over 2 steps 12% *epi*-C(8)-Irciniastatin A	1.5:1

Not withstanding the aforementioned difficulties, the Floreancig synthesis to (+)-irciniastatin A (**1.1**) proves to be the shortest linear sequence to date (14 steps, 4.4% overall yield). Their successful multicomponent sequence approach to construct directly the *N,O*-aminal significantly contributes to the brevity of this synthetic route.

1.4 Structure Activity Relationship Studies of Irciniastatin Analogues

1.4.1 The De Brabander Analogue Study

The structural similarities between the irciniastatins and pederins would suggest that they possess similar biological functions. On the other hand, notable differences in structure and biological profile may indicate they have different biological mechanisms. De Brabander and coworkers set out to construct a hybrid between the two families of natural products, psympederin (**1.49**), in order to probe how differences in the molecular structure influence biological function.[41] Psympederin (**1.49**) was designed to retain the irciniastatin's acyclic side chain, but the dihydroisocoumarin was removed.

Construction of psympederin (**1.49**) began with an 8-step sequence from diol **1.52**, an intermediate from their (+)-irciniastatin A (**1.1**) synthesis, to provide amide **1.53** (Scheme 1.9). Installation of the side chain was achieved by methoxy-imidate formation from **1.53**, acylation with acid chloride **1.17**, and *in situ* reduction to the acyl-*N,O*-aminal. Final saponification removed the remaining protecting groups to furnish psympederin (**1.49)** and *epi*-C(8)-psympederin (**1.50**) as a separable mixture (1:4) of diastereomers.

Scheme 1.9. Synthesis of Psympederin (**1.49**) and *epi*-C(8)-Psympederin (**1.50**)

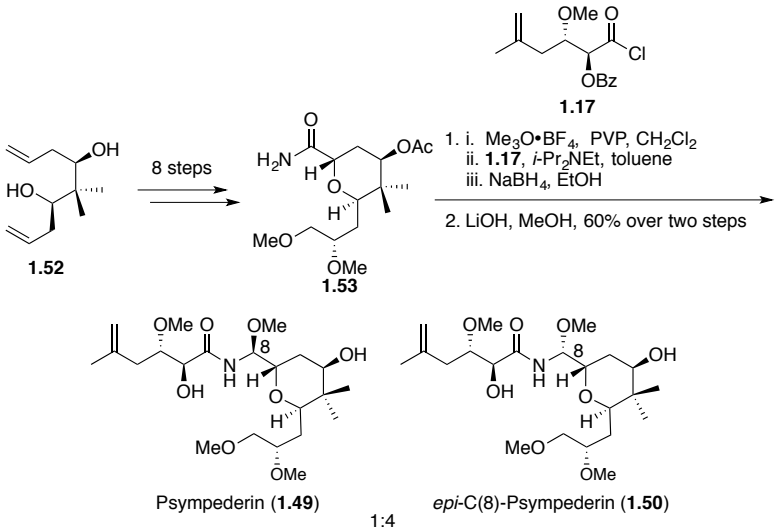

De Brabander and coworkers evaluated the cytotoxic activity of the epimers of psympederin (**1.49** and **1.50**), (+)-irciniastatin A, and the C(8) and C(4)-epimers (**1.19** and **1.20**, respectively)[10] against a series of human tumor cell lines (Table 1.5).[41] Inverting the stereochemical configuration of the *N,O*-aminal (**1.19**) and at C(4) (**1.20**) resulted in a decrease in cytotoxicity across all cell lines tests, but inhibition of proliferation of the cancer cell lines remained (37-762 nM). Most interestingly, psympederin **1.49** displayed a dramatic decrease in cytotoxicity (~1000 fold) compared to (+)-irciniastatin A (**1.1**). *epi*-C(8)-Psympederin **1.50** displayed no cytotoxic activity against three of the four cell lines evaluated, in comparison with *epi*-C(8)-irciniastatin A (**1.19**), which displayed moderate to good activity. This result suggests that the dihydroisocoumarin fragment is critical to the cytotoxic activity of the irciniastatins, but is not important for the pederins. In addition, removal of the side chain in amide **1.51**

resulted in complete loss of activity (Table 1.6), which suggests that the side chain is required for high levels of cytotoxicity.

Table 1.5. Cytotoxicity of De Brabander's Analogues Against Human Cancer Cell Lines

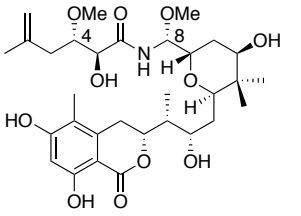

epi-C(8)-Irciniastatin A (**1.19**)

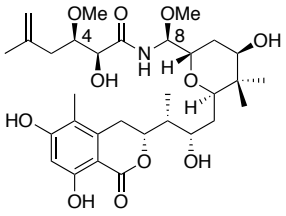

epi-C(4)-Irciniastatin A (**1.20**)

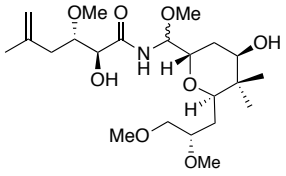

Psympederin (**1.49**)
epi-C(8)-psympederin (**1.50**)

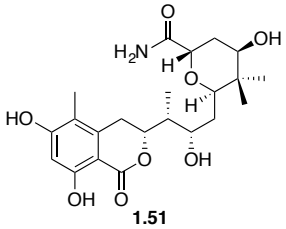

1.51

	IC_{50} [nM]			
Compound	KM12	PC3	SK-MEL-5	T98G
Irciniastatin A (**1.1**)	0.45 ± 0.01	0.98 ± 0.12	2.29 ± 0.13	1.37 ± 0.06
epi-C(8)-Irciniastatin A (**1.19**)	37.1 ± 5.5	200.2 ± 27.6	352.0 ± 12.1	85.8 ± 48.4
epi-C(4)-Irciniastatin A (**1.20**)	126.08 ± 8.6	346.5 ± 102.8	762.8 ± 70.0	186.7 ± 51.3
psympederin (**1.49**)	710.9 ± 35.8	821.8 ± 89.1	>1000	>1000
epi-C(8)-psympederin (**1.50**)	>1000	255.5 ± 11.4	>1000	>1000

Since the members of the pederin family such as mycalamide A (**1.5**) are eukaryotic protein translation inhibitors,[42] De Brabander hypothesized that (+)-irciniastatin A (**1.1**) and the analogues may also possess this biological function, because of their similarities in chemical structure. De Brabander and coworkers evaluated their analogues for protein inhibition in both cell-based and *in vitro* assays (Table 1.6).[14] In the cell-based assays, psympederin **1.49** and the epimers **1.20** and **1.19** displayed marked decrease in potency in inhibiting protein translation in both HeLa and SK-MEL-5 cells. Removal of the side chain (**1.51**) resulted in loss of all inhibition activity. In the *in vitro* assays of these analogues, De Brabander and coworkers were surprised to observe that

psympederin **1.49**, and epimers **1.20** and **1.19** were only 10 to 20-fold less active compared to (+)-irciniastatin A (**1.1**). The significant difference in the activities between the two assays suggests that removal of the dihydroisocoumarin and changes in stereochemical configuration affects other processes in the cell-based assay outside of the ribosome. Protein inhibition by psympederin **1.49** only decreased by 20-fold in the *in vitro* assays, suggesting that the dihydroisocoumarin is important for inducing cytotoxicity and not for protein translation inhibition.

Table 1.6. Cytotoxicity and Protein Inhibition of De Brabander's Analogues

	cytotoxicity (IC_{50}, nM)		Translation Inhibition (EC_{50}, nM)		
				cell-based Assay	
	Hela	SK-MEL-5	*in vitro* assay	HeLa	SK-MEL-5
(+)-Irciniastatin A (**1.1**)	0.64	0.27	28	2.2	11
psympederin (**1.49**)	>1000	>1000	641	1650	578
mycalamide A (**1.5**)	2.52	3.79	238	59	64
1.51	>1000	>1000	>10,000	>10,000	>10,000
epi-C(4)-Irciniastatin A (**1.20**)	>1000	762.8	346	4950	496
epi-C(8)-Irciniastatin A (**1.19**)	618.6	352	318	2200	843

In order to understand the inconsistencies between the *in vitro* and cell-based assays for protein inhibition, De Brabander and coworkers[14] measured the intracellular concentration of (+)-irciniastatin A (**1.1**) and the three synthetic analogues in question (Table 1.7). The HeLa cells were incubated for 2 h with 100 nM of each respective compound. The intracellular concentration of epimers **1.19** and **1.20** was about 20-fold less than that of (+)-irciniastatin A (**1.1**). Furthermore, psympederin's intracellular concentration was below the limit of detection. Therefore, the difference in the two assays was presumably due to a difference in cellular uptake of the compounds.

Table 1.7. Intracellular Concentration of (+)-Irciniastatin A (**1.1**) and Analogues in HeLa Cells

	intracellular concentration (mM)
(+)-Irciniastatin A (**1.1**)	7.14
epi-C(4)-Irciniastatin A (**1.20**)	0.21
epi-C(8)-Irciniastatin A (**1.19**)	0.31
psympederin (**1.49**)	<LD

1.4.2 The Schering-Plough Group Analogue Study

The group at Schering-Plough had constructed *epi*-C(8)-*epi*-C(9)-irciniastatin A **1.31** *via* their synthetic route to irciniastatin A (**1.1**).[15,43] They evaluated the cytotoxicity of **1.31** against a series of human cancer cell lines, and found that **1.31** displayed significant loss of cytotoxic activity compared to (+)-irciniastatin A (**1.1**), suggesting the importance of the stereochemical configuration at both C(8) and C(9) (Table 1.8).

Table 1.8. Antitumor Activity of **1.31** versus (+)-Irciniastatin A (**1.1**) by Schering-Plough (IC_{50} nM)

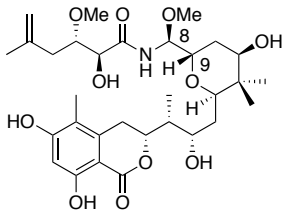

Irciniastatin A (**1.1**)

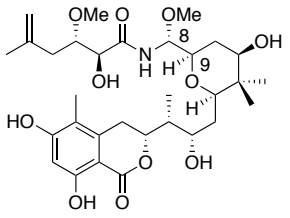

epi-C(8)-*epi*-C(9)-Irciniastatin A (**1.31**)

irciniastatin A (**1.1**)	*epi*-C(8)-C(9)-irciniastatin A (**1.31**)	cell lines	human tissue tytpe
0.76 ± 0.07	6800 ± 244	ACHN	kidney
0.30 ± 0.03	3800 ± 301	DU145	prostate
0.18 ± 0.02	2400 ± 431	H226	lung
0.81 ± 0.14	4900 ± 187	HCT116	colon
0.42 ± 0.02	4600 ± 68	HOP62	lung
0.27 ± 0.01	4200 ± 174	MB231	breast
0.28 ± 0.03	3600 ± 155	MB435	melanoma
0.28 ± 0.02	5200 ± 195	MKN45	gastric
0.19 ± 0.02	3100 ± 341	PC3	prostate
0.82 ± 0.04	4800 ± 177	SW620	colon
0.84 ± 0.08	n.d.	NHDF	normal

The Schering-Plough group conducted their next SAR study on the side chain (Table 1.9). Substantial reduction in cytotoxicity resulted when the side chain was replaced with a methyl group in compounds **1.54** and **1.55**. Next, the function of the terminal olefin was examined. Compounds **1.56** and **1.57** replaced the terminal olefin with a primary hydroxyl group. Analogue **1.56** still retained good cytotoxicity (260 nM), however the epimer **1.57** lost all activity (>10,000 nM), which suggests the terminal olefin plays an important role in the biological mode of action responsible for potent cytotoxicity. Next, a phenyl group was employed to mimic the electronic properties of the terminal olefin. Analogues **1.58** and **1.59** were constructed without substitution at C(4) and C(5), which resulted in loss of activity (>10,000 nM). When the appropriate

substitution was added to the phenyl analogues, **1.60** displayed good levels of cytotoxicity (32 nM), while **1.61** possessed moderate levels (615 nM). The biological data from these analogues suggests that the π-character in the side chain, as well as the substitution at C(4) and C(5), are important for the cytotoxic properties of (+)-irciniastatin A (**1.1**).

Table 1.9. Activity of Side Chain Analogues against HOP62 Lung Cancer Cell Line

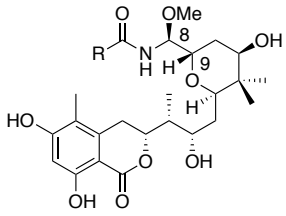

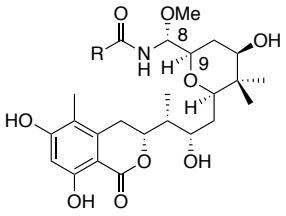

Compound	R	IC_{50} (nM)	Compound	R	IC_{50} (nM)
1.54		>10000	**1.55**		>10000
1.56	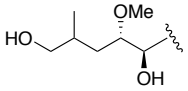	260 ± 36	**1.57**	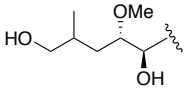	>10000
1.58	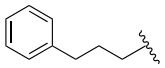	>10000	**1.59**	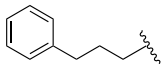	>10000
1.60	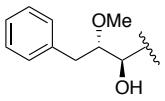	32 ± 1	**1.61**	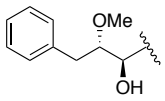	615 ± 15

Although the only difference between (+)-irciniastatin A (**1.1**) and (–)-irciniastatin B (**1.2**) is the oxidation state at C(11), **1.2** displays a 10-fold increase in cytotoxic activity compared to **1.1**.[1] In order to probe the biological function of the C(11) oxygen, the Schering-Plough group set out to construct C(11)-deoxy-irciniastatin A (**1.68**). In addition, removal of the functionality in the tetrahydropyran core would simplify the synthesis. Full carbon skeleton **1.63** was constructed from ester **1.62** in 12 synthetic steps

(Scheme 1.10). Oxidative cyclization promoted by $PhI(OAc)_2$ was achieved in 89% yield, followed by acetylation of secondary hydroxyl group and debenzylation provided a mixture of four diastereomers. The diastereomers were separated *via* flash chromatography. Final elaboration to the C(11)-deoxy analogues required conversion of alcohols **1.64, 1.65, 1.66,** and **1.67** to the *o*-nitrophenyl selenides, which upon oxidization in the presence of H_2O_2,[30] and global deprotection with TBAF revealed C(11)-deoxy-irciniastatin A (**1.68**) and corresponding epimers **1.69, 1.70,** and **1.71**.

Scheme 1.10. Synthesis of C(11)-Deoxy-Irciniastatin A Analogues

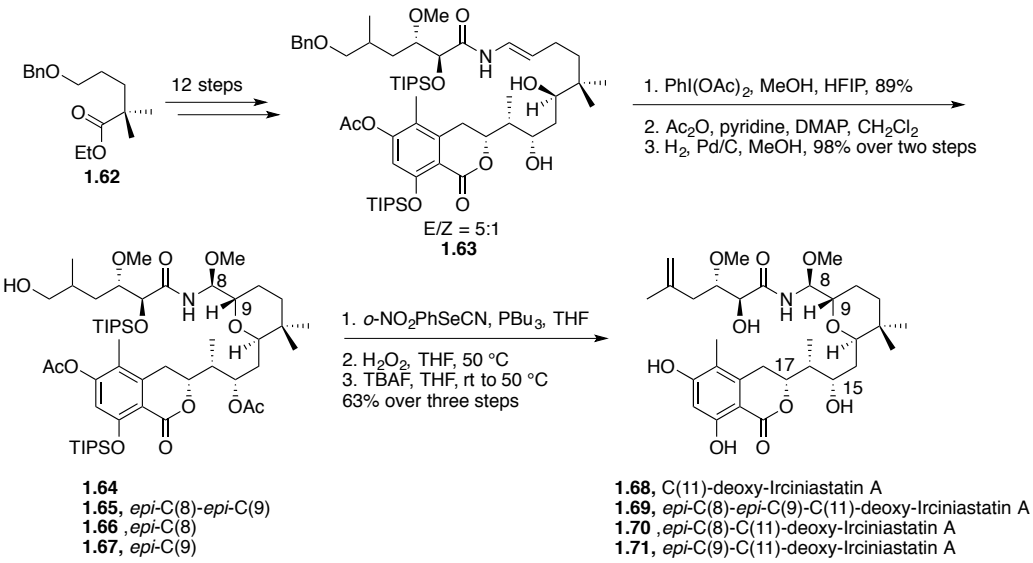

1.62

1.63

1.64
1.65, *epi*-C(8)-*epi*-C(9)
1.66 ,*epi*-C(8)
1.67, *epi*-C(9)

1.68, C(11)-deoxy-Irciniastatin A
1.69, *epi*-C(8)-*epi*-C(9)-C(11)-deoxy-Irciniastatin A
1.70 ,*epi*-C(8)-C(11)-deoxy-Irciniastatin A
1.71, *epi*-C(9)-C(11)-deoxy-Irciniastatin A

The C(11)-deoxy-irciniastatin A analogues were then tested against a variety of human cancer cell lines (Table 1.10).[43] The C(11)-deoxy-irciniastatin A congener (**1.68**) displayed very potent cytotoxicity and was 3-10 times more active compared to (+)-irciniastatin A (**1.1**). Epimer **1.71** also displayed potent activity in the nanomolar range (1.6 – 8.7 nM). These results strongly suggest the hydrogen bond donating ability of the C(11) hydroxyl and a polar C(11) substituent are not important for cytotoxicity.

Table 1.10. Biological Evaluation of C(11)-Deoxy-Irciniastatin A Analogues (IC_{50} nM)

1.68	**1.69**	**1.70**	**1.71**	cell line	human tissue
0.265 ± 0.008	n.d.	n.d.	8.7 ± 0.18	ACHN	Kidney
0.149 ± 0.005	n.d.	n.d.	5.9 ± 0.18	DU145	prostate
0.034 ± 0.004	n.d.	n.d.	1.6 ± 0.27	H226	lung
0.055 ± 0.002	177 ± 6	46 ± 7	3.0 ± 0.12	HOP62	lung
0.142 ± 0.007	n.d.	n.d.	5.3 0.15	MB231	breast
0.076 ± 0.004	n.d.	n.d.	3.9 ± 0.48	MKN45	gastric
0.073 ± 0.006	n.d.	n.d.	2.9 ± 0.21	PC3	prostate
0.160 ± 0.015	n.d.	n.d.	6.1 ± 0.22	SW620	colon
.066 ± 0.004	n.d.	n.d.	3.8 ± 0.1	NHDF	normal

1.4.3 The Iwabuchi Analogue Study

The Schering-Plough group illustrated that the terminal olefin in the side chain of (+)-irciniastatin A (**1.1**) can be replaced with an electronically similar moiety such as a phenyl group, and still retain potent cytotoxicity. Subsequently, Iwabuchi and coworkers constructed "alkymberin" (**1.80**), where the terminal olefin is substituted with an alkyne moiety.[12] They envisioned that the alkyne could be employed as a chemical handle for coupling reporter tags *via* click chemistry.[44] The construction of alkymberin (**1.80**) begins with TES protection of propargyl bromide **1.72** (Scheme 1.11) to furnish bromide **1.73**, which was treated with the alkoxide of propargyl alcohol to provide di-yne **1.74**. Directed reduction followed by Sharpless epoxidation[45] furnished epoxide **1.75** in 79% yield with good enantioselectivity (94% *ee*). Chemoselective epoxide opening was then achieved with $Eu(OTf)_3$ to furnish the desired 1,2-diol **1.76** (4:1 mixture with the 1,3-diol). Construction of primary alcohol **1.77** was next achieved by a three-step sequence: protection of primary hydroxyl group as a pivalate ester; SEM protection of the secondary hydroxyl group; and reductive removal of the pivalate ester. Alcohol **1.77** was

then directly oxidized to the carboxylic acid employing 1-Me-AZADO.[46] The carboxylic acid in turn was converted to the mixed anhydride and coupled to the *N,O*-aminal **1.79** followed by global deprotection to provide alkymberin **1.80**.

Scheme 1.11. Synthesis of Alkymberin (**1.80**)

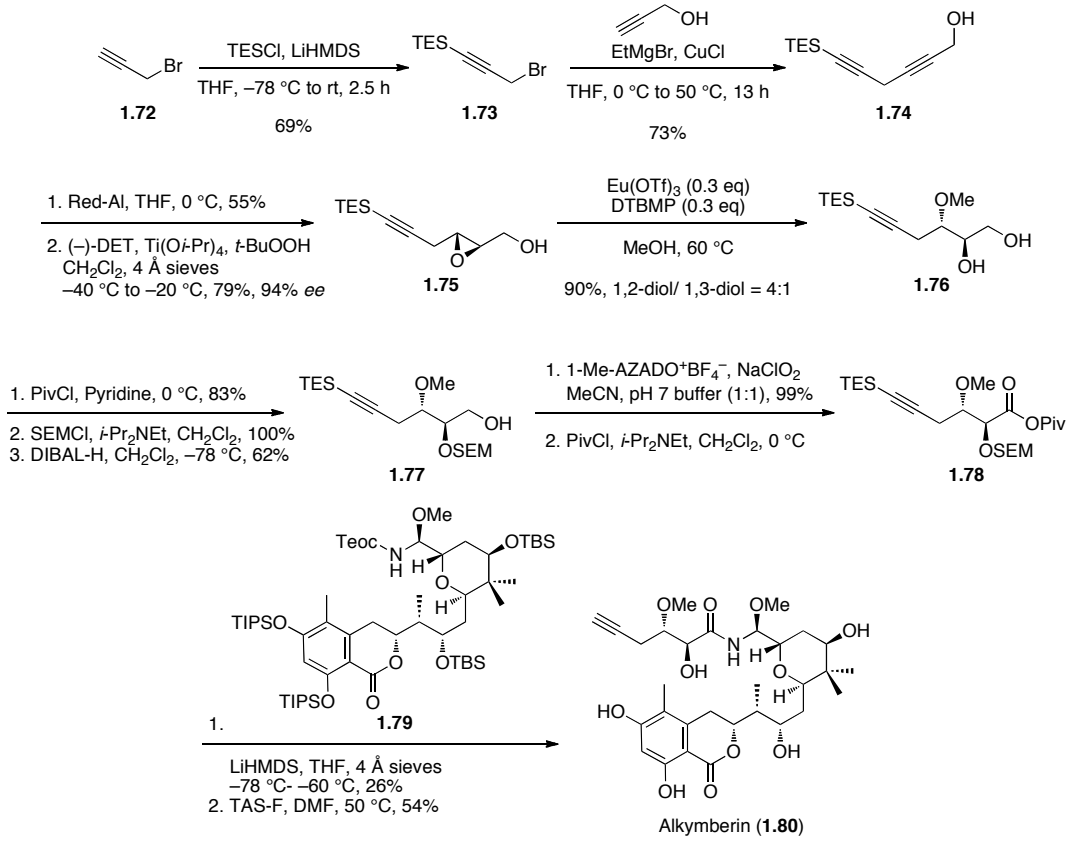

Iwabuchi and coworkers also constructed the enantiomer of (+)-irciniastatin A (**1.1**), (–)-irciniastatin A (**1.88**).[12] They were interested in whether the secondary metabolite behaved as a "ligand" or "chemical reagent" in cells, since the C(8) *N,O*-aminal could act as a good electrophilic reagent. To this end, they constructed the necessary fragments with the opposite stereochemical configurations and achieved the unions required to construct (–)-irciniastatin A (**1.88**) (Scheme 1.12).

Scheme 1.12. Synthesis of (–)-Irciniastatin A (**1.88**)

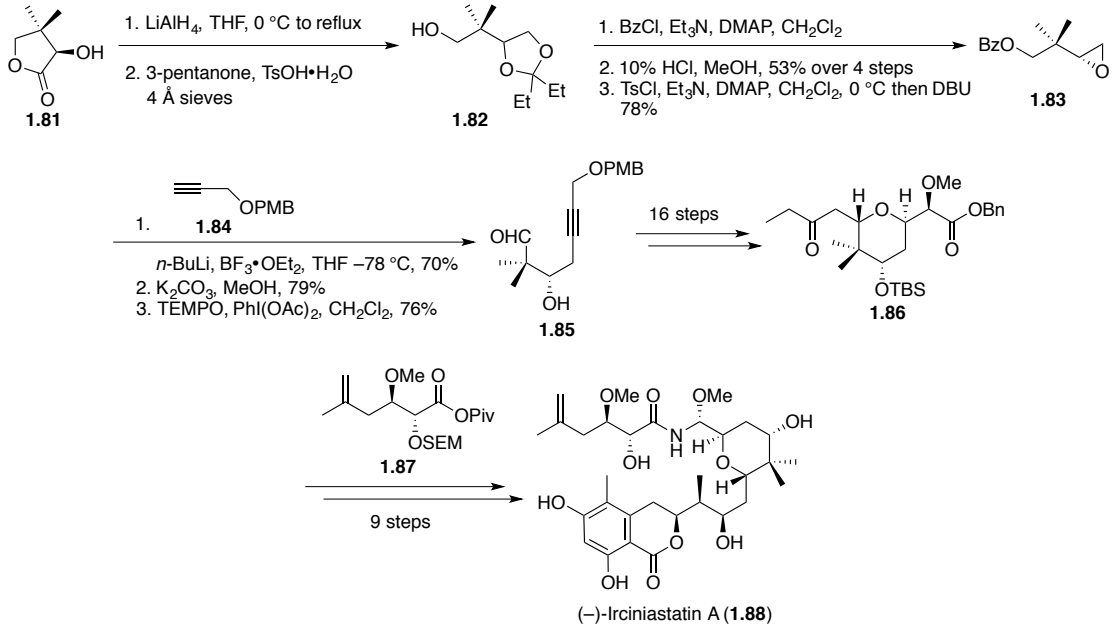

The two synthetic analogues were evaluated for cytotoxicity against HeLa cells. Alkymberin (**1.80**) possessed high levels of activity (GI_{50} = 1.2 nM compared to 0.2 nM for **1.1**). Therefore, alkymberin (**1.80**) can be employed as a probe to study the irciniastatin's biological mode of action. The enantiomer (–)-irciniastatin A (**1.88**) however, displayed no cytotoxic activity (GI_{50} > 1000 nM). Although (–)-irciniastatin A (**1.88**) possesses a highly electrophilic *N,O*-aminal moiety, the enantiomer was unable to induce any cytotoxicity in HeLa cells, suggesting that (+)-irciniastatin A acted as a enantio-specific ligand to the target protein, rather than simply an electrophilic reagent.

1.4.4 The Floreancig Analogue Study

Floreancig and coworkers also constructed several synthetic analogues to probe the biological mode of action of (+)-irciniastatin A (**1.1**). Floreancig, similar to De Brabander, was also interested in how the differences in structure of the irciniastatins and

the pederins influence their biological activity (Table 1.11). Floreancig had synthesized hybrid analogue pedastatin **1.89**, where the acyclic side chain was replaced with the pederate cyclic side chain.[18] To their surprise, pedastatin **1.89** was 10-fold more potent than (+)-irciniastatin A (**1.1**). This new result suggests that pederin (**1.3**) and (+)-irciniastatin A (**1.1**) may share the same binding site on the ribosome, and that the cyclic side chain of pederin and dihydroisocoumarin of (+)-irciniastatin A (**1.1**) play an important role *vis-a-vis* the high levels of cytotoxicity of (+)-irciniastatin A (**1.1**). In order to evaluate the biological function of the *N,O*-aminal, C(8)-desmethoxy psymberin (**1.90**) and C(10)-desmethoxy pedastatin (**1.91**) were constructed and evaluated for cytotoxic activity. Both analogues possessed potent activity, displaying only 10-fold less activity than the parent natural product/analogue, which importantly suggests that the *N,O*-aminal is not an electrophilic reagent for the protein target that is responsible for cytotoxicity, the same conclusion that Iwabuchi made from their analogue study. Taken together with the substantial loss in activity for the *epi*-C(8)-irciniastatin A analogues synthesized by De Brabander and the Schering-Plough group, the stereochemical configuration at C(8) is critical to the irciniastatin's ability to adopt the favorable binding conformation. The natural C(8)-(*S*) configuration stabilizes the binding conformation and the unnatural C(8)-(*R*) configuration destabilizes this conformation. Removal of the stereogenic center altogether does not stabilize nor destabilize the binding conformation, and thus retains potent activity.

Table 1.11. Biological Evaluation of Floreancig's Analogues

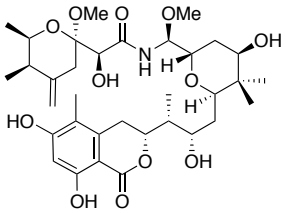

Pedastatin (**1.89**)

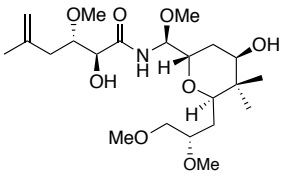

Psympederin (**1.49**)

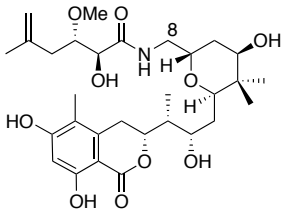

C(8)-desmethoxy psymberin (**1.90**)

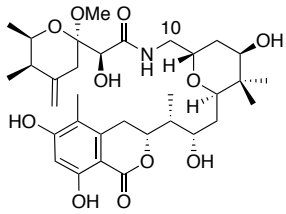

C(10)-desmethoxy pedastatin (**1.91**)

Entry	Compound	GI_{50} (nM) against HCT-116 colon cancer
1	Pederin (**1.3**)	0.6
2	Irciniastatin A/ Psymberin (**1.1**)	0.052
3	Pedastatin (**1.89**)	0.004
4	Psympederin (**1.49**)	710.9*
5	C(8)-desmethoxy psymberin (**1.90**)	0.83
6	C(10)-desmethoxy pedastatin (**1.91**)	0.068

*IC_{50} value for cytotoxicity measured against KM12 colon tumor

1.4.5 Summary of SAR Studies

Since their isolation, numerous biological and SAR studies have shed light on the biological mechanism of (+)-irciniastatin A (**1.1**) (psymberin) and (–)-irciniastatin B (**1.2**). A summary of these studies is presented in Figure 1.5. The difference in biological profiles associated with the structural differences of the alcohol (**1.1**) and the ketone (**1.2**), however, still remain unknown. In conjunction with designing and executing a synthetic route to construct (–)-irciniastatin B (**1.2**), we also aimed to construct synthetic analogues to determine the role that the C(11) substituent plays in the irciniastatins biological mechanism in an SAR study (Figure 1.6).

Figure 1.5. Summary of Analogues Studies for (+)-Irciniastatin A (**1.1**)

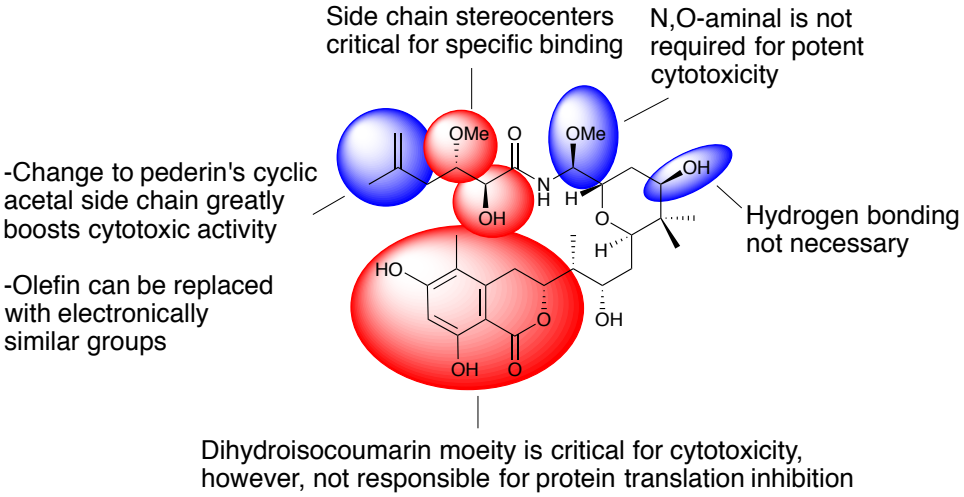

Figure 1.6. Proposed C(11)-Irciniastatin Analogues

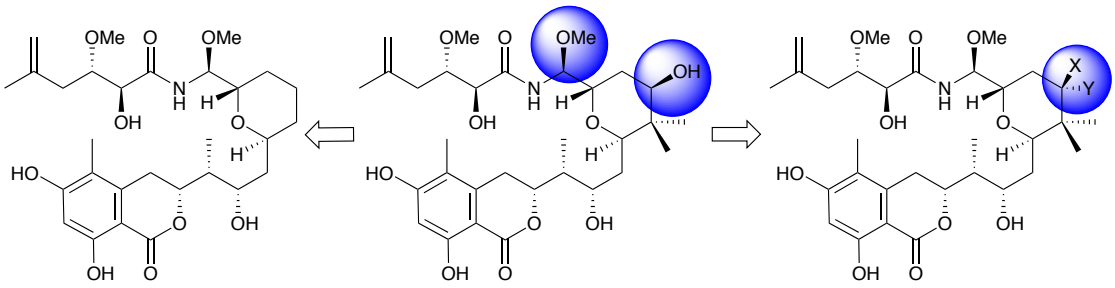

1.5 References

(1) Pettit, G. R.; Xu, J.-P.; Chapuis, J.-C.; Pettit, R. K.; Tackett, L. P.; Doubek, D. L.; Hooper, J. N. A.; Schmidt, J. M. *J. Med. Chem.* **2004**, *47*, 1149-1152.

(2) Cichewicz, R. H.; Valeriote, F. A.; Crews, P. *Org. Lett.* **2004**, *6*, 1951-1954.

(3) Pavan, M.; Bo, M. *Mem. Soc. Entom. It.* **1952**, *31*, 67.

(4) Cardani, C.; Ghiringhelli, D.; Mondelli, R.; Quilico, A. *Tetrahedron Lett.* **1965**, *6*, 2537-2545.

(5) Fusetani, N.; Sugawara, T.; Matsunaga, S. *J. Org. Chem.* **1992**, *57*, 3828-3832.

(6) Perry, N. B.; Blunt, J. W.; Munro, M. H. G.; Pannell, L. K. *J. Am. Chem. Soc.* **1988**, *110*, 4850-4851.

(7) Mosey, R. A.; Floreancig, P. E. *Nat. Prod. Rep.* **2012**, *29*, 980-995.

(8) Richter, A.; Kocienski, P.; Raubo, P.; Davies, D. *Anti-Cancer Drug Des.* **1997**, *12*, 217-227.

(9) Fukui, H.; Tsuchiya, Y.; Fujita, K.; Nakagawa, T.; Koshino, H.; Nakata, T. *Bioorg. Med. Chem. Lett.* **1997**, *7*, 2081-2086.

(10) Jiang, X.; Garcia-Fortanet, J.; De Brabander, J. K. *J. Am. Chem. Soc.* **2005**, *127*, 11254-11255.

(11) Chinen, T.; Nagumo, Y.; Watanabe, T.; Imaizumi, T.; Shibuya, M.; Kataoka, T.; Kanoh, N.; Iwabuchi, Y.; Usui, T. *Toxicol. Lett.* **2010**, *199*, 341-346.

(12) Watanabe, T.; Imaizumi, T.; Chinen, T.; Nagumo, Y.; Shibuya, M.; Usui, T.; Kanoh, N.; Iwabuchi, Y. *Org. Lett.* **2010**, *12*, 1040-1043.

(13) Lee, K.-H.; Nishimura, S.; Matsunaga, S.; Fusetani, N.; Horinouchi, S.; Yoshida, M. *Cancer Sci.* **2005**, *96*, 357-364.

(14) Wu, C.-Y.; Feng, Y.; Cardenas, E. R.; Williams, N.; Floreancig, P. E.; De Brabander, J. K.; Roth, M. G. *J. Am. Chem. Soc.* **2012**, *134*, 18998-19003.

(15) Huang, X.; Shao, N.; Palani, A.; Aslanian, R.; Buevich, A. *Org. Lett.* **2007**, *9*, 2597-2600.

(16) Smith, A. B.; Jurica, J. A.; Walsh, S. P. *Org. Lett.* **2008**, *10*, 5625-5628.

(17) Crimmins, M. T.; Stevens, J. M.; Schaaf, G. M. *Org. Lett.* **2009**, *11*, 3990-3993.

(18) Wan, S.; Wu, F.; Rech, J. C.; Green, M. E.; Balachandran, R.; Horne, W. S.; Day, B. W.; Floreancig, P. E. *J. Am. Chem. Soc.* **2011**, *133*, 16668-16679.

(19) Byeon, S. R.; Park, H.; Kim, H.; Hong, J. *Org. Lett.* **2011**, *13*, 5816-5819.

(20) An, C.; Hoye, A. T.; Smith, A. B. *Org. Lett.* **2012**, *14*, 4350-4353.

(21) An, C.; Jurica, J. A.; Walsh, S. P.; Hoye, A. T.; Smith, A. B. *J. Org. Chem.* **2013**, *78*, 4278-4296.

(22) Feng, Y.; Jiang, X.; De Brabander, J. K. *J. Am. Chem. Soc.* **2012**, *134*, 17083-17093.

(23) Ghaffar, T.; Parkins, A. W. *Tetrahedron Lett.* **1995**, *36*, 8657-8660.

(24) Shao, N.; Huang, X.; Palani, A.; Aslanian, R.; Buevich, A.; Piwinski, J.; Huryk, R.; Seidel-Dugan, C. *Synthesis* **2009**, *2009*, 2855-2872.

(25) Huang, X.; Shao, N.; Palani, A.; Aslanian, R. *Tetrahedron Lett.* **2007**, *48*, 1967-1971.

(26) Evans, D. A.; Hoveyda, A. H. *J. Org. Chem.* **1990**, *55*, 5190-5192.

(27) Dess, D. B.; Martin, J. C. *J. Org. Chem.* **1983**, *48*, 4155-4156.

(28) Takai, K.; Nitta, K.; Utimoto, K. *J. Am. Chem. Soc.* **1986**, *108*, 7408-7410.

(29) Jiang, L.; Job, G. E.; Klapars, A.; Buchwald, S. L. *Org. Lett.* **2003**, *5*, 3667-3669.

(30) Grieco, P. A.; Takigawa, T.; Schillinger, W. J. *J. Org. Chem.* **1980**, *45*, 2247-2251.

(31) Weinstock, J. *J. Org. Chem.* **1961**, *26*, 3511-3511.

(32) Smith, A. B.; Safonov, I. G.; Corbett, R. M. *J. Am. Chem. Soc.* **2002**, *124*, 11102-11113.

(33) Ayala, L.; Lucero, C. G.; Romero, J. A. C.; Tabacco, S. A.; Woerpel, K. A. *J. Am. Chem. Soc.* **2003**, *125*, 15521-15528.

(34) Corey, E. J.; Helal, C. J. *Angew. Chem. Int. Ed.* **1998**, *37*, 1986-2012.

(35) Noyori, R.; Nishida, I.; Sakata, J.; Nishizawa, M. *J. Am. Chem. Soc.* **1980**, *102*, 1223-1225.

(36) Scheidt, K. A.; Chen, H.; Follows, B. C.; Chemler, S. R.; Coffey, D. S.; Roush, W. R. *J. Org. Chem.* **1998**, *63*, 6436-6437.

(37) Erker, G.; Frömberg, W.; Atwood, J. L.; Hunter, W. E. *Angew. Chem. Int. Ed.* **1984**, *23*, 68-69.

(38) Maraval, A.; Igau, A.; Donnadieu, B.; Majoral, J.-P. *Eur. J. Org. Chem.* **2003**, *2003*, 385-394.

(39) Wan, S.; Green, M. E.; Park, J.-H.; Floreancig, P. E. *Org. Lett.* **2007**, *9*, 5385-5388.

(40) Xiao, Q.; Floreancig, P. E. *Org. Lett.* **2008**, *10*, 1139-1142.

(41) Jiang, X.; Williams, N.; De Brabander, J. K. *Org. Lett.* **2007**, *9*, 227-230.

(42) Burres, N. S.; Clement, J. J. *Cancer Res.* **1989**, *49*, 2935-2940.

(43) Huang, X.; Shao, N.; Huryk, R.; Palani, A.; Aslanian, R.; Seidel-Dugan, C. *Org. Lett.* **2009**, *11*, 867-870.

(44) Rostovtsev, V. V.; Green, L. G.; Fokin, V. V.; Sharpless, K. B. *Angew. Chem. Int. Ed.* **2002**, *41*, 2596-2599.

(45) Katsuki, T.; Sharpless, K. B. *J. Am. Chem. Soc.* **1980**, *102*, 5974-5976.

(46) Shibuya, M.; Tomizawa, M.; Suzuki, I.; Iwabuchi, Y. *J. Am. Chem. Soc.* **2006**, *128*, 8412-8413.

CHAPTER 2 Total Synthesis of (–)-Irciniastatin B

Adapted with permission from An, C.; Hoye, T. A.; Smith, A. B. III. "Total Synthesis of (−)-Irciniastatin B and Structural Confirmation via Chemical Conversion to (+)-Irciniastatin A (Psymberin)" *Organic Letters* **2012,** *14*, 4350-4353. Copyright 2012 American Chemical Society.

Adapted with permission from An, C.; Jurica, J. A.; Walsh, S. P.; Hoye, T. A.; Smith, A. B. III. "Total Synthesis of (+)-Irciniastatin A (a.k.a Psymberin) and (–)-Irciniastatin B" *Journal of Organic Chemistry.* **2013***, 78*, 4278-4296. Copyright 2013 American Chemical Society.

2.1 Synthetic Strategy Toward (–)-Irciniastatin B

Figure 2.1. (–)-Irciniastatin B

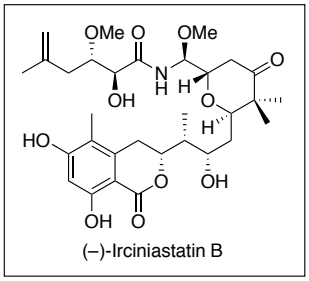

2.1.1 Retrosynthetic Analysis of (–)-Irciniastatin B (2.2)

Our strategy to construct (–)-irciniastatin B (**2.2**)[1,2] follows the same retrosynthetic disconnections as the earlier Smith synthesis of (+)-irciniastatin A (**2.1**).[2,3] The first disconnection begins at the amide linkage, leading to acid side chain **2.3** and Teoc-protected *N,O*-aminal **2.4** (Scheme 2.1). The acid-sensitive *N,O*-aminal moiety would be installed late in the synthesis, with complete retention of stereochemical configuration *via* a Curtius rearrangement,[4] a strategy first developed and successfully

exploited by the Smith group's 2002 synthesis of (+)-zampanolide, bearing a similar *N,O*-aminal group.[5] Disconnection at C(16)-C(17) next provided aldehyde **2.5** and 2,6-*trans*-tetrahydropyran **2.6,** which we envisioned would be united *via* a substrate-controlled aldol reaction. Aryl aldehyde **2.5** in turn would then derive by a [4+2] cycloaddition between known bis-silyl enol ether **2.7**[6] and allene **2.8**,[7] while 2,6-*trans*-tetrahydropyran **2.6** would arise *via* a 6-*exo*-tet-cyclization from epoxide **2.9**. Epoxide **2.9** in turn would be constructed *via* union of aldehyde **2.10** and ketene acetal **2.11**, exploiting a vinylogous Mukaiyama aldol reaction to set the first stereogenic center.[8] Importantly, the requisite stereogenicity in tetrahydropyran **2.6** would be installed *via* three reagent-controlled asymmetric reactions.

Scheme 2.1. Retrosynthetic Analysis of (+)-Irciniastatin A (**2.1**) and (–)-Irciniastatin B (**2.2**)

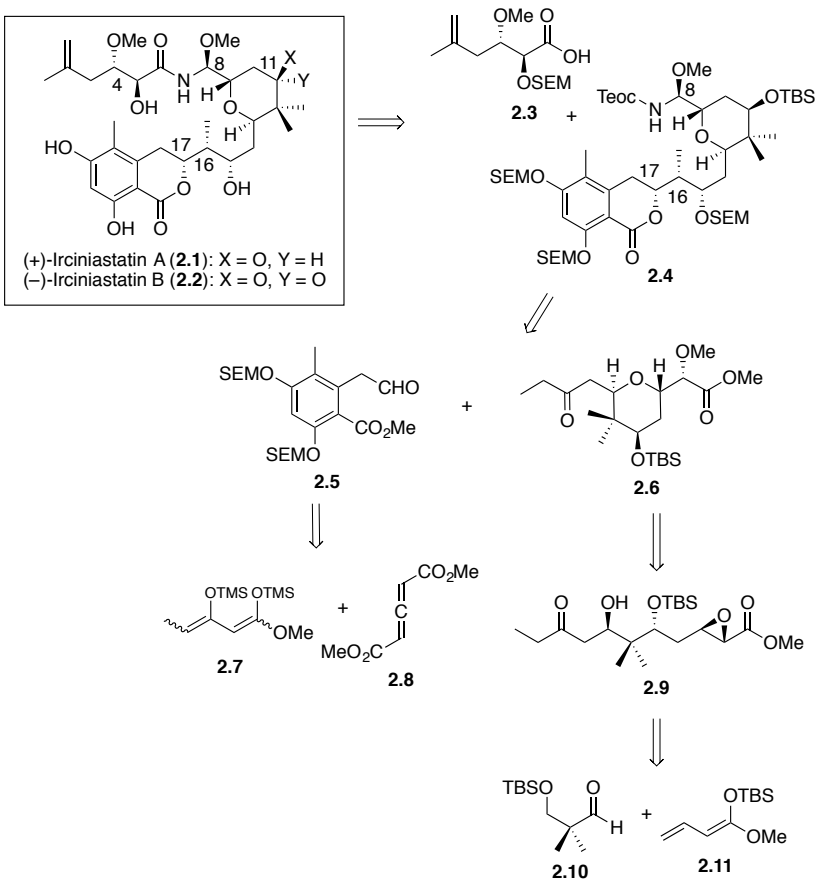

2.1.2 Divergent Strategy to the Construction of (–)-Irciniastatin B (2.2)

To achieve the requisite ketone oxidation state at C(11), the C(15) secondary hydroxyl in (+)-**2.12**, a late-stage intermediate employed in our synthesis of (+)-irciniastatin A (**1**),[3] was envisioned to be protected as a SEM ether, instead of a TBS ether employed earlier (Scheme 2.2). This protecting group was selected to permit the critical, selective deprotection of the neopentyl secondary TBS ether at C(11). The secondary alcohol would then be oxidized to the requisite ketone, followed by global deprotection to provide access to (–)-irciniastatin B (**2.2**). The advantage of this approach compared to our original strategy for (+)-irciniastatin A (**2.1**) would be ready access to a late-stage

intermediate [i.e., (+)-**2.12**] *en route* to both (+)-irciniastatin A (**2.1**) and (–)-irciniastatin B (**2.2**). Additionally, chemical modification of both the C(11) alcohol and ketone in late stage intermediates would permit access to analogues varying at the C(11) stereogenic center, thus permitting further exploration of the irciniastatin chemotype as a potent therapeutic lead.

Scheme 2.2. Divergent Strategy to (+)-Irciniastatin A (**2.1**) and (–)-Irciniastatin B (**2.2**)

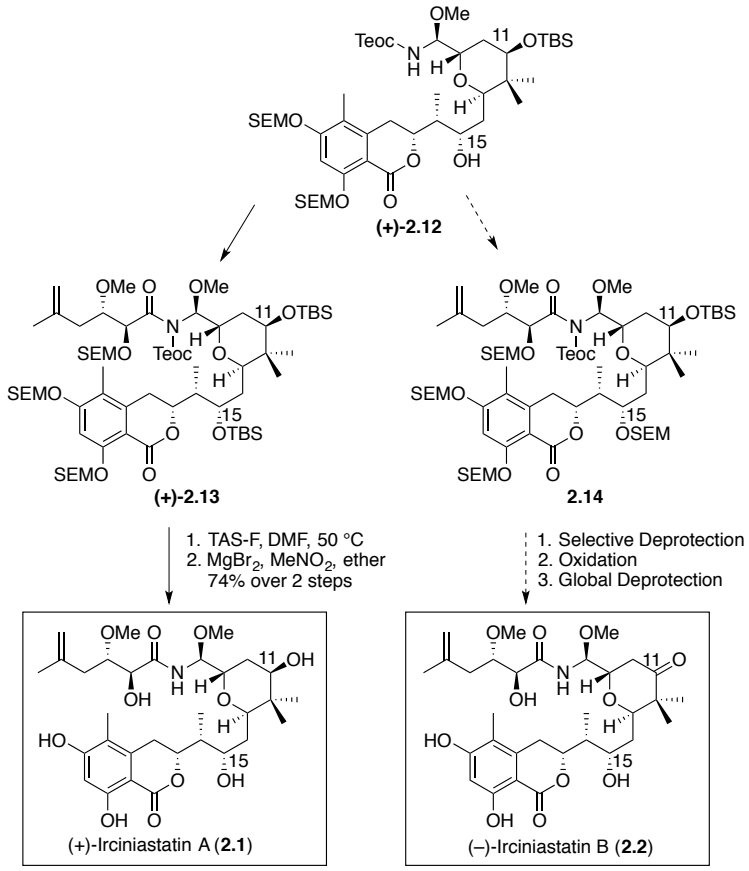

2.2 Challenges Towards the Construction of (–)-Irciniastatin B (2.2)

Although the total synthesis of (+)-irciniastatin A (**2.1**) has been reported seven times since the original isolation,[3,9-14] prior to beginning our synthetic endeavor, there had been no reported total synthesis of (–)-irciniastatin B (**2.2**). This is surprising since **2.2**

was known to be 10-fold more active compared to **2.1**.[15] The reason for no successful total synthesis of (–)-irciniastatin B (**2.2**) might be attributed to the required manipulation of a late-stage intermediate such as **2.15** that possesses two highly sensitive moieties: a base sensitive ketone and an acid labile *N,O*-aminal. For example, we envisioned the tetrahydropyranone contributes to the base sensitivity in **2.15**. Treatment with a base could lead to a retro-Michael-Michael sequence, converting the *trans*-tetrahydropyranone **2.15** into the more thermodynamically favored *cis*-tetrahydropyranone **2.16** (Scheme 2.3).[16] Mechanistically, the first step would be deprotonation of the α-position, which would initiate a retro-Michael addition, opening the THP core. The thermodynamically favored product would then be formed upon cyclization *via* an oxa-Michael addition.

Scheme 2.3. Base-Mediated Epimerization of *trans*-Tetrahydropyranone

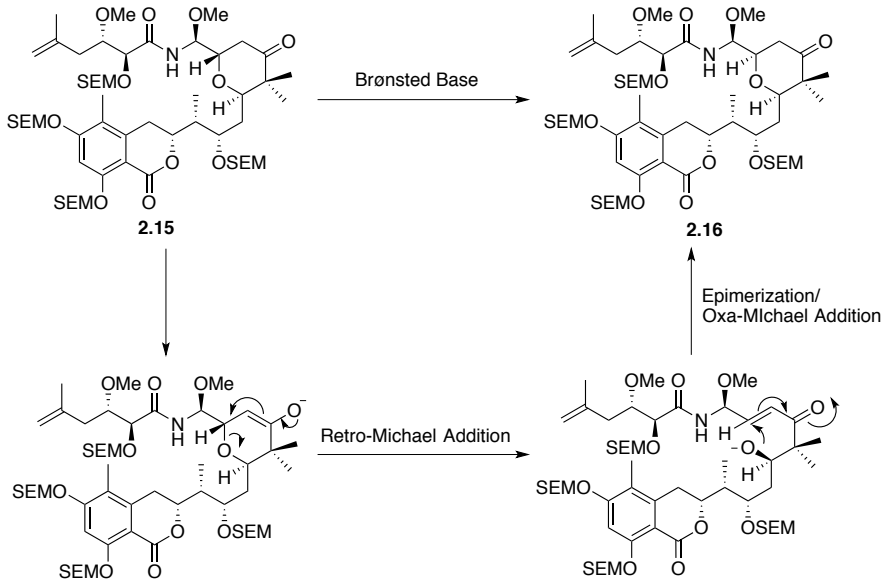

Treatment of **2.15** with acid would also result in undesired degradation products due to the sensitivity of the *N,O*-aminal moiety (Scheme 2.4).[17] For example, upon exposure to a Brønsted or Lewis acid, ionization of methanol could result in acyliminium

ion **2.17**. Acyliminium ion **2.17** could then be trapped by a nucleophile such as water to furnish the hydroxy-aminal **2.18**. With these two synthetic challenges in mind, we were prudent in our selection of a suitable protecting group strategy that would lead to the successful construction of (–)-irciniastatin B (**2.2**). To this end, we selected SEM as the optimal alcohol protecting group because of its robust nature and its successful removal with the mildly basic fluoride reagent, TAS-F,[18,19] as employed in our earlier synthesis of (+)-irciniastatin A (**2.1**).[3]

Scheme 2.4. Acid Hydrolysis of *N,O*-Aminal

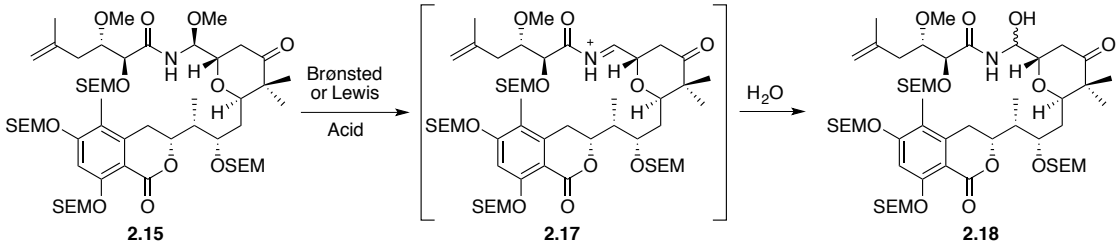

2.3 Synthesis of Acid Side Chain (–)-2.3

Synthesis of the requisite acid side chain began *via* an asymmetric Brown allylation between 2-methyl-propene and commercially available (+)-isopropylidene glyceraldehyde (+)-**2.19** (Scheme 2.5).[9] Alcohol **2.20** was then treated with methyl iodide and sodium hydride to furnish methyl ether (+)-**2.21** in 41% yield over the two steps with excellent stereochemical control (*dr* > 20:1). Removal of the acetonide was next achieved by treatment of (+)-**2.21** with aqueous hydrochloric acid. The primary alcohol was in turn protected chemoselectively as pivalate ester (+)-**2.22**, followed by protection of the secondary alcohol as SEM ether (–)-**2.23**. Reduction with DIBAL-H provided primary alcohol (+)-**2.24**, which was then oxidized *via* a two-step Parikh-Doering[20]/Pinnick[21] oxidation sequence to provide the desired acid side chain (–)-**2.3**.

Scheme 2.5. Synthesis of Acid Side Chain (–)-**2.3**

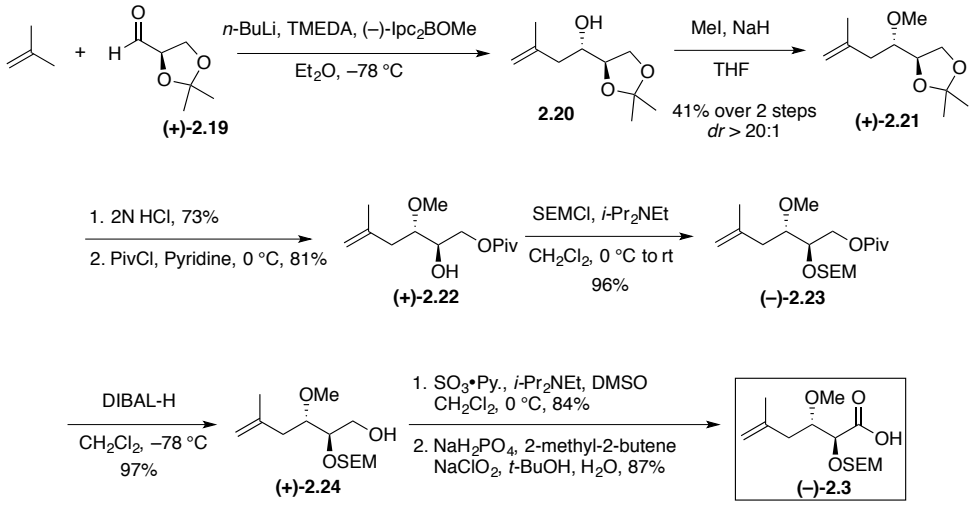

2.4 Synthesis of Aryl Aldehyde 2.5

The requisite aryl aldehyde **2.5** was constructed *via* a Diels-Alder cycloaddition between 1,3-bis(trimethylsiloxy)-1,3-diene **2.7** (constructed in 3 steps),[6] and dimethyl-1,3-allene-dicarboxylate **2.8** (constructed in 2 steps)[7] (Scheme 2.6). Their union was followed by a fluoride-mediated aromatization to furnish known homophthalate **2.25**[22] in good yield (42%–77%). Bis-phenol **2.25** was next protected as bis-SEM ether **2.26** followed by chemoselective reduction to furnish aryl aldehyde **2.5**.

Scheme 2.6. Synthesis of Aryl Aldehyde **2.5**

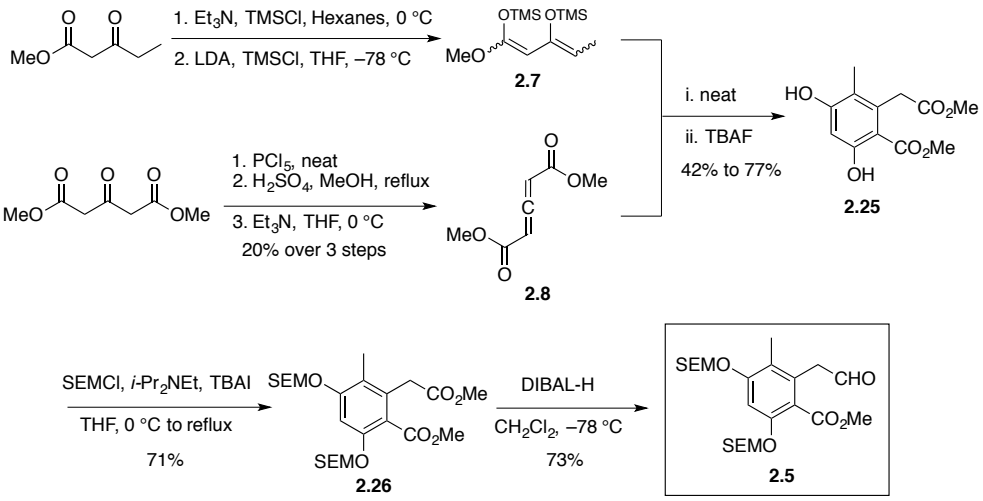

2.5 Synthesis of *trans*-Tetrahydropyran (+)-2.6

Figure 2.2. *trans*-Tetrahydropyran (+)-**2.6**

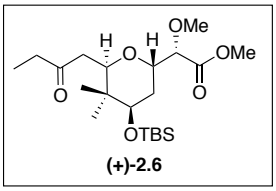

2.5.1 Synthesis of Bis-TBS Ether (+)-2.31

We began the synthesis of *trans*-tetrahydropyran (+)-**2.6** *via* monoprotection of commercially available 2,2-dimethyl-1,3-propanediol **2.27** (Scheme 2.7), followed by oxidation of the second hydroxyl group *via* the Parikh-Doering[20] protocol to provide aldehyde **2.10**. Treatment of aldehyde **2.10** and ketene acetal **2.11**[8] employing the chiral oxazaborolidinone derived from L-tryptophan, led to a vinylogous Mukaiyama aldol reaction,[8] thereby installing the first stereocenter to furnish (+)-**2.29** as a single enantiomer. Mosher's ester analysis demonstrated that the desired *(R)*-isomer was obtained.[23,24] Alcohol (+)-**2.29** was then protected as the TBS ether, followed by reduction of the methyl ester with DIBAL-H to furnish the corresponding allylic alcohol.

A second reagent controlled transformation, asymmetric epoxidation *via* the Sharpless[25] protocol, next provided the desired β-epoxide (+)-**2.30** with 10:1 diastereoselectivity, which in turn was converted directly to the corresponding acid *via* a one-pot TEMPO[26] oxidation; subsequent methylation provided methyl ester (+)-**2.31**.

Scheme 2.7. Synthesis of Bis-TBS Ether (+)-**2.31**

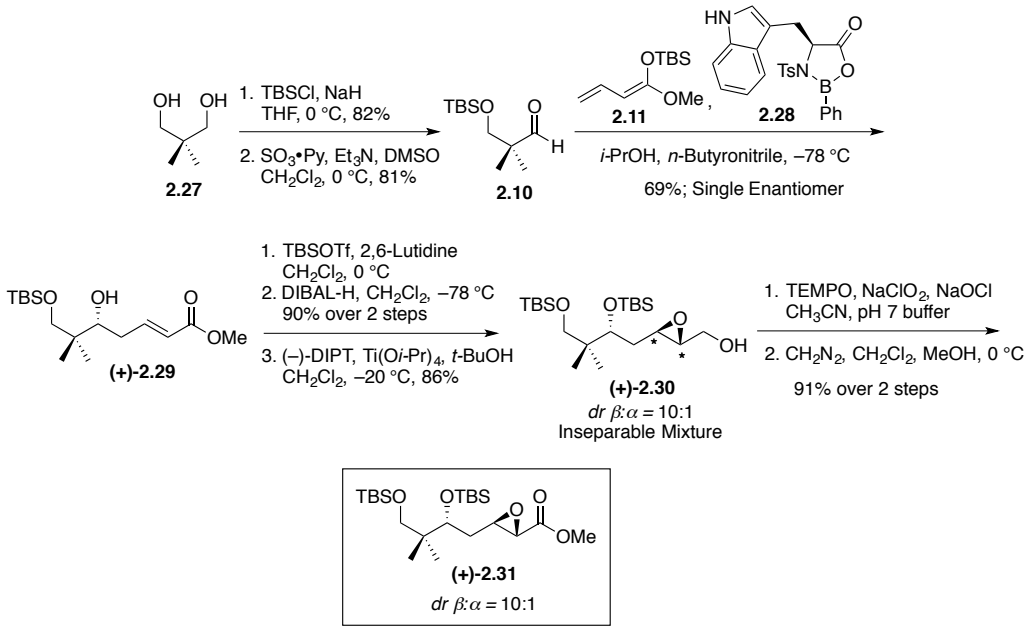

2.5.2 Chemoselective Deprotection of Bis-TBS Ether (+)-2.31

Chemoselective deprotection of the primary TBS ether was achieved by treatment of (+)-**2.31** with hydrogen fluoride, buffered with pyridine (Scheme 2.8). Unfortunately, the acidic medium activates the epoxide to nucleophilic attack, leading to the formation of undesired pyran **2.33**. Separation of the desired primary alcohol (+)-**2.32** and pyran **2.33** could be achieved by column chromatography. However, when the reaction was conducted on large scale (> 5 g), the purification *via* silica gel flash column chromatography became a challenge due the acid sensitivity of (+)-**2.32**. In order to isolate the desired product without the undesired conversion of (+)-**2.32** to **2.33** during

the purification step, the crude mixture, after the deprotection step, was carried without further purification through the Parikh-Doering[20] oxidation. At this stage, aldehyde (+)-**2.34** could be isolated from undesired pyran products *via* column chromatography without visible degradation.

Scheme 2.8. Chemoselective Deprotection of Primary TBS Ether (+)-**2.31**

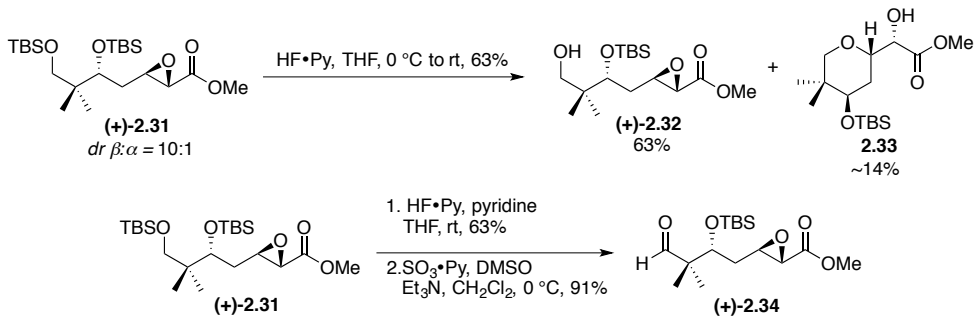

2.5.3 One-Pot Paterson Aldol/Reduction Sequence: Completion of *trans*-Tetrahydropyran (+)-2.6

The final stereocenter required for the tetrahydropyran core was introduced *via* Paterson aldol union[27,28] with aldehyde (+)-**2.34** and 2-butanone, employing (−)-B-chlorodiisopinocampheylborane (DIP-Cl) as the chiral Lewis acid. The desired β-hydroxyketone **2.9** was obtained in 38% yield as a 6:1 (β:α) diastereomeric mixture (Scheme 2.9). The stereochemical outcome for the methyl ketone aldol reaction can be understood by a favorable boat transition state. This conformation minimizes the unfavorable steric interactions between one of the isopinocampheyl (Ipc) ligands and the ethyl substituent. On the other hand, the opposite stereochemical outcome would arise with the ethyl ketone aldol case, where a chair conformation is favored in order to

minimize the steric interactions between the Ipc ligand and the methyl substituent of the boron enolate.

Scheme 2.9. Stereochemical Rationale of Paterson Aldol Reactions

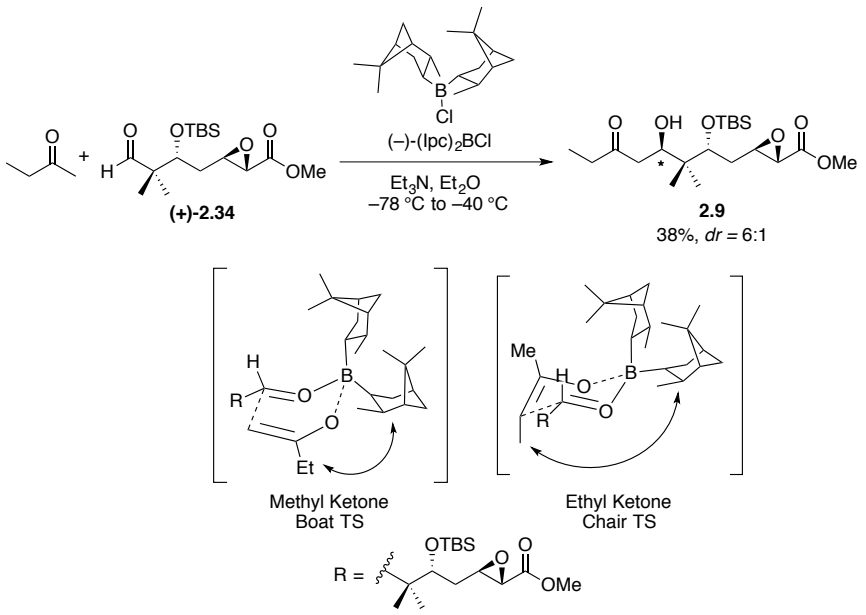

The lower than expected yield realized on larger scale (38%, 500 mg) was explained by the formation of dioxaborinane **2.35** (Table 2.1). This unexpected side product was formed after completion of the aldol union. During the oxidative quench step, the boronate ester aldol adduct was not completely oxidized to aldol product **2.9**, instead reduction of the aldol adduct leads to dioxaborinane **2.35**. We had hypothesized that the source of hydride came from one of the Ipc ligands. In order to optimize the yield of **2.9**, conditions for the oxidative quench step were screened (Table 2.1). We discovered that temperatures greater than –40 °C triggered the formation of **2.35** (Table 2.1, entries 1 and 2). Therefore, upon completion of the aldol union, cryogenic temperatures (–78 °C to –65 °C) with *m*-CPBA employed as the oxidant instead of hydrogen peroxide resulted in the sole formation of the desired aldol product **2.9** (Table 2.1, entry 3), inhibiting the

undesired reduction pathway. Unfortunately, the product of the aldol union was obtained with no diastereoselectivity (1:1). The unexpected absence of facial bias was rationalized by our hypothesis that the aldol union was actually not stereoselective. However, in order to obtain a 6:1 *dr* (Table 2.1, entry 1), reduction of the boronate ester aldol adduct to dioxaborinane **2.35** must be stereospecific. Similar to a kinetic resolution, only the undesired α-isomer of the boronate aldol adduct was reduced to dioxaborninane **2.35**, while the desired β-isomer was hydrolyzed to aldol product **2.9**, resulting in the enhanced diastereoselectivity of 6:1.

Table 2.1. Optimization of Oxidative Quench Conditions

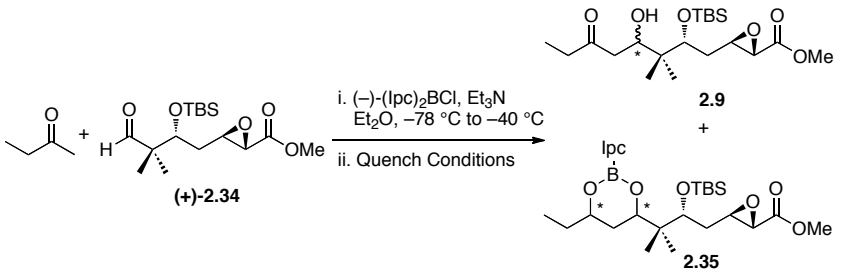

Entry	Quench Conditions	Yield **2.9**	*dr* **2.9** = β:α	Yield **2.35**
1	H_2O_2: MeOH: pH 7 buffer, 1:1:1, 0 °C	38%	6:1	46%
2	H_2O_2: MeOH: pH 7 buffer, 1:1:1, –40 °C to 0 °C	58%	2:1	27%
3	MeOH: pH 7 buffer, 2:1, 6 eq. *m*-CPBA, –78 °C to –65 °C	75%	1:1	0%

Evidence for the proposed mechanism of the above reduction began with formation of boronate aldol adduct **2.36** (Scheme 2.10). Under standard oxidative conditions, the expected aldol product **2.9** would be formed. However, in this case, when the reaction was warmed to temperatures greater than –40 °C, the reduction pathway proceeded. The hydride was delivered from one of the Ipc ligands *via* a 6-membered ring transition state, releasing one equivalent of α-pinene and **2.35**. This mechanistic pathway

was recently confirmed by Menche and coworkers in their synthesis of 1,3-diols *via* Ipc-mediated aldol/reduction sequence.[29] All attempts to remove the boronate ester under oxidative conditions failed to provide the desired diol. Only acid treatment provided tetrahydropyran (–)-**2.37** as a single diastereomer. Isolation of a single diastereomer at this stage confirms that the reduction pathway proceeds with stereospecificity and excellent diastereoselectivity.

Scheme 2.10. Mechanistic Rationale for Reduction Product **2.35**

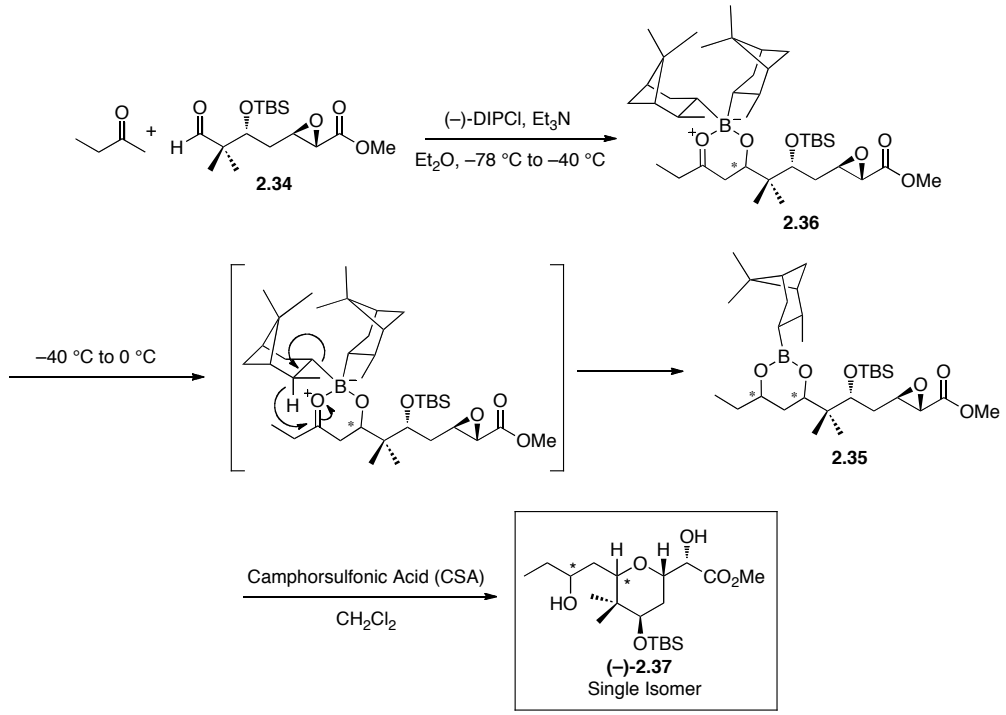

In order to obtain a higher diastereomeric ratio in the formation of **2.9** (6:1), the reduction pathway was induced after completion of the aldol reaction. With **2.9** in hand, we examined the acid-promoted cyclization to generate the tetrahydropyran core. Baldwin rules[30] suggested that both the desired 6-*exo*-tet and undesired 7-*endo*-tet cyclization pathways could operate. However, the six-membered ring transition state, in conjunction with the electron-withdrawing nature of the ester, destabilizing the partial

cationic character at the α-carbon under Lewis- or Brønsted-acidic conditions, suggested that the tetrahydropyran would predominate. Indeed, treatment with 20 mol % of camphorsulfonic acid (CSA) in methylene chloride achieved the desired 6-*exo*-tet cyclization, furnishing (+)-**2.38** and (–)-**2.39** with no trace of seven-membered ring congeners (Scheme 2.11). Fortunately, the *trans*- and *cis*-diastereomers could be readily separated by column chromatography to yield 2,6-*trans*-tetrahydropyran (+)-**2.38** in 33% yield for the 2 steps. Methylation of the secondary hydroxyl group was then achieved (84% yield) by treatment with Me_3•OBF_4 and proton sponge [1,8-bis(dimethylamino)naphthalene] to complete the second-generation synthesis of the 2,6-*trans*-tetrahydropyran core (+)-**2.6**.

Scheme 2.11. Completion of *trans*-Tetrahydropyran (+)-**2.6**

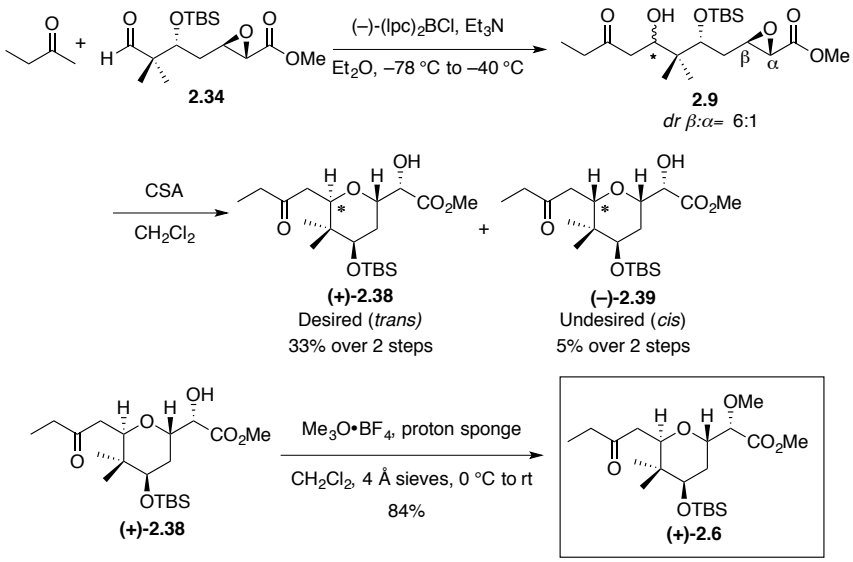

2.6 Fragment Unions

Having constructed the three fragments for the proposed synthesis of (–)-irciniastatin B (**2.2**), we set out to achieve their union employing the synthetic sequence

employed in our earlier (+)-irciniastatin A (**2.1**) synthesis. Unfortunately, we had discovered that the phenolic SEM ethers utilized as our protecting group strategy proved to be too labile in the synthesis of SEM ether **2.4**. This subchapter will outline the problematic steps in this synthetic sequence while subchapters 2.7 and 2.8 will detail the application of a revised protecting group strategy employing 3,4-dimethoxybenzyl ethers toward the completion of (–)-irciniastatin B (**2.2**).

2.6.1 Aldol Union and Elaboration Towards Acid (+)-2.43

The union of tetrahydropyran (+)-**2.6** with aryl aldehyde **2.5** (Scheme 2.12) was achieved *via* a substrate-controlled aldol reaction. Generation of the *Z*-boron enolate of (+)-**2.6**, achieved by treatment of (+)-**2.6** with dichlorophenylborane,[31] was followed by addition of aldehyde **2.5** to furnish (+)-**2.40**, the desired *syn*-aldol product, in 68% yield. The stereochemical outcome was dictated by 1,4-substrate stereoinduction.[32] Subsequent chelation-controlled reduction,[33] resulted in a mixture of the desired *syn* diol **2.41** and the corresponding lactone **2.42** (ca. 4:1) in 75% overall yield. The mixture was treated with LiOH, followed by addition of acetic acid (5% aqueous solution), to mediate lactonization, providing dihydroisocoumarin (+)-**2.43** in 72% yield for the two steps. It is important to note, however, that the acetic acid required for lactonization often results in the unforeseen hydrolysis of one of the phenolic SEM ethers. Therefore, the pH of the reaction during the quench stage must be carefully monitored in order to obtain optimal yields.

Scheme 2.12. Fragment Union and Elaboration to Acid (+)-**2.43**

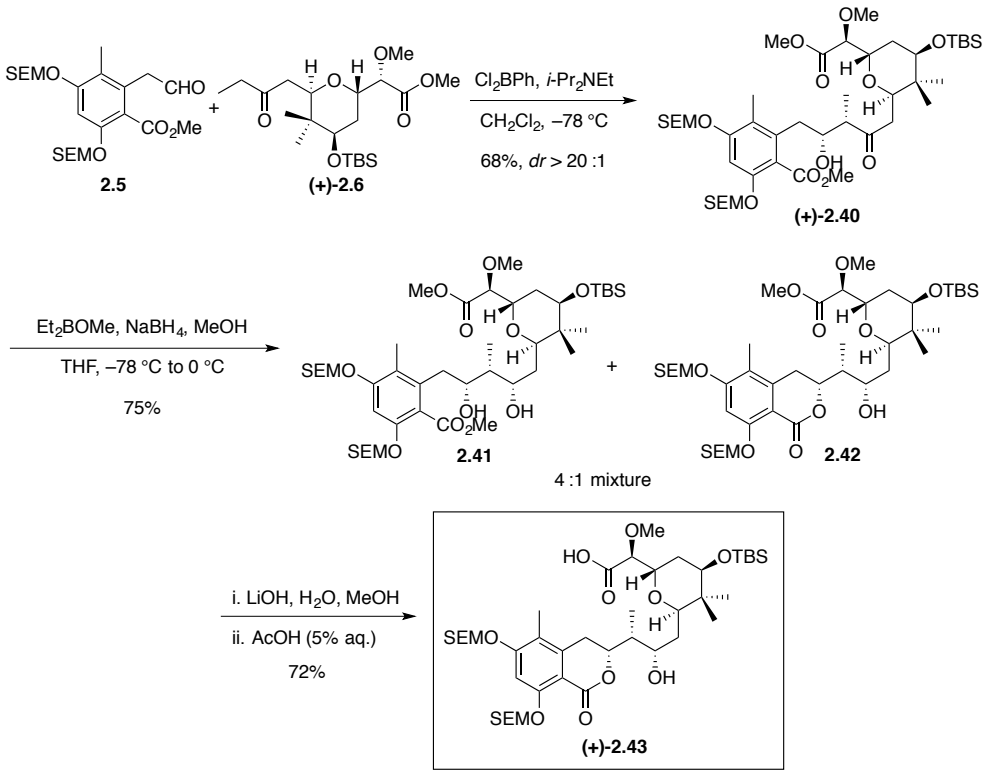

2.6.2 Curtius Rearrangement and Protecting Group Challenges

At this juncture we called upon a Curtius rearrangement, the strategy that was previously exploited in our synthesis of (+)-zampanolide[5] and (+)-irciniastatin A (**2.1**)[3] to install the *N,O*-aminal (Scheme 2.13). In this case, acid (+)-**2.43** was converted to the corresponding acyl azide, followed by thermal rearrangement in toluene (ca. 80 °C) to provide the isocyanate, which was intercepted by the addition of 2-trimethylsilylethanol to furnish the desired *N,O*-aminal (+)-**2.12** (61%), with complete retention of configuration at the methyl ether carbon (determined by ^{1}H NMR).

Scheme 2.13. Curtius Rearrangement and Protecting Group Challenges

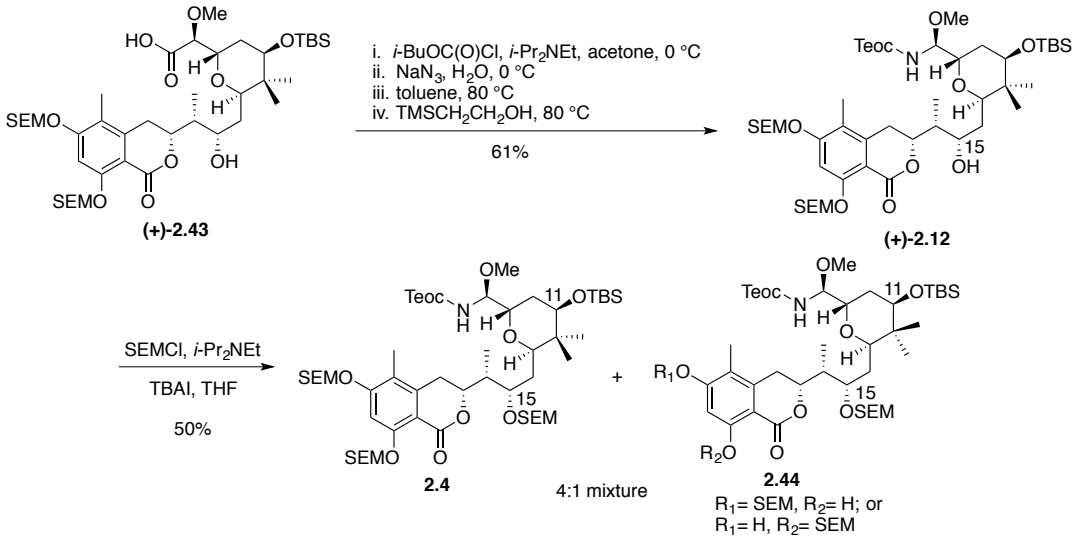

As outlined in subchapter 2.1.2, we envisioned the remaining secondary alcohol in *N,O*-aminal (+)-**2.12** to be protected as a SEM ether, instead of TBS ether employed in our earlier (+)-irciniastatin A (**2.1**) synthesis.[3] In order to construct (–)-irciniastatin B (**2.2**), installation of a SEM ether at C(15) was envisioned to permit orthogonal deprotection of the sterically hindered secondary C(11) TBS ether at a later step in the synthesis, which would permit installation of the requisite ketone. To our surprise, protection of (+)-**2.12** not only proved to be extremely sluggish (50% yield), but also resulted in the heightened sensitivity of the phenolic SEM ethers (Scheme 2.13). Standard workup conditions and silica gel column chromatography (buffered with Et_3N) resulted in a mixture of the desired SEM ether **2.4** and monophenol **2.44**. For unexplained reasons, the introduction of a third SEM ether resulted in the increased sensitivity of the phenolic SEM ethers to acid-hydrolysis. Attempts at reprotection of the phenolic hydroxyls proved ineffective, even at elevated temperatures. Since the phenolic SEM

ethers were easily hydrolyzed at multiple points in the late-stage synthesis, a more robust protecting group strategy was required.

2.7 Revising the Protecting Group Strategy

2.7.1 Model Study-4-Methoxybenzyl Ether

4-Methoxybenzyl ether (PMB) was initially selected as a potential replacement for the phenolic SEM ethers because of the superior stability under acidic conditions and ease of removal under oxidative conditions (DDQ). A model study was therefore designed in order both to examine the feasibility of removing the PMB ethers in late-stage intermediates and to assess the stability of the highly sensitive *N,O*-aminal moiety (Scheme 2.14). To this end, a Hirschmann mixture experiment was carried out.[34] Mono-PMB ether **2.45** was synthesized and *mixed with a late-stage intermediate **2.46***, which had a SEM ether hydrolyzed from earlier manipulations. The mixture was treated with DDQ. To our surprise, exposure to DDQ for three days at elevated temperatures (40 °C) resulted in no loss of the protecting group. Pleasingly, however, *N,O*-aminal **2.46** proved to be stable under standard PMB removal conditions.

Scheme 2.14. Model Study-4-Methoxybenzyl Ether

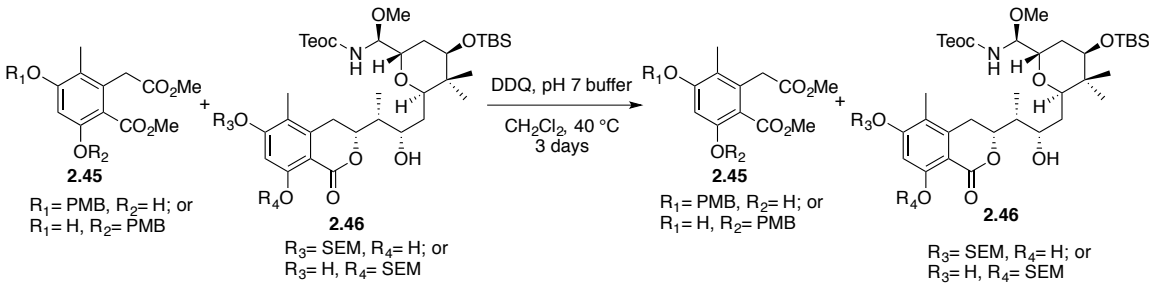

2.7.2 Model Studies-3,4-Dimethoxybenzyl Ether (DMB)

From our model study, we learned the *N,O*-aminal moiety was stable when treated with DDQ for prolonged reaction times. Therefore, 3,4-dimethoxybenzyl ether (DMB) was next examined because this group was known to be much more sensitive to DDQ compared to PMB (Scheme 2.15). Bis-DMB ether **2.47** was constructed by protection of bis-phenol **2.25** with DMB-Br and K_2CO_3 in acetone. Bis-DMB ether **2.47** was then treated with the same standard deprotection conditions employed in the previous model study to achieve cleanly the hydrolysis of both protecting groups, providing bis-phenol **2.25.** Bis-DMB ether **2.47** also proved to be stable under the mild acidic conditions employed in the synthetic sequence.

Scheme 2.15. Model Study-3,4-Dimethoxybenzyl Ether

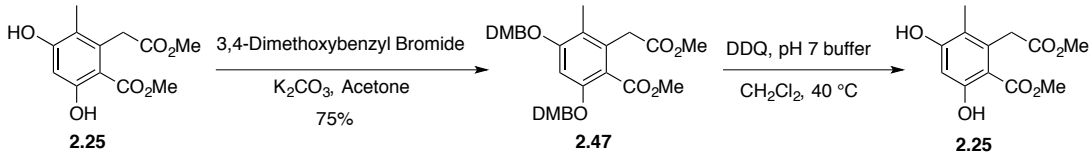

2.8 Fragment Union Employing the Revised Protecting Group Strategy

The synthesis toward (–)-irciniastatin B (**2.2**) continued with the newly designed DMB ether protecting group strategy. Reduction of the ester **2.47** with DIBAL-H furnished the aryl aldehyde **2.48** (Scheme 2.16). From here, the synthetic route continued in similar fashion to the sequence leading to (+)-irciniastatin A (**2.1**) as presented in subchapter 2.6. Aldol union[31] between aldehyde **2.48** and ketone (+)-**2.6** pleasingly furnished β-hydroxyketone (+)-**2.49** in 70% yield, again with excellent diastereoselectivity (>20:1).[32] As before, a chelation-controlled reduction[33] protocol

furnished a mixture of the desired *syn* diol **2.50** and lactone **2.51** (ca. 8:1), which upon treatment with LiOH followed by an acid work-up (50% AcOH) led to the desired acid (+)-**2.52** in 69% yield for the two steps. This time, the DMB ethers proved to be stable under the acetic acid quench after saponification; no hydrolysis of the protecting groups was observed! With acid (+)-**2.52** in hand, the corresponding acyl azide was generated and subjected to Curtius rearrangement conditions;[5] the resulting isocyanate intermediate was treated with 2-trimethylsilylethanol to furnish the Teoc-protected *N,O*-aminal in 67% yield, again with complete retention of stereogenicity at C(8) (determined by NMR). The remaining secondary alcohol was then protected as the SEM ether (+)-**2.53** in 82% yield. Importantly, the workup and purification steps proceeded without the formation of undesired side products.

Scheme 2.16. New Protecting Group Strategy: Elaboration to *N,O*-Aminal (+)-**2.53**

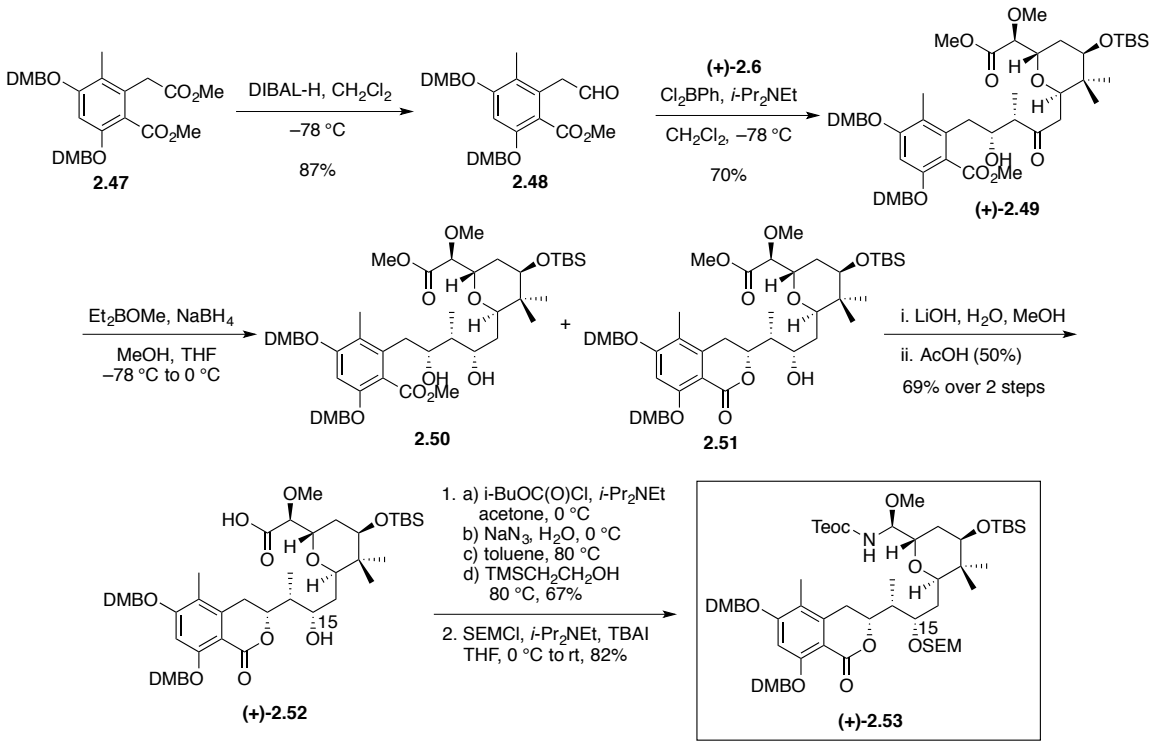

Employing the revised protecting group strategy successfully provided SEM ether (+)-**2.53** in 26.5% yield over 5 steps (>300 mg synthesized), which represents a 3-fold improvement over our original protecting group strategy, to provide (+)-**2.4** in 8.8% yield. The problem of facile hydrolysis of the protecting groups was thus overcome by utilizing robust 3,4-dimethoxybenzyl ethers.

2.9 Amide Coupling to the Complete Carbon Skeleton of (–)-Irciniastatin B

Achieving the requisite amide union to provide (+)-**2.56** proved challenging (Table 2.2). The conditions employed in our earlier (+)-irciniastatin A (**2.1**) synthesis,[3] (Table 2.2, entry 1) involving LiHMDS as the base with mixed anhydride **2.54**, resulted in low yields (ca. 15%). Warming the coupling reaction to 0 °C failed to enhance the efficiency of the transformation (Table 2.2, entry 2). Switching to a stronger base (*n*-BuLi, Table 2.2, entry 3) resulted in a complex mixture of products with no desired product observed. We had predicted that the more electrophilic acid chloride **2.55**, would be sufficiently reactive to undergo amide formation with the sterically hindered carbamate (+)-**2.53**. Unfortunately, employing LiHMDS as the base and acid chloride **2.55** failed to react (Table 2.2, entry 4). Fortunately, conditions employed by Crimmins and coworkers,[11] in their synthesis of (+)-irciniastatin A (**1.1**), namely the use of *i*-PrMgCl as the base and acid chloride **2.55**, provided the desired amide (+)-**2.56** in 72% yield (Table 2.2, entry 5). Interestingly, the previous (+)-irciniastatin A (**1.1**) syntheses also required significant screening and optimization of this very challenging coupling, even though the substrates possessed almost identical structures, except for the different protecting groups.[3,11,13] Therefore, slight differences in molecular structure, even in

regions distal to the reactive site, seem to play a significant role in the successful construction of this challenging amide bond.

Table 2.2. Amide Coupling Conditions

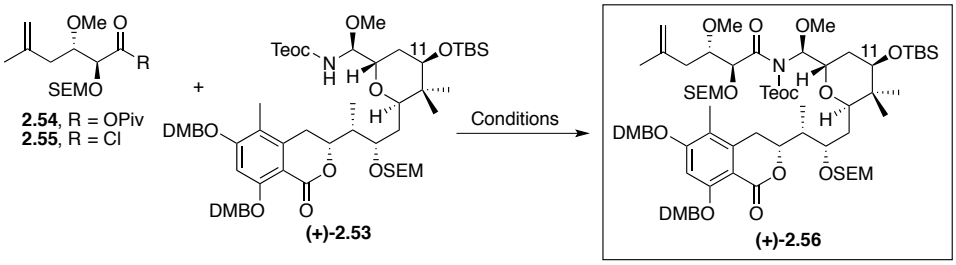

Entry	Conditions	Yield
1	**2.54**, LiHMDS, THF, –78 °C to –60 °C	15%
2	**2.54**, LiHMDS, THF, –78 °C to 0 °C	7%
3	**2.54**, *n*-BuLi, THF, –78 °C	0% (Decomp.)
4	**2.55**, LiHMDS, THF, –78 °C to –40 °C	NR
5	**2.55,** *i*-PrMgCl, THF, –78 °C	72%

2.10 Final Elaboration to (–)-Irciniastatin B (2.2)

2.10.1 Selective Deprotection and Oxidation

Having arrived at the full carbon skeleton of (–)-irciniastatin B (**2.2**), we set out to effect the selective deprotection of the hindered neopentyl secondary C(11) TBS ether (Scheme 2.17). The TBS ether (+)-**2.56** was first treated with TBAF at room temperature, which resulted in hydrolysis of the Teoc carbamate. Subsequent warming the reaction mixture to 50 °C then led to selective removal of the C(11) TBS group in an overall yield of 79%. Oxidation with Dess-Martin periodinane[35] provided ketone (–)-**2.57** in 87% yield.

Scheme 2.17. Late-Stage Selective Deprotection/Oxidation Sequence

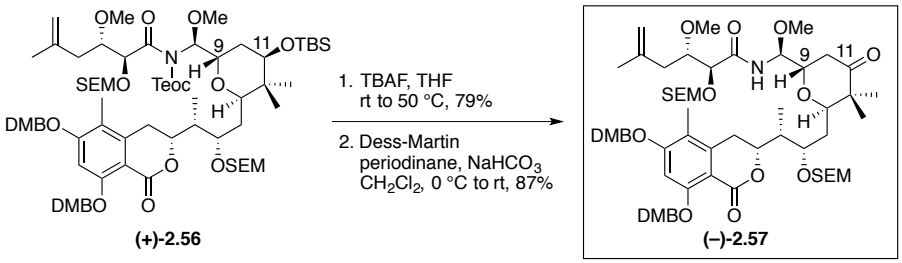

2.10.2 Global Deprotection of (–)-2.57: Completion of the First Total Synthesis of (–)-Irciniastatin B (2.2)

We had predicted tetrahydropyranone (–)-**2.57** to be very sensitive to both basic and acidic conditions; therefore prudent selection of mild reagents would be required. Global deprotection was first attempted with the mild Lewis acid $MgBr_2$ to remove both pairs of protecting groups in a single operation (Scheme 2.18).[36] One DMB ether and both SEM ethers proceeded to undergo hydrolysis to furnish mono-DMB ether **2.58**. The chemoselectivity of DMB hydrolysis was not determined; however, DMB ethers *ortho* to lactones should be more labile due to neighboring group effect. Since treatment with a Lewis acid did not provide the desired natural product, a two-stage deprotection sequence would be required. Unfortunately, attempts to remove the final DMB ether with DDQ resulted in decomposition. On the other hand, when (–)-**2.57** was treated with DDQ first, bis-phenol **2.59** was isolated cleanly. However, hydrolysis of the SEM ethers with mild basic fluoride reagents, TAS-F[18,19] or TBAF resulted in a complex mixture. This undesired result highlights the heightened base sensitivity of tetrahydropyranone (–)-**2.57**, compared to the late-stage intermediates in previous (+)-irciniastatin A (**2.1**) syntheses. Both TAS-F and TBAF had been utilized successfully in the construction of (+)-irciniastatin A (**2.1**). [3,10-14]

Scheme 2.18. Attempted Global Deprotection of (–)-**2.57**

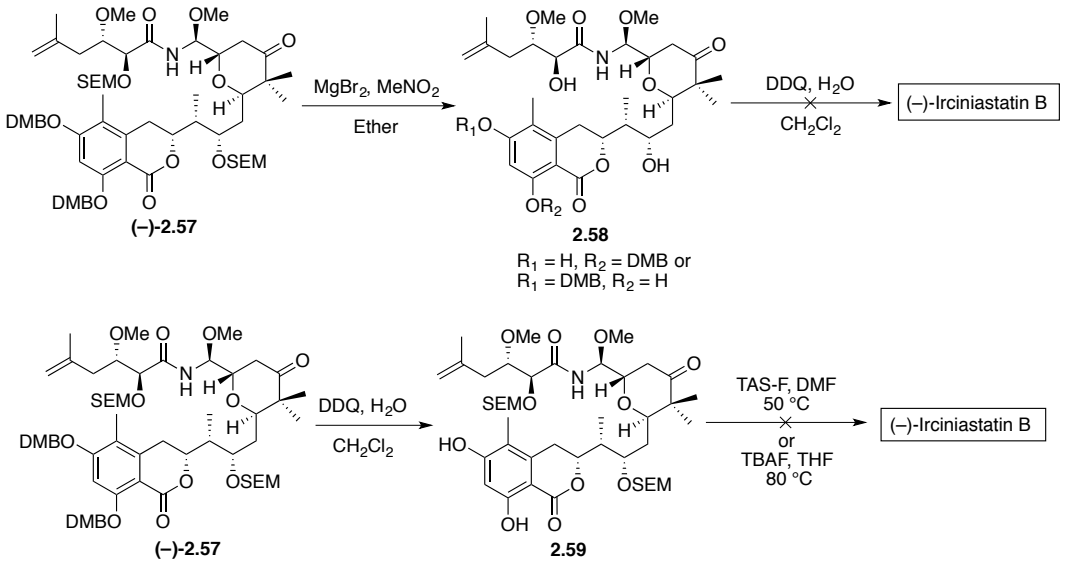

Ultimately, we discovered that treatment of ketone (–)-**2.57** with DDQ followed by a premixed solution of $MgBr_2$, *n*-butanethiol, and nitromethane[37] in Et_2O furnished (–)-irciniastatin B (**2.2**) in 78% yield over two steps (Scheme 2.19). Pleasingly, the spectral data of totally synthetic (–)-irciniastatin B (**2.2**) was identical in all respects with the spectral data kindly provided to us by Pettit and coworkers.[15]

Scheme 2.19. Global Deprotection of (–)-**2.57** and Completion of (–)-Irciniastatin B (**2.2**)

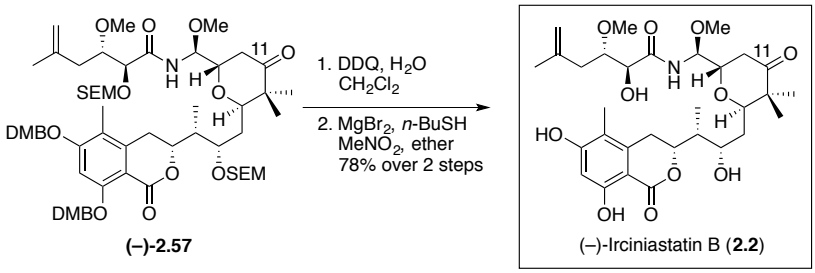

2.11 Structural Confirmation of (–)-Irciniastatin B (2.2) by Chemical Conversion to (+)-Irciniastatin A (2.1) and *epi*-C(11)-Irciniastatin A (2.60)

To verify the structural relationship of (–)-irciniastatin B (**2.2**) with (+)-irciniastatin A (**2.1**), we carried out a chemical interconversion of **2.2** to **2.1** (Scheme 2.20). To this end, (–)-irciniastatin B (**2.2**) was treated with $NaBH_4$, which resulted in a mixture (1:1) of (+)-irciniastatin A **2.1** and *epi*-C(11)-irciniastatin A (**2.60**). The two diastereomers were separated *via* preparative TLC, and the spectral data of the faster moving diastereomer (TLC) proved to be identical in all respects with the spectral data of (+)-irciniastatin A (i.e., ^{1}H, ^{13}C NMR and HRMS), thereby confirming the structural relationship of (+)-irciniastatin A (**2.1**) and (–)-irciniastatin B (**2.2**).

Scheme 2.20. Structural Confirmation of (–)-Irciniastatin B (**2.1**) by Chemical Conversion to (+)-Irciniastatin A (**2.1**)

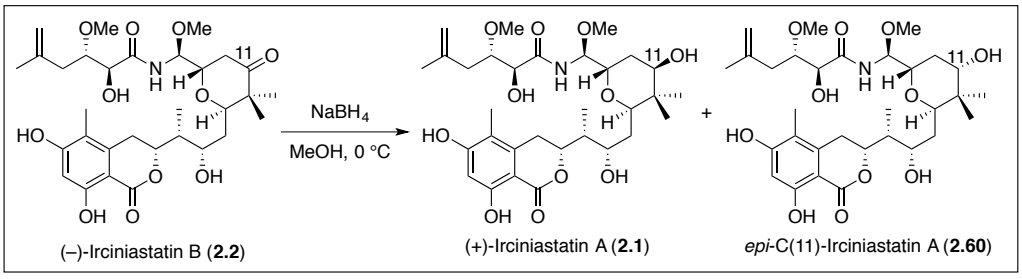

2.12 Summary

In summary, the first total synthesis of (–)-irciniastatin B (**2.2**) has been achieved with a longest linear sequence of 23 steps. The central features of this synthetic venture entailed a modified protecting group strategy that is amenable to scalable synthesis, and a late stage selective deprotection and oxidation sequence. Importantly, the structural relationship of the two metabolites has been confirmed *via* chemical conversion of (–)-

irciniastatin B (**2.2**) to (+)-irciniastatin A (**2.1**) and the corresponding C(11) epimer (**2.60**). Importantly, the successful synthesis leading to (–)-irciniastatin B (**2.2**) now holds the promise for elaboration of C(11)-irciniastatin analogues. The design and synthesis of these analogues will be outlined in Chapter 3.

2.12 References

(1) An, C.; Hoye, A. T.; Smith, A. B. *Org. Lett.* **2012**, *14*, 4350-4353.

(2) An, C.; Jurica, J. A.; Walsh, S. P.; Hoye, A. T.; Smith, A. B. *J. Org. Chem.* **2013**, *78*, 4278-4296.

(3) Smith, A. B.; Jurica, J. A.; Walsh, S. P. *Org. Lett.* **2008**, *10*, 5625-5628.

(4) Weinstock, J. *J. Org. Chem.* **1961**, *26*, 3511-3511.

(5) Smith, A. B.; Safonov, I. G.; Corbett, R. M. *J. Am. Chem. Soc.* **2002**, *124*, 11102-11113.

(6) Yamamoto, K.; Suzuki, S.; Tsuji, J. *Chem. Lett.* **1978**, *7*, 649-652.

(7) Byrson, T. A.; Dolak, T. M. *Org. Synth.* **1977**, *57*, 62.

(8) Simsek, S.; Horzella, M.; Kalesse, M. *Org. Lett.* **2007**, *9*, 5637-5639.

(9) Jiang, X.; Garcia-Fortanet, J.; De Brabander, J. K. *J. Am. Chem. Soc.* **2005**, *127*, 11254-11255.

(10) Huang, X.; Shao, N.; Palani, A.; Aslanian, R.; Buevich, A. *Org. Lett.* **2007**, *9*, 2597-2600.

(11) Crimmins, M. T.; Stevens, J. M.; Schaaf, G. M. *Org. Lett.* **2009**, *11*, 3990-3993.

(12) Byeon, S. R.; Park, H.; Kim, H.; Hong, J. *Org. Lett.* **2011**, *13*, 5816-5819.

(13) Watanabe, T.; Imaizumi, T.; Chinen, T.; Nagumo, Y.; Shibuya, M.; Usui, T.; Kanoh, N.; Iwabuchi, Y. *Org. Lett.* **2010**, *12*, 1040-1043.

(14) Wan, S.; Wu, F.; Rech, J. C.; Green, M. E.; Balachandran, R.; Horne, W. S.; Day, B. W.; Floreancig, P. E. *J. Am. Chem. Soc.* **2011**, *133*, 16668-16679.

(15) Pettit, G. R.; Xu, J.-P.; Chapuis, J.-C.; Pettit, R. K.; Tackett, L. P.; Doubek, D. L.; Hooper, J. N. A.; Schmidt, J. M. *J. Med. Chem.* **2004**, *47*, 1149-1152.

(16) Allevi, P.; Anastasia, M.; Ciuffreda, P.; Fiecchi, A.; Scala, A. *J. Chem. Soc., Perkin Trans. 1* **1989**, 1275-1280.

(17) Mori, M.; Uozumi, Y.; Ban, Y. *J. Chem. Soc., Chem. Commun.* **1986**, 841-842.

(18) Noyori, R.; Nishida, I.; Sakata, J.; Nishizawa, M. *J. Am. Chem. Soc.* **1980**, *102*, 1223-1225.

(19) Scheidt, K. A.; Chen, H.; Follows, B. C.; Chemler, S. R.; Coffey, D. S.; Roush, W. R. *J. Org. Chem.* **1998**, *63*, 6436-6437.

(20) Parikh, J. R.; Doering, W. v. E. *J. Am. Chem. Soc.* **1967**, *89*, 5505-5507.

(21) Bal, B. S.; Childers Jr, W. E.; Pinnick, H. W. *Tetrahedron* **1981**, *37*, 2091-2096.

(22) Langer, P.; Kracke, B. *Tetrahedron Lett.* **2000**, *41*, 4545-4547.

(23) Ohtani, I.; Kusumi, T.; Kashman, Y.; Kakisawa, H. *J. Am. Chem. Soc.* **1991**, *113*, 4092-4096.

(24) Hoye, T. R.; Jeffrey, C. S.; Shao, F. *Nat. Protoc.* **2007**, *2*, 2451-2458.

(25) Katsuki, T.; Sharpless, K. B. *J. Am. Chem. Soc.* **1980**, *102*, 5974-5976.

(26) Zhao, M. M.; Li, J.; E, M.; Song, Z. J.; Taschaen, D. M. *Org. Synth.* **2005**, 195.

(27) Paterson, I.; Goodman, J. M. *Tetrahedron Lett.* **1989**, *30*, 997-1000.

(28) Paterson, I.; Goodman, J. M.; Anne Lister, M.; Schumann, R. C.; McClure, C. K.; Norcross, R. D. *Tetrahedron* **1990**, *46*, 4663-4684.

(29) Dieckmann, M.; Menche, D. *Org. Lett.* **2012**, *15*, 228-231.

(30) Baldwin, J. E. *J. Chem. Soc., Chem. Commun.* **1976**, 734-736.

(31) Hamana, H.; Sasakura, K.; Sugasawa, T. *Chem. Lett.* **1984**, *13*, 1729-1732.

(32) Evans, D. A.; Calter, M. A. *Tetrahedron Lett.* **1993**, *34*, 6871-6874.

(33) Chen, K.-M.; Hardtmann, G. E.; Prasad, K.; Repič, O.; Shapiro, M. J. *Tetrahedron Lett.* **1987**, *28*, 155-158.

(34) Private Conversation to Amos B. Smith III from Ralph Hirschmann.

(35) Dess, D. B.; Martin, J. C. *J. Org. Chem.* **1983**, *48*, 4155-4156.

(36) Vakalopoulos, A.; Hoffmann, H. M. R. *Org. Lett.* **2000**, *2*, 1447-1450.

(37) Denmark, S. E.; Kobayashi, T.; Regens, C. S. *Tetrahedron* **2010**, *66*, 4745-4759.

CHAPTER 3 Design and Synthesis of Irciniastatin Analogues

3.1 Synthesis of Irciniastatin Analogues *via* Modification of Late-Stage Alcohol (–)-3.4 and Ketone (–)-3.5

Initial studies revealed that (–)-irciniastatin B (**3.2**) is 10-fold more cytotoxic compared to (+)-irciniastatin A (**3.1**) against pancreas, breast, and central nervous system cancer cell lines (Figure 3.1).[1] Subsequent analogue studies conducted by the Schering-Plough group revealed that C(11)-deoxy-irciniastatin A (**3.3**)[2] is also up to 10-fold more active than (+)-irciniastatin A (**3.1**) against the variety of cancer cell lines tested. Taken together, the C(11) position in the irciniastatins would appear to play a critical role in irciniastatin's biological mode of action.

Figure 3.1. Natural and Unnatural C(11)-Irciniastatin Derivatives

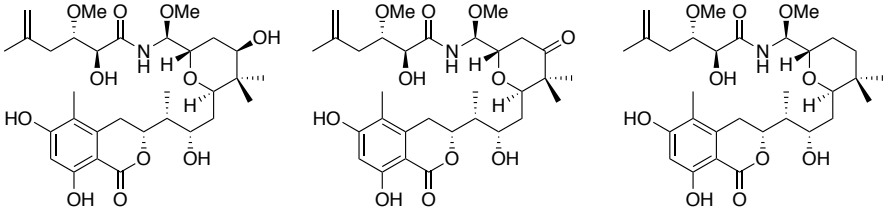

We therefore set out to modify late-stage synthetic intermediates, alcohol (–)-**3.4** and ketone (–)-**3.5**,[3,4] to construct a small series of C(11)-irciniastatin analogues (Scheme 3.1), with the expectation of possibly identifying an even more cytotoxic compound. We hypothesized the introduction of less polar substituents would improve the cytotoxic activity. Important in the synthesis of these analogues was the observed chemosynthetic strategy that led to the total synthesis of (–)-irciniastatin B (**3.2**). However, challenges to accessing C(11)-irciniastatin analogues remain, including limited reactivity of the

sterically hindered alcohol and ketone as well as the highly sensitive moieties present in both (–)-**3.4** and (–)-**3.5**. Therefore, the analogues were carefully designed such that they can be synthesized under mild reaction conditions.

Scheme 3.1. Synthetic Strategy to C(11)-Irciniastatin Analogues

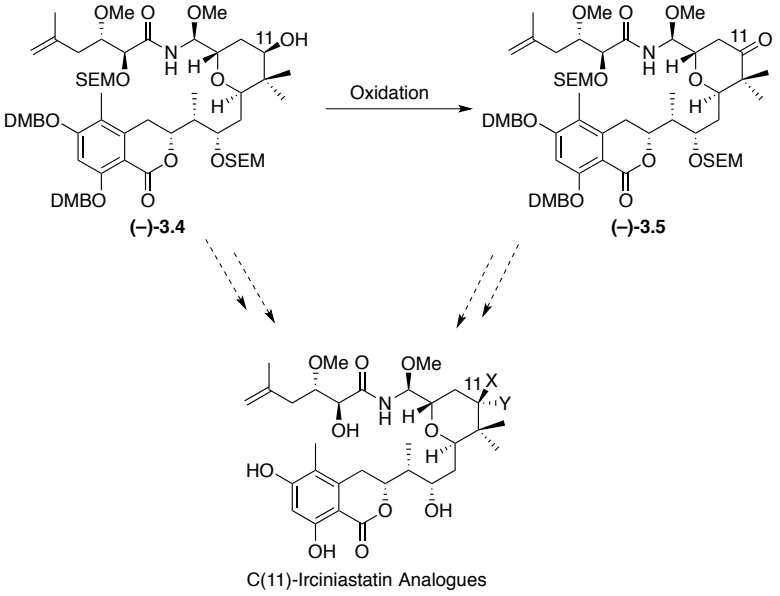

At the outset, our SAR studies focused on lowering the hydrophilicity of the C(11) substituent, and in particular removing the hydrogen-bond donating ability of the C(11) substituent (Schemes 3.2 and 3.3). Alcohol (–)-**3.4** was capped with an acetate moiety in 87% yield. The two-stage global deprotection furnished C(11)-OAc-irciniastatin A (+)-**3.7** in 75% yield over the 2 steps. Benzoyl protection of alcohol (–)-**3.4** successfully provided the corresponding benzoate in 55% yield. Removal of the protecting groups then furnished C(11)-OBz-irciniastatin A (–)-**3.6** in 50% yield over the 2 steps.

A common strategy in medicinal chemistry is the addition of a fluorine substituent to enhance metabolic stability.[5] We therefore proposed the synthesis of *epi*-C(11)-fluoro-irciniastatin A **3.8**. To this end, treatment of alcohol (–)-**3.4** with diethylamino-sulfurtrifluoride (DAST) resulted in the introduction of fluorine with inversion of stereochemistry.[6] Future work includes hydrolysis of the remaining protecting groups to complete construction of analogue **3.8**.

Scheme 3.2. Synthesis of C(11)-Irciniastatin A Analogues from Alcohol (–)-**3.4**

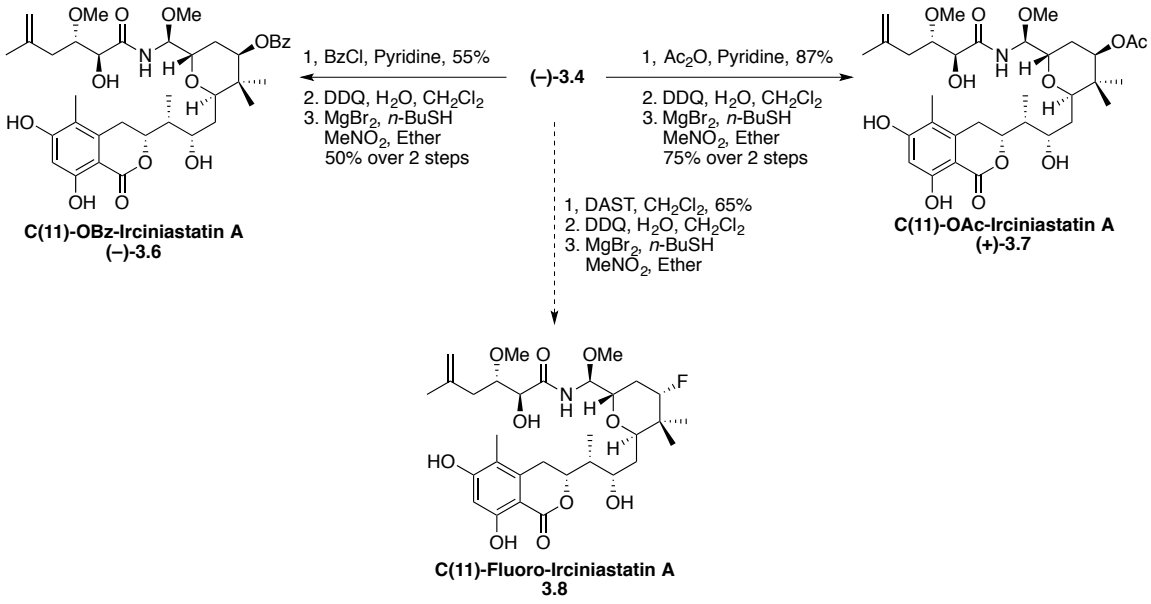

The congener, C(11)-exomethylene-irciniastatin B (+)-**3.9**, was constructed *via* Wittig methenylation[7] of ketone (–)-**3.5**, followed by global deprotection (Scheme 3.3). We envisioned that the exomethylene analogue would be an excellent bioisostere of the ketone since they bear a similar geometry and also further increases the hydrophobicity of the C(11) position, which should result in higher cytotoxicity.

Scheme 3.3. Synthesis of C(11)-Irciniastatin B Analogue from ketone (–)-**3.5**

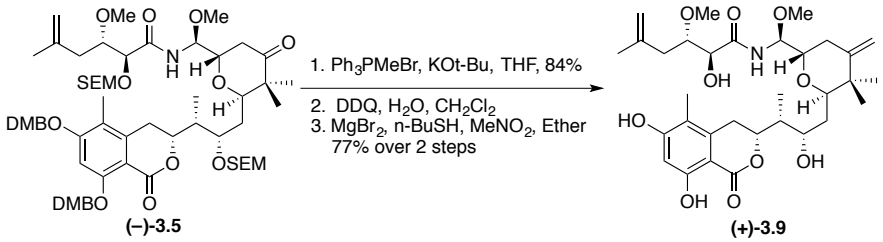

3.2 Progress Toward Disubstituted Irciniastatin Analogues

To simplify the synthetic route to cytotoxic irciniastatin analogues, we proposed the construction of disubstituted pyran analogues **3.10** (Scheme 3.4). Since removal of the C(11) substituent enhances cytotoxicity,[2] we sought to remove the *gem*-dimethyl group along with the C(11) substitution from the tetrahydropyran core. We proposed to target both *trans* and *cis* analogues **3.10**, which would derive from the unions of acid (–)-**3.11**,[4,8] aldehyde **3.12**,[3,4] and disubstituted pyrans **3.13**. Epoxides **3.14** would be utilized as the cyclization precursors to generate the desired pyran intermediates **3.13** *via* a 6-*exo*-tet-cyclization pathway as employed in our syntheses of (+)-irciniastatin A (**3.1**) and (–)-irciniastatin B (**3.2**).[3,4,8]

Scheme 3.4. Retrosynthetic Analysis of Disubstituted Irciniastatin Analogues **3.10**

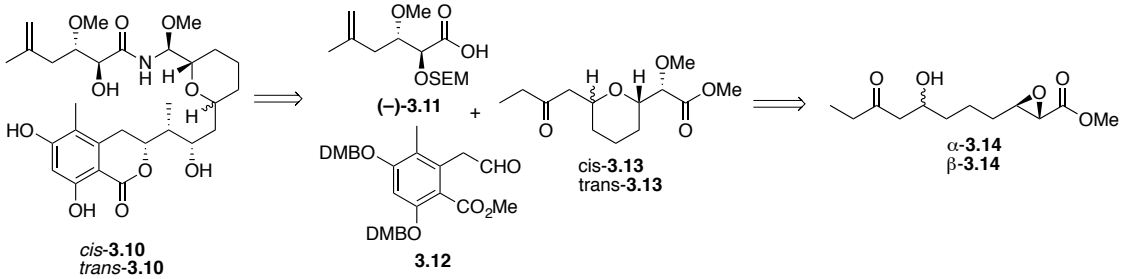

Synthesis of this novel analogue began with asymmetric epoxidation of known allylic alcohol **3.15**,[9] employing the Sharpless protocol.[10] After column chromatography, the resulting epoxy alcohol **3.16** was contaminated with (–)-DIPT. The mixture was then subjected to a three-step sequence to obtain methyl ester (+)-**3.17**: oxidation to the corresponding acid in a two-step sequence,[11,12] followed by methylation. Only a single purification step was required after the methylation step to obtain (+)-**3.17** in 59% yield over the 4 steps. Removal of the primary TBS ether to furnish alcohol (+)-**3.18** occurred without event. Importantly, no pyran byproduct was observed under the acidic conditions employed. The absence of substitution in (+)-**3.18** raised the activation barrier to the cyclization pathway.

Scheme 3.5. Synthesis of Alcohol (+)-**3.18**

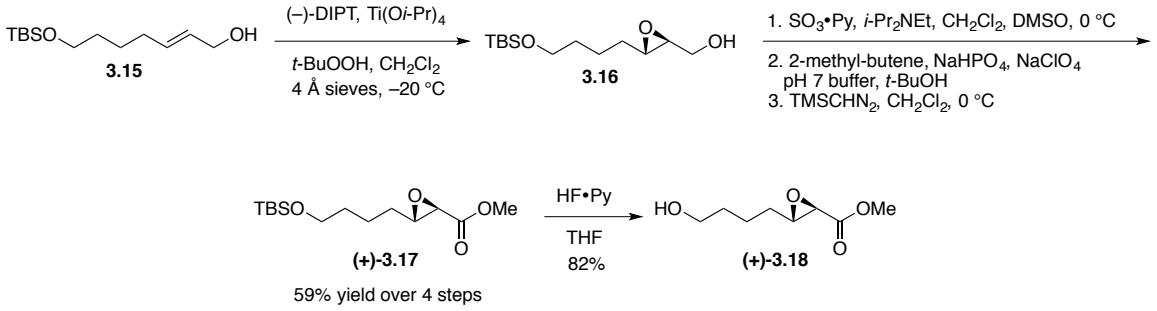

Future plans to complete the synthesis of disubstituted pyran analogues **3.10** are outlined in Scheme 3.6. Primary alcohol (+)-**3.18** will be oxidized to aldehyde **3.19**. Aldol union with 2-butanone, followed by acid-mediated cyclization will then furnish a mixture of *trans*-**3.20** and *cis*-**3.20**. Following their separation, the two diastereomers will be individually methylated employing $Me_3O•BF_4$ and proton sponge to provide *trans*-**3.21** and *cis*-**3.21**. With the two diastereomeric pyran fragments in hand, further

elaboration following our irciniastatin B synthetic route[3,4] will complete the synthesis of disubstituted pyran analogues *trans*-**3.10** and *cis*-**3.10**.

Scheme 3.6. Synthetic Plan to Construction of Analogues **3.10**

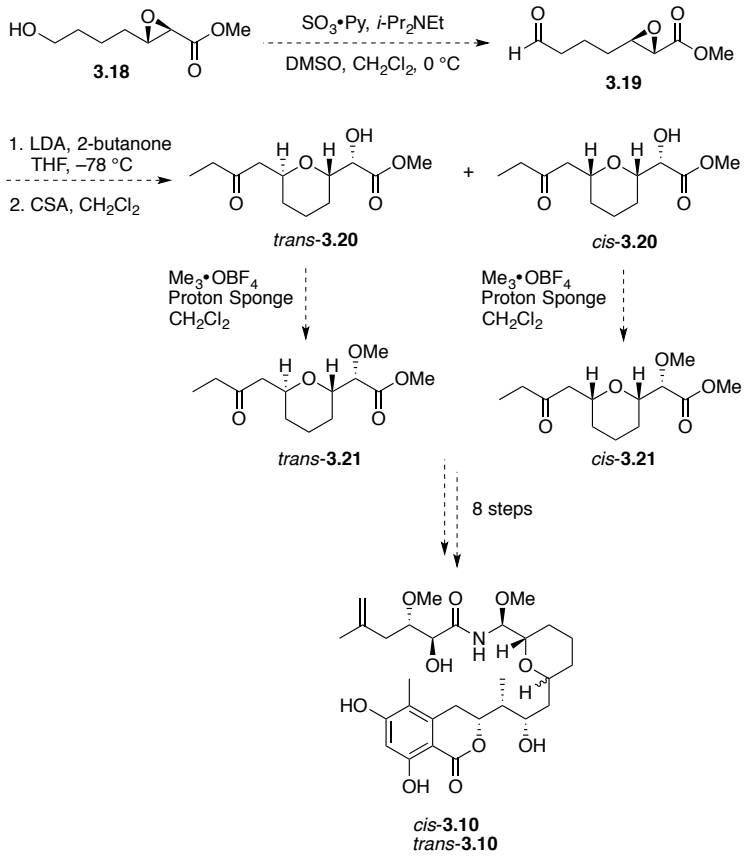

3.3 References

(1) Pettit, G. R.; Xu, J.-P.; Chapuis, J.-C.; Pettit, R. K.; Tackett, L. P.; Doubek, D. L.; Hooper, J. N. A.; Schmidt, J. M. *J. Med. Chem.* **2004**, *47*, 1149-1152.

(2) Huang, X.; Shao, N.; Huryk, R.; Palani, A.; Aslanian, R.; Seidel-Dugan, C. *Org. Lett.* **2009**, *11*, 867-870.

(3) An, C.; Hoye, A. T.; Smith, A. B. *Org. Lett.* **2012**, *14*, 4350-4353.

(4) An, C.; Jurica, J. A.; Walsh, S. P.; Hoye, A. T.; Smith, A. B. *J. Org. Chem.* **2013**, *78*, 4278-4296.

(5) Müller, K.; Faeh, C.; Diederich, F. o. *Science* **2007**, *317*, 1881-1886.

(6) Roth, G. P.; Marshall, D. R.; Chen, S.-H. *Tetrahedron Lett.* **1995**, *36*, 1609-1612.

(7) Wittig, G.; Schöllkopf, U. *Chem. Ber.* **1954**, *87*, 1318-1330.

(8) Smith, A. B.; Jurica, J. A.; Walsh, S. P. *Org. Lett.* **2008**, *10*, 5625-5628.

(9) Jung, M. E.; Berliner, J. A.; Koroniak, L.; Gugiu, B. G.; Watson, A. D. *Org. Lett.* **2008**, *10*, 4207-4209.

(10) Katsuki, T.; Sharpless, K. B. *J. Am. Chem. Soc.* **1980**, *102*, 5974-5976.

(11) Parikh, J. R.; Doering, W. v. E. *J. Am. Chem. Soc.* **1967**, *89*, 5505-5507.

(12) Bal, B. S.; Childers Jr, W. E.; Pinnick, H. W. *Tetrahedron* **1981**, *37*, 2091-2096.

Chapter 4. Experimental Information

4.1 Materials and Methods

Reactions were carried out in flame-dried or oven dried glassware under a nitrogen atmosphere. Anhydrous diethyl ether (Et_2O), tetrahydrofuran (THF), dichloromethane (CH_2Cl_2) and toluene were obtained from a Pure Solv™ PS-400 solvent purification system. Triethylamine, diisopropylethylamine and pyridine were freshly distilled from calcium hydride under a nitrogen atmosphere. All chemicals were purchased from Aldrich, Acros or TCI. Reactions were magnetically stirred unless stated otherwise and monitored by thin layer chromatography (TLC) with 0.25 mm Silacycle pre-coated silica gel plates. Silica gel chromatography was performed utilizing ACS grade solvents and silica gel from either Silacycle or Sorbent Technologies.

Infrared spectra were obtained either neat or as a thin film using a Jasco FT/IR-480 plus spectrometer. Optical rotations were obtained using a Jasco P2000 polarimeter. All melting points were obtained on a Thomas-Hoover apparatus and are uncorrected. ^{1}H NMR spectra (500 MHz field strength) and ^{13}C NMR spectra (125 MHz field strength) were obtained on a Bruker Avance III 500 MHz spectrometer with dual inverse probe or a 5mm DCH cyroprobe or a Bruker Avance III cryomagnet (500MHZ/52mm) with a 5 mm dual cryoprobe. Chemical shifts are reported relative to chloroform (δ 7.26) or methanol (δ 3.31) or benzene (δ 7.16) for ^{1}H NMR spectra and chloroform (δ 77.23) or methanol (δ 49.15) or benzene (δ 128.06) for ^{13}C spectra. High-resolution mass spectra (HRMS) were measured at the University of Pennsylvania on either a Waters LC-TOF mass spectrometer (model LCT-XE Premier) or a Waters GCT Premier Spectrometer.

4.2 Detailed Experimental Procedures

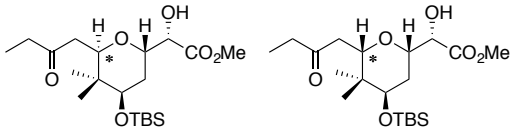

(+)-2.38 (–)-2.39

Tetrahydropyrans (+)-3.8 and (–)-3.9: (–)-DIP-Cl was weighed into a round bottom flask in a glovebox and placed under vacuum for 25 min to remove residual HCl. To a solution of (–)-DIP-Cl (950 mg, 2.96 mmol, 2.01 equiv) in ether (9.6 mL) at – 78 °C was added freshly distilled triethylamine (0.61 mL, 4.41 mmol, 3.0 equiv) dropwise over 5 min. Butanone, freshly distilled from $CaSO_4$ (0.26 mL, 2.96 mmol, 2.01 equiv) was added to the reaction solution dropwise over 5 minutes. The reaction mixture immediately becomes cloudy white upon addition of the first drop of butanone. The boron enolate solution was stirred for 2 h. Next, aldehyde (+)-**2.34** (485.7 mg, 1.47 mmol, azeotroped in benzene 3x, placed under high vacuum overnight) as a solution in ether (9.6 mL) was added to the reaction *via* syringe pump over 30 min. The aldehyde flask was washed with additional ether (5.0 mL) and added to reaction mixture *via* syringe pump over 30 min. The reaction solution was allowed to stir for 4 h at –78 °C. The reaction vessel was warmed slowly to –40 °C over 45 min and held at this temperature for 12 h. The reaction vessel was then warmed to 0 °C and quenched with a 1:1:1 solution (23 mL) of pH 7 buffer, methanol, and hydrogen peroxide (35% aq. solution) and stirred for 1 h. The remaining peroxides were quenched with a saturated solution of sodium thiosulfate. The aqueous phase was extracted with EtOAc (3x 20 mL). The combined organic phases were further washed with a saturated solution of $NaHCO_3$ (1x) and brine (1x). The resulting organic phase was dried over $MgSO_4$, filtered

and concentrated *in vacuo*. The resultant oil was purified *via* flash chromatography on SiO_2 (10% to 15% to 20% EtOAc: hexanes) to furnish aldol product **2.9** (~224 mg, 0.56 mmol, ~38% yield, 6:1 mixture of diastereomers) and dioxaborninane **2.35** (~379.8 mg, 0.67 mmol, ~46% yield).

To a solution of mixture of diastereomers **2.9** (6:1) (224 mg, 0.56 mmol) in CH_2Cl_2 (11.2 mL) was added (*R*)-CSA (25.5 mg, 0.11 mmol, 0.2 equiv). The reaction mixture was stirred for 2 h. The reaction mixture was then quenched with a saturated solution of $NaHCO_3$ and extracted with CH_2Cl_2 (3 x 15 mL). The combined organic layers were dried over $MgSO_4$, filtered and concentrated *in vacuo*. The crude mixture was purified *via* flash chromatography on SiO_2 (10% to 15% to 20% EtOAc: hexanes) to furnish tetrahydropyran (+)-**2.38** (196.3 mg, 0.49 mmol, 33% over 2 steps) and (–)-**2.39** (30.0 mg, 0.07 mmol, 5.0% over 2 steps). ^1H and ^{13}C NMR spectral data was in complete agreement with the spectral data previously reported.[1]

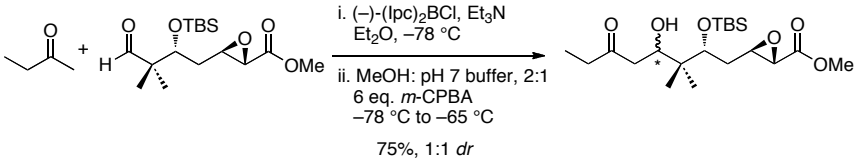

Ketone 2.9 (1:1 *dr*): (–)-DIP-Cl was weighed out into a glovebox and placed under vacuum for 25 min to remove residual HCl. To a solution of (–)-DIP-Cl (127.9 mg, 0.40 mmol, 1.8 equiv) in ether (1.4 mL) at – 78 °C was added freshly distilled triethylamine (0.09 mL, 0.66 mmol, 3.0 equiv) dropwise over 5 min. Butanone, distilled from $CaSO_4$ (0.04 mL, 0.44 mmol, 2.0 equiv, distilled over $CaSO_4$) was added to the reaction solution dropwise over 5 minutes. The reaction mixture immediately becomes cloudy white upon addition of the first drop of butanone. The boron enolate solution was stirred for 2 h,

next, aldehyde (+)-**2.34** (71.1 mg, 0.22 mmol, azeotroped in benzene 3x, placed under high vacuum overnight) in a solution of ether (1.4 mL) was added to the reaction *via* syringe pump over 1 h. The aldehyde flask was washed with additional ether (1.4 mL) and added to reaction mixture *via* syringe pump over 30 min. The reaction solution was allowed to stir for 22 h at –78 °C. The reaction mixture was quenched with 2:1 solution (2.0 mL) of MeOH and pH 7 buffer solution, followed by addition of *m*-CPBA (300 mg, 1.32 mmol, 6 equiv). The reaction vessel was warmed to –65 °C and allowed to stir overnight. The reaction mixture was cooled to –78 °C and the remaining peroxides were quenched with dimethylsulfide (1.0 mL). The reaction mixture was warmed to rt and stirred for 30 min. The aqueous phase was extracted with EtOAc (3 x 10 mL). The combined organic phases were further washed with a solution of K_2CO_3 (0.1 N) (4x) and brine (1x). The resulting organic phase was dried over $MgSO_4$, filtered and concentrated *in vacuo*. The resultant crude oil was purified *via* flash chromatography on SiO_2 (10% to 15% to 20% EtOAc: hexanes) to furnish aldol product **2.9** (~66.0 mg, 0.164 mmol, 75% yield, 1:1 *dr*).

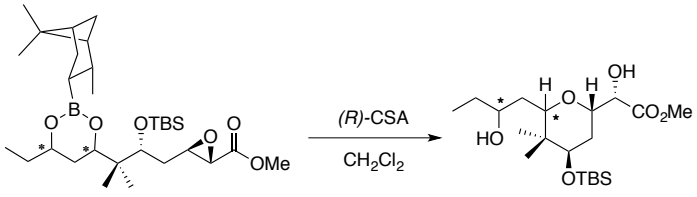

2.35 **(–)-2.37** Single Isomer

Tetrahydropyran (–)-2.37: To a solution of dioxaborinane **2.35** (170 mg, 0.46 mmol) in CH_2Cl_2 (6.2 mL) was added (*R*)-CSA (14.4 mg, 0.062 mmol, 0.13 equiv). The reaction mixture was stirred overnight. Starting **2.35** was still observed by TLC (20% EtOAc: hexanes). (*R*)-CSA (51 mg, 0.22, 0.50 equiv) was added and the reaction was stirred for

10 h. The reaction mixture was quenched with a saturated solution of $NaHCO_3$ and extracted with CH_2Cl_2 (3 x 15 mL). The combined organic layers were dried over $MgSO_4$, filtered and concentrated *in vacuo*. The crude mixture was purified *via* flash chromatography on SiO_2 (10% to 15% to 20% to 25% to 30% EtOAc: hexanes) to furnish tetrahydropyran (–)-**2.37** (44.0 mg, 0.109 mmol, 24%, single isomer) as a colorless solid: Melting Point= 61.0-64.0 °C; $[\alpha]_D^{20}$ –39.8 (*c* 0.18 CH_2Cl_2); IR (neat) 3436, 2956, 2857, 1741, 1465, 1389, 1254, 1094 cm^{-1}; ^1H NMR (500 MHz, $CDCl_3$) δ 4.22 (d, *J* = 2.0 Hz, 1 H) 4.06 (ddd, *J* = 2.4, 3.8, 11.9 Hz, 1 H), 3.96 (dd, *J* = 2.2, 11.1 Hz, 1 H), 3.79 (s, 3 H), 3.71 (m, 1 H), 3.54 (ap t, *J* = 2.4 Hz, 1 H), 2.50 (bs, 1 H), 2.03 (ddd, *J* = 2.4, 12.1, 14.0 Hz, 1 H), 1.65 (ddd, *J* = 2.8, 10.9, 14.2 Hz, 1 H), 1.56-1.43 (m, 3 H), 1.35 (ddd, *J* = 2.7, 2.7, 13.8 Hz, 1 H), 0.94 (t, *J* = 7.3 Hz, 3 H), 0.90 (s, 9 H), 0.88 (s, 3 H), 0.80 (s, 3 H), 0.04 (s, 3 H), 0.03 (s, 3 H); ^{13}C NMR (125 MHz, $CDCl_3$) δ 173.3, 76.2, 75.0, 74.2, 73.5, 71.0, 52.8, 37.5, 34.7, 30.7, 30.0, 29.9, 26.1, 23.8, 19.7, 18.3, 10.6, –4.3, 4.7; HRMS (ES+) *m/z* 405.2668 [$(M+H)^+$; calcd for $C_{20}H_{41}O_6Si$: 405.2672].

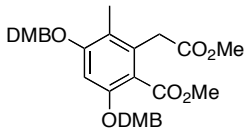

Bis-DMB ether 2.47: To a solution of bis-phenol **2.25** (519 mg, 2.043 mmol) in acetone (25.0 mL) was added K_2CO_3 (1.03 g, 7.452 mmol, 3.7 equiv) followed by dropwise addition of a solution of 3,4-dimethoxybenzylbromide[2] (2.0 mL, 2.2 M in acetone, 2.2 equiv). The yellow reaction mixture was stirred for 24 h and quenched with H_2O (20 mL). The layers were separated and the aqueous layer was extracted with EtOAc (3 x 20 mL). The combined organic layers were dried over $MgSO_4$, filtered and concentrated *in vacuo*. The crude mixture was purified *via* flash chromatography on SiO_2 (40% to 50%

EtOAc: hexanes) to provide **2.47** (850 mg, 1.532 mmol, 75%) as a colorless solid: Melting point= 102.0-103.0 °C; IR (neat) 2947, 1732, 1594, 1515, 1459, 1264, 1152, 1025 cm^{-1}; ^{1}H NMR (500 MHz, $CDCl_3$) 6.97-6.81 (m, 6 H), 6.52 (s, 1 H), 4.99 (s, 2 H), 4.95 (s, 2 H), 3.89 (s, 3 H), 3.88 (s, 3 H), 3.88 (s, 3 H), 3.87 (s, 3 H), 3.83 (s, 3 H), 3.69 (s, 2 H), 3.67 (s, 3 H), 2.14 (s, 3 H); ^{13}C NMR (125 MHz, $CDCl_3$) δ 171.2, 158.7, 155.2, 149.4, 149.3, 149.1, 148.9, 132.7, 129.6, 129.4, 120.0, 119.7, 119.6, 117.8, 111.3, 111.1, 110.9, 110.1, 98.3, 71.2, 70.7, 56.1, 56.1, 56.1, 56.0, 52.2, 36.2, 11.7; HRMS (ES+) *m/z* 577.2047 [$(M+Na)^+$; calcd for $C_{30}H_{34}O_{10}Na$: 577.2050].

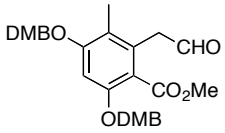

Aldehyde 2.48: To a solution of bis-DMB ether **2.47** (850 mg, 1.53 mmol) in CH_2Cl_2 (15.3 mL) was cooled to –78 °C and DIBAL-H (2.1 mL, 1.0 M in hexanes, 1.4 equiv) was added over 20 min *via* syringe pump. The reaction mixture was allowed to stir for an additional 5 min before it was quenched by the addition of MeOH (7.0 mL) and was warmed to room temperature, then diluted with EtOAc (2 mL) and a saturated aq. solution of Rochelle's salt (2 mL). The biphasic reaction mixture was allowed to stir for 1 h at room temperature to allow the organic layer to transition from cloudy to clear. The layers were separated and the aqueous layer was extracted with EtOAc (3 x 3 mL). The combined organic layers were dried over $MgSO_4$, filtered and concentrated *in vacuo*. The crude mixture was purified *via* flash chromatography on SiO_2 (40% to 50% EtOAc: hexanes) to provide **2.48** (697 mg, 1.33 mmol, 87%) as a colorless solid: Melting point= 122.5-124.0 °C; IR (neat) 2944, 2838, 2726, 1722, 1594, 1515, 1459, 1265, 1153, 1030 cm^{-1}; ^{1}H NMR (500 MHz, $CDCl_3$) 9.65 (t, J = 1.8 Hz, 1 H), 6.97 (d, J = 1.7 Hz, 1 H),

6.94-6.83 (m, 5 H), 6.55 (s, 1 H), 5.02 (s, 2 H), 4.97 (s, 2 H), 3.90 (s, 3 H), 3.89 (s, 9 H), 3.84 (s, 3 H), 3.68 (d, J = 1.6 Hz, 2 H), 2.10 (s, 3 H); ^{13}C NMR (125 MHz, MeOD) δ 198.6, 168.7, 158.9, 155.4, 149.4, 149.4, 149.2, 149.0, 131.0, 129.4, 129.2, 120.1, 119.8, 119.7, 118.0, 111.3, 111.1, 110.0, 110.7, 98.5, 71.2, 70.7, 56.3, 56.1, 56.1, 56.1, 52.3, 46.1, 11.9; HRMS (ES+) m/z 525.2141 [(M+Na)$^+$; calcd for $C_{29}H_{33}O_9$: 525.2125].

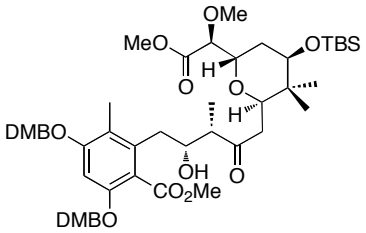

β-Hydroxy Ketone (+)-2.49: To a solution of ketone (+)-**2.6** (114 mg, 0.274 mmol, azeotroped in benzene 3x, placed under high vacuum overnight) in CH_2Cl_2 (1.35 mL) was cooled to –78 °C and Cl_2BPh (0.05 mL, 0.383 mmol, 1.4 equiv) was added dropwise. After 20 min, i-Pr_2NEt (0.10 mL, 0.574 mmol, 2.1 equiv) was introduced dropwise. After 1 h, the reaction mixture was warmed to 0 °C, where it was stirred for 1 h then cooled back down to –78 °C. Aldehyde **2.48** (205 mg, 0.391 mmol, 1.5 equiv) was dissolved in CH_2Cl_2 (0.7 mL) and was added to the boron enolate solution at –78 °C over 15 min *via* syringe pump. After 4 h at –78 °C, the reaction mixture was quenched with a 1:1 mixture of MeOH and pH 7 buffer (4 mL). While warming to 0 °C, pH 8 buffer solution was added to neutralize the reaction mixture to pH 7 and the biphasic mixture was stirred for 1 h at 0 °C. The layers were separated and the aqueous layer was extracted with CH_2Cl_2 (3 x 5 mL). The combined organic layers were dried over $MgSO_4$, filtered and concentrated *in vacuo*. The resulting crude mixture was purified *via* flash chromatography on deactivated SiO_2 (2% v/v triethylamine, 7.5% to 10% EtOAc:

CH_2Cl_2) to provide a mixture (ca. 10:1) of β-hydroxy ketone (+)-**2.49** and corresponding lactone (176 mg, 0.192 mmol, 70%) as a colorless foam: $[\alpha]_D^{20}$ +29.8 (*c* 0.68 $CHCl_3$); IR (neat) 3417, 2924, 2855, 1719, 1590, 1516, 1461, 1264, 1154 cm^{-1}; ^1H NMR (500 MHz, $CDCl_3$) Major: δ 6.95-6.91 (m, 3 H), 6.88-6.82 (m, 3 H), 6.49 (s, 1 H), 5.02-4.97 (m, 2 H), 4.95 (s, 2 H), 4.10 (dd, *J* = 5.3, 10.9 Hz, 1 H), 4.06 (dd, *J* = 2.9, 9.1 Hz, 1 H), 4.06-4.03 (m, 1 H), 3.94 (d, *J* = 6.3 Hz, 1 H), 3.89 (s, 3 H), 3.89 (s, 3 H), 3.88 (s, 3 H), 3.88 (s, 3 H), 3.85 (s, 3 H), 3.72 (s, 3 H), 3.64 (dd, *J* = 3.7, 7.7 Hz, 1 H), 3.46 (d, *J* = 5.6 Hz, 1 H), 3.41 (s, 3 H), 3.06 (dd, *J* = 9.4, 16.0 Hz, 1 H), 2.87 (dd, *J* = 3.4, 14.3 Hz, 1 H), 2.68 (dq, *J* = 7.1, 5.4 Hz, 1 H), 2.62 (dd, *J* = 10.1, 14.1 Hz, 1 H), 2.54 (dd, *J* = 3.0, 16.4 Hz, 1 H), 2.20 (s, 3 H), 1.96 (ddd, *J* = 3.9, 6.0, 13.9 Hz, 1 H), 1.58 (ddd, *J* = 5.0, 7.9, 13.3 Hz, 1 H), 1.21 (d , *J* = 6.9 Hz, 3 H), 0.96 (s, 3 H), 0.90 (s, 9 H), 0.85 (s, 3 H), 0.04 (s, 3 H), 0.04 (s, 3 H); Distinct peaks from minor byproduct: δ 6.54 (s), 5.16 (dab, *J* = 12.2 Hz), 5.10 (dab, *J* = 11.8 Hz), 1.33 (d, *J* = 7.0 Hz); ^{13}C NMR (125 MHz, $CDCl_3$) δ 212.5, 171.5, 170.7, 159.0, 155.2, 149.4, 149.3, 149.1, 148.9, 137.1, 129.5, 129.5, 120.0, 119.8, 119.3, 117.9, 111.3, 111.1, 110.8, 110.7, 97.6, 82.3, 77.4, 76.7, 73.0, 71.6, 71.2, 70.6, 70.1, 58.8, 56.1, 56.1, 56.1, 56.1, 53.2, 52.6, 52.1, 42.4, 38.0, 35.8, 30.0, 26.0, 24.9, 18.2, 11.8, 11.4, –4.3, –4.9; HRMS (ES+) *m/z* 963.4525 [$(M+Na)^+$; calcd for $C_{50}H_{72}O_{15}SiNa$: 963.4538].

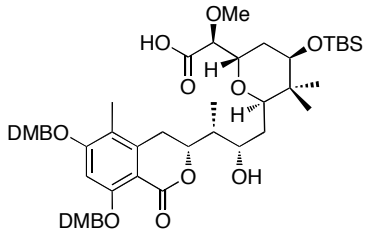

Acid (+)-2.52: To a solution of β-hydroxy ketone (+)-**2.49** (203 mg, 0.215 mmol) in THF (2.20 mL) and MeOH (0.73 mL) cooled to –78 °C was added a solution of Et_2BOMe

(0.31 mL, 1M in THF, 1.4 equiv). The reaction mixture was stirred for 25 min before $NaBH_4$ (45 mg, 1.189 mmol, 5.4 equiv) was added. After 5.5 h, the reaction was warmed to 0 °C and quenched with a 1:1 mixture of MeOH and pH 7 buffer (4.0 mL) followed by the addition of *m*-CPBA (0.330 g, 1.31 mmol, 6.0 equiv) portion-wise. After 30 min, the reaction mixture was warmed to room temperature, and dimethylsulfide was added slowly to quench remaining peroxides. After 10 min, aq. solution of K_2CO_3 (5 mL, 0.1 N) was added and the layers were separated. The aqueous layer was extracted with EtOAc (3 x 5 mL). The combined organic layers were washed with brine, then dried over $MgSO_4$, filtered and concentrated *in vacuo*. The crude mixture was purified *via* flash chromatography (50% to 60% EtOAc: hexanes then flushed with 10% MeOH: EtOAc) to provide a mixture (ca. 8:1) of diol **2.50** and lactone **2.51** (183 mg).

The mixture of diol **2.50** and lactone **2.51** was dissolved in MeOH (10.0 mL) and cooled to 0 °C followed by the addition of H_2O (70 μL, 3.889 mmol, 20.0 equiv) and LiOH (191 mg, 7.975 mmol, 40.0 equiv). The reaction mixture was allowed to warm to room temperature and after 35 h, the reaction mixture was quenched with 50% aqueous acetic acid solution (5 mL). Brine (6 mL) and H_2O (2 mL) were added and the layers were separated. The aqueous layer was extracted with EtOAc (5 x 15 mL). The combined organic layers were dried over $MgSO_4$, filtered and concentrated *in vacuo*. Crude mixture was purified *via* column chromatography on SiO_2 (0.1% acetic acid in 60% EtOAc: hexanes to 0.1% acetic acid in 80% EtOAc: hexanes) to provide acid (+)-**2.52** (136 mg, 0.152 mmol, 69% over two steps) as a colorless foam: $[\alpha]_D^{20}$ +22.4 (*c* 0.9 $CHCl_3$); IR (neat) 3522, 3058, 2937, 2862, 2862, 1712, 1590, 1515, 1461, 1381, 1261, 1153, 1090

cm^{-1}; ^1H NMR (500 MHz, $CDCl_3$) δ 7.33 (d, *J* = 1.7 Hz, 1 H), 6.92 (m, 3 H), 6.86 (d, *J* = 8.0 Hz, 1 H), 6.82 (d, *J* = 8.3 Hz, 1 H), 6.51 (s, 1 H), 5.15 (dab, *J* = 11.8 Hz, 1 H), 5.09 (dab *J* = 12.2 Hz, 1 H), 4.99 (s, 2 H), 4.33 (ddd, *J* = 2.3, 5.5, 8.0 Hz, 1 H) 4.19 (dd, *J* = 6.0, 11.7 Hz, 1 H), 4.13 (m, 1 H), 3.91 (s, 3 H), 3.89 (s, 3 H), 3.88 (s, 3 H), 3.86 (s, 3 H), 3.85 (d, *J* = 4.1 Hz, 1 H), 3.60 (d, *J* = 12.3 Hz, 1 H), 3.57 (dd, *J* = 4.0, 7.6 Hz, 1 H) 3.41 (s, 3 H), 3.02 (dd, *J* = 2.7, 17.2 Hz, 1 H), 2.88 (dd, *J* = 12.3, 16.4 Hz, 1 H), 2.11 (s, 3 H), 2.08 (m, 1 H), 2.01-1.93 (m, 2 H), 1.66 (ddd, *J* = 5.1, 8.0, 13.6 Hz, 1 H), 1.56 (app d, *J* = 14 Hz, 1 H), 1.07 (d, *J* = 6.9 Hz, 3 H), 0.94 (s, 3 H), 0.89 (s, 9 H), 0.87 (s, 3 H), 0.05 (s, 3 H), 0.04 (s, 3 H); ^{13}C NMR (125 MHz, $CDCl_3$) δ 172.3, 164.4, 161.4, 160.4, 149.5, 149.4, 149.2, 148.7, 142.2, 129.6, 128.9, 120.2, 119.0, 116.3, 111.3, 111.0, 110.9, 110.7, 107.7, 97.9, 82.0, 81.8, 79.0, 72.6, 71.6, 71.1, 70.5, 69.8, 58.7, 56.2, 56.1, 41.5, 38.7, 33.1, 30.6, 29.4, 26.0, 25.0, 18.2, 11.3, 9.5, –4..2, –4.8; HRMS (ES+) *m/z* 919.4287 [$(M+Na)^+$; calcd for $C_{48}H_{68}O_{14}SiNa$: 919.4276].

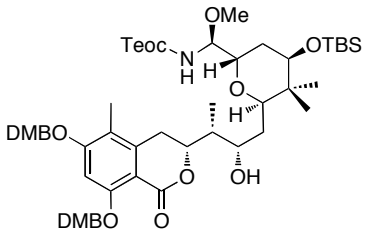

N,O-aminal (+)-S1: A solution of acid (+)-**2.52** (116 mg, 0.129 mmol) in freshly distilled acetone (6.6 mL, distilled from $CaSO_4$) was cooled to 0 °C followed by the dropwise addition of *i*-Pr_2NEt (0.05 mL, 0.287 mmol, 2.2 equiv) and a solution of isobutylchloroformate (0.50 mL, 0.64 M in acetone, 2.4 equiv). After 1 h, a solution of NaN_3 (0.85 mL, 0.78 M in H_2O, 5 equiv) was added to the reaction mixture dropwise. After an additional 20 min at 0 °C, the reaction mixture was diluted with cold H_2O (15

mL). The layers were separated and the aqueous layer was extracted with cold EtOAc (3 x 10 mL). The combined organic layers were dried over $MgSO_4$, filtered and concentrated *in vacuo*. The crude acyl azide was azeotroped (benzene x3) and placed under high vacuum (~0.1 mmHg) for 30 min. The acyl azide was dissolved in toluene (6.6 mL) and reaction flask was fitted with a reflux condenser and heated to 80 °C. After 45 min, 2-TMS-ethanol (0.67 mL, 4.674 mmol, 36.2 equiv) was added *via* syringe through the top of the condenser. After 5 h at 80 °C, the reaction mixture was cooled to room temperature and concentrated *in vacuo*. The crude mixture was purified *via* flash chromatography on SiO_2 (40% to 50% EtOAc: hexanes) to provide *N,O*-aminal (+)-**S1** (90 mg, 0.087 mmol, 67%) as a colorless foam: $[\alpha]_D^{20}$ +3.7 (*c* 0.5, $CHCl_3$); IR (neat) 3502, 3340, 2947, 2859, 1713, 1589, 1515, 1462, 1253, 1151, 1078, 1034, 840 cm^{-1}; ^1H NMR (500 MHz, $CDCl_3$) δ 7.34 (d, *J* = 1.8 Hz, 1 H), 6.93 (m, 3 H), 6.87 (d, *J* = 8.0 Hz, 1 H), 6.82 (d, *J* = 8.3 Hz, 1 H), 6.52 (s, 1 H), 5.38, (d, *J* = 8.8 Hz, 1 H), 5.16 (dab, *J* = 12.0, 1 H), 5.09 (dab, *J* = 11.9 Hz, 1 H), 4.99 (s, 2H), 4.89 (d, *J* = 9.6 Hz, 1 H), 4.31 (ddd, *J* = 2.2, 6.6, 10.5 Hz, 1 H), 4.19 (ddd, *J* = 8.3, 10.3, 18.2 Hz, 1 H), 4.12 (m 2 H), 3.98 (d, *J* = 9.1 Hz, 1 H), 3.92 (s, 3 H), 3.89 (s, 3 H), 3.88 (s, 3 H), 3.87 (m, 1 H), 3.86 (s, 3 H), 3.66 (s, 1 H), 3.62 (d, *J* =11.5 Hz, 1 H), 3.56 (m, 1 H), 3.35 (s, 3 H), 3.10 (app d, *J* = 16.5 Hz, 1 H), 2.83 (dd, *J* = 12.1, 16.0 Hz, 1 H), 2.37 (m , 1 H), 2.12 (s, 3 H), 1.85 (m, 2 H), 1.45-1.41 (m, 2 H), 1.11 (d, *J* = 6.9 Hz, 3 H), 0.10 (s, 3 H), 0.97 (t, *J* = 8.6 Hz, 2 H), 0.89 (s, 9 H), 0.87 (s, 3 H), 0.04 (s, 3 H), 0.03 (s, 3 H), 0.01 (s, 9 H); ^{13}C NMR (125 MHz, $CDCl_3$) δ 163.7, 161.2, 160.3, 157.1, 149.6, 149.4, 149.2, 148.7, 142.2, 129.7, 129.0, 120.1, 119.0, 116.2, 111.3, 111.0, 110.9, 110.8, 108.2, 97.9, 83.7, 83.6, 79.3, 77.4, 73.0, 72.7, 71.1, 70.5, 63.7, 56.2, 56.1, 56.1, 55.8, 43.4, 38.0, 32.9, 31.1, 29.7, 26.1, 26.0, 18.1, 17.8,

11.4, 10.1, –1.3, –4.4, –4.8. HRMS (ES+) *m/z* 1034.5088 [$(M+Na)_+$; calcd for $C_{53}H_{81}NO_{14}Si_2Na$: 1034.5093].

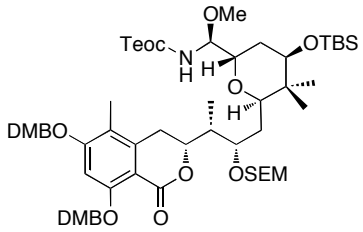

SEM-ether (+)-2.53: A solution of *N,O*-aminal (+)-**S1** (86 mg, 0.085 mmol) in THF (0.6 mL) was cooled to 0 °C followed by the addition of *i*-Pr_2NEt (0.13 mL, 0.746 mmol, 9 equiv), SEMCl (0.09 mL, 0.509 mmol, 6 equiv), and TBAI (8 mg, 0.022 mmol, 0.2 equiv). The reaction mixture was stirred at 0 °C for 15 min and was allowed to warm to room temperature and stirred for 23 h. The reaction mixture was quenched with a saturated aq. solution of $NaHCO_3$ (1 mL). The aqueous layer was extracted with EtOAc (3 x 3 mL). The combined organic layers were dried over $MgSO_4$, filtered and concentrated *in vacuo*. The crude mixture was purified *via* flash chromatography on SiO_2 (35% to 40% EtOAc: hexanes) to provide desired SEM ether (+)-**2.53** (0.080 g, 0.070 mmol, 82%) as a colorless foam: $[\alpha]_D^{20}$ +31.6 (*c* 0.8, $CHCl_3$); IR (neat) 3336, 2952, 2929, 2858, 1716, 1593, 1518, 1464, 1264, 1249, 1160, 1078, 1027, 836 cm^{-1}; ^1H NMR (500 MHz, $CDCl_3$) δ 7.33 (d, *J* = 1.8 Hz, 1 H), 6.98-6.93 (m, 3 H), 6.88 (d, *J* = 8.7 Hz, 1 H), 6.83 (d, *J* = 8.3 Hz, 1 H), 6.54 (s, 1 H), 5.60 (bd, *J* = 9.2 Hz, 1 H), 5.19 (dab, *J* = 11.7 Hz, 1 H), 5.10 (dab, *J* = 11.6 Hz, 1 H), 4.98 (s, 2 H), 4.81 (bd, *J* = 7.9 Hz, 1 H), 4.69-4.59 (m, 2 H), 4.26 (ddd, *J* = 2.3, 8.4, 11.4 Hz, 1 H), 4.17 (dd, *J* = 7.5, 10.5 Hz, 1 H), 4.10 (m, 1 H), 3.98-3.94 (m, 2 H), 3.94 (s, 3 H), 3.93 (s, 3 H), 3.89 (s, 3 H), 3.88 (s, 3 H), 3.58 (dd, *J* = 4.2 Hz, 1 H), 3.54 -3.48 (m, 1 H), 3.44-3.39 (m, 1 H), 3.36 (s, 3 H), 3.34-3.27 (m, 2 H),

2.65 (dd, *J* = 7.8, 16.0 Hz, 1 H), 2.47 (m, 1 H), 2.15 (s, 3 H), 2.04 (m, 1 H), 1.82 (ddd, *J* = 2.4, 9.5, 12.9 Hz, 1 H), 1.66 (m , 1 H), 1.51 (ddd, *J* = 3.9, 8.5, 14.2 Hz, 1 H), 1.13 (d, *J* = 7.1 Hz, 3 H), 0.98 (s, 3 H), 0.94 (m, 2 H), 0.90 (s, 9 H), 0.87 (s, 3 H), 0.85-0.77 (m, 1 H), 0.71-0.65 (m, 1 H), 0.05 (s, 3 H), 0.04 (s, 3 H), 0.004 (s, 9 H), –0.13 (s, 9 H) ; ^{13}C NMR (125 MHz, $CDCl_3$) δ 163.6, 161.3, 160.4, 157.2, 149.6, 149.5, 149.3, 148.8, 142.2, 129.7, 129.0, 120.2, 119.2, 116.3, 111.4, 111.2, 111.0, 110.9, 108.3, 98.0, 93.6, 84.4, 79.4, 77.4, 75.0, 73.5, 71.2, 70.5, 67.6, 65.7, 63.6, 56.3, 56.2, 56.2, 56.1, 56.0, 39.3, 37.7, 31.7, 29.9, 29.3, 26.3, 26.0, 18.2, 18.1, 17.9, 11.4, 9.9, –1.3, –1.4, –4.3, –4.8. high resolution mass spectrum (ES+) *m/z* 1164.5879 [$(M+Na)^+$; calcd for $C_{59}H_{95}NO_{15}Si_3Na$: 1164.5907].

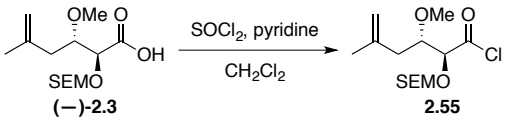

Acid Chloride 2.55:[3] To a solution of carboxylic acid (–)-**2.3** (31 mg, 0.102 mmol) in CH_2Cl_2 was added a solution of pyridine (0.66 mL, 0.62 M in CH_2Cl_2, 4 equiv) and a solution of thionyl chloride (0.64 mL, 0.48 M in CH_2Cl_2, 3 equiv) and stirred at rt for 2 h. The resulting solution was concentrated under a stream of positive N_2 then placed under vacuum (~0.1 mmHg). The crude mixture was dissolved in toluene (0.4 mL) and transferred to an oven-dried vial *via* cannula transfer (flask rinsed with 2 x 0.4 mL toluene). Crude acid chloride **2.55** was concentrated *in vacuo,* dissolved in THF (1.0 mL, 0.1 M), and used in the next step without further purification.

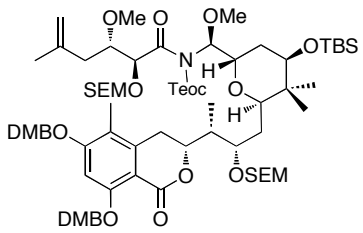

Amide (+)-2.56: To a solution of carbamate (+)-**2.53** (0.030 mg, 0.026 mmol) in THF (0.65 mL) cooled to –78 °C and added a solution of *i*-PrMgCl (55 μL, 2.0 M in THF, 4 equiv) over 2 min. The yellow solution was stirred for 30 min at –78 °C then a solution of acid chloride **2.55** (1.0 mL, 0.1 M in THF, 3.9 equiv) was added dropwise over 20 min. After 2.5 h, the reaction mixture was quenched with a saturated aq. solution of $NaHCO_3$ (1.5 mL) and warmed to rt. The aqueous layer was extracted with EtOAc (3 x 2 mL) and the combined organic layers were washed with brine, then dried over $MgSO_4$, filtered and concentrated *in vacuo*. The crude mixture was purified *via* flash chromatography on deactivated silica gel (1% v/v triethylamine, 25% to 30% EtOAc: hexanes) to furnish amide (+)-**2.56** (27 mg, 0.019 mmol, 72%) as a white foam: $[\alpha]_D^{20}$ +27.0 (*c* 0.3, $CHCl_3$); IR (neat) 2928, 2856, 1716, 1593, 1518, 1464, 1250, 1160, 1083, 1029, 859, 837 cm^{-1}; ^1H NMR (500 MHz, $CDCl_3$) δ 7.34 (d, *J* = 1.9 Hz, 1 H), 6.97-6.93 (m, 3 H), 6.88 (d, *J* = 8.0 Hz, 1 H), 6.83 (d, *J* = 8.2 Hz, 1 H), 6.54 (s, 1 H), 5.62 (d, *J* = 5.7 Hz, 1 H), 5.17 (d, *J* = 4.4 Hz, 1 H), 5.16 (d, *J* = 12.7 Hz, 1 H), 5.10 (d, *J* = 11.9 Hz, 1 H), 4.98 (s, 2 H), 4.75 (s, 1 H), 4.73 (s, 1 H), 4.67 (dd, *J* = 6.4, 12.7 Hz, 2 H), 4.59 (dd, *J* = 7.1, 25.3 Hz, 2 H), 4.35 (m, 1 H), 4.32 (dd, *J* = 3.6, 6.8 Hz, 1 H), 4.30-4.25 (m, 2 H), 3.93 (s, 3 H), 3.91 (s, 3 H), 3.90 (s, 3 H), 3.88 (s, 3 H), 3.83 (m, 1 H), 3.64 (m, 1 H), 3.58 (ddd, *J* = 1.6, 9.8, 13.1 Hz, 2 H), 3.53 (m, 1 H), 3.47-3.38 (m, 2 H), 3.36 (s, 3 H), 3.31 (s, 3 H), 3.24 (dd, *J* = 1.8, 17.7 Hz, 1 H), 3.20 (m, 1 H), 2.86 (dd, *J* = 12.4, 15.9 Hz, 1 H), 2.26 (m, 1 H), 2.25 (m, 1

H), 2.21 (s, 3 H), 2.05 (m, 1 H), 1.96 (ddd, J = 4.0, 4.0, 13.7 Hz, 1 H), 1.86 (m, 2 H), 1.73 (s, 3 H), 1.70 (m, 1 H), 1.14 (d, J = 7.6 Hz, 3 H), 1.09 (dd J = 7.1, 9.2 Hz, 2 H), 0.92 (s, 3 H), 0.90 (s, 9 H), 0.86 (s, 3 H), 0.84 (m, 2 H), 0.78 (ddd, J = 5.7, 11.6, 13.6 Hz, 1 H), 0.66 (ddd, J = 5.5, 11.6, 13.6 Hz, 1 H), 0.06 (s, 3 H), 0.05 (s, 3 H), 0.05 (s, 9 H), –0.05 (s, 9 H), –0.15 (s, 9 H) ; ^{13}C NMR (125 MHz, $CDCl_3$) δ 175.2, 163.9, 161.2, 160.4, 154.5, 149.5, 149.4, 149.2, 142.9, 148.7 142.6, 129.7, 129.0, 120.2, 119.1, 116.4, 112.8, 111.2, 111.0, 110.8, 110.7, 108.2, 97.7, 95.1, 94.1, 88.5, 81.1, 79.6, 77.4, 77.0, 75.9, 73.0, 71.2, 70.4, 66.3, 66.0, 65.7, 58.4, 57.0, 56.2, 56.1, 56.1, 56.1, 39.8, 39.1, 38.8, 31.8, 31.1, 29.9, 29.9, 26.1, 24.7, 23.1, 18.2, 18.2, 18.1, 17.7, 11.5, 9.8, –1.3, –1.4, –1.4, –4.1, –4.8. HRMS (ES+) m/z 1450.7513 [$(M+Na)^+$; calcd for $C_{73}H_{121}NO_{19}Si_4Na$: 1450.7508].

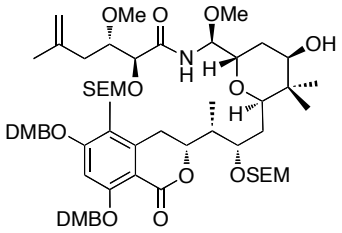

Alcohol (–)-3.4: To a solution of amide (+)-**2.56** (7.0 mg, 0.005 mmol) in THF (0.1 mL) was added a solution of TBAF (15 µL, 1 M in THF, 3.0 equiv). The yellow solution was stirred at rt for 1 h then warmed to 50 °C. After 19 h, additional TBAF (10 µL, 0.010 mmol, 2.0 equiv) was added. The reaction mixture was stirred at 50 °C for an additional 23 h, then cooled to rt, quenched with water and extracted with EtOAc (4 x 0.5 mL). The combined organic layers were dried over $MgSO_4$, filtered and concentrated *in vacuo*. The crude mixture was purified *via* flash chromatography on SiO_2 (40% to 60% to 70% EtOAc: hexanes) to furnish alcohol (–)-**3.4** (4.5 mg, 0.004 mmol, 79%) as a colorless oil: $[\alpha]_D^{20}$ –3.2 (*c* 0.3, $CHCl_3$); IR (neat) 3426, 2951, 2835, 1715, 1685, 1593, 1517, 1265,

1248, 1160, 1028 cm^{-1}; ^1H NMR (500 MHz, $CDCl_3$) δ 7.32 (d, *J* = 1.6 Hz, 1 H), 7.25 (d, *J* = 9.4 Hz, 1 H), 6.97-6.92 (m, 3 H), 6.87 (d, *J* = 8.8 Hz, 1 H), 6.83 (d, *J* = 8.0 Hz, 1 H), 6.53 (s, 1 H), 5.13 (ABq, *J* = 11.7 Hz, 2 H), 5.09 (dd, *J* = 2.5, 5.6 Hz, 1 H), 4.98 (s, 2 H), 4.83 (d, *J* = 6.6 Hz, 1 H), 4.77 (s, 1 H), 4.76 (s, 1 H), 4.70 (ABq, *J* = 5.5 Hz, 2 H), 4.60 (d, *J* = 7.7 Hz, 1 H), 4.40 (d, *J* = 2.1 Hz, 1 H), 4.27 (ddd, *J* = 1.9, 7.8, 11.9 Hz, 1 H), 4.08 (m, 1 H), 3.99 (m, 1 H), 3.93 (s, 3 H), 3.90 (s, 3 H), 3.89 (s, 3 H), 3.87 (s, 3 H), 3.74 (m, 2 H), 3.67 (dd, *J* = 4.5, 4.5 Hz, 1 H), 3.58 (ddd, *J* = 6.5, 10.3, 10.3 Hz, 1 H), 3.50-3.43 (m, 2 H), 3.37 (s, 3 H), 3.32 (s, 3 H), 3.27 (dd, *J* = 2.2, 16.7 Hz, 1 H), 2.65 (dd, *J* = 12.7, 16.4 Hz, 1 H), 2.46 (m, 1 H), 2.37 (dd, *J* = 8.5, 14.5 Hz, 1 H), 2.19 (dd, *J* = 4.7, 14.8 Hz, 1 H), 2.14 (s, 3 H), 2.10 (ddd, *J* = 2.6, 8.4, 8.4 Hz, 1 H), 2.01 (m, 1 H), 1.81 (ddd, *J* = 2.54, 9.4, 13.5 Hz, 1 H), 1.73 (m, 1 H), 1.70 (s, 3 H), 1.56 (dd, *J* =4.7, 9.6 Hz, 1 H), 1.54 (dd, *J* = 5.0, 9.3 Hz, 1 H), 1.15 (d, *J* = 6.7 Hz, 3 H), 1.00 (s, 3 H), 0.94 (s, 3 H), 0.91 (m, 2 H), 0.85-0.79 (m, 1 H), 0.71-0.69 (m, 1 H), 0.01 (s, 9 H), –0.13 (s, 9 H); ^{13}C NMR (125 MHz, $CDCl_3$) δ 171.2, 163.9, 161.3, 160.4, 149.5, 149.4, 149.2, 148.7, 142.4, 142.2, 129.6, 128.9, 120.2, 119.2, 116.7, 113.0, 111.2, 111.0, 110.9, 110.7, 108.1, 97.7, 94.8, 94.4, 81.8, 81.4, 79.6, 77.4, 75.5, 72.9, 71.1, 70.5, 68.0, 66.2, 65.6, 58.0, 56.3, 56.2, 56.2, 56.1, 56.1, 39.2, 38.3, 37.3, 30.7, 30.0, 29.9, 29.5, 26.0, 22.9, 19.4, 18.2, 18.1, 11.4, 9.6, –1.2, –1.4; HRMS (ES+) *m/z* 1192.6072 [$(M+Na)^+$; calcd for $C_{61}H_{95}NO_{17}Si_2Na$: 1192.6036].

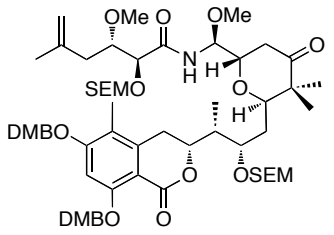

Ketone (–)-2.57: To a solution of alcohol (–)-**3.4** (3.5 mg, 0.003 mmol) in CH_2Cl_2 (0.05 mL) was added $NaHCO_3$ (4.2 mg, 16.6 equiv). The reaction mixture was cooled to 0 °C and Dess-Martin periodinane (6.0 mg, 0.015 mmol, 5.0 equiv) was added and the resulting mixture was stirred for 3 h. Reaction was quenched with a saturated aq. solution of $NaHCO_3$ and extracted with EtOAc (4 x 0.5 mL). The combined organic layers were dried over $MgSO_4$, filtered and concentrated *in vacuo*. The crude mixture was purified *via* flash chromatography on SiO_2 (40% to 50% EtOAc: hexanes) to furnish ketone (–)-**2.57** (3.0 mg, 0.0026 mmol, 87%) as a colorless oil: $[\alpha]_D^{20}$ –14.5 (*c* 0.2, $CHCl_3$); IR (neat) 3403, 2951, 2928, 2835, 1713, 1687, 1593, 1517, 1463, 1265, 1248, 1159, 1080.9, 1029 cm^{-1}; ^1H NMR (500 MHz, $CDCl_3$) δ 7.31 (ap s, 1 H), 7.27 (ap s, 1 H), 6.97 (d, *J* = 8.4 Hz, 1 H), 6.93 (m, 2 H), 6.88 (d, *J* = 8.4 Hz, 1 H), 6.83 (d, *J* = 8.2 Hz, 1 H), 6.55 (s, 1 H), 5.18 (dab, *J* = 12.0 Hz, 1 H), 5.11 (dab, *J* = 11.7 Hz, 1 H), 5.09 (d, *J* = 9.8 Hz, 1 H), 4.98 (s, 2 H), 4.83 (dab, *J* = 6.4 Hz, 1 H), 4.81 (s, 1 H), 4.79 (s, 1 H), 4.73 (dab, *J* = 6.6 Hz, 1 H), 4.65 (dab, *J* = 7.0 Hz, 1 H), 4.61 (dab, *J* = 7.0 Hz, 1 H), 4.38 (d, *J* = 2.0 Hz, 1 H), 4.29-4.23 (m, 2 H), 3.99 (m, 1 H), 3.93 (s, 3 H), 3.90 (s, 3 H), 3.89 (s, 3 H), 3.88 (s, 3 H), 3.75 (m, 1 H), 3.72 (m, 1 H), 3.56 (ddd, *J* = 6.4, 10.0, 10.0 Hz, 1 H), 3.51-3.42 (m, 2 H), 3.40 (s, 3 H), 3.35 (aps, 1 H), 3.34 (s, 3 H), 3.21 (d, *J* = 15.9 Hz, 1 H), 2.68 (dd, *J* = 12.7, 16.4 Hz, 1 H), 2.60 (dd, *J* = 11.4, 14.9 Hz, 1 H), 2.38 (dd, *J* = 8.9, 14.9 Hz, 1 H), 2.27 (dd, *J* = 3.8, 10.9, 1 H), 2.24 (dd, *J* = 5.2, 12.3, 1 H), 2.14 (s, 3 H), 2.17 -2.09 (m, 1 H), 1.86-1.75 (m, 2 H), 1.73 (s, 3 H), 1.25 (s, 3 H), 1.16 (d, *J* = 6.6 Hz, 3 H), 1.01 (s, 3 H), 0.96-0.86 (m, 2 H), 0.82-0.76 (m, 1 H), 0.74-0.68 (m, 1 H), 0.01 (s, 9 H), –0.10 (s, 9 H); ^{13}C NMR (125 MHz, $CDCl_3$) δ 210.8, 171.4, 163.7, 161.4, 160.4, 149.5, 149.4, 149.3, 148.7, 142.2, 141.8, 129.5, 128.8, 120.3, 119.2, 116.1, 113.3, 111.2, 111.0, 110.9,

110.7, 108.0, 97.8, 95.0, 94.8, 81.7, 81.4, 79.8, 79.2, 77.6, 74.6, 72.8, 71.1, 70.5, 66.3, 65.8, 58.1, 56.4, 56.2, 56.2, 56.1, 56.1, 49.6, 39.6, 38.8, 38.3, 30.2, 29.9, 24.8, 23.0, 19.5, 18.2, 18.1, 11.4, 9.7, –1.2, –1.4; high resolution mass spectrum (ES+) *m/z* 1190.5880 [$(M+Na)^+$; calcd for $C_{61}H_{93}NO_{17}Si_2Na$: 1190.5880].

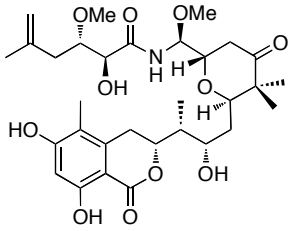

(–)-Irciniastatin B (2.2): To a solution of fully protected irciniastatin B (–)-**2.57** (5.0 mg, 0.0043 mmol) in CH_2Cl_2 (0.05 mL) and H_2O (15 μL) was added a suspension of 2,3-dichloro-5,6-dicyano-1,4-benzoquinone (0.1 mL, 0.33 M in CH_2Cl_2, 8 equiv). After 24 h, the reaction mixture was quenched with a saturated aq. solution of $NaHCO_3$ and extracted with EtOAc (5 x 0.5 mL). The combined organic layers were dried over $MgSO_4$, filtered and concentrated *in vacuo*. The crude mixture was purified *via* flash chromatography (40% EtOAc: hexanes) to afford a mixture (1:2) of desired bis-phenol and 3,4-dimethoxybenzalehyde respectively. The mixture was treated with a stock solution of $MgBr_2$/*n*-BuSH/$MeNO_2$ in Et_2O (0.21 mL: 25 equiv $MgBr_2$, 25 equiv *n*-BuSH, stock solution made up of 75.4 mg $MgBr_2$, 44 μL *n*-BuSH, 82 μL, $MeNO_2$ and 0.82 mL Et_2O). After 10 h, the reaction mixture was diluted with EtOAc, and quenched with a saturated aq. solution of $NaHCO_3$ and extracted with EtOAc (5 x 0.5 mL). The combined organic layers were dried over $MgSO_4$, filtered and concentrated *in vacuo*. The crude mixture was purified *via* flash chromatography with water washed SiO_2 [50 g of SiO_2 washed with H_2O (500 mL) then MeOH (500 mL) then EtOAc (500 mL) then hexanes (500 mL) and

dried under vacuum overnight, then deactivated with 5% v/v triethylamine, 35% to 80% EtOAc: hexanes] to afford (–)-irciniastatin B (**2.2**) (2.0 mg, 0.0033 mmol, 78% over two steps) as a colorless solid: $[\alpha]_D^{20}$ –28.7 (*c* 0.2, MeOH) [$[\alpha]_D^{20}$ –4.7 (*c* 0.15, MeOH) lit.][4] IR (neat) 3356, 2925, 2873, 1710, 1651, 1612, 1510, 1461, 1380, 1266, 1174, 1103 cm^{-1}; ^1H NMR (500 MHz, $CDCl_3$) δ 11.11 (s, 1 H), 7.37 (d, *J* = 10.4 Hz, 1 H), 6.64 (bs, 1 H), 6.30 (s, 1 H), 5.20 (dd, *J* = 6.4 Hz, 10.1 Hz, 1 H), 4.82 (s, 1 H), 4.79 (s, 1 H), 4.55 (ddd, *J* = 4.2, 4.2, 11.8 Hz, 1 H), 4.47 (ap t, *J* = 2.9 Hz, 1 H), 4.21 (ap q, *J* = 6.4 Hz, 1 H), 4.09 (d, *J* = 8.4 Hz, 1 H), 4.00 (dd, *J* = 1.8, 11.2 Hz, 1 H), 3.79-3.77 (m, 1 H), 3.77 (bs, 1H), 3.65 (bs, 1 H), 3.39 (s, 3 H), 3.36 (s, 3 H), 2.94-2.83 (m, 2 H), 2.67 (ap d, *J* = 6.4 Hz, 2 H), 2.36 (dd, *J* = 9.4, 14.5 Hz, 1 H), 2.14 (dd, *J* = 3.7, 14.5 Hz, 1 H), 2.04 (s, 3 H), 1.91 (1 H, m), 1.84 (ddd, *J* = 10.1, 14.6, 24.8 Hz, 1 H), 1.75 (s, 3 H), 1.59 (ap d, *J* = 14.0 Hz, 1 H), 1.16 (s, 3 H), 1.11 (d, *J* = 7.2 Hz, 3 H), 1.10 (s, 3H); ^{13}C NMR (125 MHz, $CDCl_3$) δ 210.3, 173.2, 170.7, 162.5, 161.3, 142.1, 139.9, 113.5, 113.3, 101.7, 101.5, 83.2, 80.5, 80.5, 80.3, 73.8, 72.7, 72.4, 57.9, 56.6, 49.6, 42.8, 38.8, 37.4, 33.0, 28.3, 22.8, 22.3, 19.4, 10.7, 9.2; HRMS (ES+) *m/z* 608.3058 [$(M+1)^+$; calcd for $C_{31}H_{46}NO_{11}$: 608.3071].

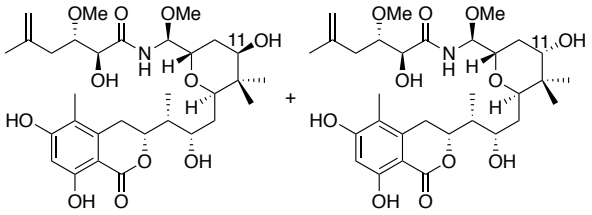

(+)-Irciniastatin A (**2.1**)
(Psymberin)

epi-C(11)-Irciniastatin A (**2.60**)

(+)-Irciniastatin A (2.1) and *epi*-C(11)-Irciniastatin A (2.60): To neat (–)-irciniastatin B (**2.2**) (1 mg, 1.6 μmol) was treated with a solution of $NaBH_4$ (0.1 mL, 0.024 M in MeOH, 1.5 equiv) at 0 °C. After 15 min, the reaction mixture was quenched with a

saturated aq. solution of $NaHCO_3$ (0.4 mL) and extracted with EtOAc (3 x 0.5 mL). The combined organic layers were dried over $MgSO_4$, filtered and concentrated *in vacuo*. The crude mixture (1:1) of (+)-**2.1** and **2.60** was purified *via* preparatory TLC (70% EtOAc: hexanes, 250 micron SiO_2 plate) to provide (+)-irciniastatin A (**2.1**) (0.3 mg, 0.5 μmol 31%) and *epi*-C(11)-irciniastatin A (**2.60**) (0.3 mg, 0.5 μmol, 31%).

Characterization data for (+)-irciniastatin A (**2.1**): ^{1}H NMR (500 MHz, MeOD) δ 6.24 (s, 1 H), 5.39 (d, *J* = 8.3 Hz, 1 H), 4.74 (s, 1 H), 4.71 (s, 1 H), 4.51-4.47 (ddd, *J* = 3.0, 5.9, 12.0 Hz, 1 H), 4.35 (d, *J* = 2.6 Hz, 1 H), 3.94 (m, 2 H), 3.67 (ddd, *J* = 2.6, 3.5, 9.5 Hz, 1 H), 3.60 (dd, *J* = 4.4, 10.9 Hz, 1 H), 3.50 (dd, *J* = 2.0, 10.1 Hz, 1 H), 3.35 (s, 3 H), 3.23 (s, 3 H), 3.13 (dd, *J* = 3.3, 16.7 Hz, 1 H), 2.86 (dd, *J* = 12.0, 16.6 Hz, 1 H), 2.35 (dd, *J* = 9.4, 14.8 Hz, 1 H), 2.11 (m, 1 H), 2.10 (s, 3 H), 2.02 (ddd, *J* = 2.6, 4.5, 13.4 Hz, 1 H), 1.91 (m, 1 H), 1.86-1.74 (m, 2 H), 1.72 (s, 3 H), 1.68 (ddd, *J* = 2.1, 3.8, 14.6 Hz, 1 H), 1.10 (d, *J* = 7.1 Hz, 3 H), 0.97 (s, 3 H), 0.90 (s, 3 H); ^{13}C NMR (125 MHz, $CDCl_3$) *Observable peaks* δ 176.3, 172.5, 163.9, 144.0, 141.2, 115.5, 113.1, 101.6, 82.8, 82.3, 82.1, 79.9, 73.6, 73.3, 72.1, 57.8 56.7, 43.4, 39.9, 38.8, 34.5, 30.6, 29.6, 23.8, 23.0, 14.0, 11.0, 9.3; HRMS (ES+) *m/z* 632.3033 [$(M+Na)^+$; calcd for $C_{31}H_{47}NO_{11}Na$: 632.3047].

Characterization data for *epi*-C(11)-irciniastatin A (**2.60**): ^{1}H NMR (500 MHz, MeOD) *Observable peaks* δ 6.25 (s, 1 H), 5.25 (d, *J* = 3.6 Hz, 1 H), 4.76 (s, 1 H), 4.73 (s, 1 H), 4.51-4.47 (ddd, *J* = 3.1, 6.8, 12.2 Hz, 1 H), 4.37 (d, *J* = 2.8 Hz, 1 H), 4.04 (m, 1 H), 3.97 (dd, *J* = 4.0, 13.2 Hz, 1 H), 3.78 (dd, *J* = 3.1, 11.8 Hz, 1 H), 3.73-3.67 (m, 2 H), 3.33 (s, 3 H), 3.17 (dd, *J* = 3.3, 16.7 Hz, 1 H), 2.83 (dd, *J* = 11.9, 16.2 Hz, 1 H), 2.35 (dd, *J* = 9.7, 15.0 Hz, 1 H), 2.12 (dd, *J* = 3.9, 14.2 Hz, 1 H), 2.09 (s, 3 H), 1.96 (m, 2 H), 1.79 (m, 1 H), 1.73 (s, 3 H), 1.63 (m, 2 H), 1.12 (d, *J* = 7.0 Hz, 3 H), 1.01 (s, 3 H), 0.93 (s, 3 H); ^{13}C

NMR (125 MHz, $CDCl_3$) *Observable peaks* δ 176.0, 172.6, 164.7, 163.8, 144.0, 141.2, 115.4, 113.2, 101.5, 101.5, 83.0, 82.5, 73.0, 72.7, 72.0, 57.9, 56.7, 42.8, 39.0, 38.7, 30.9, 29.6, 23.1, 22.8, 21.3, 10.9, 9.7; HRMS (ES+) *m/z* 632.3029 [$(M+Na)^+$; calcd for $C_{31}H_{47}NO_{11}Na$: 632.3047].

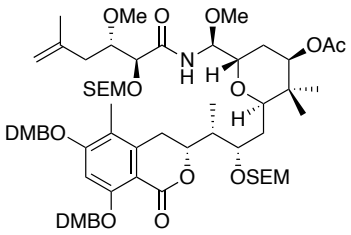

Acetate (+)-S2: To a solution of alcohol (–)-**3.4** (7.0 mg, 0.006 mmol) in pyridine (0.42 mL) was added acetic anhydride (0.18 mL) dropwise. The reaction mixture was stirred for 7.5 h at rt. Reaction was quenched with a saturated aq. solution of $NaHCO_3$ and extracted with EtOAc (3 x 0.5 mL). The combined organic layers were dried over $MgSO_4$, filtered and concentrated *in vacuo*. The crude mixture was purified *via* flash chromatography on SiO_2 (40% to 45% EtOAc: hexanes) to furnish acetate (+)-**S2** (6.3 mg, 0.0051 mmol, 87%) as a colorless oil: $[\alpha]_D^{20}$ +5.3 (*c* 0.5, $CHCl_3$); IR (neat) 3391, 2925, 2858, 1716, 1687, 1592, 1516, 1462, 1371, 1249, 1150 cm^{-1}; ^1H NMR (500 MHz, $CDCl_3$) δ 7.31 (ap s, 1 H), 7.23 (d, *J* = 9.7 Hz, 1 H), 6.98 -6.92 (m, 3 H), 6.87 (d, *J* = 8.7 Hz, 1 H), 6.83 (d, *J* = 8.0 Hz, 1 H), 6.54 (s, 1 H), 5.16 (dab, *J* = 11.5 Hz, 1 H), 5.10 (dab, *J* = 12.3 Hz, 1 H), 5.07 (d, *J* = 10.6 Hz, 1 H), 4.98 (s, 2 H), 4.87 (ap t, *J* = 3.9 Hz, 1 H), 4.82 (d, *J* = 6.8 Hz, 1 H), 4.78 (s, 1 H), 4.77 (s, 1 H), 4.71 (ap t, *J* = 7.6 Hz, 2 H), 4.63 (d, *J* = 7.2 Hz, 1 H), 4.38 (ap s, 1 H), 4.31 (m, 1 H), 4.00 (dd, *J* = 2.9, 9.6 Hz, 2 H), 3.92 (s, 3 H), 3.90 (s, 3 H), 3.88 (s, 3 H), 3.87 (s, 3 H), 3.76 -3.71 (m, 2 H), 3.58 (dd, *J* = 6.9, 10.0 Hz, 1 H), 3.56-3.49 (m, 2 H), 3.49-3.44 (m, 1 H), 3.37 (s, 3 H), 3.31 (s, 3 H), 3.23 (d, *J* =

15.4 Hz, 1 H), 2.67 (dd, *J* = 12.8, 16.4 Hz, 1 H), 2.36 (dd, *J* = 8.8, 14.6 Hz, 2 H), 2.20 (dd, *J* = 4.3, 14.5 Hz, 1 H), 2.14 (s, 3 H), 2.11 (m, 1 H), 2.08 (s, 3 H), 1.83-1.74 (m, 2 H), 1.71 (s, 3 H), 1.57 (ddd, *J* = 4.1, 7.9, 18.2 Hz, 1 H), 1.16 (d, *J* = 6.8 Hz, 3 H), 1.05 (s, 3 H), 0.95-0.90 (m 1 H), 0.88 (s, 3 H), 0.86-0.84 (m, 1 H), 0.86-0.79 (ddd, *J* = 5.9, 11.5, 17.5 Hz, 1 H), 0.74-0.69 (ddd, *J* = 5.9, 11.7, 17.7 Hz, 1 H), 0.01 (s, 9 H), –0.11 (s, 9 H); ^{13}C NMR (125 MHz, $CDCl_3$) δ 171.2, 170.3, 163.7, 161.3, 160.4, 149.6, 149.4, 149.3, 148.8, 142.4, 142.1, 129.6, 128.9, 120.2, 119.2, 116.2, 113.0, 111.3, 111.1, 111.0, 110.8, 108.1, 97.9, 94.8, 94.4, 81.7, 81.5, 79.3, 75.6, 74.5, 71.2, 70.5, 66.2, 65.7, 58.0, 56.4, 56.2, 56.1, 56.1, 39.3, 38.4, 36.4, 30.2, 30.0, 29.9, 29.6, 27.9, 26.1, 22.9, 21.4, 20.2, 18.2, 18.2, 11.4, 9.7, –1.2, –1.4; high resolution mass spectrum (ES+) *m/z* 1212.6318 [$(M+H)^+$; calcd for $C_{63}H_{98}NO_{18}Si_2$: 1212.6322].

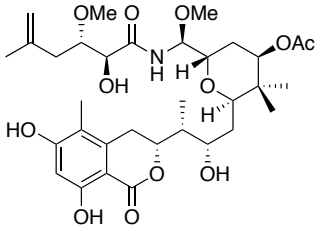

C(11)-OAc-Irciniastatin A (+)-3.7: To a solution of fully protected acetate (+)-**S2** (5.1 mg, 0.0042 mmol) in CH_2Cl_2 (50 μL) and H_2O (15 μL) was added a suspension of 2,3-dichloro-5,6-dicyano-1,4-benzoquinone (0.1 mL, 0.33 M in CH_2Cl_2, 8 equiv). After 10 h, the reaction mixture was quenched with a saturated aq. solution of $NaHCO_3$ and extracted with EtOAc (5 x 0.5 mL). The combined organic layers were dried over $MgSO_4$, filtered and concentrated *in vacuo*. The crude mixture was purified *via* flash chromatography on SiO_2 (50% EtOAc: hexanes) to afford a mixture (1:2) of the desired bis-phenol and 3,4-dimethoxybenzalehyde respectively. The mixture was treated with a stock solution of $MgBr_2$/*n*-BuSH/$MeNO_2$ in Et_2O (0.155 mL: 25 equiv $MgBr_2$, 25 equiv *n*-BuSH, stock

solution made up of 57.4 mg $MgBr_2$, 33 μL *n*-BuSH, 62 μL, $MeNO_2$ and 0.62 mL Et_2O). After 9 h, the reaction mixture was diluted with EtOAc, and quenched with a saturated aq. solution of $NaHCO_3$ and extracted with EtOAc (5 x 0.5 mL). The combined organic layers were dried over $MgSO_4$, filtered and concentrated *in vacuo*. The crude mixture was purified *via* flash chromatography on SiO_2 [deactivated with 5% v/v triethylamine, 40% to 80% EtOAc: hexanes] to afford (+)-C(11)-OAc-irciniastatin A (+)-**3.7** (1.9 mg, 0.0031 mmol, 75% over two steps) as a colorless solid: $[\alpha]_D^{20}$ +3.9 (*c* 0.15, $CHCl_3$); IR (neat) 3372, 2923, 2850, 1737, 1661, 1617, 1515, 1461, 1373, 1251, 1172, 1108, 1071 cm^{-1}; ^1H NMR (500 MHz, $CDCl_3$) δ 11.15 (s, 1 H), 7.17 (d, *J* = 9.7 Hz, 1 H), 6.59 (bs, 1 H), 6.30 (s, 1 H), 5.43 (dd, *J* = 1.6, 10.3 Hz, 1 H), 4.89 (dd, *J* = 4.4, 9.3 Hz, 1 H), 4.81 (s, 1 H), 4.80 (s, 1 H), 4.59 (ddd, *J* = 3.8, 8.3, 11.8 Hz, 1 H), 4.43 (app bs, 1 H), 4.24 (app bs, 1 H), 3.97-3.90 (m, 2 H), 3.77-3.74 (m, 2 H), 3.65 (d, *J* = 10.5 Hz, 1 H), 3.44-3.35 (m, 1H), 3.40 (s, 3 H), 3.39 (s, 3 H), 2.91-2.80 (m, 2 H), 2.37 (dd, *J* = 8.8, 14.6 Hz, 1 H), 2.18 (dd, *J* = 3.9, 14.8 Hz, 1 H), 2.10 (s, 3 H), 2.03 (s, 3 H), 1.91 (m, 2 H), 1.83-1.78 (m, 1 H), 1.76 (s, 3 H), 1.63 (d, *J* = 15.0 Hz, 1 H), 1.11 (d, *J* = 7.1 Hz, 3 H), 0.97 (s, 3 H), 0.96 (s, 3 H); ^{13}C NMR (125 MHz, $CDCl_3$) δ 173.3, 170.7, 162.5, 161.1, 142.2, 140.0, 113.3, 113.3, 101.9, 101.5, 82.6, 80.6, 79.4, 79.0, 74.0, 73.4, 72.8, 71.8, 58.0, 56.7, 56.1, 42.8, 37.6, 37.5, 31.9, 29.9, 28.7, 27.1, 24.1, 22.9, 21.4, 10.7, 9.6; HRMS (ES+) *m/z* 674.3155 [$(M+Na)^+$; calcd for $C_{33}H_{49}NO_{12}Na$: 674.3152].

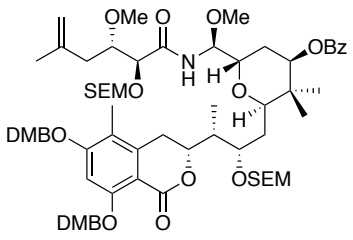

Benzoate (+)-S3: To a solution of alcohol (–)-**3.4** (6.0 mg, 0.005 mmol) in pyridine (0.30 mL) was added benzoyl chloride (30 μL, 0.43 mmol, 85 equiv) dropwise. The reaction mixture was stirred for 1 h at rt. Additional benzoyl chloride (50 μL) was then added reaction mixture was stirred for 30 min. The reaction mixture was quenched with a saturated aq. solution of $NaHCO_3$ and extracted with EtOAc (3 x 0.5 mL). The combined organic layers were dried over $MgSO_4$, filtered and concentrated *in vacuo*. The crude mixture was purified *via* flash chromatography on SiO_2 (30% to 40% EtOAc: hexanes) to furnish benzoate (+)-**S3** (3.6 mg, 0.003 mmol, 55%) as a colorless foam: $[\alpha]_D^{20}$ +12.8 (*c* 0.3, CH_2Cl_2); IR (neat) 3454, 3351, 2954, 2926, 2855, 1729, 1438, 1251, 1157, 1101, 1066, 1011, 1066, 833, 772 cm^{-1}; ^1H NMR (500 MHz, MeOD) δ 8.17-8.00 (m, 3 H), 7.59 (t, *J* = 8.3 Hz, 1 H), 7.49 (t, *J* = 7.7 Hz, 2 H), 7.26 (s, 1 H), 7.08 (s, 1 H), 6.97 (d, *J* = 8.3 Hz, 1 H), 6.94 (s, 2 H), 6.89 (d, *J* = 8.4 Hz, 1 H), 6.74 (s, 1 H), 5.22 (dd, *J* = 5.2, 5.7 Hz, 1 H), 5.20 (dab, *J* = 12.7 Hz, 1 H), 5.16-5.14 (m, 1 H), 5.14 (dab, *J* = 12.7 Hz, 1 H), 5.09 (ap s, 2 H), 4.76-4.68 (m, 6 H), 4.42 (ddd, *J* = 1.7, 5.4, 10.9 Hz, 1 H), 4.28 (d, *J* = 3.2 Hz, 1 H), 4.04 (m, 1 H), 3.93 (m, 1 H), 3.84 (s, 3 H), 3.82 (s, 3 H), 3.82 (bs, 6 H), 3.70 (ddd, *J* = 6.5, 10.0, 10.0 Hz, 1 H), 3.63 (m, 2 H), 3.62-3.60 (m, 3 H), 3.38 (s, 3 H), 3.24 (s, 3 H), 2.79 (dd, *J* = 12.6, 16.6 Hz, 1 H), 2.30 (dd, *J* = 9.0, 14.7 Hz, 1 H), 2.20 (d, *J* = 3.4 Hz, 1 H), 2.17 (s, 3 H), 2.14 (dd, *J* = 4.5, 8.3 Hz, 1 H), 2.11 (dd, *J* = 2.9, 6.5 Hz, 1 H), 1.99 (m, 1 H), 1.90-1.85 (m, 1 H), 1.69 (s, 3 H), 1.15 (d, *J* = 6.8 Hz, 3 H), 1.11 (s, 3 H), 1.05 (s, 3 H), 0.88-0.78 (m, 3 H), 0.68 (ddd, *J* = 5.6, 11.4, 13.4 Hz, 1 H), –0.04 (s, 9 H), –0.13 (s, 9 H); ^{13}C NMR (125 MHz, CD_3OD) δ 173.9, 173.8, 167.5, 166.4, 163.3, 162.1, 150.8, 150.8, 150.7, 150.2, 143.8, 143.4, 136.1, 134.6, 133.9, 131.7, 131.6, 131.2, 130.8, 130.7, 130.4, 129.6, 121.6, 120.9, 117.2, 113.5, 113.0, 112.8, 112.7, 112.4, 107.8, 99.1, 96.0,

95.5, 83.0, 82.9, 82.7, 80.7, 78.5, 78.5, 78.3, 76.7, 71.7, 71.5, 67.1, 66.8, 58.5, 57.0, 56.6, 56.6, 40.7, 39.7, 38.4, 32.4, 31.3, 28.2, 25.6, 23.2, 19.1, 19.1, 11.8, 9.4, –1.1, –1.3; high resolution mass spectrum (ES+) *m/z* 1296.6295 [$(M+Na)^+$; calcd for $C_{68}H_{99}NO_{18}Si_2Na$: 1296.6298].

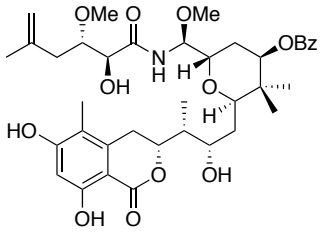

C(11)-OBz-Irciniastatin A (–)-3.6: To a solution of fully protected benzoate (+)-**S3** (3.6 mg, 0.0028 mmol) in CH_2Cl_2 (100 μL) and H_2O (18 μL) was added a suspension of 2,3-dichloro-5,6-dicyano-1,4-benzoquinone (80 μL, 0.29 M in CH_2Cl_2, 8 equiv). After 10 h, the reaction mixture was quenched with a saturated aq. solution of $NaHCO_3$ and extracted with EtOAc (5 x 0.5 mL). The combined organic layers were dried over $MgSO_4$, filtered and concentrated *in vacuo*. The crude mixture was purified *via* flash chromatography on SiO_2 (50% EtOAc: hexanes) to afford a mixture (1:2) of the desired bis-phenol and 3,4-dimethoxybenzalehyde respectively. The mixture was treated with a stock solution of $MgBr_2$/*n*-BuSH/$MeNO_2$ in Et_2O (0.140 mL: 25 equiv $MgBr_2$, 25 equiv *n*-BuSH, stock solution made up of 89.9 mg $MgBr_2$, 36 μL *n*-BuSH, 100 μL, $MeNO_2$ and 0.98 mL Et_2O). After 9.5 h, the reaction mixture was diluted with EtOAc, and quenched with a saturated aq. solution of $NaHCO_3$ and extracted with EtOAc (5 x 0.5 mL). The combined organic layers were dried over $MgSO_4$, filtered and concentrated *in vacuo*. The crude mixture was purified *via* flash chromatography on SiO_2 (40% to 50% EtOAc: hexanes) to afford (+)-C(11)-OBz-irciniastatin A (–)-**3.6** (1.0 mg, 0.0014 mmol, 50% over two steps)

as a colorless solid: $[\alpha]_D^{20}$ –13.7 (*c* 0.08, $CHCl_3$); IR (neat) 3372, 2943, 1726, 1663, 1599, 1446, 1377, 1253, 1114 cm^{-1}; ^1H NMR (500 MHz, C_6D_6) δ 11.93 (bs, 1 H), 8.17 (d, *J* = 7.5 Hz, 3 H), 7.10 (t, *J* = 7.5 Hz, 2 H), 6.31 (s, 1 H), 5.67 (t, *J* = 8.3 Hz, 1 H), 5.27 (dd, *J* = 4.4, 9.9 Hz, 1 H), 5.04 (s, 1 H), 4.92 (s, 1 H), 4.61 (bs, 1 H), 4.33 (m, 3 H), 4.17 (d, *J* = 9.7 Hz, 1 H), 3.91 (ddd, *J* = 3.5, 3.5, 4.0 Hz, 1 H), 3.73 (d, *J* = 10.4 Hz, 1 H), 3.59 (bs, 1 H), 3.32 (s, 3 H), 3.25 (s, 3 H), 2.63 (d, *J* = 16.3 Hz, 1 H), 2.65-2.51 (ddd, *J* = 8.7, 12.4, 12.4 Hz, 1 H), 2.46 (dd, *J* = 4.6, 14.0 Hz, 2 H), 2.26 (m, 1 H), 2.02 (s, 3 H), 1.93 (m, 1 H), 1.79 (s, 3 H), 1.58 (bs, 1 H), 1.46 (d, *J* = 13.9 Hz, 1 H), 1.06 (d, *J* = 6.6 Hz, 3 H), 0.96 (s, 3 H), 0.79 (s, 3 H); ^{13}C NMR (125 MHz, C6D6) δ 173.7, 170.9, 165.7, 163.2, 161.8, 142.6, 140.1, 133.2, 130.9, 129.9, 128.8, 127.5, 113.6, 113.5, 102.0, 101.6, 82.2, 81.5, 80.1, 78.9, 74.3, 73.8, 73.5, 57.8, 56.3, 43.1, 38.1, 37.8, 33.0, 32.4, 30.2, 30.1, 28.4, 27.2, 23.1, 14.4, 10.6, 9.2; HRMS (ES+) *m/z* 736.3286 [$(M+Na)^+$; calcd for $C_{38}H_{51}NO_{12}Na$: 736.3309].

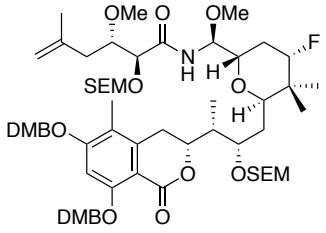

Fluoride (+)-S4: To a solution of alcohol (+)-**3.4** (4.0 mg, 0.003 mmol) in CH_2Cl_2 (0.15 mL) was added DAST (0.05 mL, 0.2 M in CH_2Cl_2, 4 equiv) dropwise. The reaction mixture was stirred for 15 min at rt. The reaction was quenched with a saturated aq. solution of $NaHCO_3$ and extracted with EtOAc (3 x 0.5 mL). The combined organic layers were dried over $MgSO_4$, filtered and concentrated *in vacuo*. The crude mixture was purified *via* flash chromatography on SiO_2 (35% to 40% to 45% EtOAc: hexanes) to

furnish fluoride (+)-**S4** (2.6 mg, 0.0022 mmol, 65%) as a colorless oil: $[\alpha]_D^{20}$ +5.6 (*c* 0.3, $CHCl_3$); IR (neat) 3428, 2921, 2851, 1715, 1683, 1592, 1516, 1462, 1247, 1158, 1083 cm^{-1}; ^1H NMR (500 MHz, $CDCl_3$) δ 7.33 (d, *J* = 1.9 Hz, 1 H), 7.01-6.92 (m, 4 H), 6.88 (d, *J* = 8.0 Hz, 1 H), 6.84 (d, *J* = 8.2 Hz, 1 H), 6.54 (s, 1 H), 5.16 (dab, *J* = 11.4 Hz, 1 H), 5.09 (dab, *J* = 11.8 Hz, 1 H), 5.07 (dd, *J* = 3.1, 10.0 Hz, 1 H), 4.99 (s, 2 H), 4.82 (m, 1 H), 4.80 (m, 1 H), 4.71 (d, *J* = 6.3 Hz, 1 H), 4.68 (d, *J* = 7.1 Hz, 1 H), 4.60 (d, *J* = 7.1 Hz, 1 H), 4.36 (d, *J* = 2.3 Hz, 1 H), 4.29 (ddd, *J* = 2.3, 7.5, 12.0 Hz, 1 H), 4.22-4.18 (ddd, *J* = 4.9, 5.8, 10.3 Hz, 1 H), 4.16-4.12 (ddd, *J* = 3.2, 4.6, 9.4 Hz, 1 H), 3.97-3.94 (m, 1 H), 3.93 (s, 3 H), 3.90 (s, 3 H), 3.89 (s, 3 H) 3.88 (s, 3 H), 3.78-3.70 (m, 2 H), 3.61-3.56 (ddd, *J* = 6.9, 9.8, 19.9 Hz, 1 H), 3.52-3.43 (m, 2 H), 3.40 (s, 3 H), 3.33 (s, 3 H), 3.19 (dd, *J* = 2.4, 16.3 Hz, 1 H), 2.70 (dd, *J* = 11.8, 16.1 Hz, 1 H), 2.37 (dd, *J* = 8.6, 14.6 Hz, 1 H), 2.33-2.25 (ddd, *J* = 3.1, 8.7, 18.3 Hz, 1 H), 2.23 (dd, *J* = 4.7, 14.3 Hz, 1 H), 2.14 (s, 3 H), 2.13-2.10 (m, 2 H), 1.89 (m, 2 H), 1.83 (ddd, *J* = 4.5, 8.3, 12.9 Hz, 1 H), 1.75 (s, 3 H), 1.40 (d, *J* = 15.1 Hz, 3 H), 1.36 (d, *J* = 15.8 Hz, 3 H), 1.17 (d, *J* = 6.8 Hz, 3 H), 1.02-0.84 (m, 2 H), 0.84-0.78 (ddd, *J* = 6.4, 11.2, 13.9 Hz, 1 H), 0.73-0.67 (ddd, *J* = 6.1, 11.0, 13.6 Hz, 1 H), 0.01 (s, 9 H), –0.10 (s, 9 H); ^{19}F NMR (470 MHz, $CDCl_3$) δ 147.4; ^{13}C NMR (125 MHz, $CDCl_3$) δ 171.3, 163.6, 161.3, 160.5, 149.6, 149.5, 149.4, 148.9, 142.4, 142.0, 129.7, 129.0, 120.3, 119.2, 116.3, 113.1, 111.4, 111.2, 111.1, 110.9, 108.2, 98.1, 95.0, 94.4 (d, *J* = 171.0 Hz), 94.5 82.1, 81.5, 78.9, 77.9, 77.4, 76.1, 71.3, 70.6, 66.4, 65.8, 58.1, 56.4, 56.3, 56.2, 56.2, 51.3 (d, *J* = 21.2 Hz), 40.2, 38.4, 32.0 (d, *J* = 5.1 Hz), 30.1, 29.9, 27.7, 27.6, 27.5 (d, *J* = 25.6 Hz), 27.0 (d, 24.6 Hz), 23.0, 18.3, 18.2, 11.4, 10.1, –1.2, –1.4; high resolution mass spectrum (ES+) *m/z* 1172.6189 [$(M+H)^+$; calcd for $C_{61}H_{95}NO_{16}Si_2F$: 1172.6173].

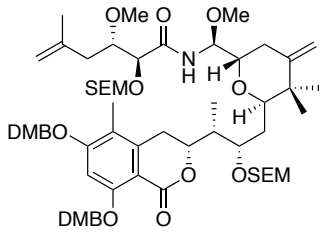

Olefin (–)-S5: To a solution of Ph_3MeBr (75.4 mg, 0.211 mmol) in THF (0.46 mL) was added KO*t*-Bu (0.20 mL, 0.20 mmol) to provide a yellow solution, which was stirred for 5 minutes. The ylide solution (40 μL, 0.32 M in THF, 2.5 equiv) was added to a separate vial containing a solution of ketone (–)-**3.5** (6.0 mg, 0.0051 mmol) in THF (0.26 mL) and the yellow reaction mixture was allowed to stir for 1 h at rt. The reaction mixture was quenched with water and extracted with EtOAc (4 x 0.5 mL). The combined organic layers were dried over $MgSO_4$, filtered and concentrated *in vacuo*. The crude mixture was purified *via* flash chromatography on SiO_2 (40% EtOAc: hexanes) to furnish olefin (–)-**S5** (5.0 mg, 0.0043 mmol, 84%) as a colorless oil: $[\alpha]_D^{20}$ –3.4 (*c* 0.4, $CHCl_3$); IR (neat) 3422, 2951, 1715, 1686, 1592, 1515, 1463, 1417, 1378, 1246, 1157, 1083, 1027 cm^{-1}; ^1H NMR (500 MHz, $CDCl_3$) δ 7.41 (d, *J* = 9.7 Hz, 1 H), 7.31 (ap s, 1 H), 6.97-6.93 (m, 3 H), 6.87 (d, *J* = 8.5 Hz, 1 H), 6.88 (d, *J* = 8.3 Hz, 1 H), 6.54 (s, 1 H), 5.17 (dab, *J* = 11.7 Hz, 1 H), 5.10 (dab, *J* = 11.7 Hz, 1 H), 5.03 (d, *J* = 19.9 Hz, 1 H), 4.98 (s, 2 H), 4.87 (d, *J* = 5.5 Hz, 1 H), 4.86 (s, 1 H), 4.78 (ap s, 2 H), 4.70 (d, *J* = 13.6 Hz, 1 H), 4.64 (dab, *J* = 7.0 Hz, 1 H), 4.60 (dab, *J* = 6.8 Hz, 1 H), 4.42 (ap s, 1 H), 4.22 (ap t, *J* = 10.8 Hz, 1 H), 3.96 (m, 2 H), 3.92 (s, 3 H), 3.90 (s, 3 H), 3.88 (s, 3 H), 3.87 (s, 3 H), 3.80-3.74 (m, 2 H), 3.58 (ddd, *J* = 64, 9.7, 9.7 Hz, 1 H), 3.53-3.48 (m, 2 H), 3.42 (dd, *J* = 5.3, 11.0 Hz, 1 H), 3.40 (s, 3 H), 3.30 (s, 3 H), 3.23 (d, *J* = 16.1 Hz, 1 H), 2.64 (dd, *J* = 12.3, 16.2 Hz, 1 H), 2.38 (dd, *J* = 9.0, 14.9 Hz, 1 H), 2.30-2.22 (m, 2 H), 2.13 (s, 3 H), 2.06-1.97 (m, 2 H), 1.72 (s,

3 H), 1.66-1.63 (m, 1 H), 1.19 (s, 3 H), 1.16 (d, J = 6.7 Hz, 3 H), 0.99 (s, 3 H), 0.95-0.86 (m, 2 H), 0.84-0.78 (ddd, J = 5.6, 12.0, 14.0 Hz, 1 H), 0.75-0.67 (ddd, J = 6.1, 12.2, 13.8 Hz, 1 H), 0.01 (s, 9 H), –0.10 (s, 9 H); ^{13}C NMR (125 MHz, $CDCl_3$) δ171.5, 163.8, 161.3, 160.4, 149.6, 149.4, 149.3, 148.8, 148.3, 142.4, 142.1, 129.6, 128.9, 120.2, 119.2, 116.1, 113.0, 111.3, 111.1, 111.0, 110.8, 109.7, 108.2, 97.9, 94.9, 94.7, 81.6, 81.5, 79.7, 79.4, 74.6, 72.2, 71.2, 70.5, 66.1, 65.5, 58.1, 56.3, 56.2, 40.2, 39.5, 38.4, 33.8, 29.9, 28.7, 27.5, 23.2, 23.0, 18.2, 11.4, 9.6, –1.2, –1.4; high resolution mass spectrum (ES+) *m/z* 1188.6088 [$(M+Na)^+$; calcd for $C_{62}H_{95}NO_{16}Si_2Na$: 1188.6087].

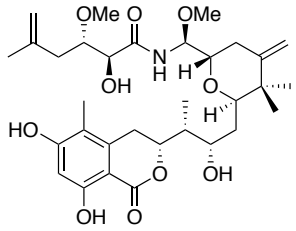

C(11)-Exomethylene-Irciniastatin B (+)-3.9: To a solution of olefin (–)-**S6** (5.0 mg, 0.0043 mmol) in CH_2Cl_2 (0.05 mL) and H_2O (15 μL) was added a suspension of 2,3-dichloro-5,6-dicyano-1,4-benzoquinone (0.1 mL, 0.34 M in CH_2Cl_2, 8 equiv). After 11.5 h, the reaction mixture was quenched with a saturated aq. solution of $NaHCO_3$ and extracted with EtOAc (5 x 0.5 mL). The combined organic layers were dried over $MgSO_4$, filtered and concentrated *in vacuo*. The crude mixture was purified *via* flash chromatography (50% EtOAc: hexanes) to afford a mixture (1:2) of desired bis-phenol and 3,4-dimethoxybenzalehyde respectively. The mixture was treated with a stock solution of $MgBr_2$/*n*-BuSH/$MeNO_2$ in Et_2O (0.200 mL: 25 equiv $MgBr_2$, 25 equiv *n*-BuSH, stock solution made up of 42.3 mg $MgBr_2$, 18 μL *n*-BuSH, 46 μL, $MeNO_2$ and 0.46 mL Et_2O). After 10 h, the reaction mixture was diluted with EtOAc, and quenched with a saturated aq. solution of $NaHCO_3$ and extracted with EtOAc (5 x 0.5 mL). The

combined organic layers were dried over $MgSO_4$, filtered and concentrated *in vacuo*. The crude mixture was purified *via* flash chromatography with SiO_2 [deactivated with 5% v/v triethylamine, 40% to 80% EtOAc: hexanes] to afford (+)-C(11)-exomethylene-irciniastatin A (+)-**3.9** (2.0 mg, 0.0033 mmol, 77% over two steps) as a colorless solid: $[\alpha]_D^{20}$ +12.7 (*c* 0.17, $CHCl_3$); IR (neat) 3379, 2921, 1732, 1659, 1623, 1514, 1454, 1379, 1254, 1109 cm^{-1}; ^1H NMR (500 MHz, $CDCl_3$) δ 11.15 (s, 1 H), 7.28 (d, *J* = 6.7, 10.3 Hz, 1 H), 6.68 (bs, 1 H), 6.30 (s, 1 H), 5.28 (dd, *J* = 6.7, 10.3 Hz, 1 H), 4.87 (s, 2 H), 4.81 (s, 1 H), 4.79 (s, 1 H), 4.52 (ddd, *J* = 4.0, 8.0, 16.4 Hz, 1 H), 4.45 (d, *J* = 3.0 Hz, 1 H), 4.01 (d, *J* = 10.1 Hz, 1 H), 3.92-3.88 (m, 2 H), 3.77-3.74 (ddd, *J* = 3.8, 9.4, 12.7 Hz, 1 H), 3.63 (d, *J* = 10.7 Hz, 1 H), 3.40 (s, 3 H), 3.35 (s, 3 H), 3.34-3.31 (m, 1 H), 2.93-2.80 (m, 2 H), 2.52 (dd, *J* = 5.4, 14.2 Hz, 1 H), 2.42-2.35 (m, 2 H), 2.16 (dd, *J* = 3.9, 14.8 Hz, 1 H), 2.02 (s, 3 H), 1.88 (m, 1 H), 1.79 (dd, *J* = 2.8, 10.6 Hz, 1 H), 1.75 (3 H, s), 1.55 (d, *J* = 14.5 Hz, 1 H), 1.14 (s, 3 H), 1.10 (d, *J* = 7.0 Hz, 3 H), 1.06 (s, 3 H); ^{13}C NMR (125 MHz, $CDCl_3$) δ 173.3, 170.7, 162.5, 161.2, 148.2, 142.2, 140.0, 113.4, 113.2, 110.0, 101.7, 101.5, 83.4, 80.6, 80.2, 79.1, 73.9, 73.2, 72.7, 58.0, 56.5, 43.0, 39.9, 37.5, 33.0, 32.1, 28.5, 25.0, 22.9, 21.7, 10.7, 9.5; HRMS (ES^-) *m/z* 606.3280 [$(M–H)^-$; calcd for $C_{32}H_{48}NO_{10}$: 606.3278].

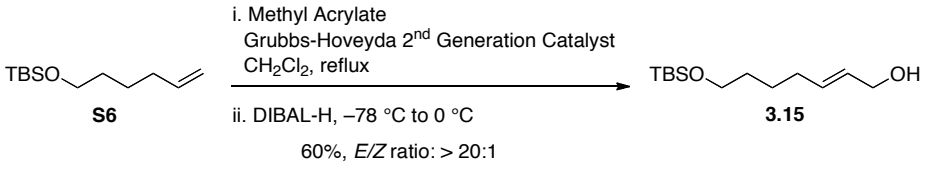

Allylic Alcohol 3.15: To a solution of alkene **S6**[5] (232.9 mg, 1.09 mmol) in THF was added methyl acrylate (0.30 mL, 3.26 mmol, 3.0 equiv), followed by Grubbs-Hoveyda second-generation catalyst (17.8 mg, 0.027 mmol, 0.025 equiv). The reaction mixture

was warmed to reflux and stirred for 2.5 h. The reaction mixture was then cooled to –78 °C and added DIBAL-H (7.6 mL, 1 M in THF, 7 equiv). After 1 h, the reaction mixture was warmed to 0 °C and stirred at this temperature for 30 min and quenched with MeOH. The reaction mixture was warmed to rt and diluted with EtOAc and added saturated solution of Rochelle's salt. The mixture was stirred for 1 h in which the reaction mixture became a homogenous solution. The layers were separated and the aqueous layer was extracted with EtOAc (3 x 15 mL). The combined organic layers were dried over $MgSO_4$, filtered and concentrated *in vacuo*. The crude mixture was purified *via* flash chromatography on SiO_2 (10% to 20% EtOAc: hexanes) to provide allylic alcohol **3.15** (159.0 mg, 0.65 mmol, 60% yield) as a yellow oil (*E*/*Z* ratio > 20:1). Spectral data of **3.15** was in complete agreement with spectral data presented in the literature:[6] ^{1}H NMR (500 MHz, $CDCl_3$) δ 5.70-5.58 (m, 2 H), 4.06 (d, *J* = 5.5 Hz, 2 H), 3.59 (t, *J* = 6.3 Hz, 2 H), 2.04 (dt, *J* = 7.3, 6.7 Hz, 2 H), 1.76 (bs, 1 H), 1.54-1.48 (m, 2 H), 1.44-1.38 (m, 2 H), 0.87 (s, 9 H), 0.028 (s, 6 H); ^{13}C NMR (125 MHz, $CDCl_3$) δ 133.3, 129.3, 63.9, 63.2, 32.5, 32.1, 26.1, 25.5, 18.5, 5.1.

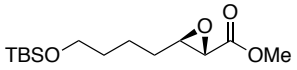

Epoxy Ester 3.17: To freshly activated 4 Å molecular sieves (2.0 g, beads) was added (–)-DIPT (0.27 mL, 0.15 equiv). The solution was cooled to –20 °C and Ti(O*i*-Pr)$_4$ (0.23 mL, 0.10 equiv) was added followed by *t*-BuOOH (3.30 mL, 5 M in decane, 2.0 equiv). The reaction was stirred for 30 min and then allylic alcohol **3.15** (2.012 g, 8.24 mol) dissolved in CH_2Cl_2 (50 ml) was added *via* addition funnel. After 3 h, aq. citric acid solution (1.0 M) was added and the reaction was warmed to rt. After 1 h at rt, the layers were separated, and the aqueous layer was extracted with CH_2Cl_2 (3 x 25 mL). The

combined organic layers were dried over $MgSO_4$, filtered and concentrated *in vacuo*. The crude mixture was purified *via* flash chromatography on SiO_2 (10% to 15% to 20% EtOAc: hexanes) to provide epoxide **3.16** [1.986 g, contaminated with (–)-DIPT] as a yellow oil.

To a solution of epoxide **3.16** containing (–)-DIPT contaminant (1.986 g total mass, ~6.5 mol of **3.16**) in CH_2Cl_2 (65 mL) and DMSO (4.6 mL, 65 mol, 10 equiv) at 0 °C was added *i*-Pr_2NEt (5.7 mL, 32.5 mol, 5 equiv) followed by SO_3•pyridine (5.21 g, 32.5 mol, 5 equiv) in one portion. After 30 min, aqueous saturated $NaHCO_3$ solution (50 mL) was added and the layers were separated. The aqueous layer was extracted with CH_2Cl_2 (3 x 50 mL) and the combined organic layers were dried over $MgSO_4$, filtered and concentrated *in vacuo*. The unpurified aldehyde was used in the step without further purification.

The unpurified aldehyde was dissolved in *t*-BuOH (70 mL) and pH 7 buffer (24 mL). The solution was cooled to 0 °C, followed by addition of 2-methyl-2-butene (7.1 mL), NaH_2PO_4•H_2O (5.12 g, 32.5, 5 equiv), and $NaClO_2$ (3.70 g, 80 wt%, 32.5 mol, 5 equiv). After 2 h, the reaction was quenched with brine and extracted with EtOAc (5 x 100 mL). The combined organic layers were dried over $MgSO_4$ and concentrated. The unpurified acid was used in the next step without further purification.

The unpurified acid was dissolved in CH_2Cl_2 (32.5 mL) and the solution was cooled to 0 °C, followed by dropwise addition of TMS-diazomethane (4.2 mL, 2.0 M in Et_2O, 1.3 equiv) until the solution remained yellow in color. Glacial acetic acid was added dropwise until bubbling stopped to quench the excess TMS-diazomethane. The reaction

mixture was concentrated *in vacuo* and the crude oil obtained was purified *via* flash chromatography on SiO_2 (5% EtOAc: hexanes) to provide ester (+)-**3.17** (1.4076 g, 4.88 mol, 59% yield, 4 steps) as a colorless oil: $[\alpha]_D^{20}$ +13.7 (*c* 2.23, CH_2Cl_2); IR (neat) 2932, 2858, 1757, 1446, 1389, 1359, 1290, 1253, 1204, 1100, 837, 777 cm^{-1}; ^1H NMR (500 MHz, $CDCl_3$) δ 3.77 (s, 3 H), 3.61 (t, *J* = 5.9 Hz, 2 H), 3.23 (d, *J* = 1.9 Hz, 1 H), 3.17-3.15 (ddd, *J* = 1.9, 4.8, 6.2 Hz, 1 H), 1.71-1.64 (m, 2 H), 1.62-1.48 (m, 4 H), 0.88 (s, 9 H), 0.04 (s, 6 H); ^{13}C NMR (125 MHz, $CDCl_3$) δ 170.0, 62.9, 58.7, 53.2, 52.6, 32.5, 31.4, 26.1, 22.4, 18.5, –5.1; high resolution mass spectrum (ES+) *m/z* 311.1659 [$(M+Na)^+$; calcd for $C_{14}H_{28}O_4SiNa$: 311.1655].

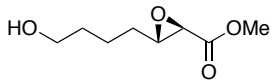

Alcohol (+)-3.18: A solution of HF•Py. [2.7 M in THF, 3.9 mL, 10 equiv; stock solution made up of 0.4 mL HF•Py, 0.8 mL pyridine, 4.0 mL THF] was added to neat TBS ether (+)-**3.17** (295.4 mg, 1.03 mmol). The reaction mixture was stirred at rt for 5 h before quenching with saturated solution of $NaHCO_3$. The layers were separated and the aqueous layer was extracted with EtOAc (3 x 20 mL). The combined organic layers were dried over $MgSO_4$, filtered, and concentrated *in vacuo*. The crude oil was purified *via* flash chromatography on SiO_2 (40% to 60% EtOAc: hexanes) to afford alcohol (+)-**3.18** (148.3 mg, 0.85 mmol, 82%) as a colorless oil: $[\alpha]_D^{20}$ +20.4 (*c* 0.8, CH_2Cl_2); IR (neat) 3394, 2942, 2863, 1743, 1447, 1293, 1250, 1208, 1022 cm^{-1}; ^1H NMR (500 MHz, $CDCl_3$) δ 3.77 (s, 3H), 3.61 (t, *J* = 6.0 Hz, 2 H), 3.24 (d, *J* = 1.9 Hz, 1 H), 3.17 (ddd, *J* = 1.9, 4.7, 5.7 Hz, 1 H), 1.75-1.67 (m, 1 H), 1.66-1.60 (m, 3 H), 1.59-1.52 (m, 2 H); ^{13}C

NMR (125 MHz, $CDCl_3$) δ 169.9, 62.7, 58.6, 53.1, 52.7, 32.4, 31.4, 22.3; HRMS (ES+) *m/z* 197.0799 [$(M+Na)^+$; calcd for $C_8H_{14}O_4$: 197.0790].

4.3 References

(1) Smith, A. B.; Jurica, J. A.; Walsh, S. P. *Org. Lett.* **2008**, *10*, 5625-5628.

(2) Zeng, W.; Chemler, S. R. *J. Org. Chem.* **2008**, *73*, 6045-6047.

(3) Crimmins, M. T.; Stevens, J. M.; Schaaf, G. M. *Org. Lett.* **2009**, *11*, 3990-3993.

(4) Pettit, G. R.; Xu, J.-P.; Chapuis, J.-C.; Pettit, R. K.; Tackett, L. P.; Doubek, D. L.; Hooper, J. N. A.; Schmidt, J. M. *J. Med. Chem.* **2004**, *47*, 1149-1152.

(5) Li, P.; Li, J.; Arikan, F.; Ahlbrecht, W.; Dieckmann, M.; Menche, D. *J. Org. Chem.* **2010**, *75*, 2429-2444.

(6) Jung, M. E.; Berliner, J. A.; Koroniak, L.; Gugiu, B. G.; Watson, A. D. *Org. Lett.* **2008**, *10*, 4207-4209.

Appendix. Spectroscopic Data

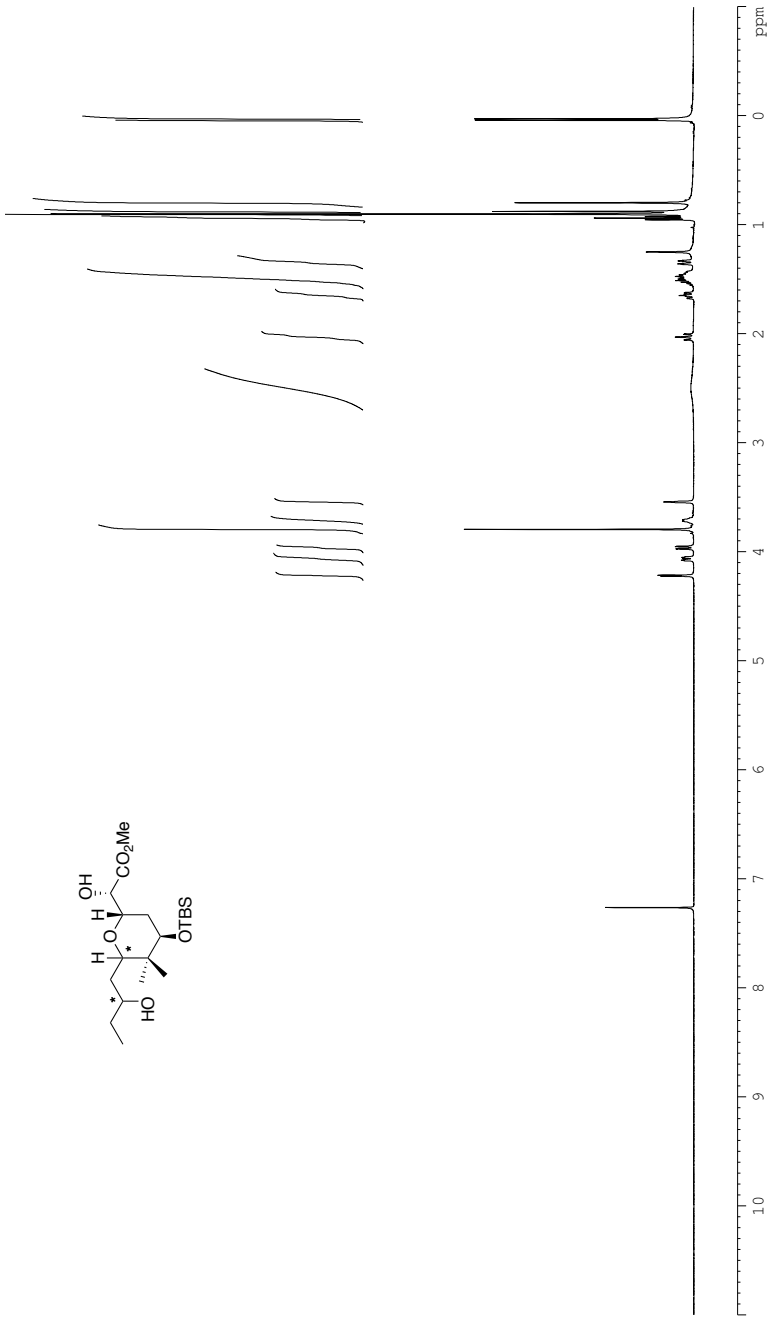

Figure A2.1. ^{1}H NMR Spectrum (500 MHz) of Compound (–)-**2.37** in $CDCl_3$

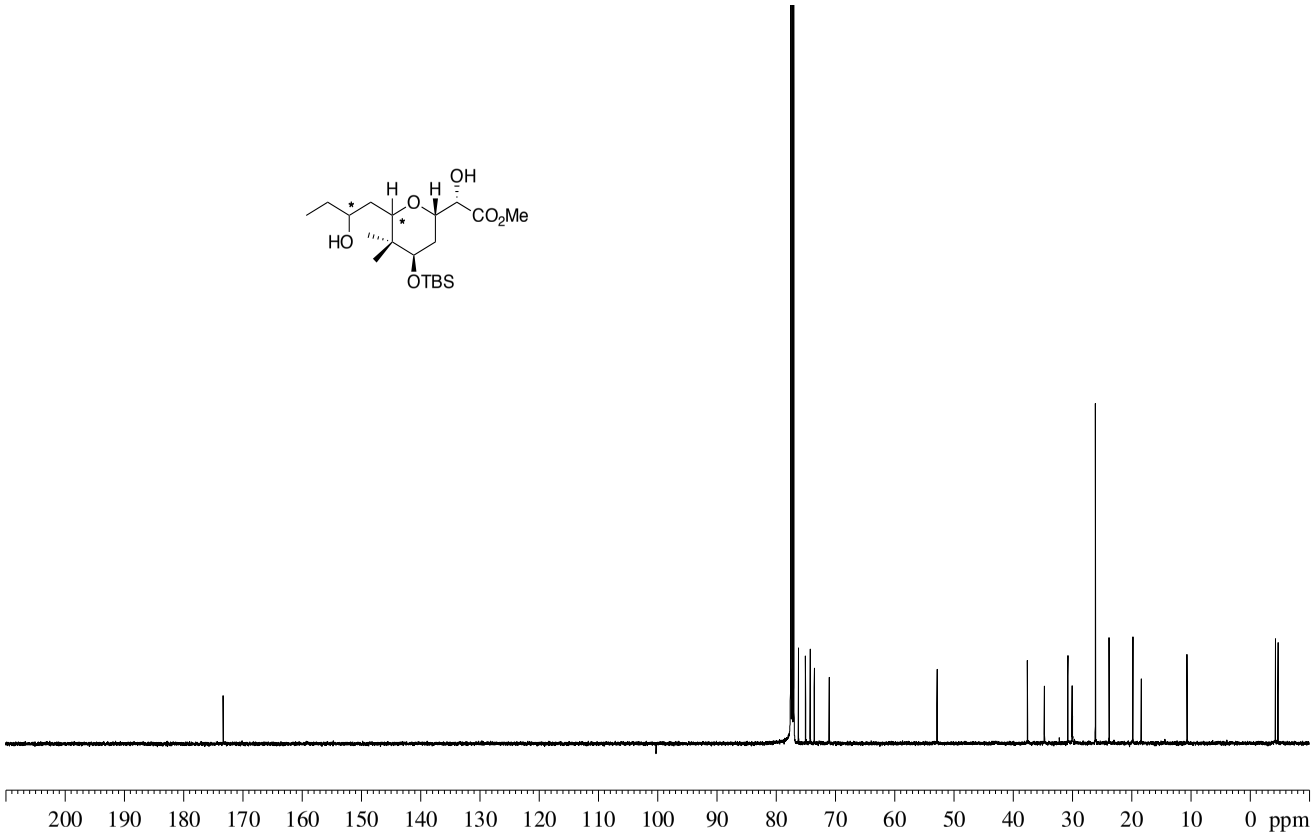

Figure A2.2. ^{13}C NMR Spectrum (125 MHz) of Compound (–)-**2.37** in $CDCl_3$

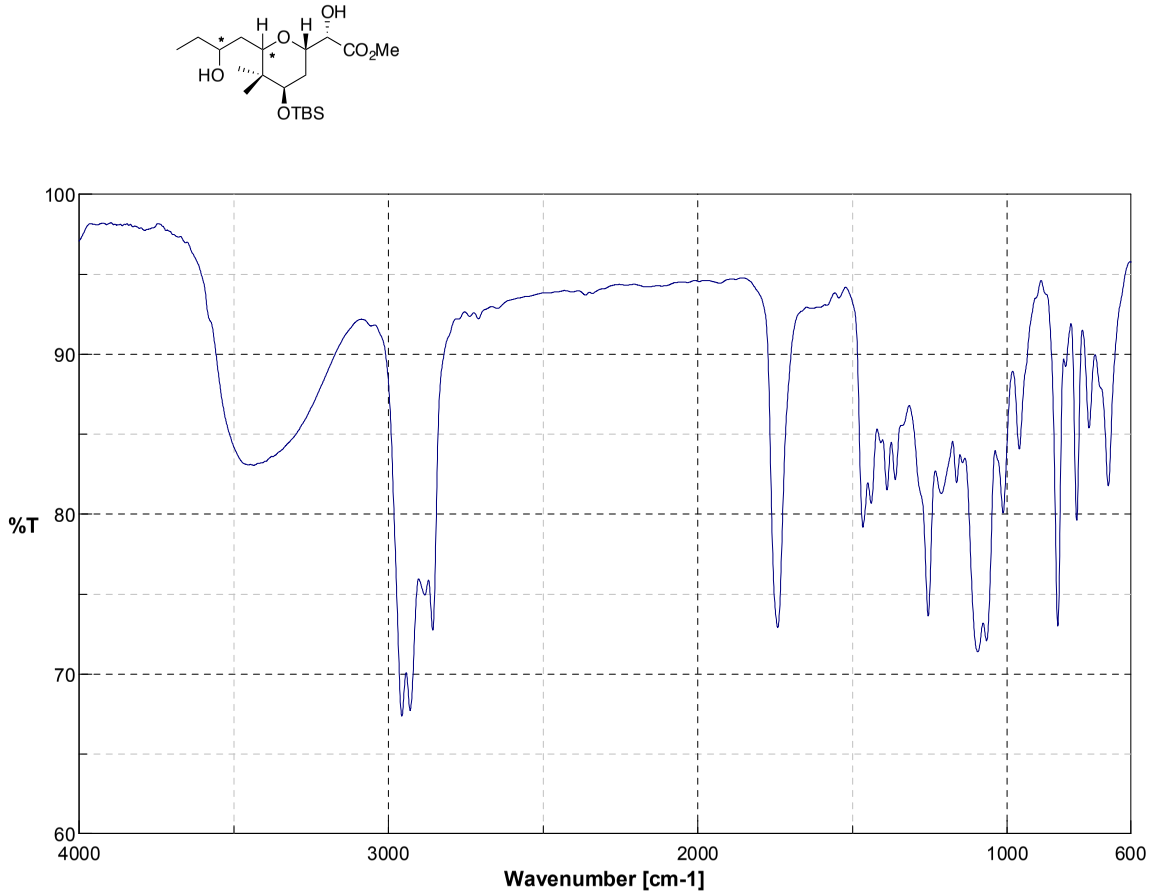

Figure A2.3. Infrared Spectrum of Compound (+)-**2.37**

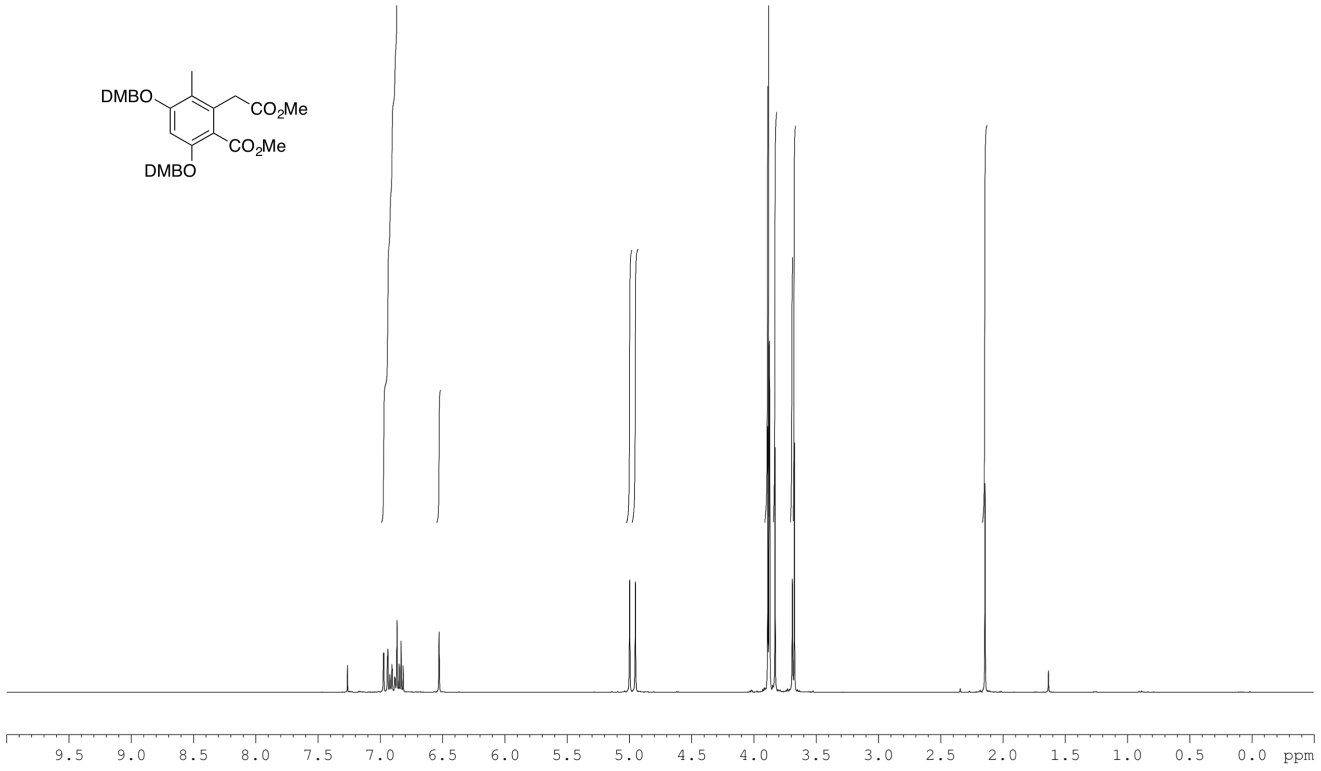

Figure A2.4. ^{1}H NMR Spectrum (500 MHz) of Compound **2.47** in $CDCl_3$

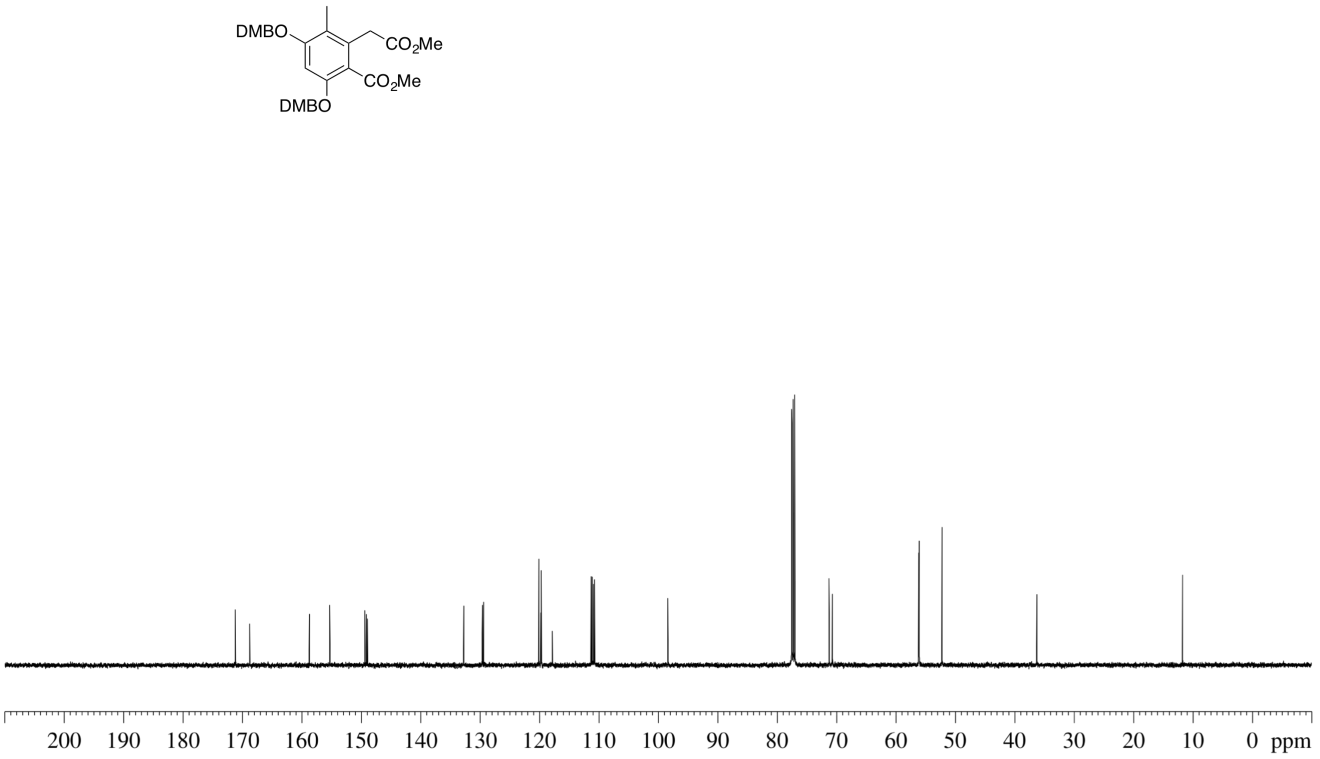

Figure A2.5. ^{13}C NMR Spectrum (125 MHz) of Compound **2.47** in $CDCl_3$

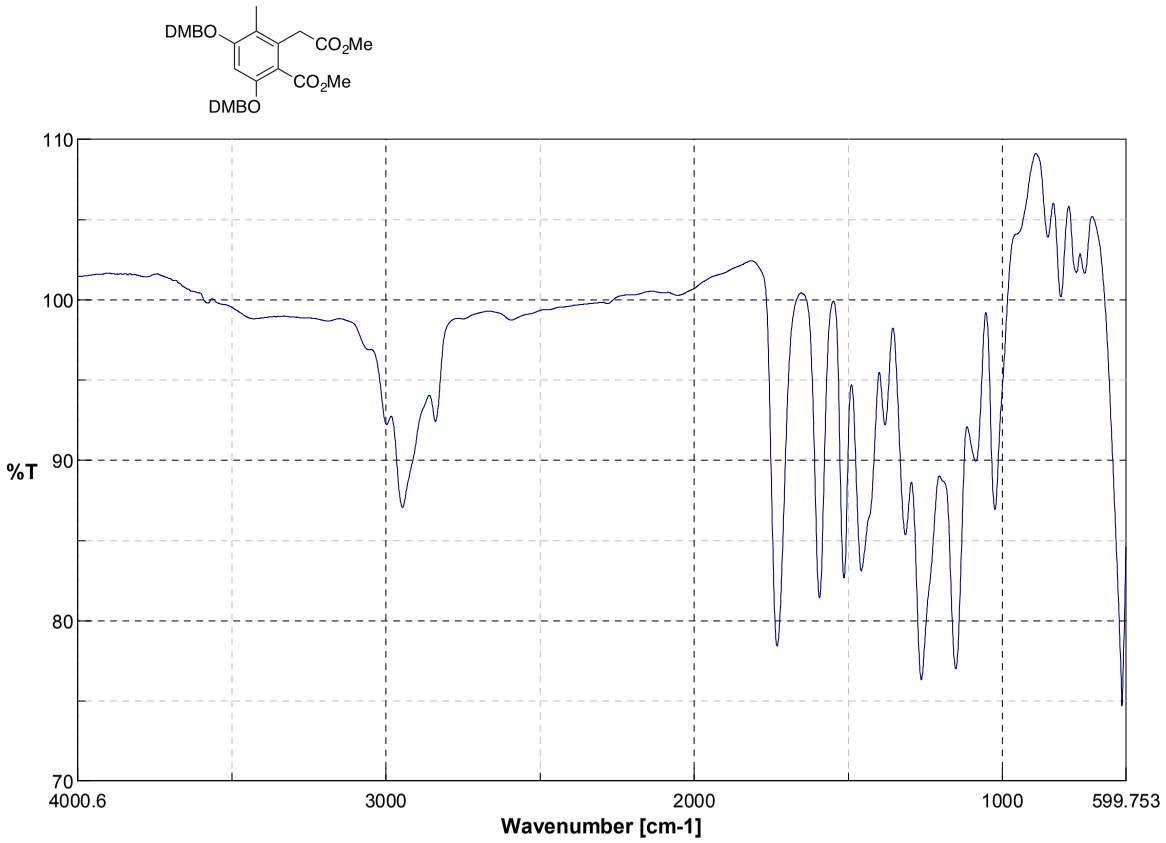

Figure A2.6. Infrared Spectrum of Compound **2.47**

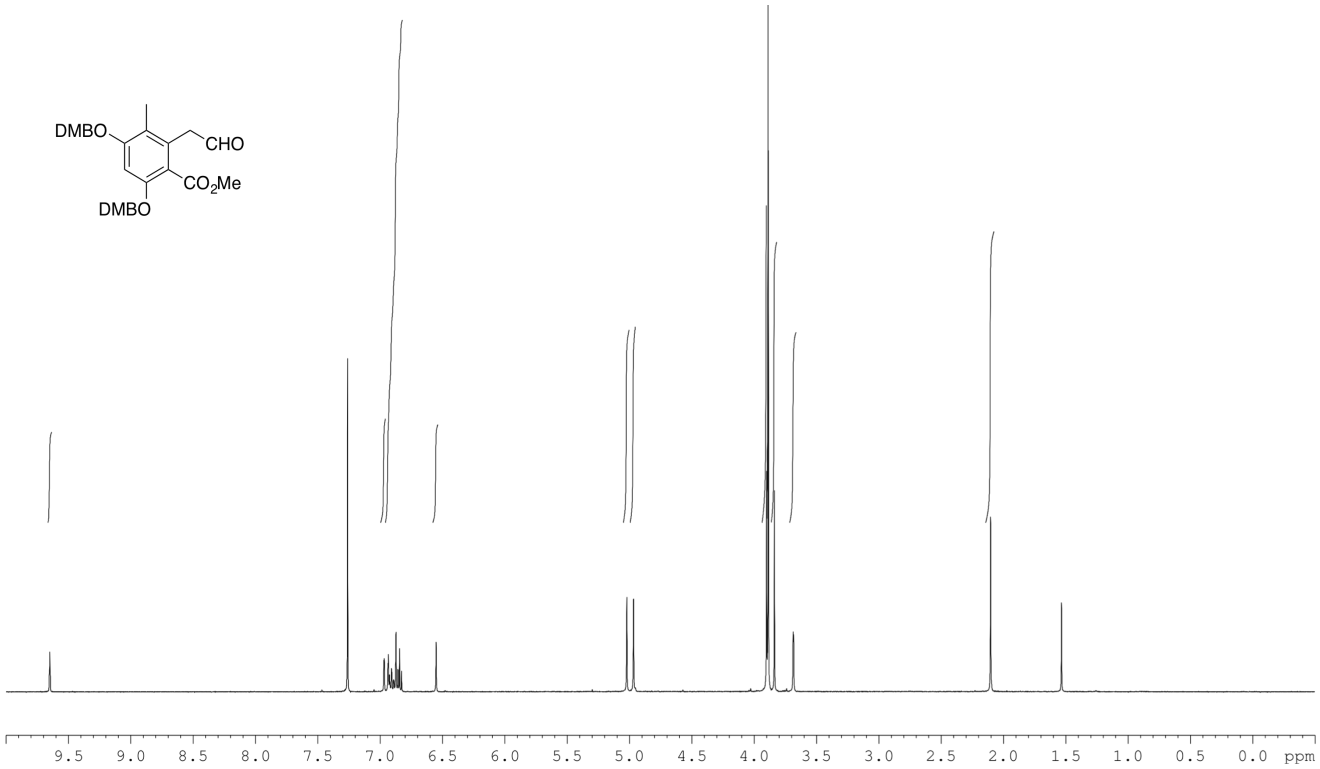

Figure A2.7. ^{1}H NMR Spectrum (500 MHz) of Compound **2.48** in $CDCl_3$

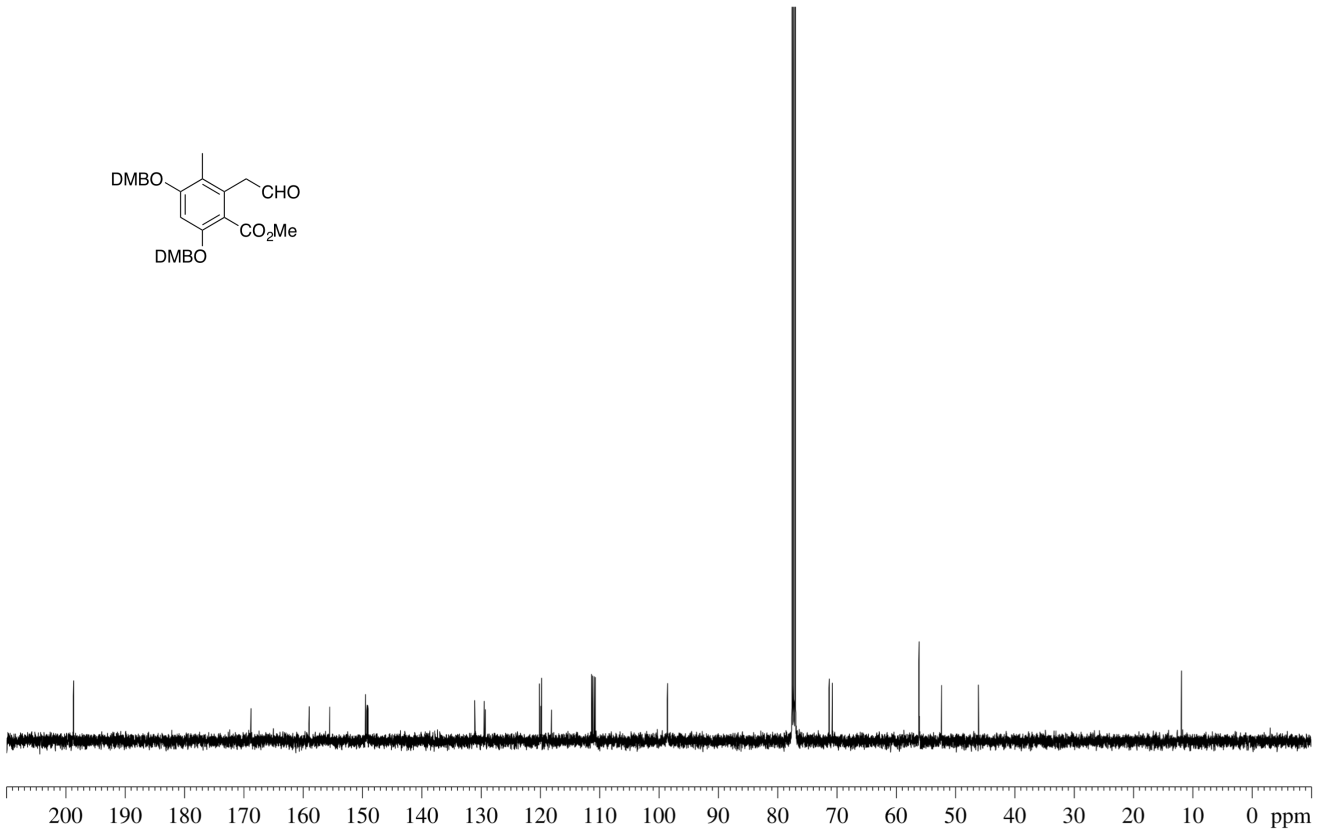

Figure A2.8. ^{13}C NMR Spectrum (125 MHz) of Compound **2.48** in $CDCl_3$

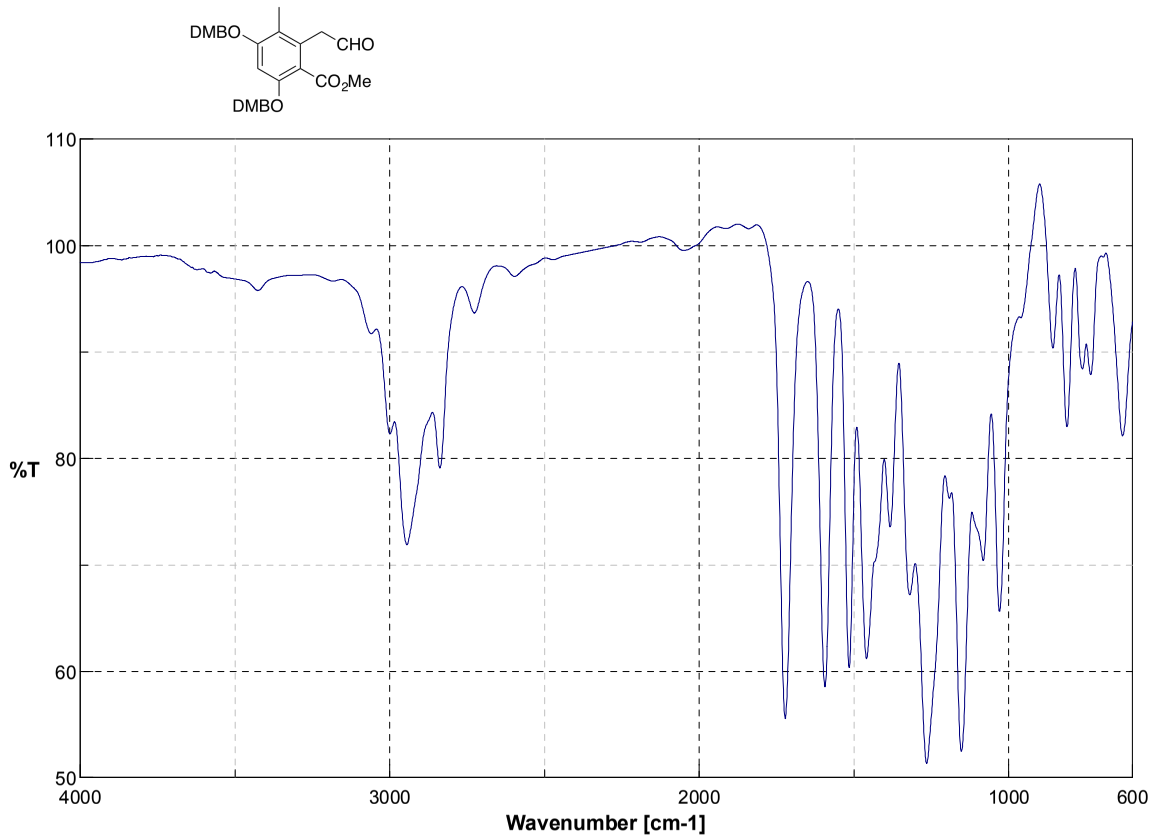

Figure A2.9. Infrared Spectrum of Compound **2.48**

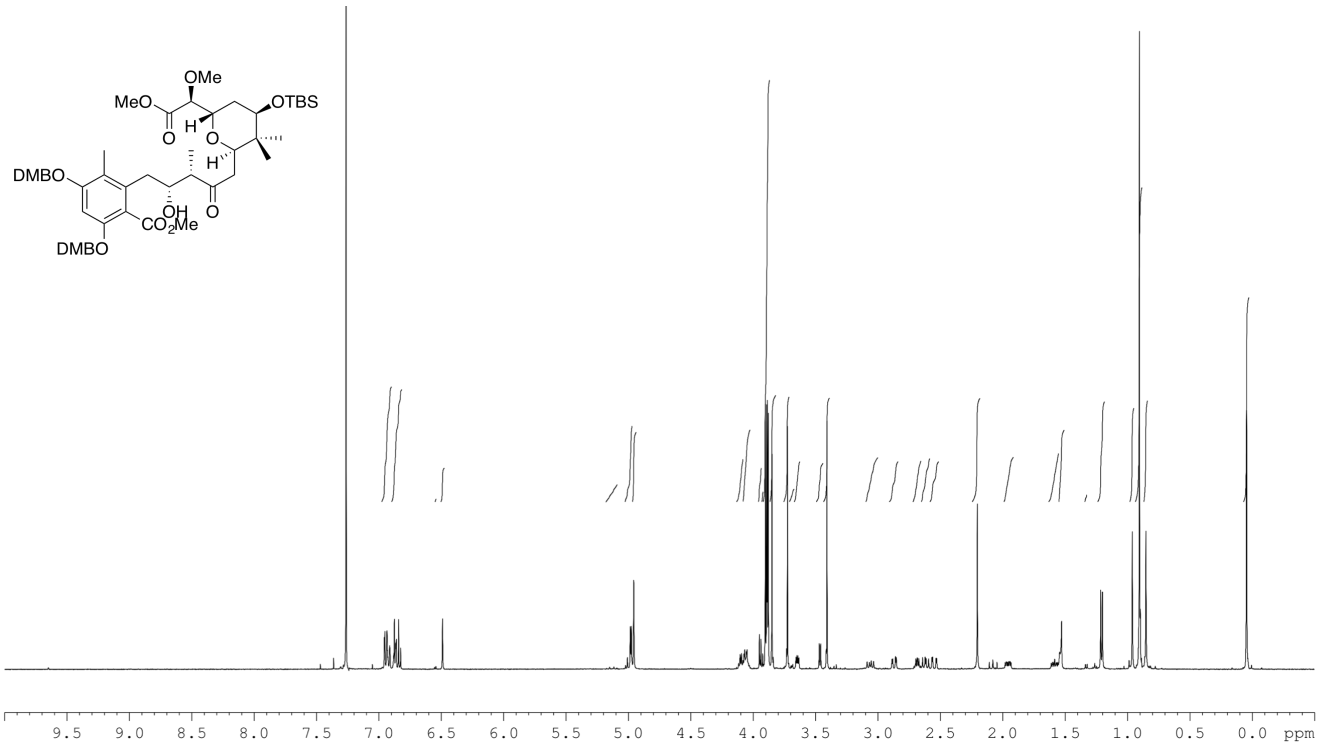

Figure A2.10. ^{1}H NMR Spectrum (500 MHz) of Compound (+)-**2.49** in $CDCl_3$

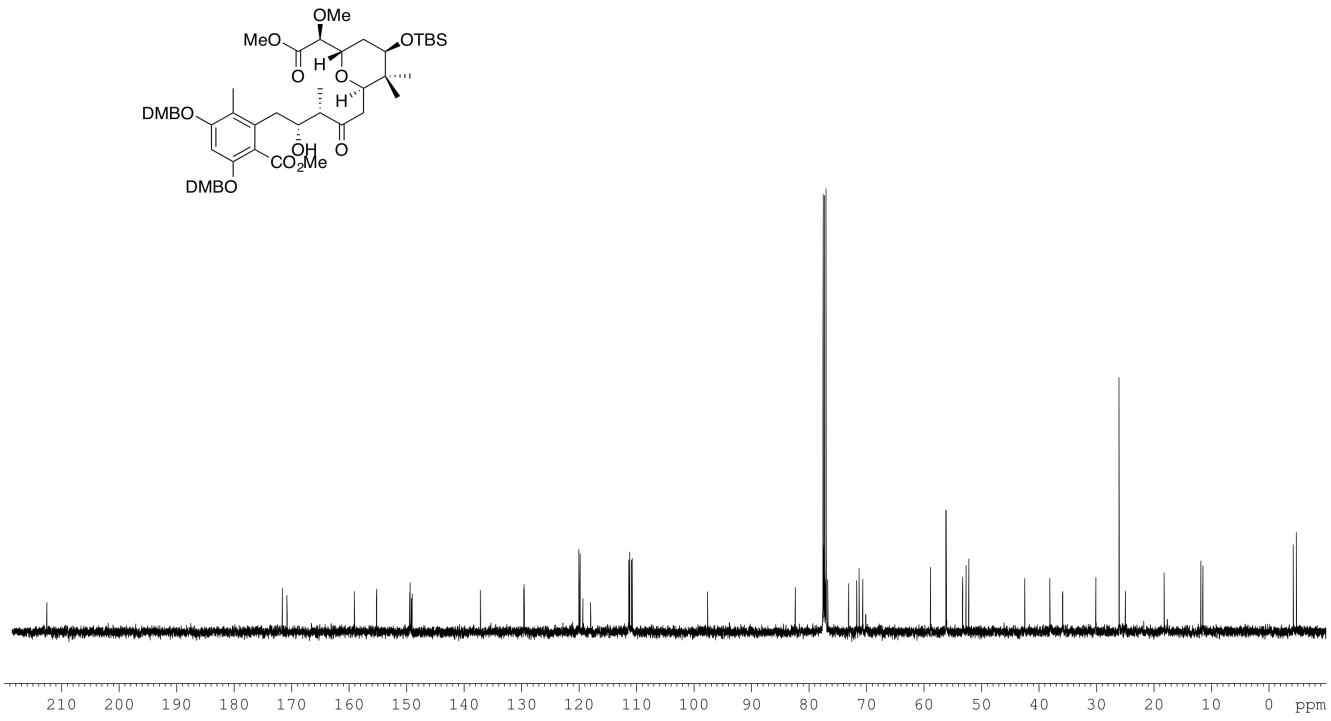

Figure A2.11.^{13}C NMR Spectrum (125 MHz) of Compound (+)-**2.49** in $CDCl_3$

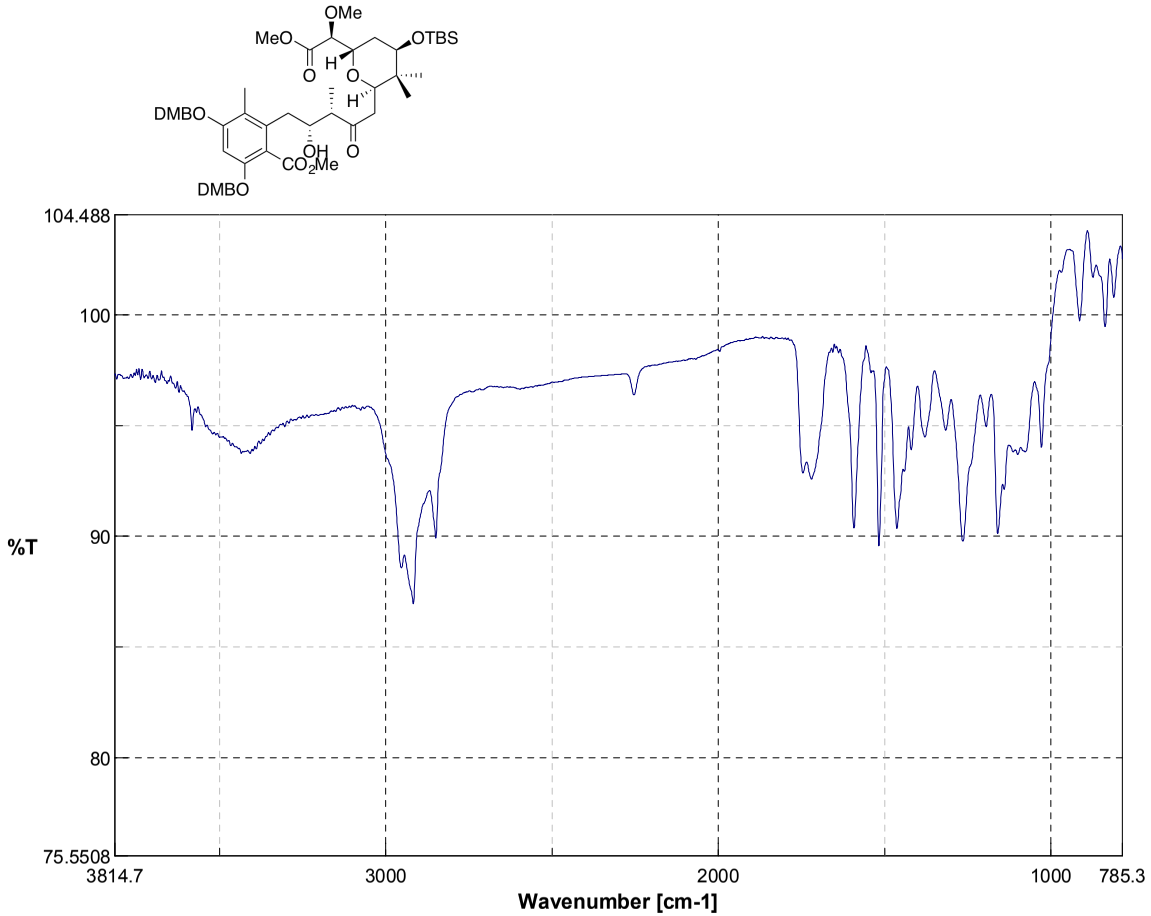

Figure A2.12. Infrared Spectrum of Compound (+)-**2.49**

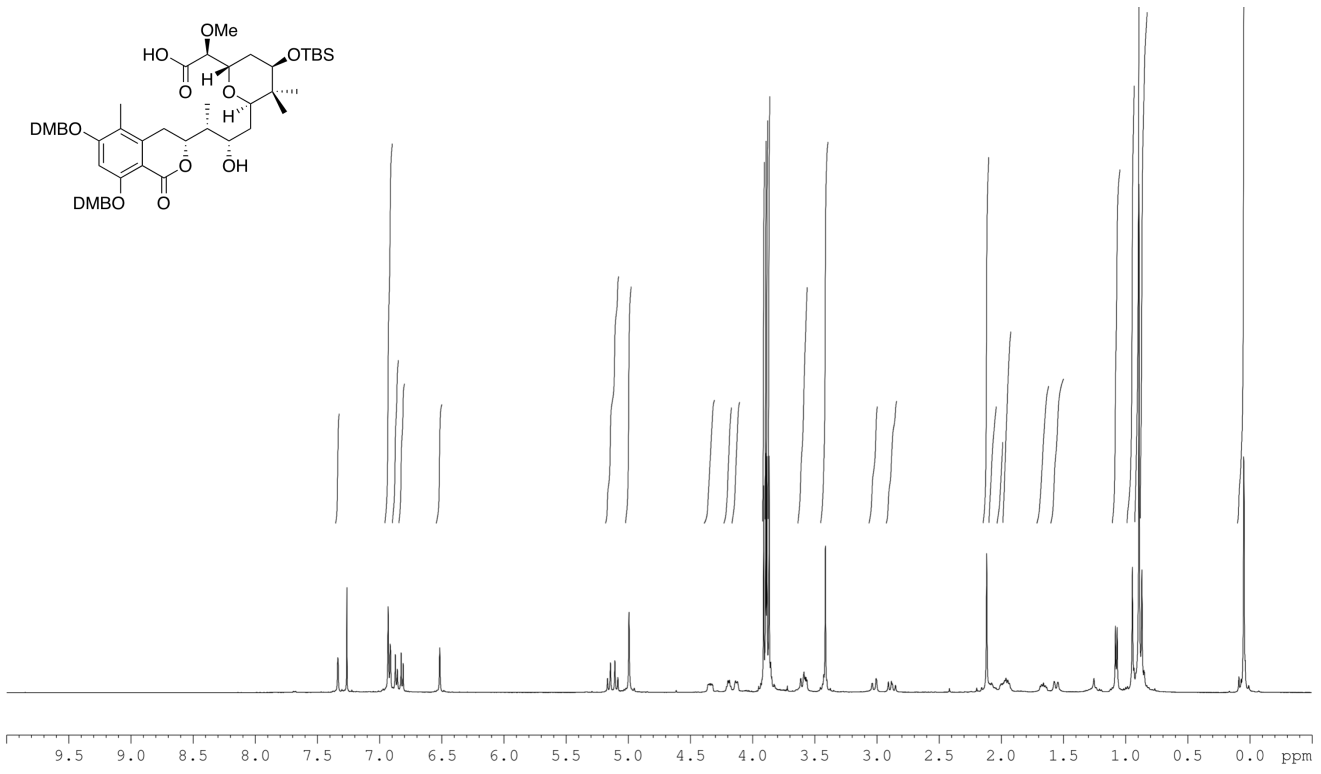

Figure A2.13. ^{1}H NMR Spectrum (500 MHz) of Compound (+)-**2.52** in $CDCl_3$

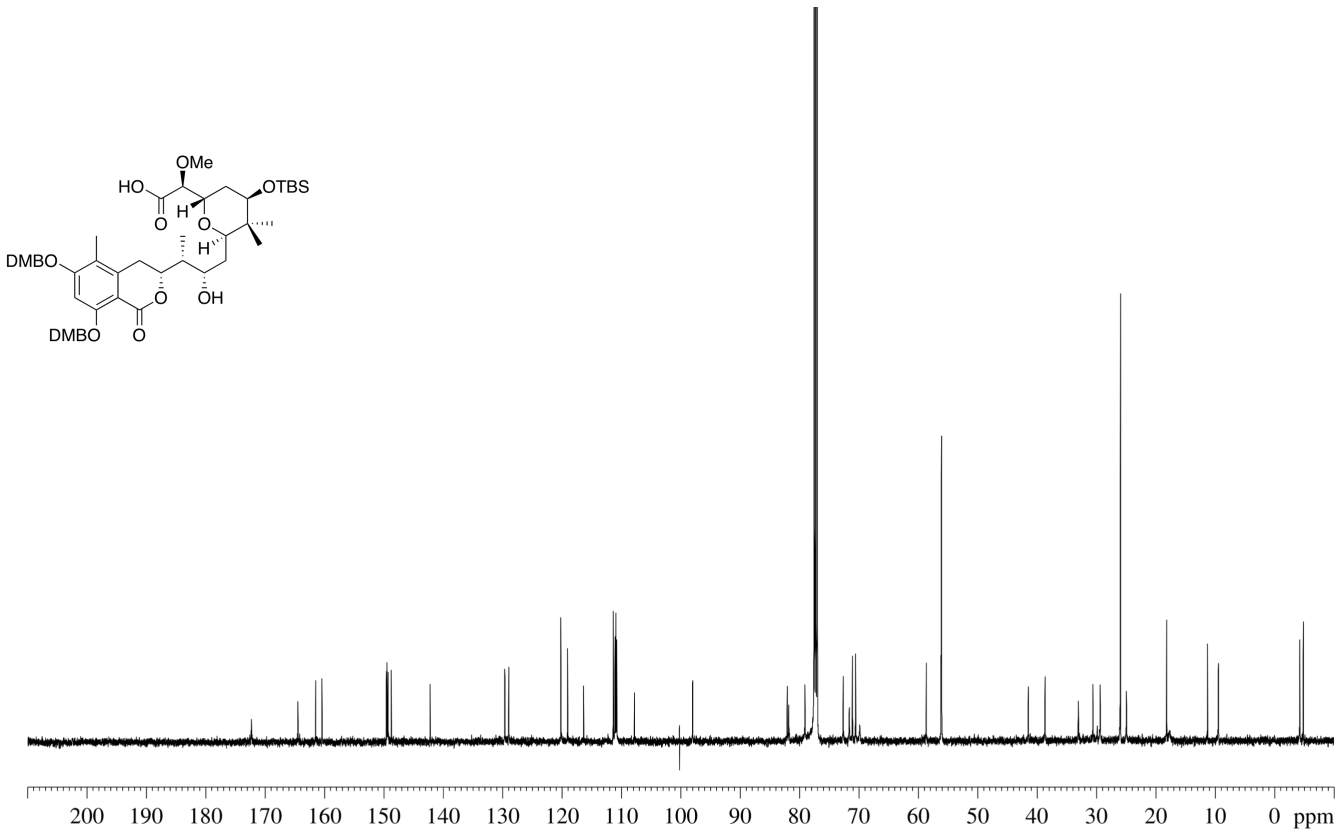

Figure A2.14. ^{13}C NMR Spectrum (125 MHz) of Compound (+)-**2.52** in $CDCl_3$

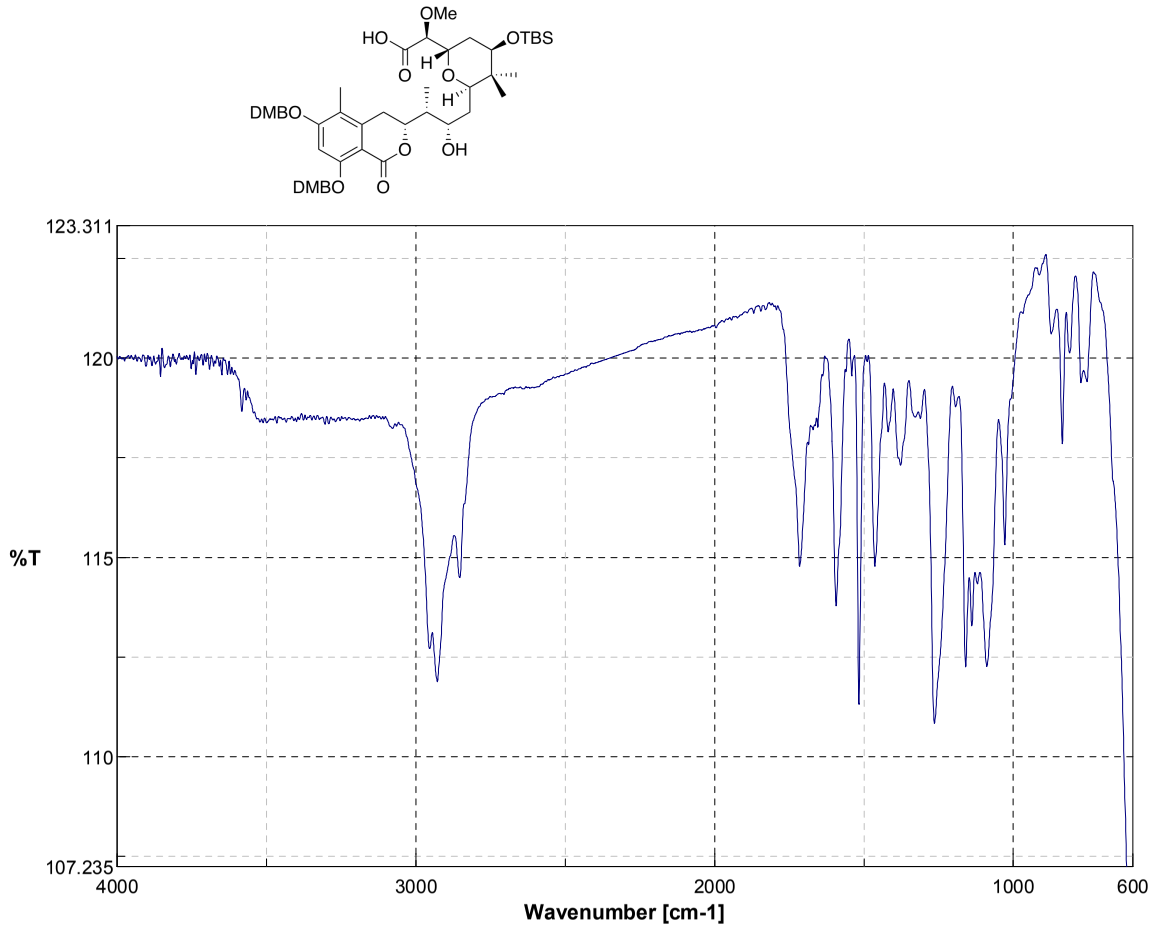

Figure A2.15. Infrared Spectrum of Compound (+)-**2.52**

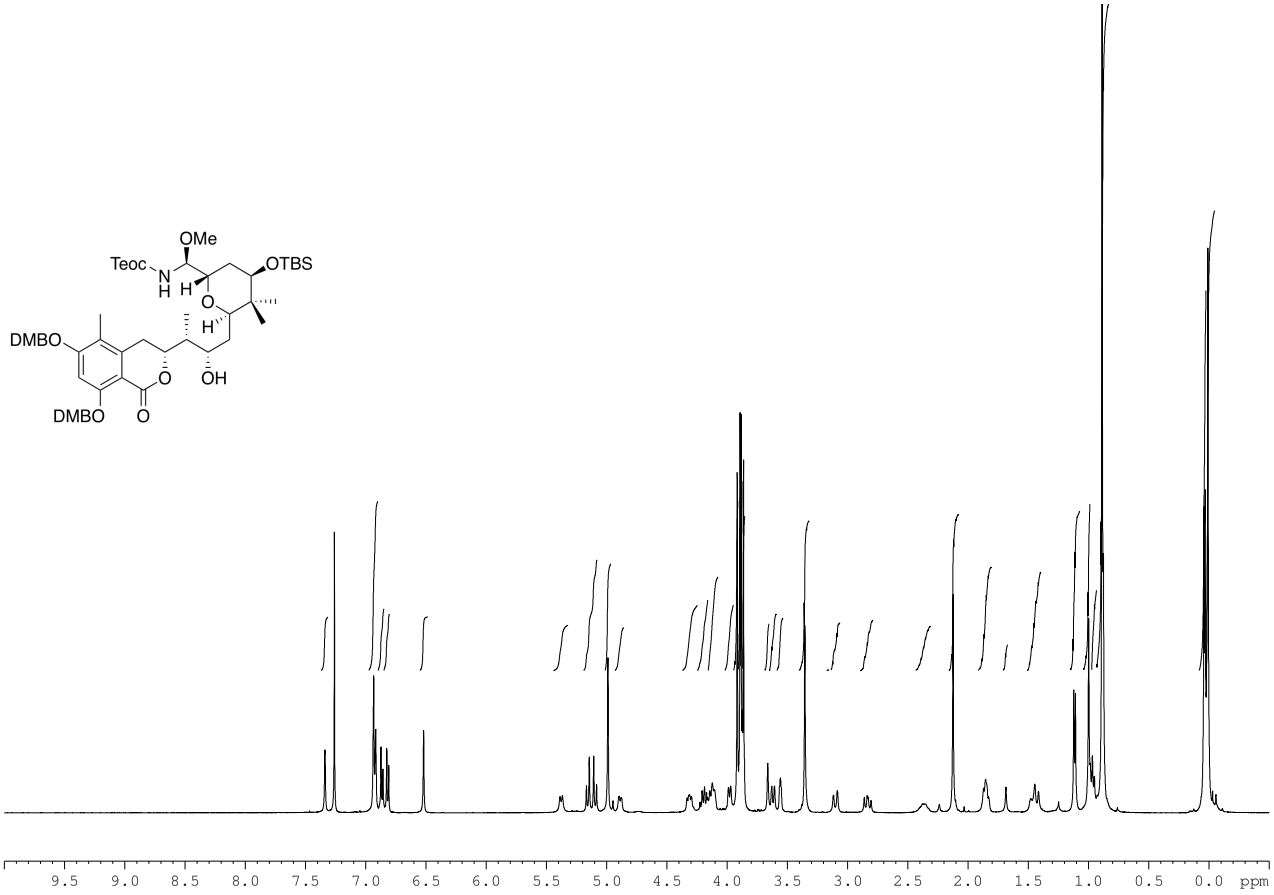

Figure A2.16. ^{1}H NMR Spectrum (500 MHz) of Compound (+)-**S1** in $CDCl_3$

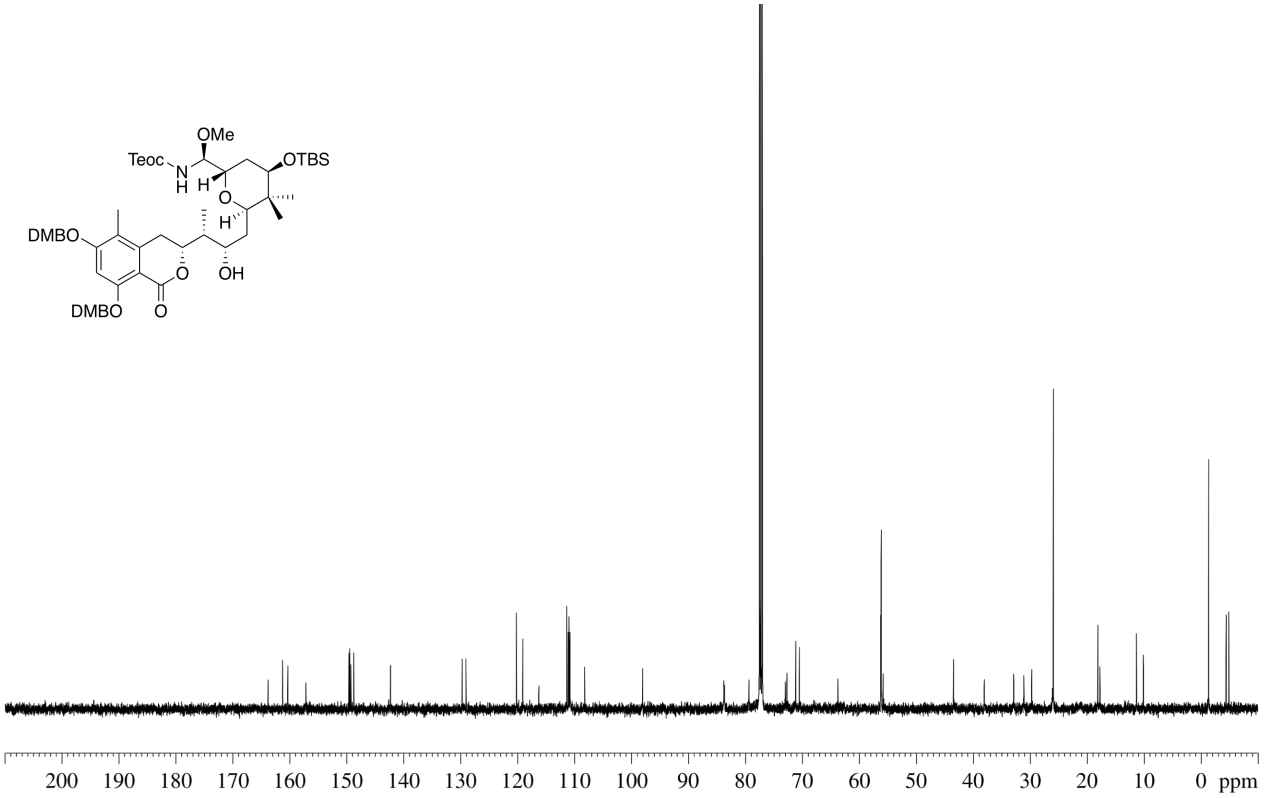

Figure A2.17. ^{13}C NMR Spectrum (125 MHz) of Compound (+)-**S1** in $CDCl_3$

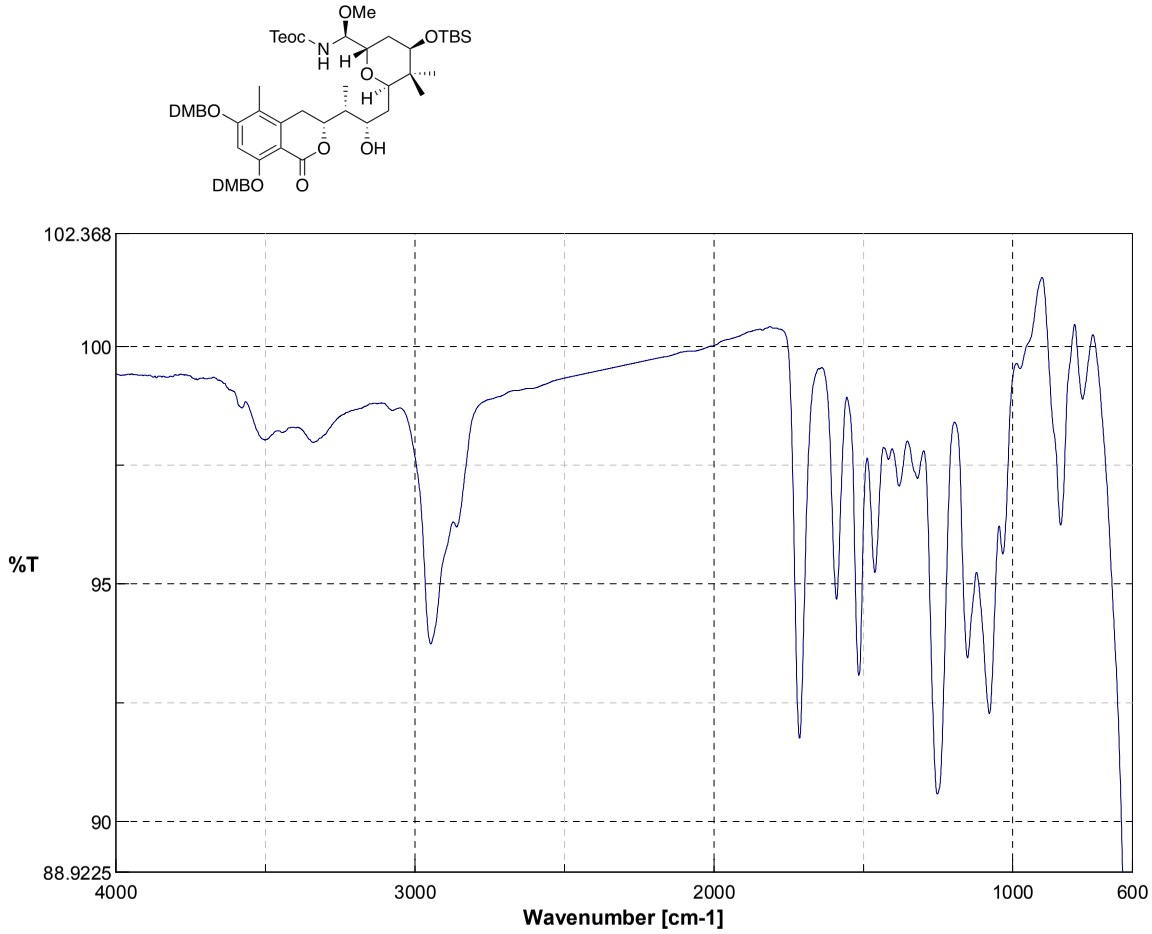

Figure A2.18. Infrared Spectrum of Compound (+)-**S1**

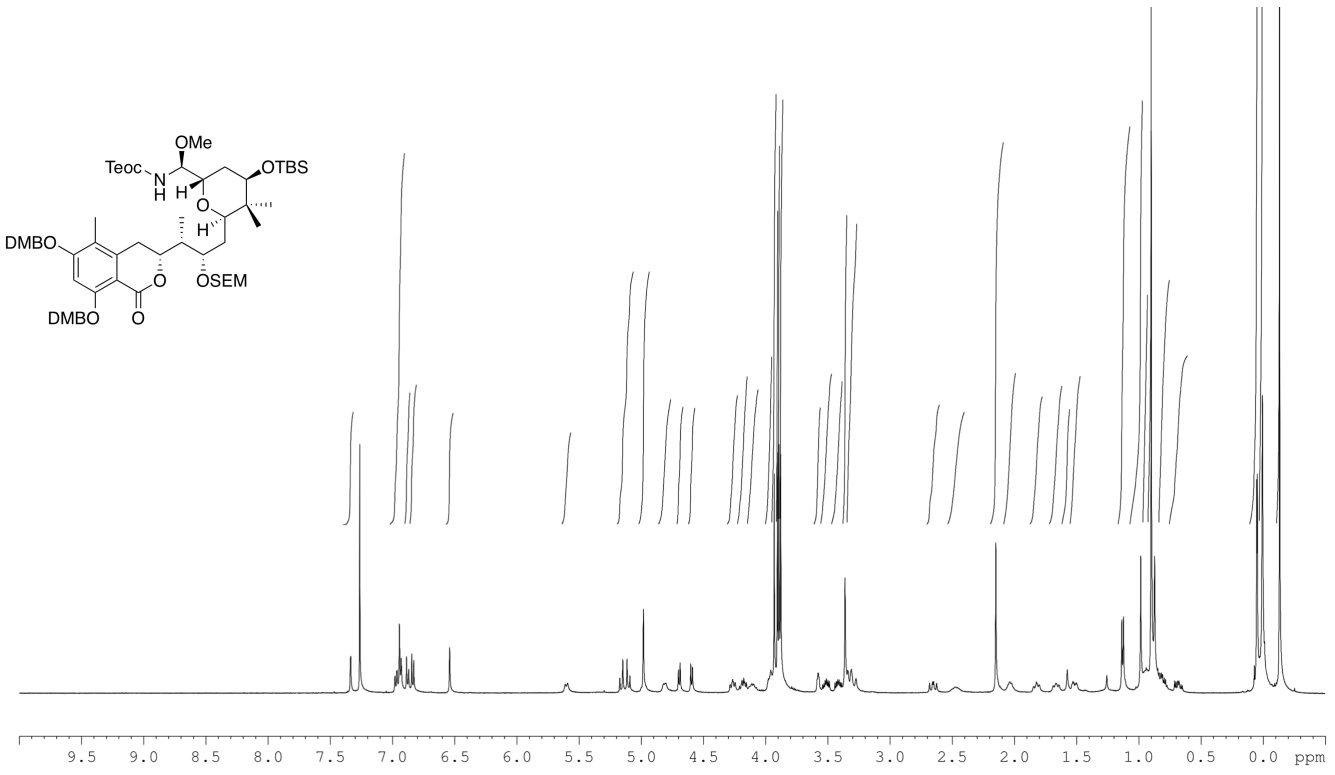

Figure A2.19. ^{1}H NMR Spectrum (500 MHz) of Compound (+)-**2.53** in $CDCl_3$

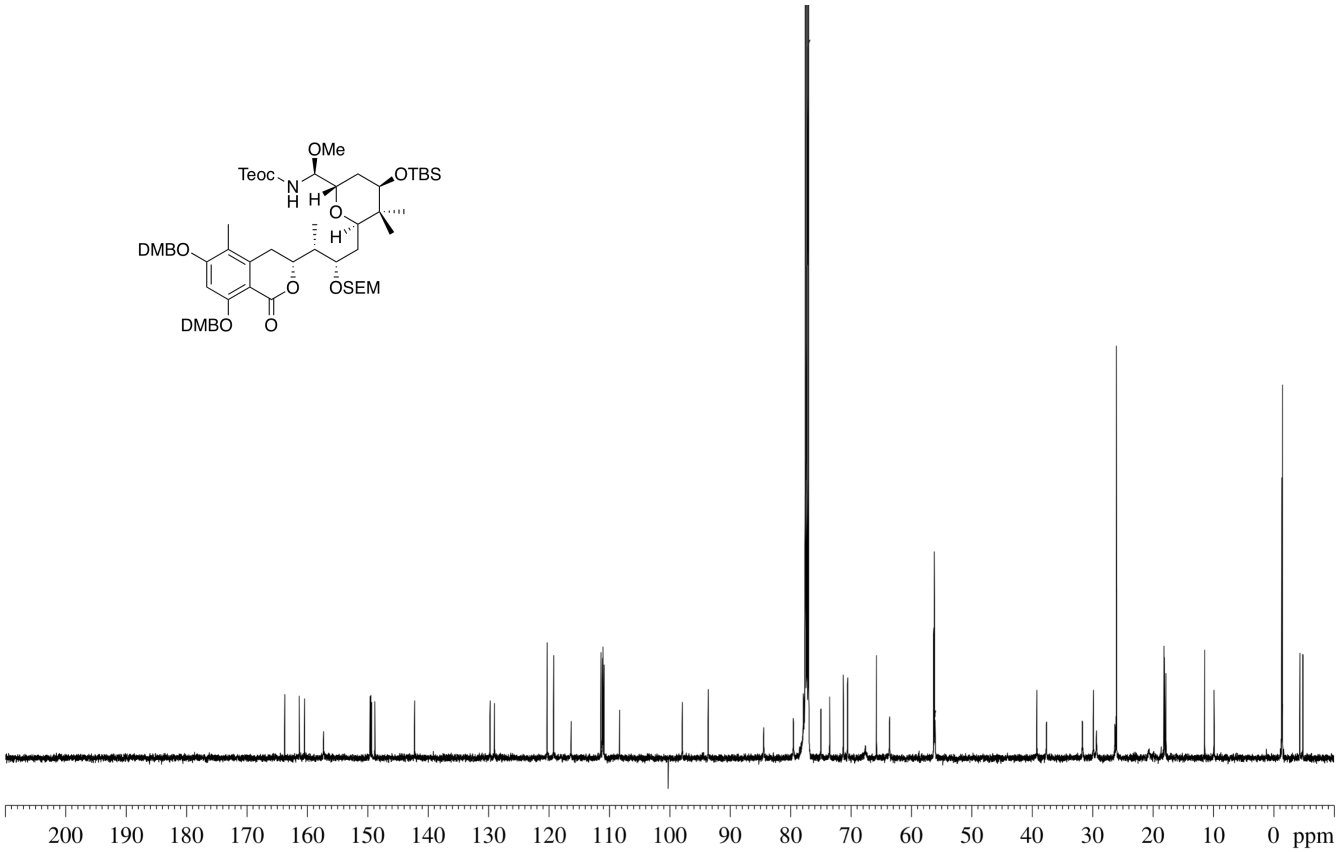

Figure A2.20. ^{13}C NMR Spectrum (125 MHz) of Compound (+)-**2.53** in $CDCl_3$

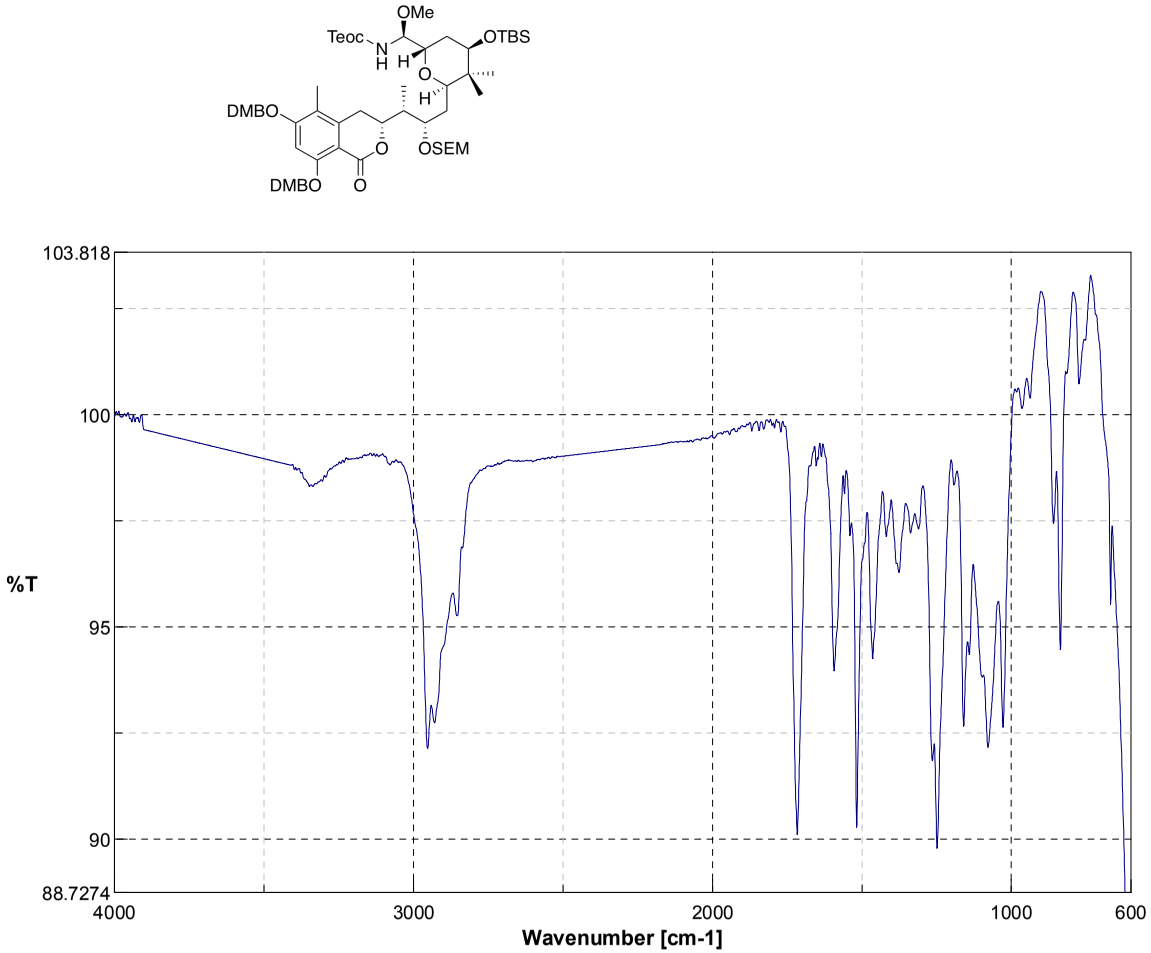

Figure A2.21. Infrared Spectrum of Compound (+)-**2.53**

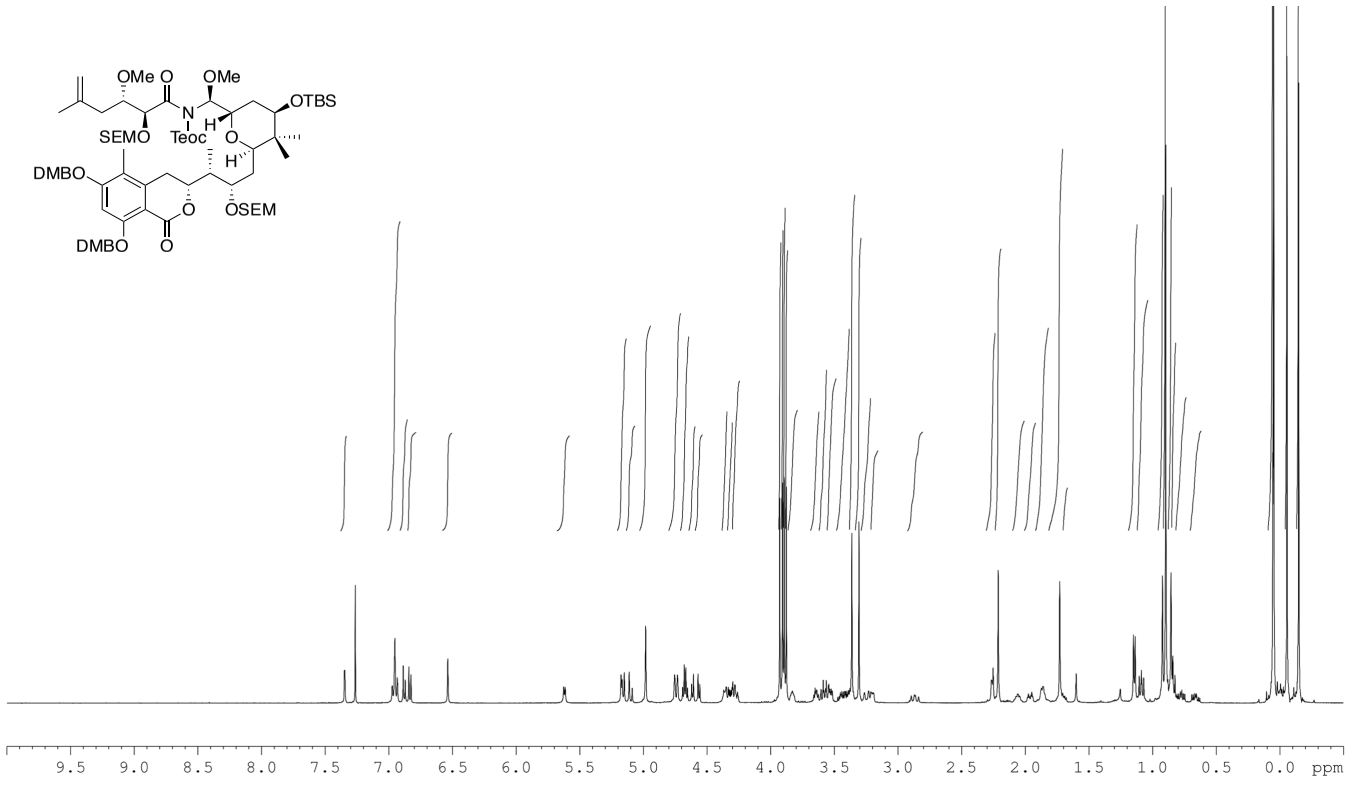

Figure A2.22. ^{1}H NMR Spectrum (500 MHz) of Compound (+)-**2.56** in $CDCl_3$

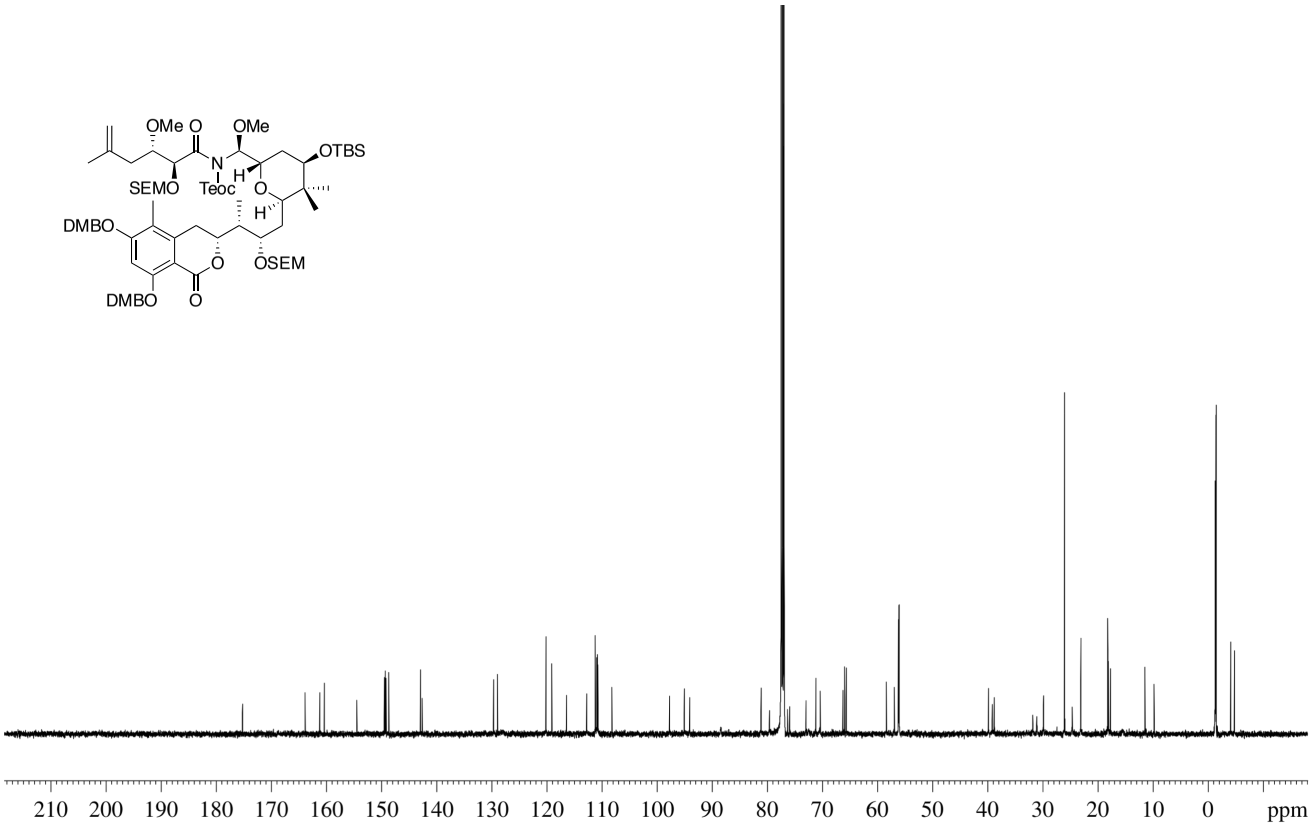

Figure A2.23. ^{13}C NMR Spectrum (125 MHz) of Compound (+)-**2.56** in $CDCl_3$

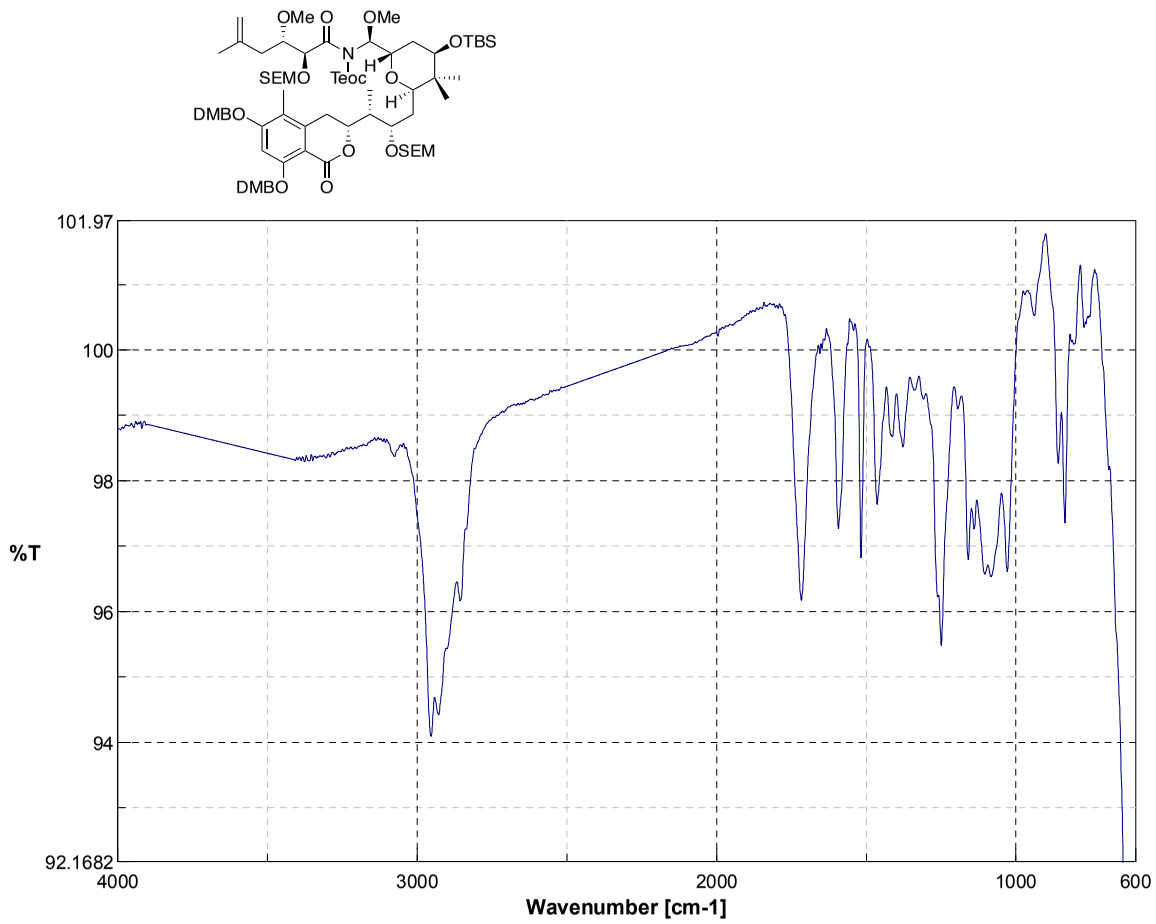

Figure A2.24. Infrared Spectrum of Compound (+)-**2.56**

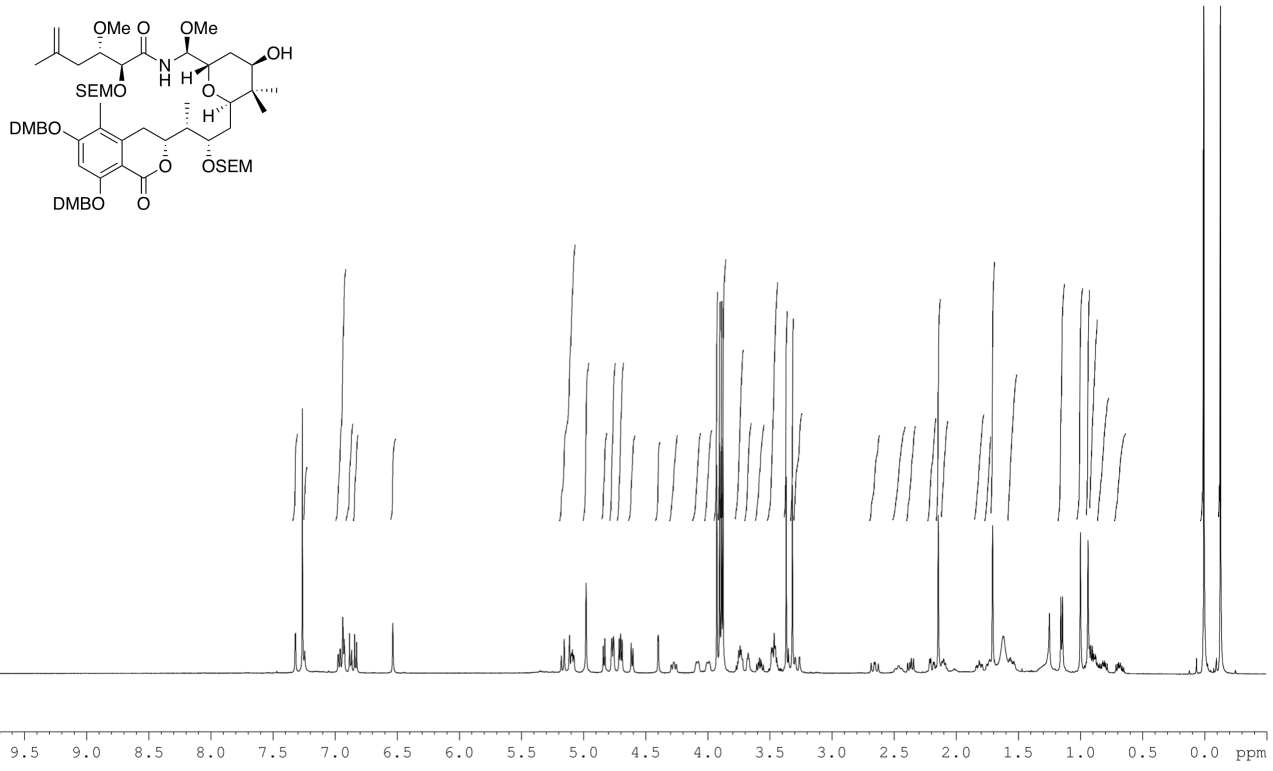

Figure A2.25. ^{1}H NMR Spectrum (500 MHz) of Compound (–)-**3.4** in $CDCl_3$

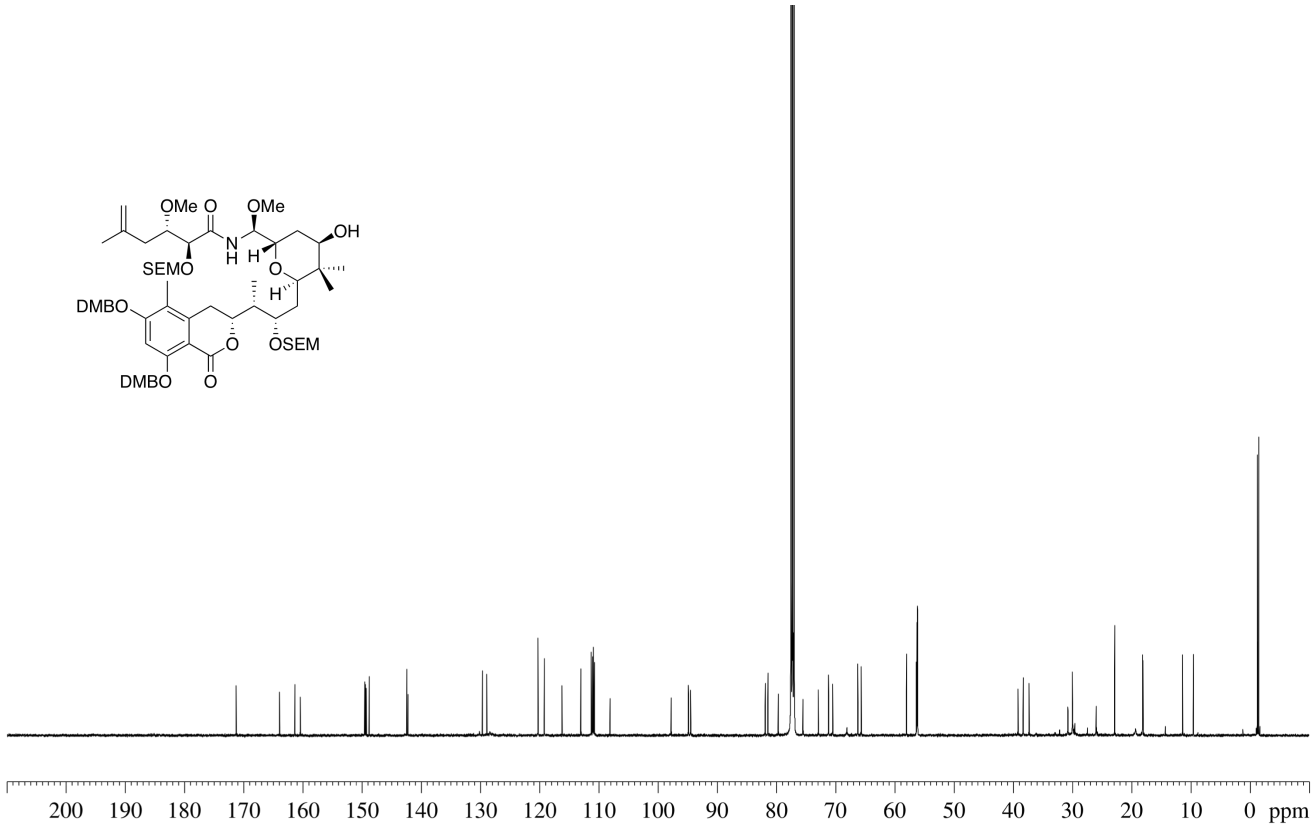

Figure A2.26. ^{13}C NMR Spectrum (125 MHz) of Compound (–)-**3.4** in $CDCl_3$

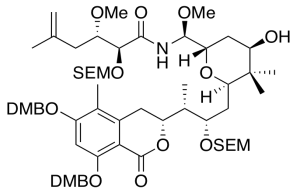

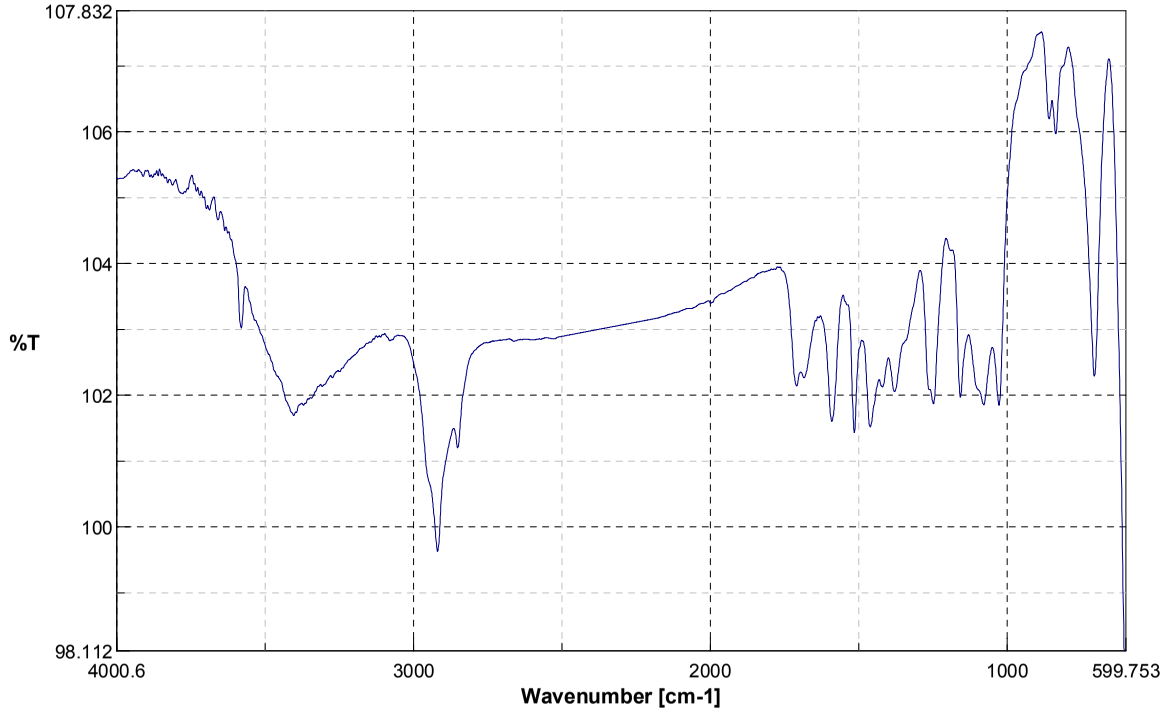

Figure A2.27. Infrared Spectrum of Compound (–)-**3.4**

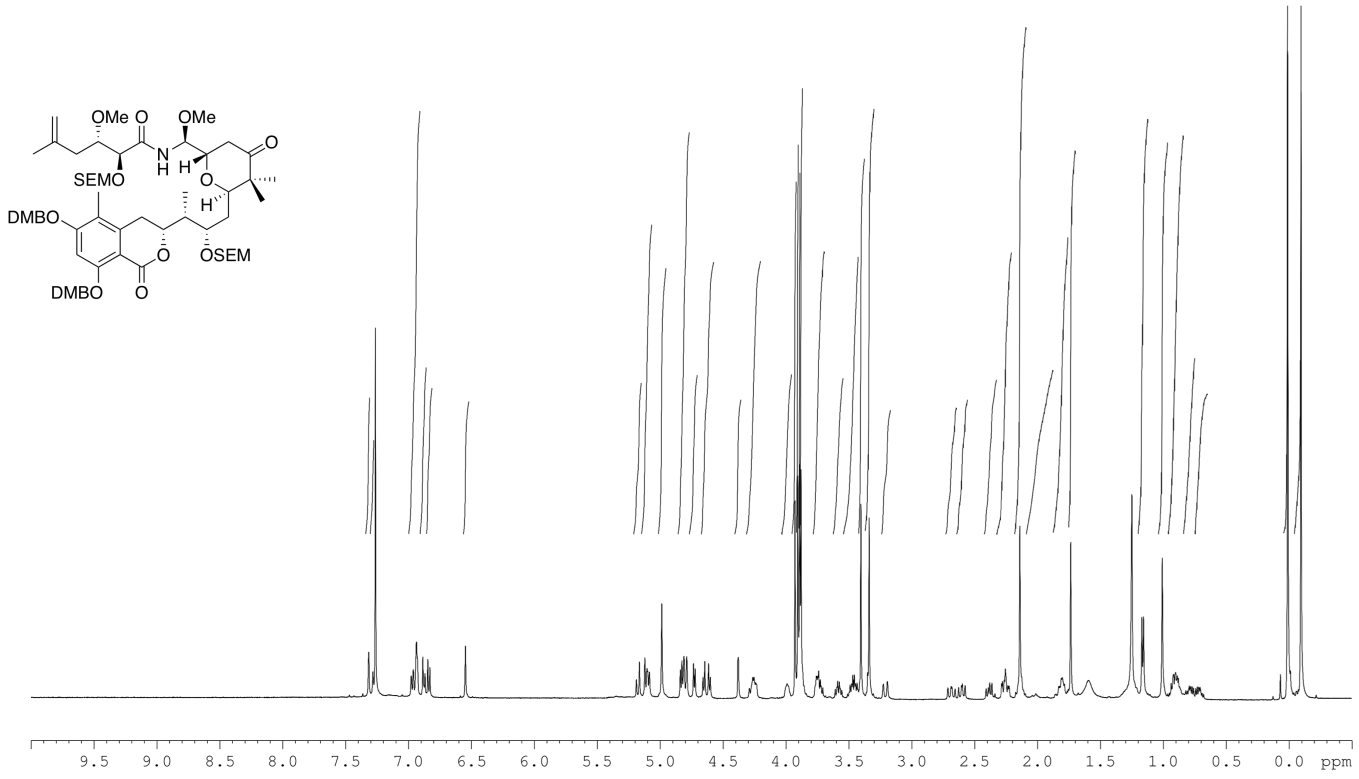

Figure A2.28. ^{1}H NMR Spectrum (500 MHz) of Compound (–)-**2.57** in $CDCl_3$

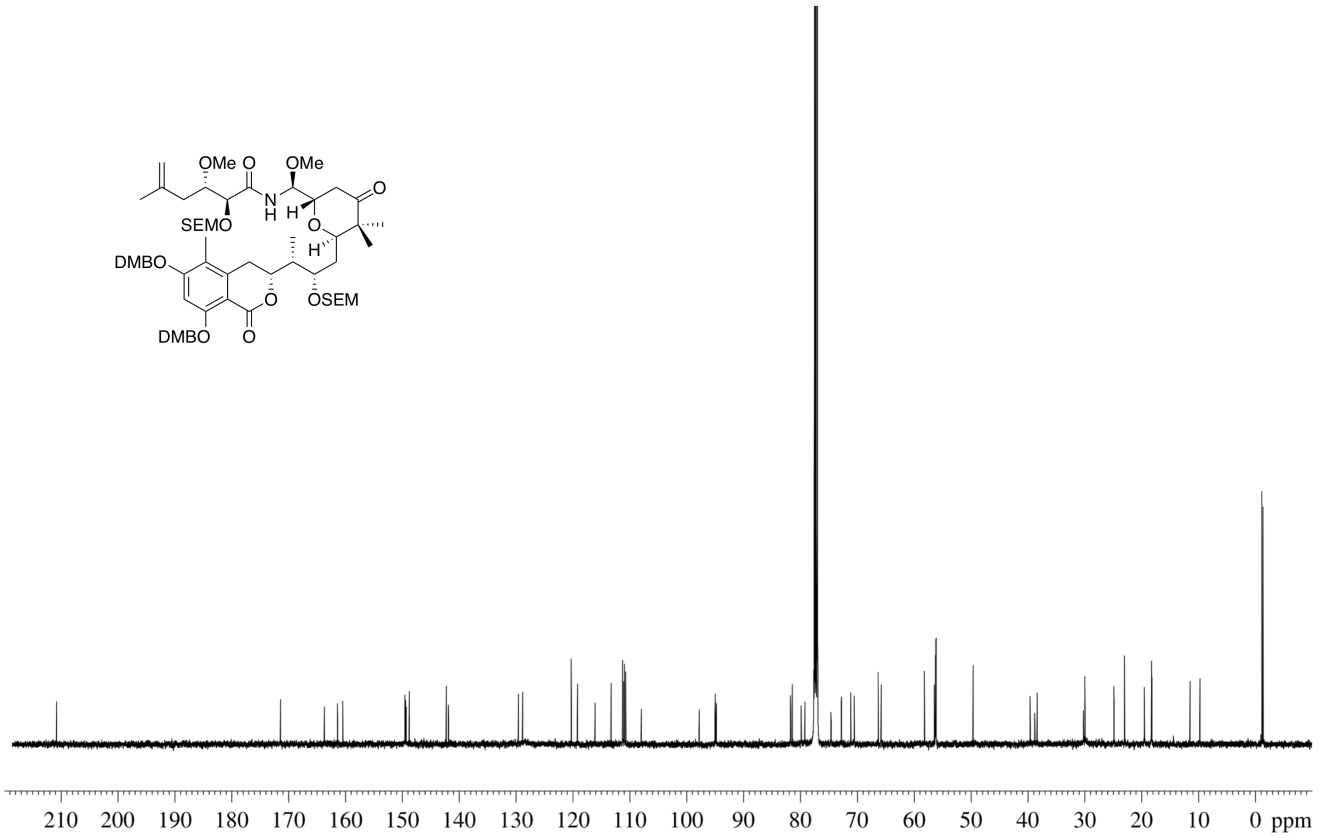

Figure A2.29. ^{13}C NMR Spectrum (125 MHz) of Compound (–)-**2.57** in $CDCl_3$

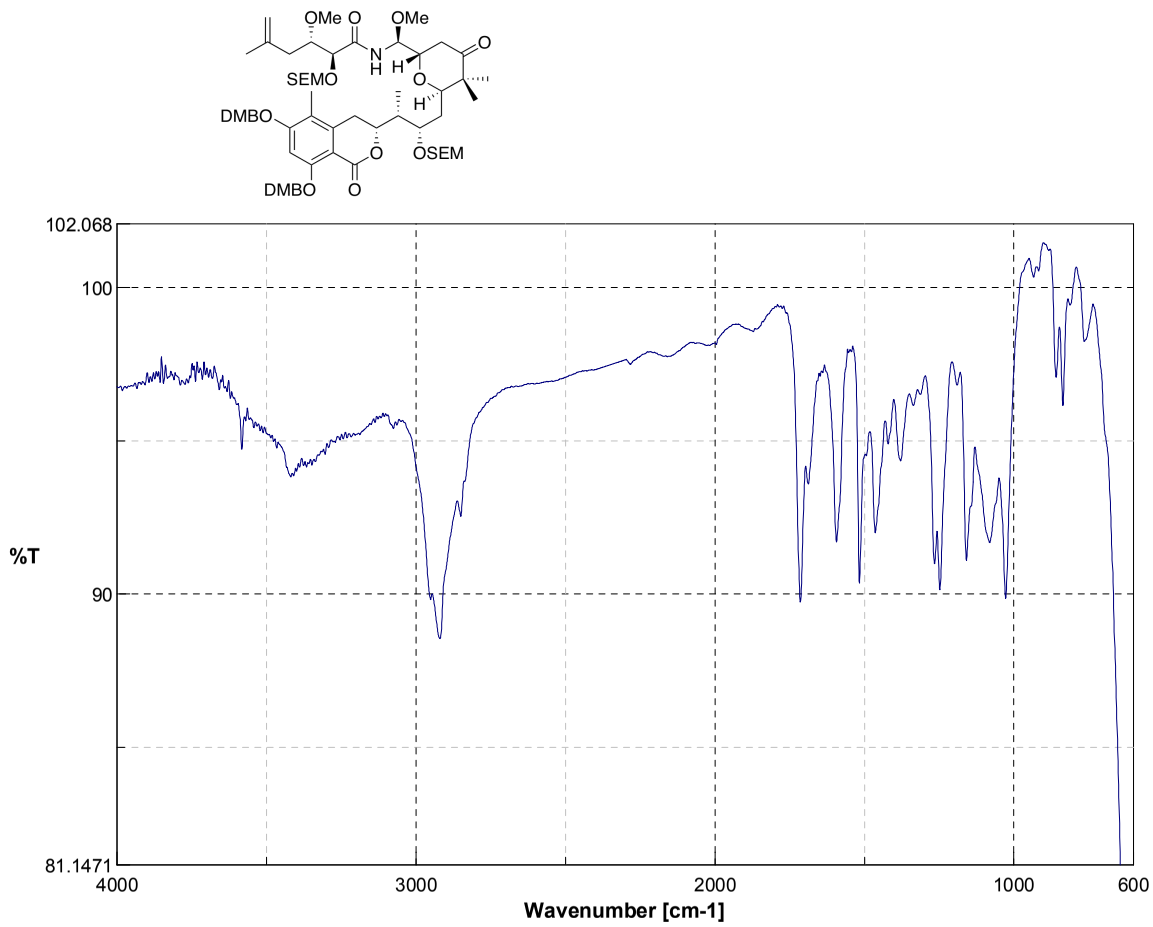

Figure A2.30. Infrared Spectrum of Compound (–)-**2.57**

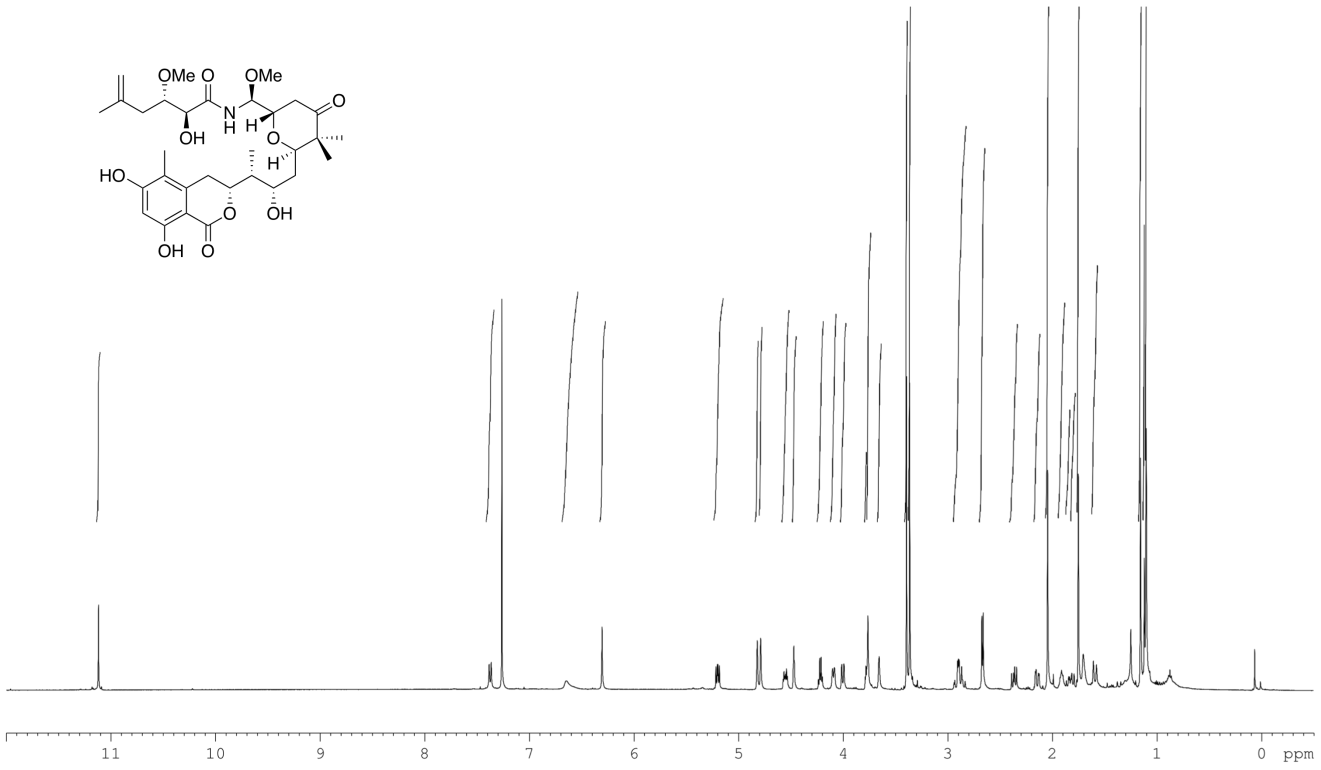

Figure A2.31. ^{1}H NMR Spectrum (500 MHz) of Compound (–)-**2.2** in $CDCl_3$

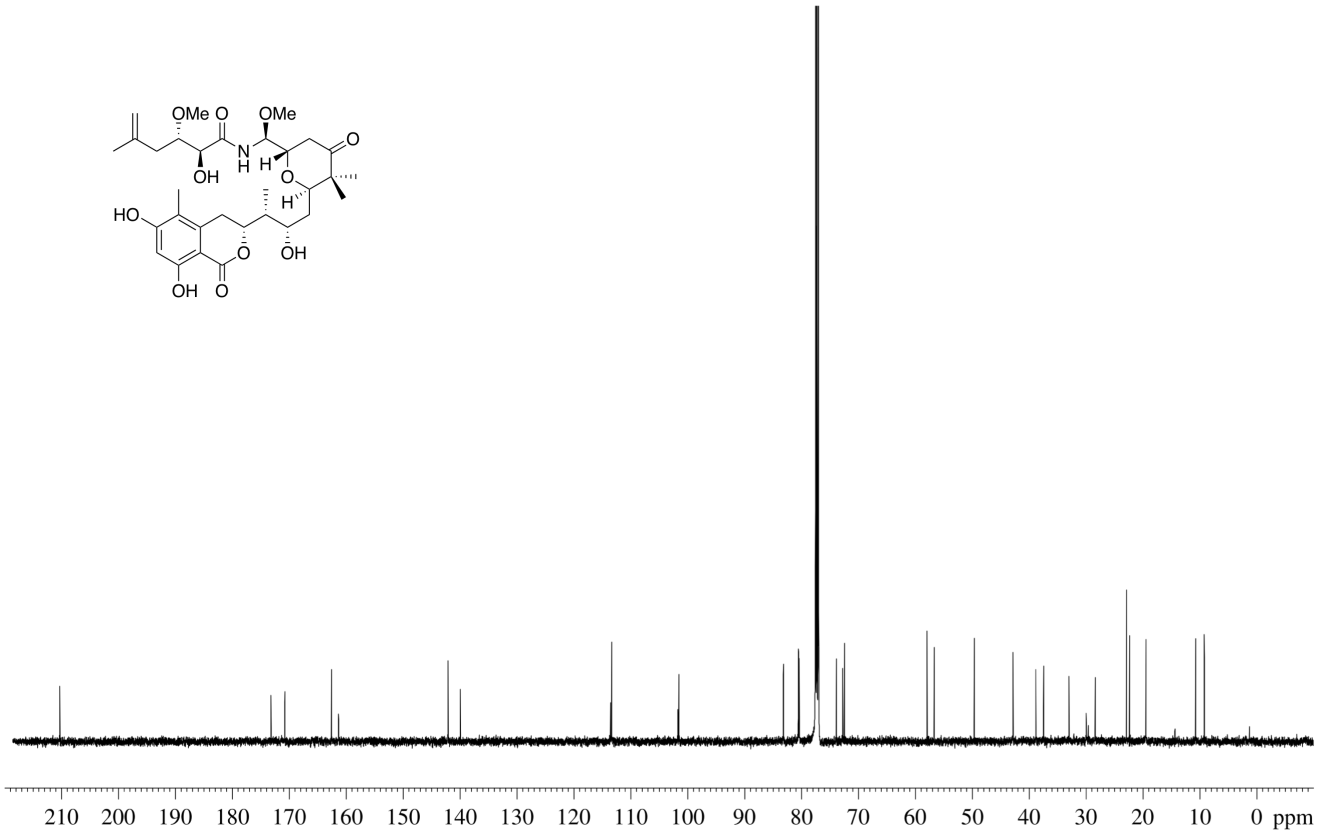

Figure A2.32. ^{13}C NMR Spectrum (125 MHz) of Compound (–)-**2.2** in $CDCl_3$

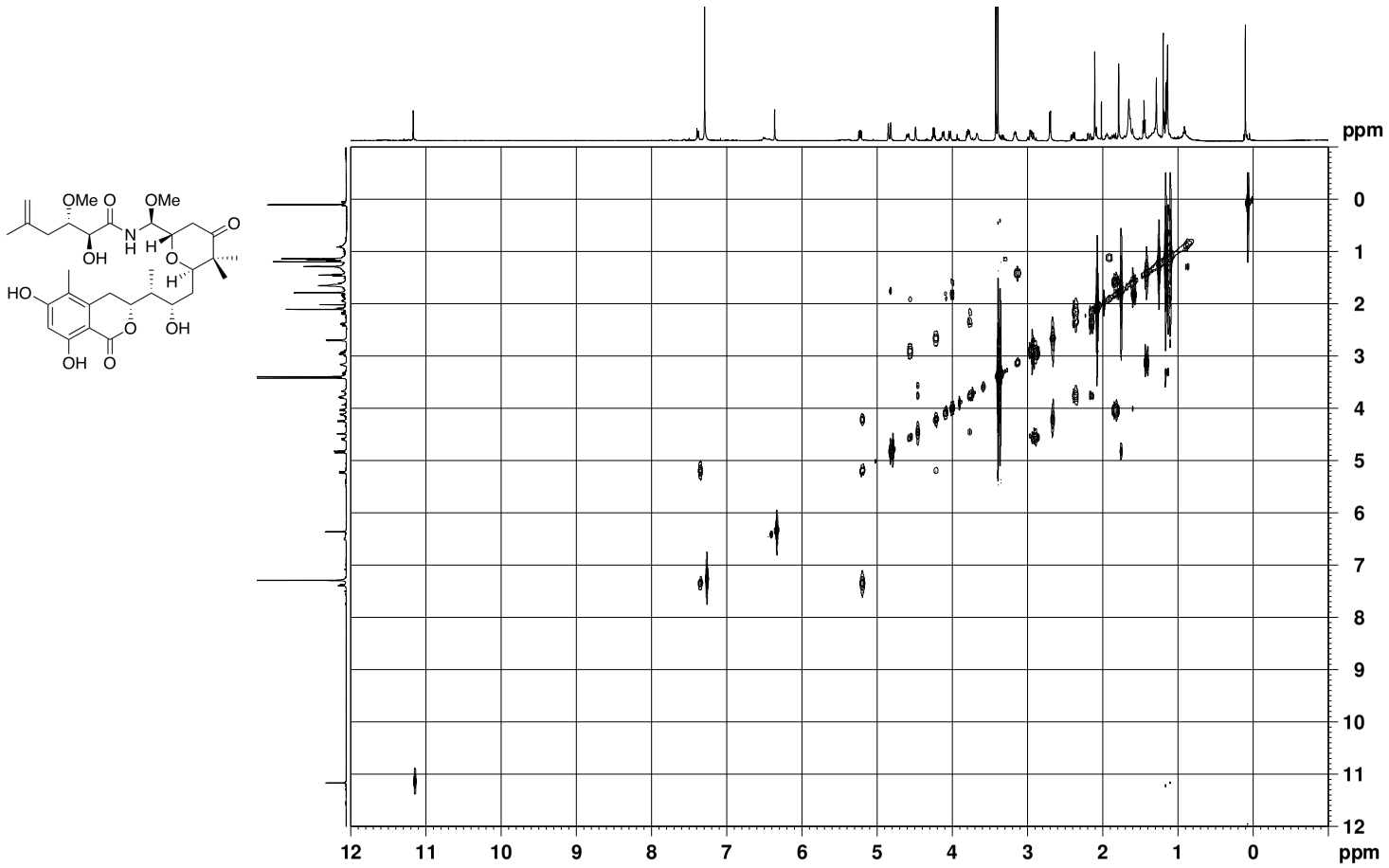

Figure A2.33. COSY Spectrum of Compound (–)-**2.2** in $CDCl_3$

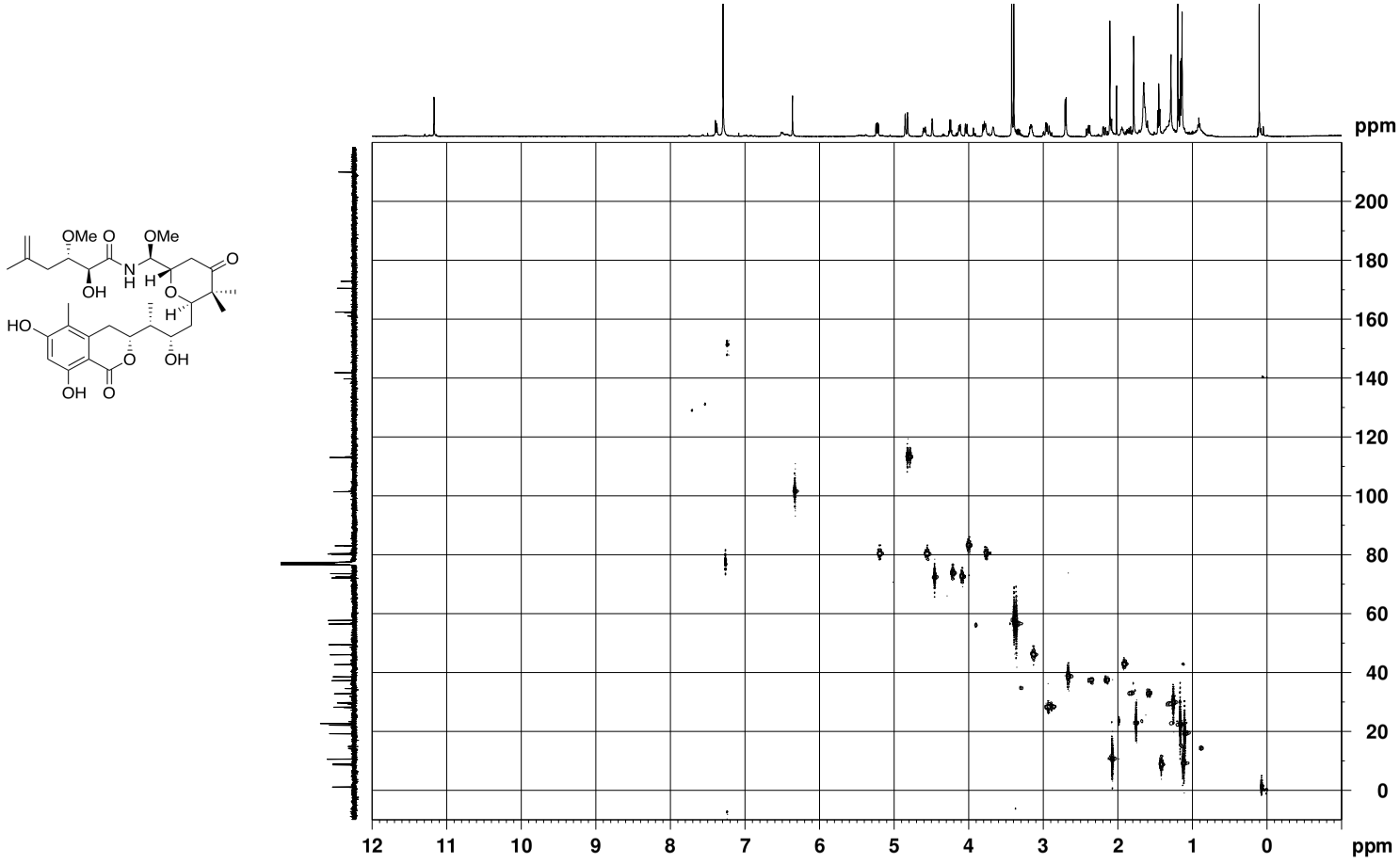

Figure A2.34. HSQC Spectrum of Compound (–)-**2.2** in $CDCl_3$

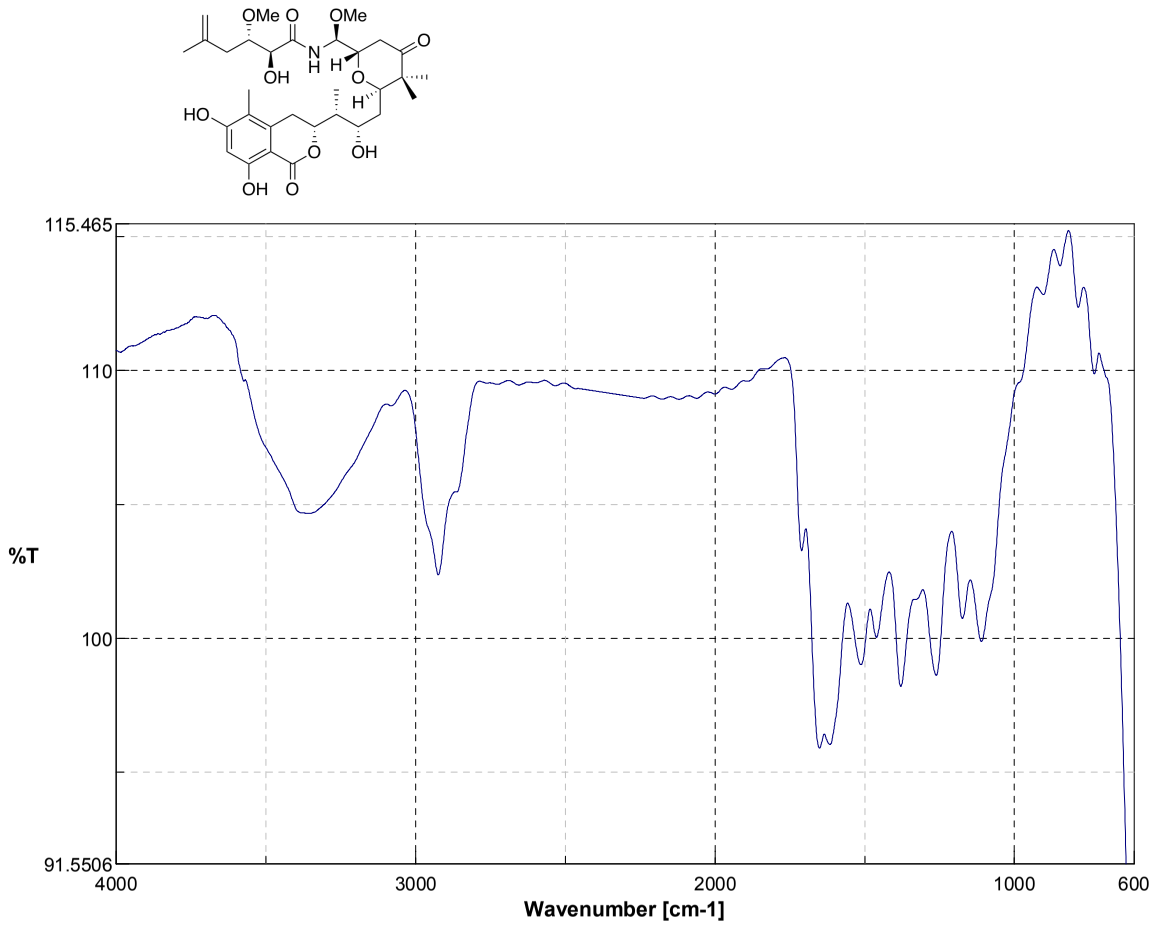

Figure A2.35. Infrared Spectrum of Compound (–)-**2.2**

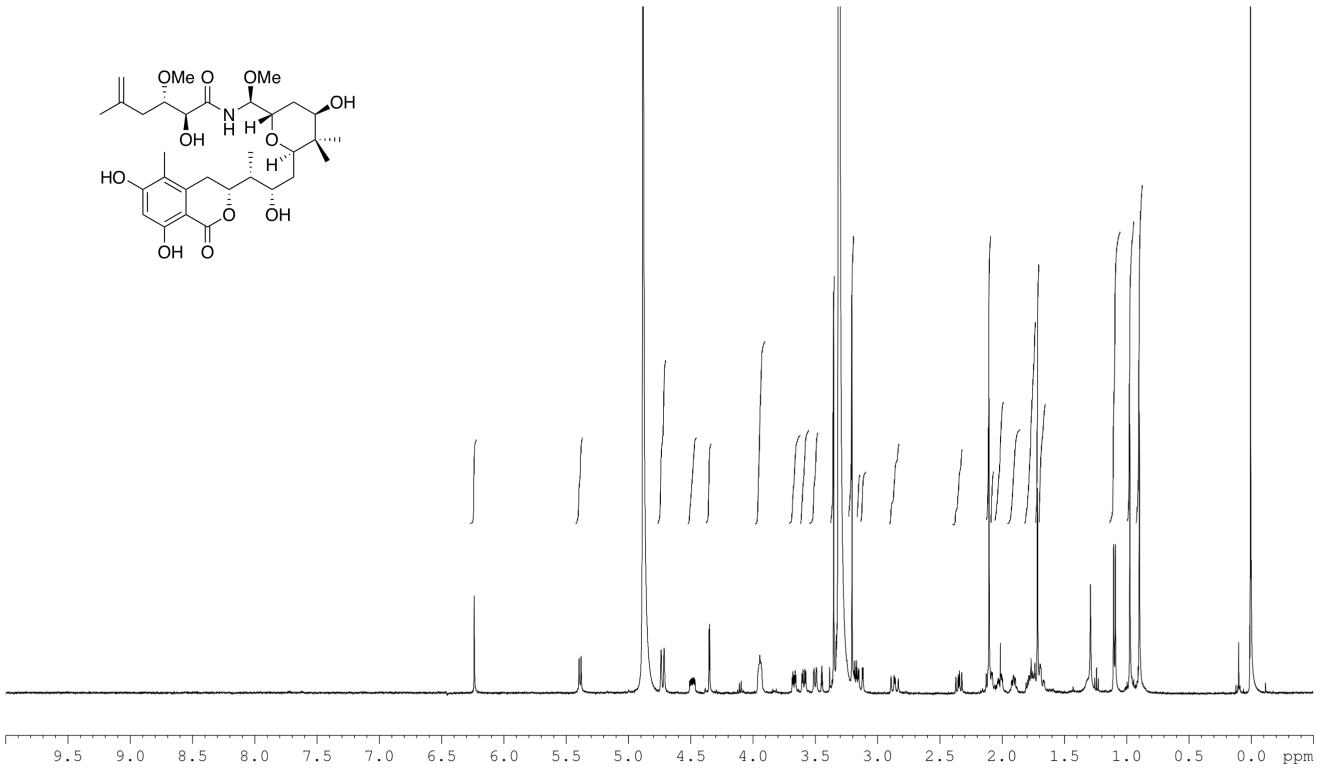

Figure A2.36. ^{1}H NMR Spectrum (500 MHz) of Compound (+)-**2.1** in MeOD

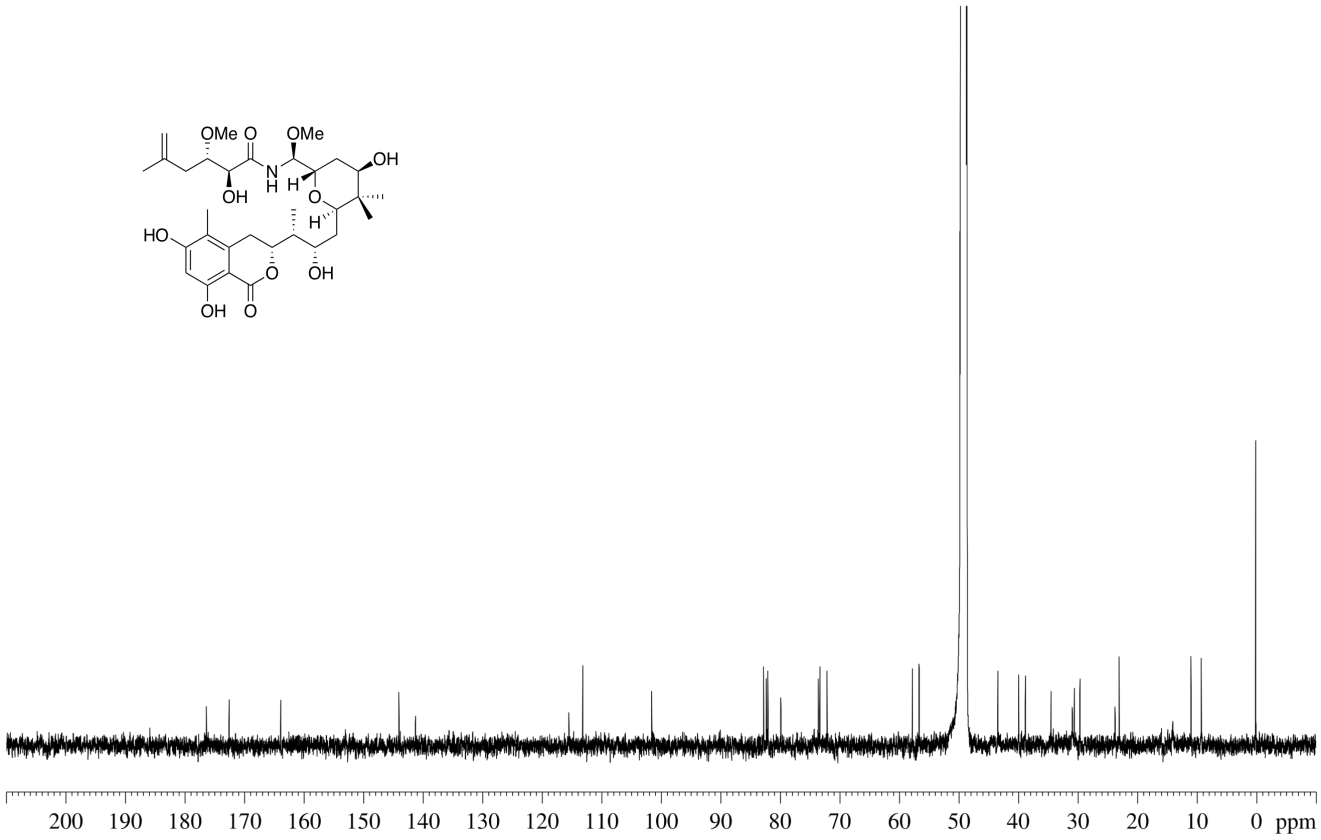

Figure A2.37. ^{13}C NMR Spectrum (125 MHz) of Compound (+)-**2.1** in MeOD

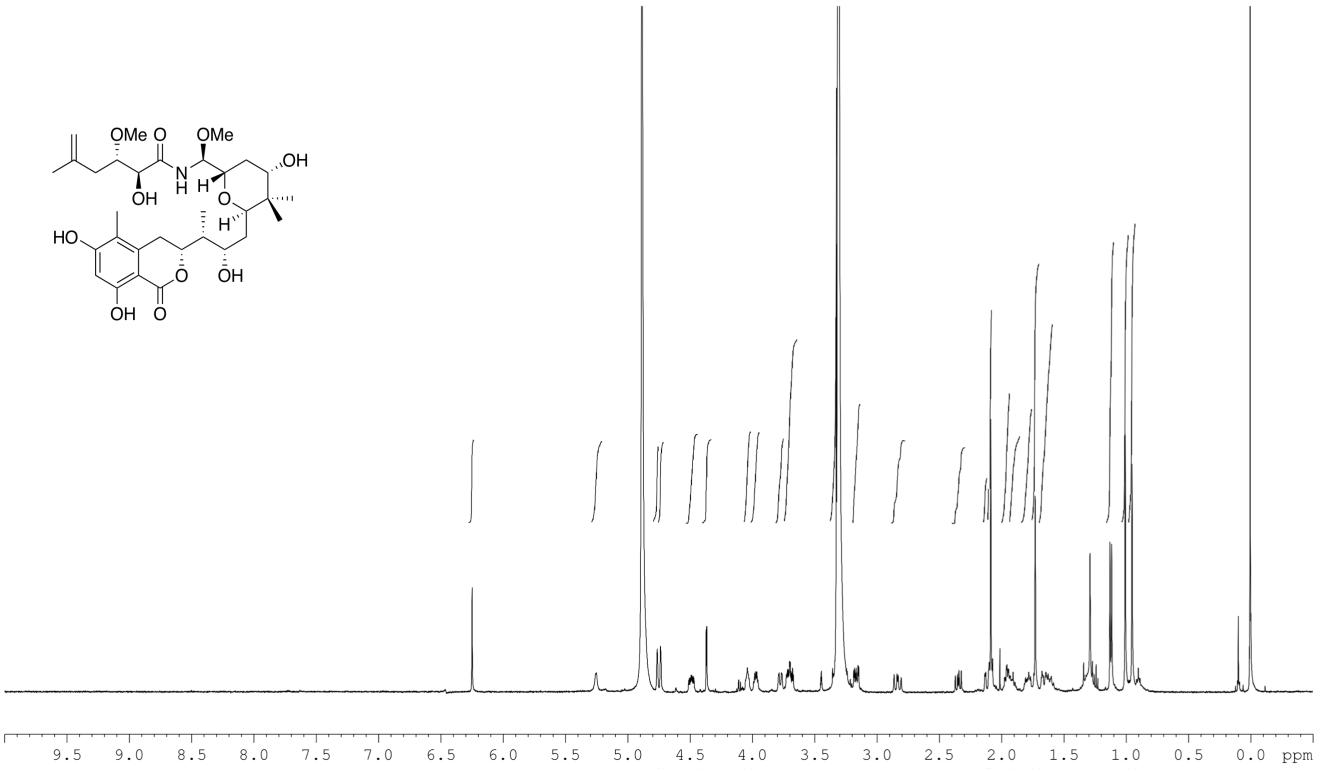

Figure A2.38. ^{1}H NMR Spectrum (500 MHz) of Compound **2.60** in MeOD

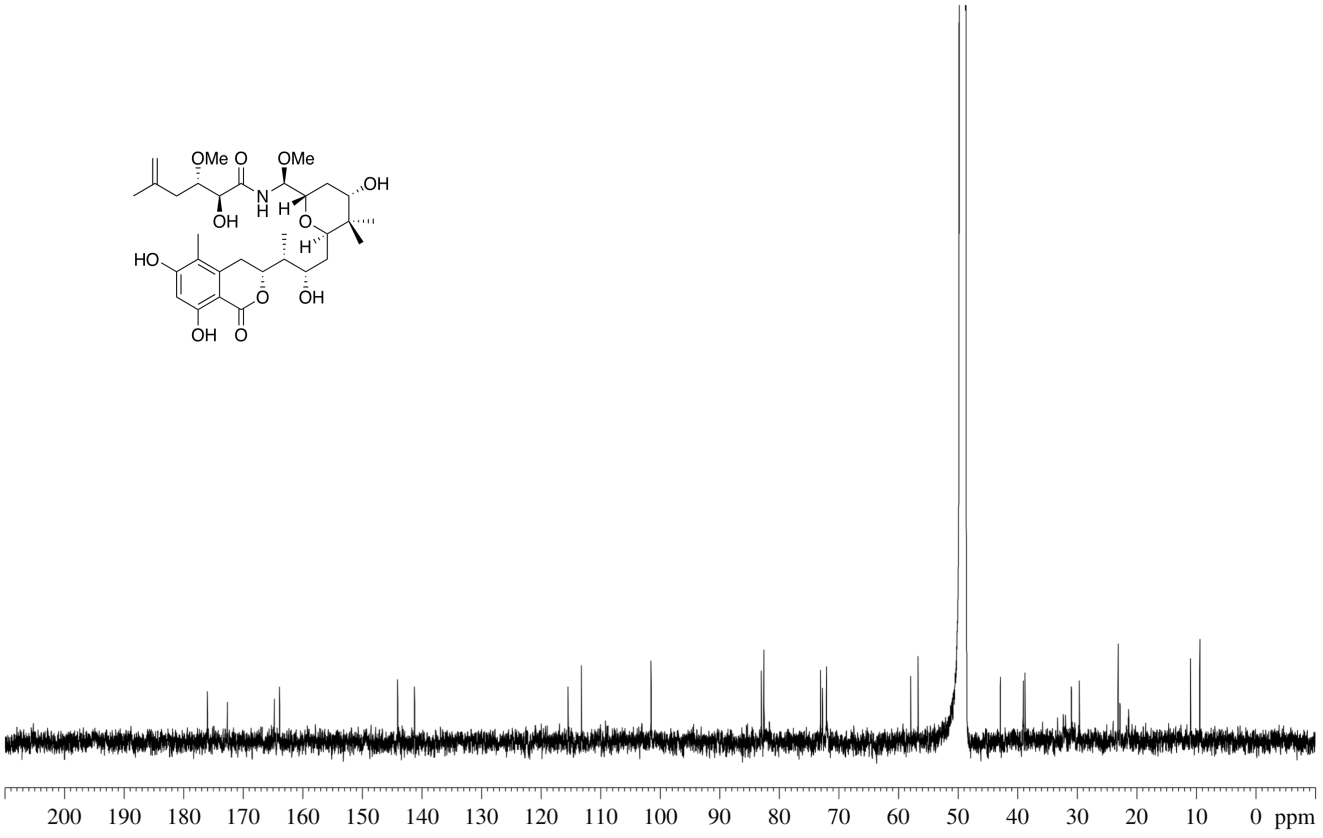

Figure A2.39. ^{13}C NMR Spectrum (125 MHz) of Compound **2.60** in MeOD

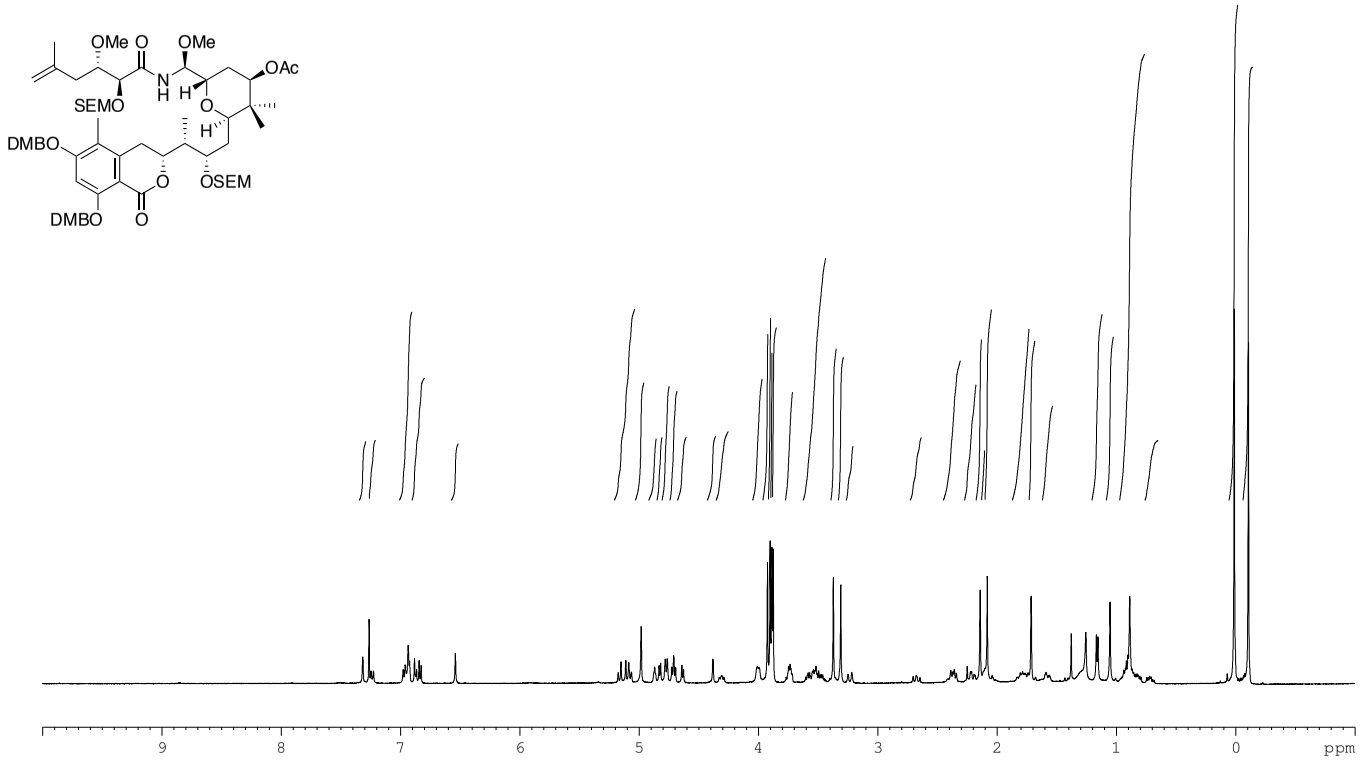

Figure A3.1. ^{1}H NMR Spectrum (500 MHz) of Compound (+)-**S2** in $CDCl_3$

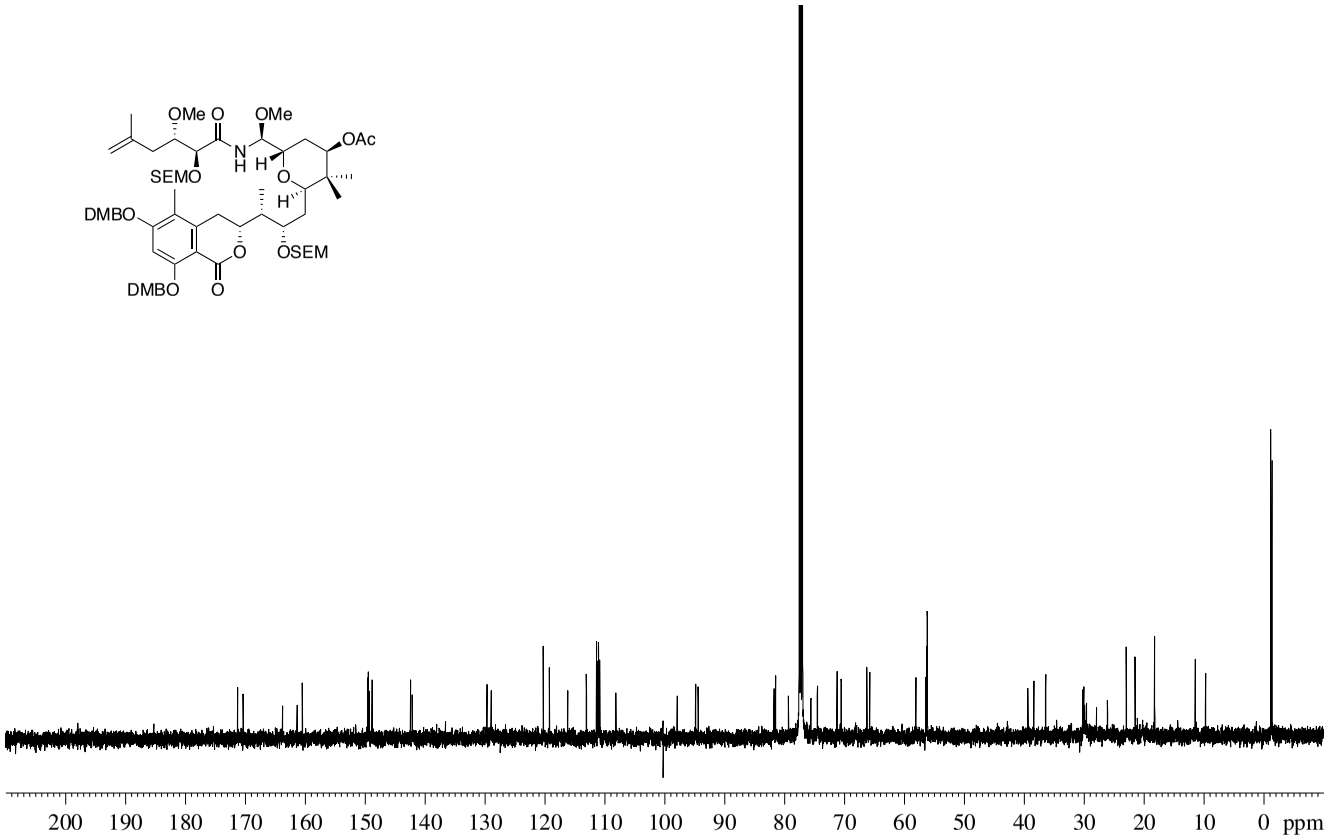

Figure A3.2. ^{13}C NMR Spectrum (125 MHz) of Compound (+)-**S2** in $CDCl_3$

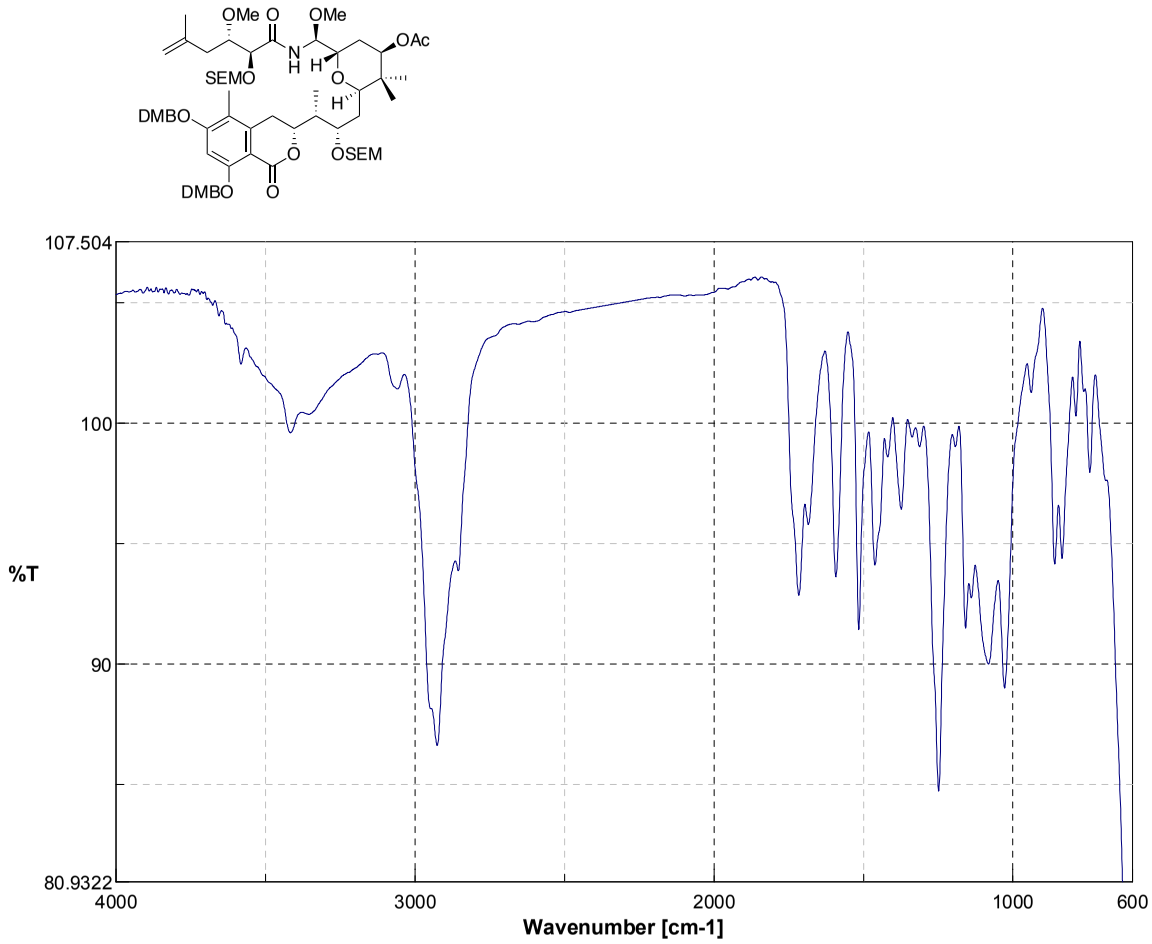

Figure A3.3. Infrared Spectrum of Compound (+)-**S2**

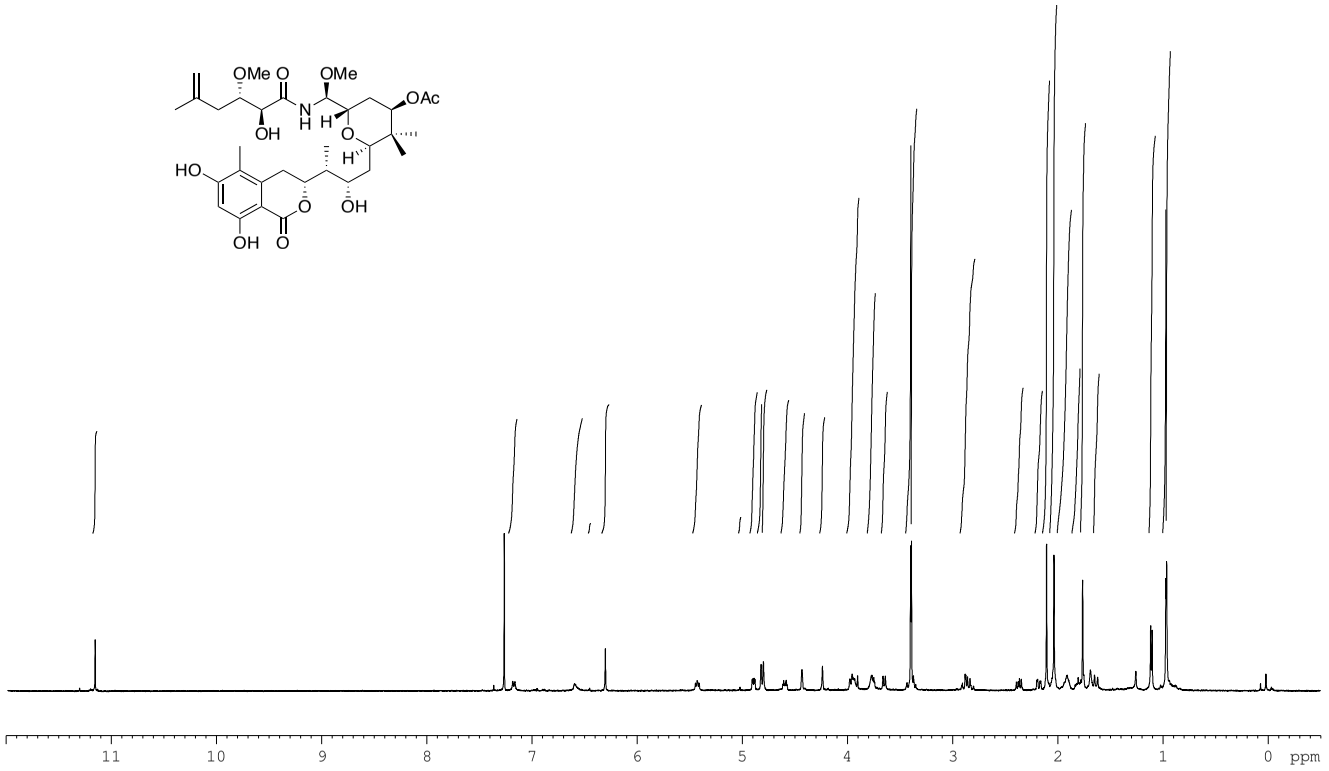

Figure A3.4. ^{1}H NMR Spectrum (500 MHz) of Compound (+)-**3.7** in $CDCl_3$

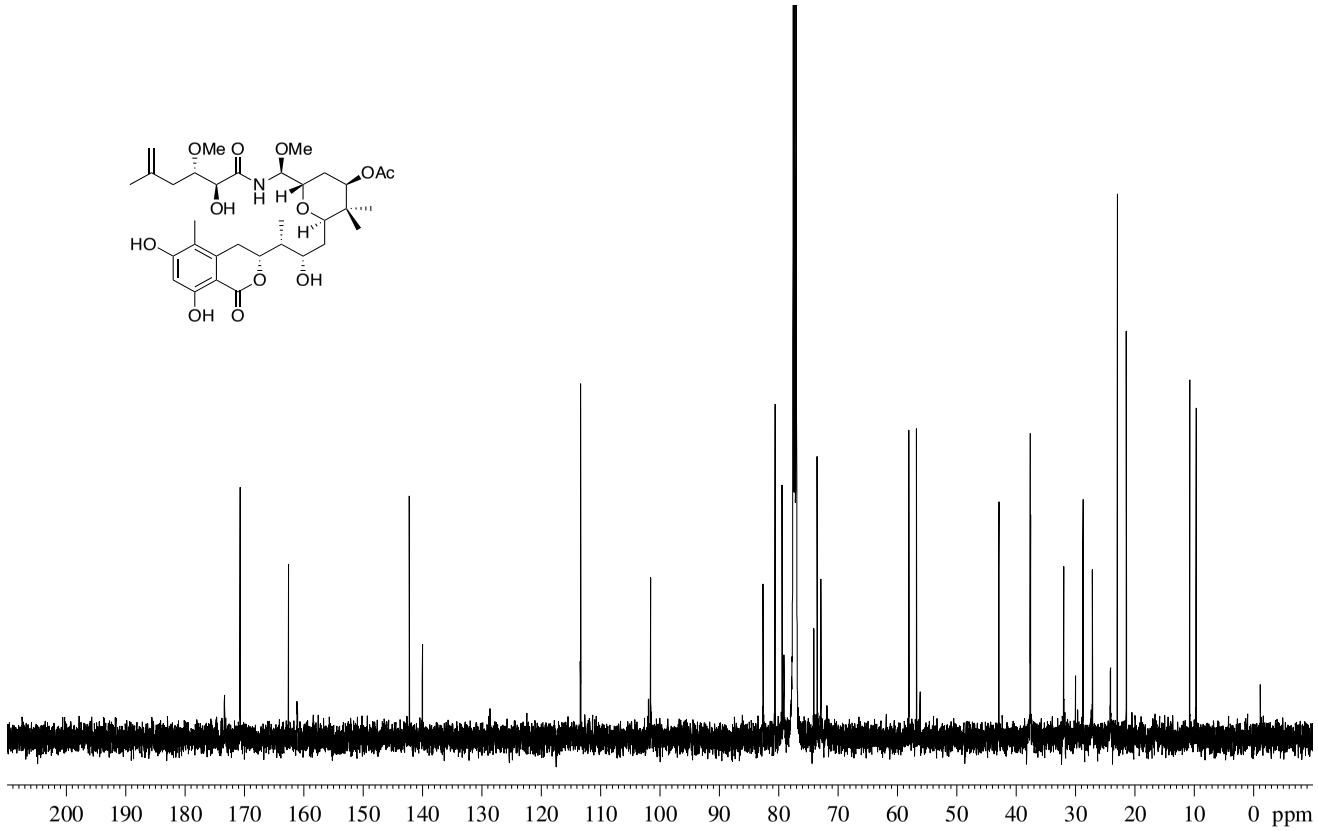

Figure A3.5. ^{13}C NMR Spectrum (125 MHz) of Compound (+)-**3.7** in $CDCl_3$

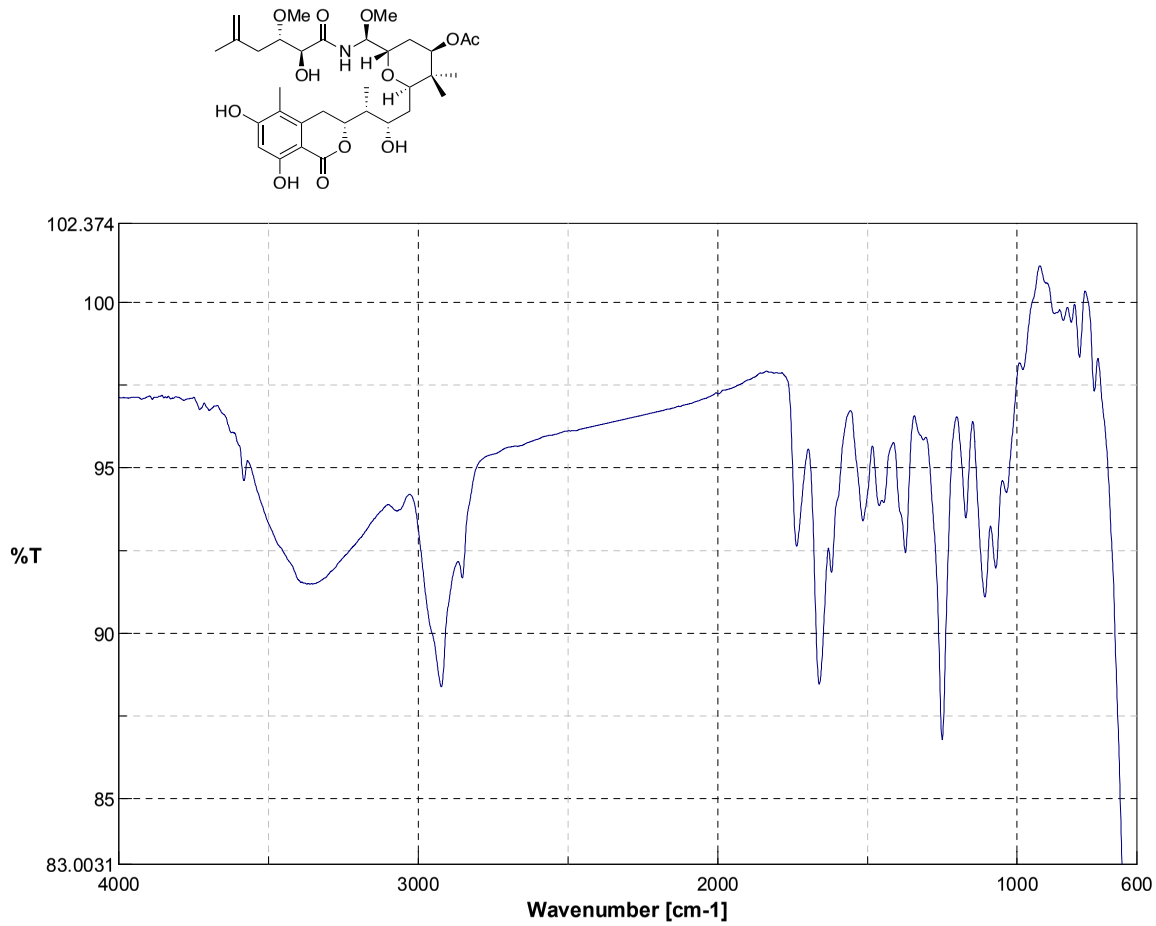

Figure A3.6. Infrared Spectrum of Compound (+)-**3.7**

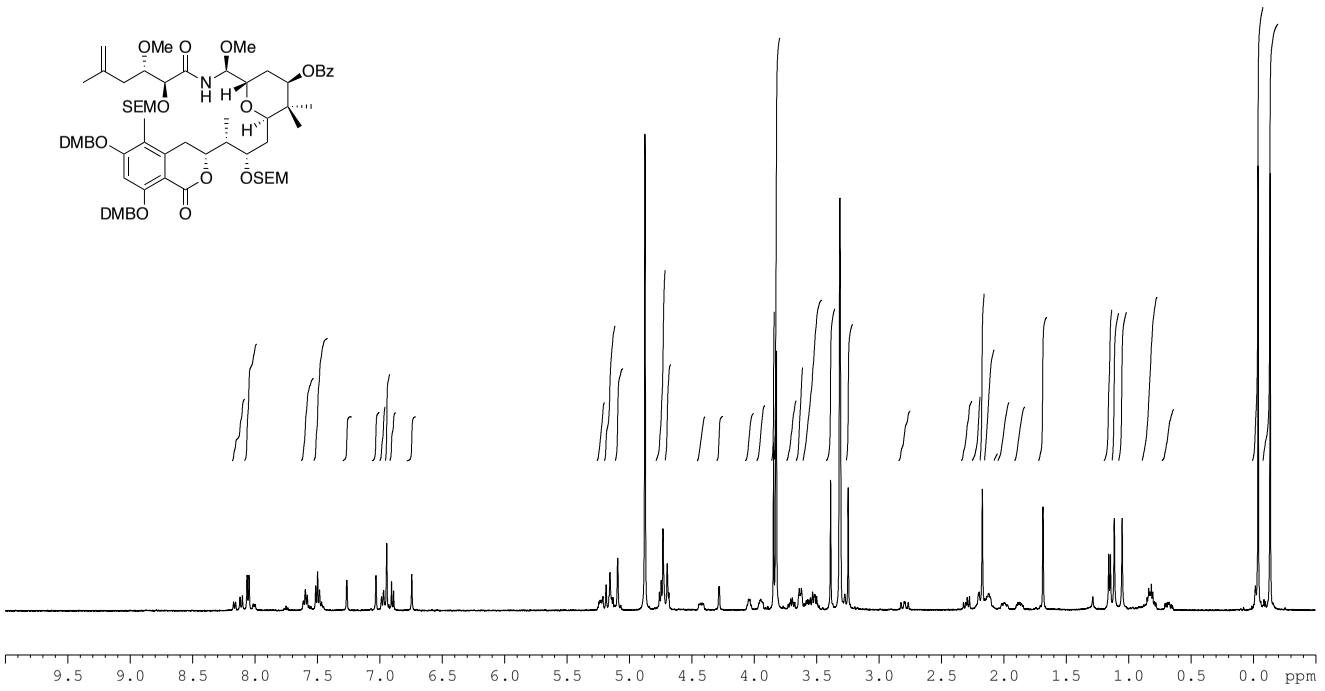

Figure A3.7. ^{1}H NMR Spectrum (500 MHz) of Compound (+)-**S3** in MeOD

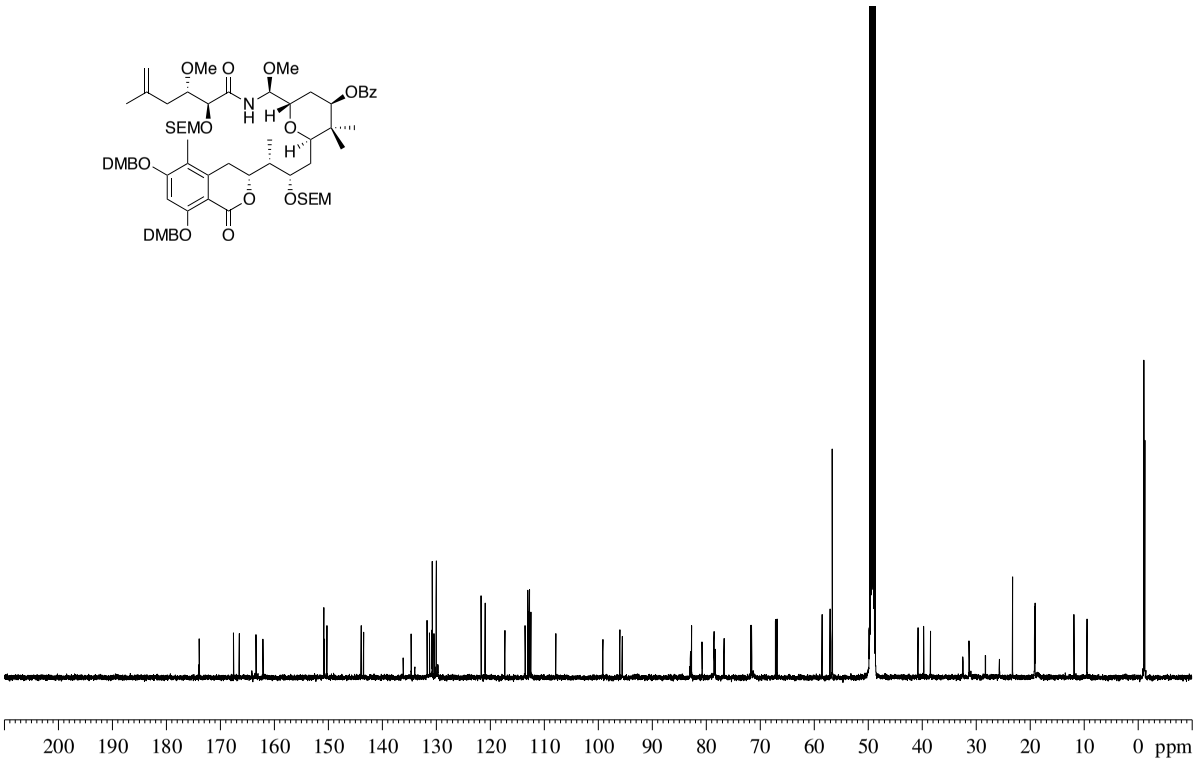

Figure A3.8. ^{13}C NMR Spectrum (125 MHz) of Compound (+)-**S3** in MeOD

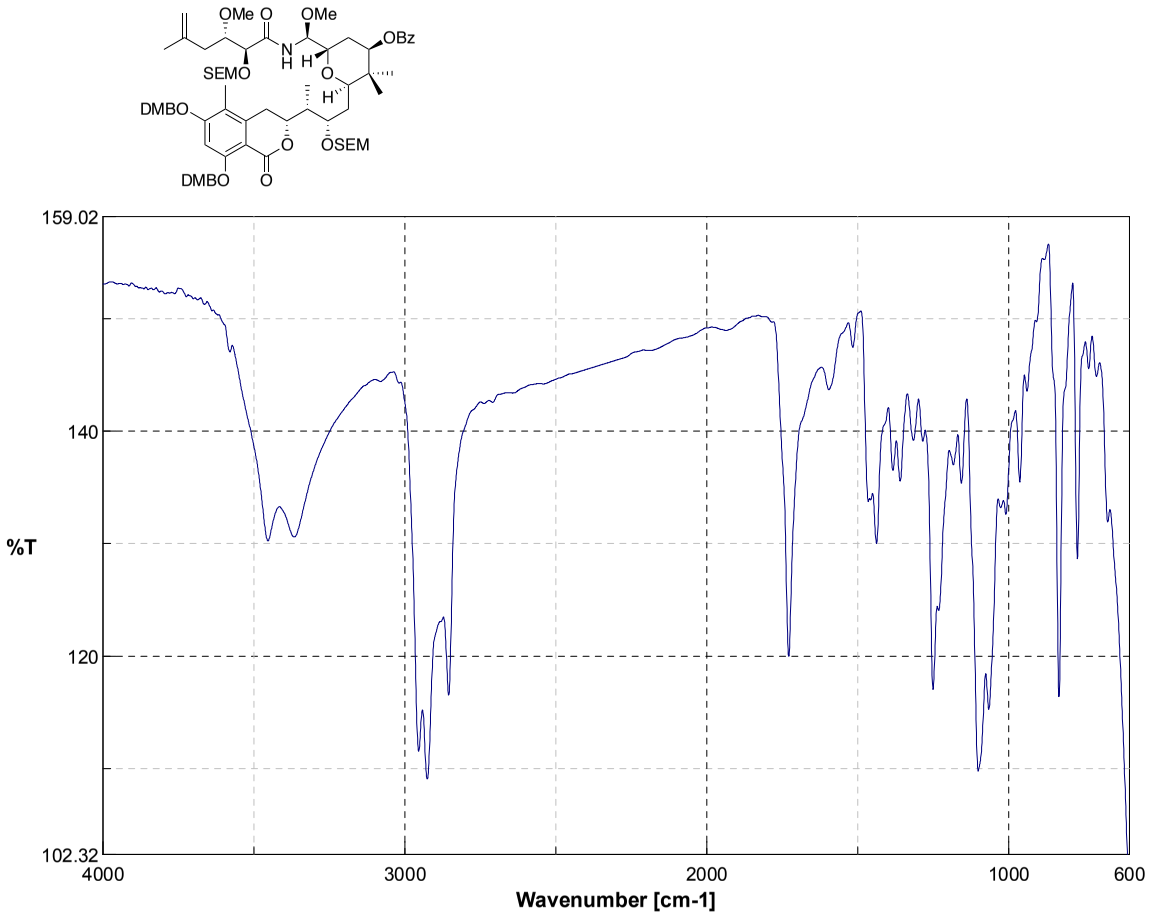

Figure A3.9. Infrared Spectrum of Compound (+)-**S3**

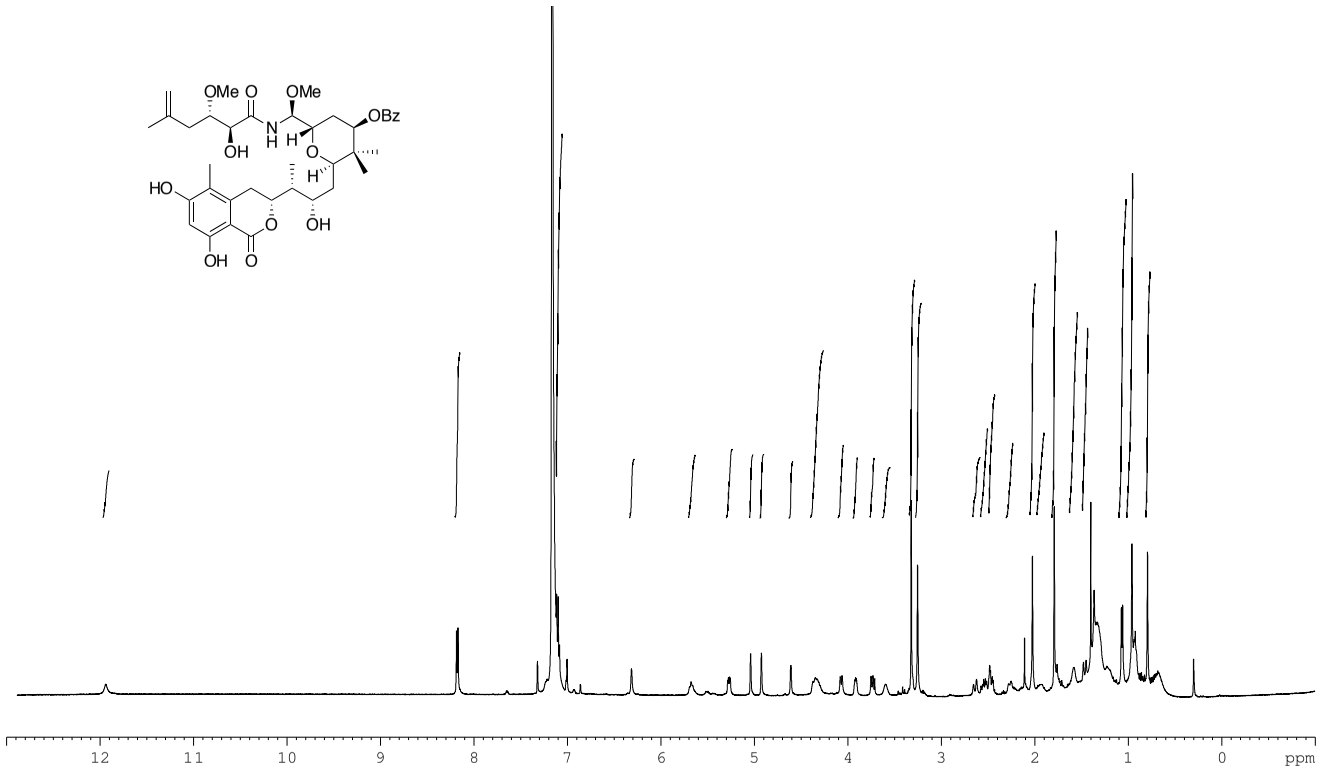

Figure A3.10. ^{1}H NMR Spectrum (500 MHz) of Compound (–)-**3.6** in C_6D_6

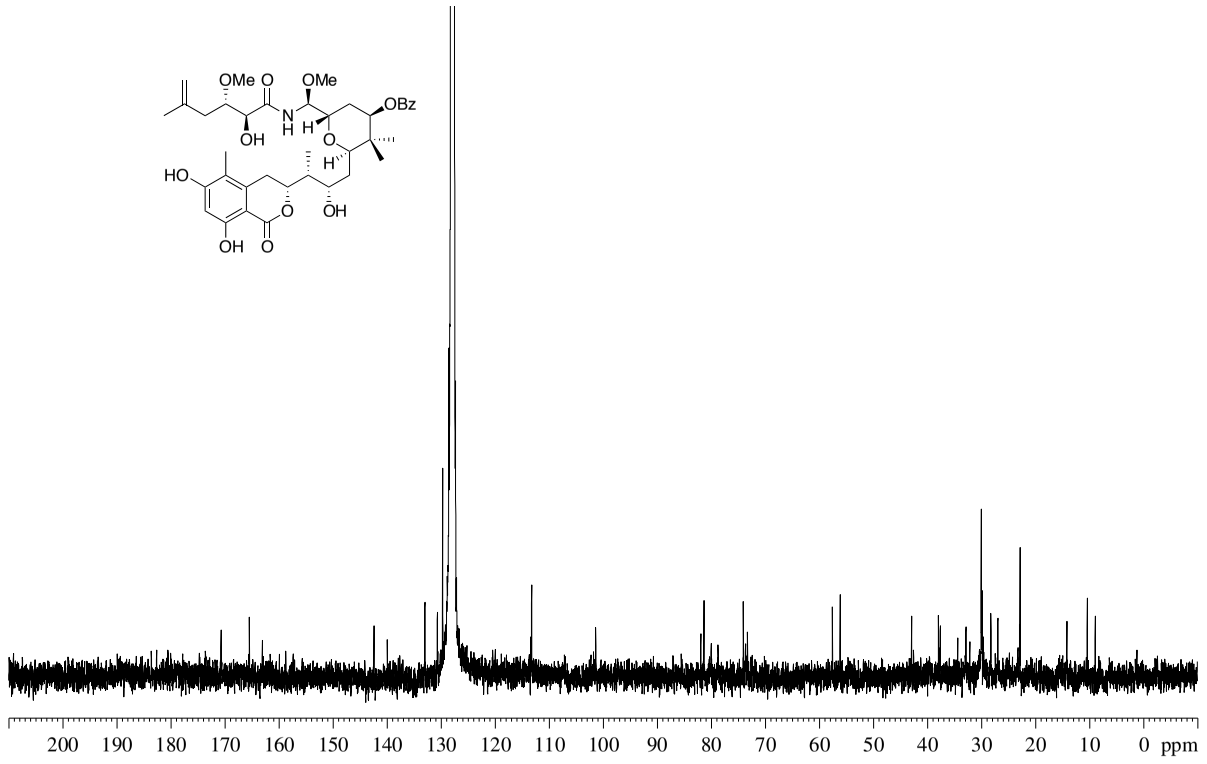

Figure A3.11. ^{13}C NMR Spectrum (125 MHz) of Compound (–)-**3.6** in C_6D_6

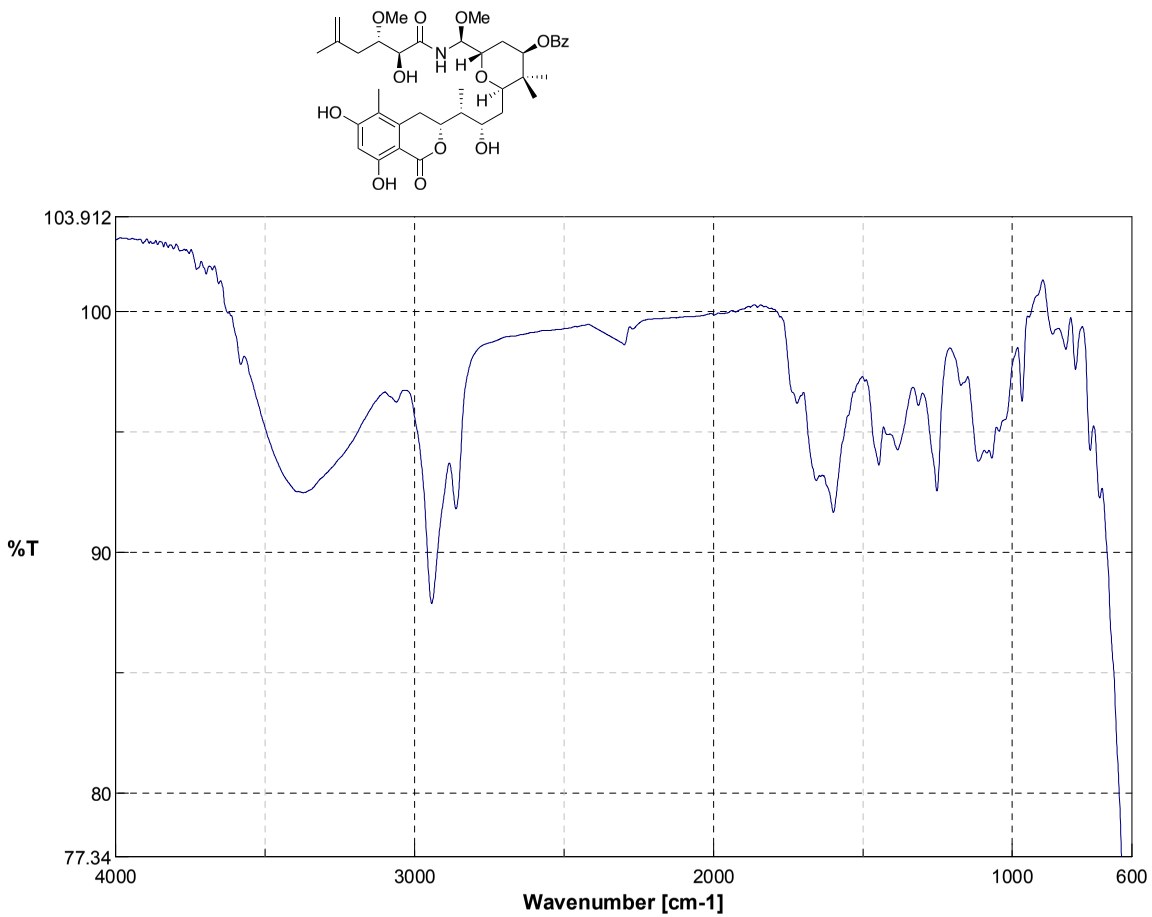

Figure A3.12. Infrared Spectrum of Compound (–)-**3.6**

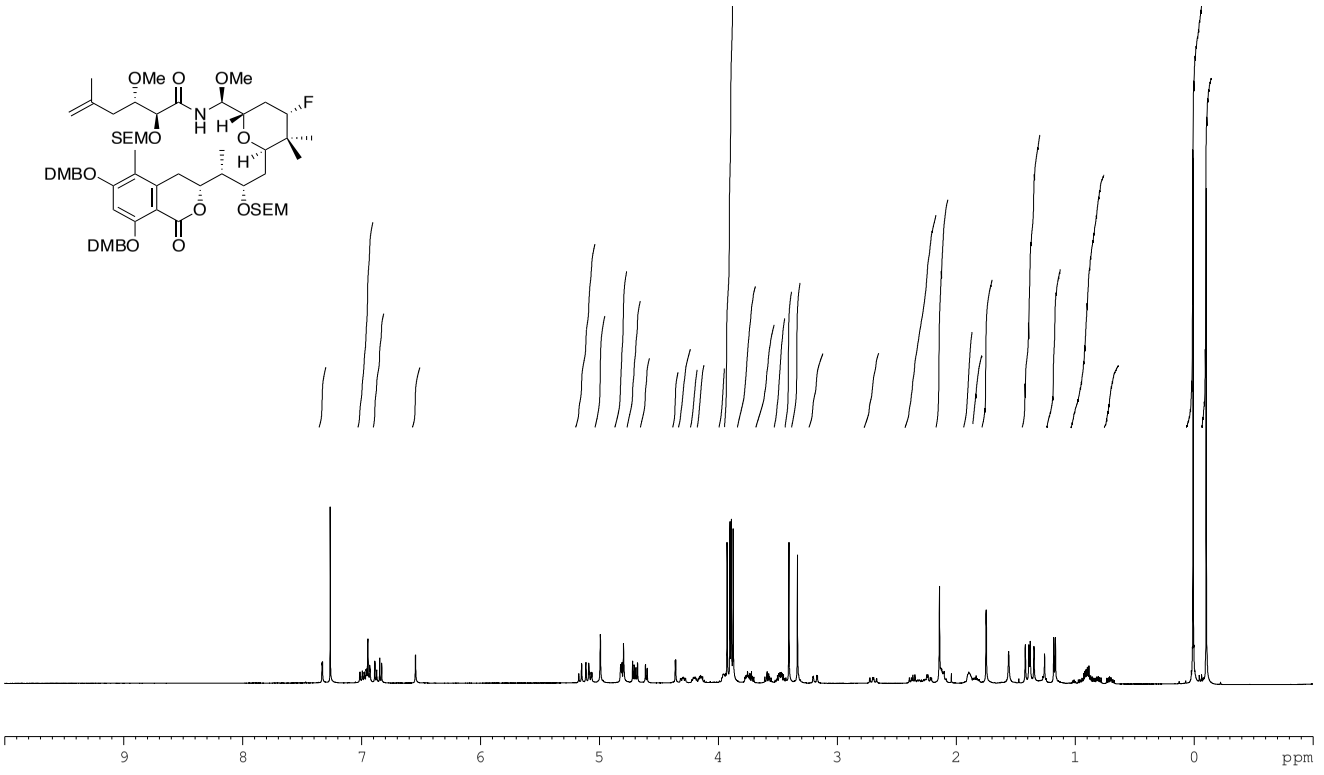

Figure A3.13. ^{1}H NMR Spectrum (500 MHz) of Compound (+)-**S4** in $CDCl_3$

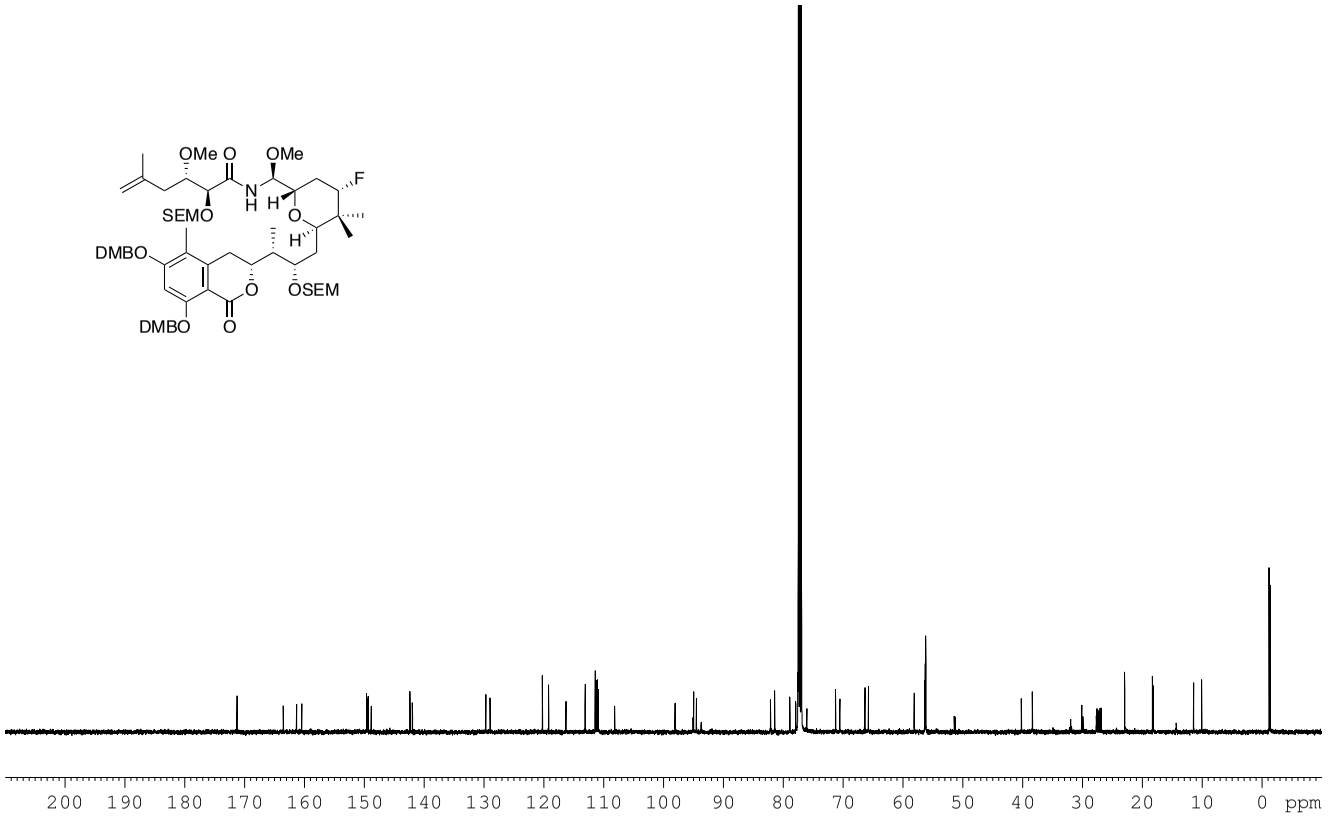

Figure A3.14. ^{13}C NMR Spectrum (125 MHz) of Compound (+)-**S4** in $CDCl_3$

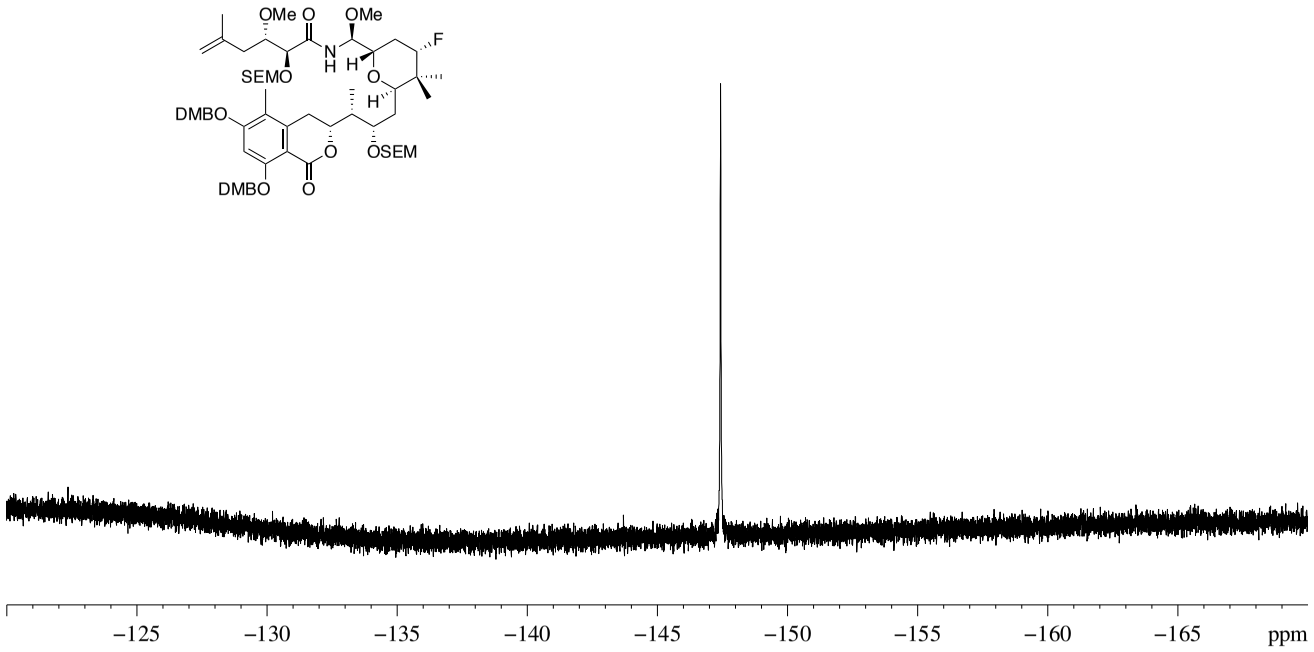

Figure A3.15. ^{19}F NMR Spectrum (470 MHz) of Compound (+)-**S4** in $CDCl_3$

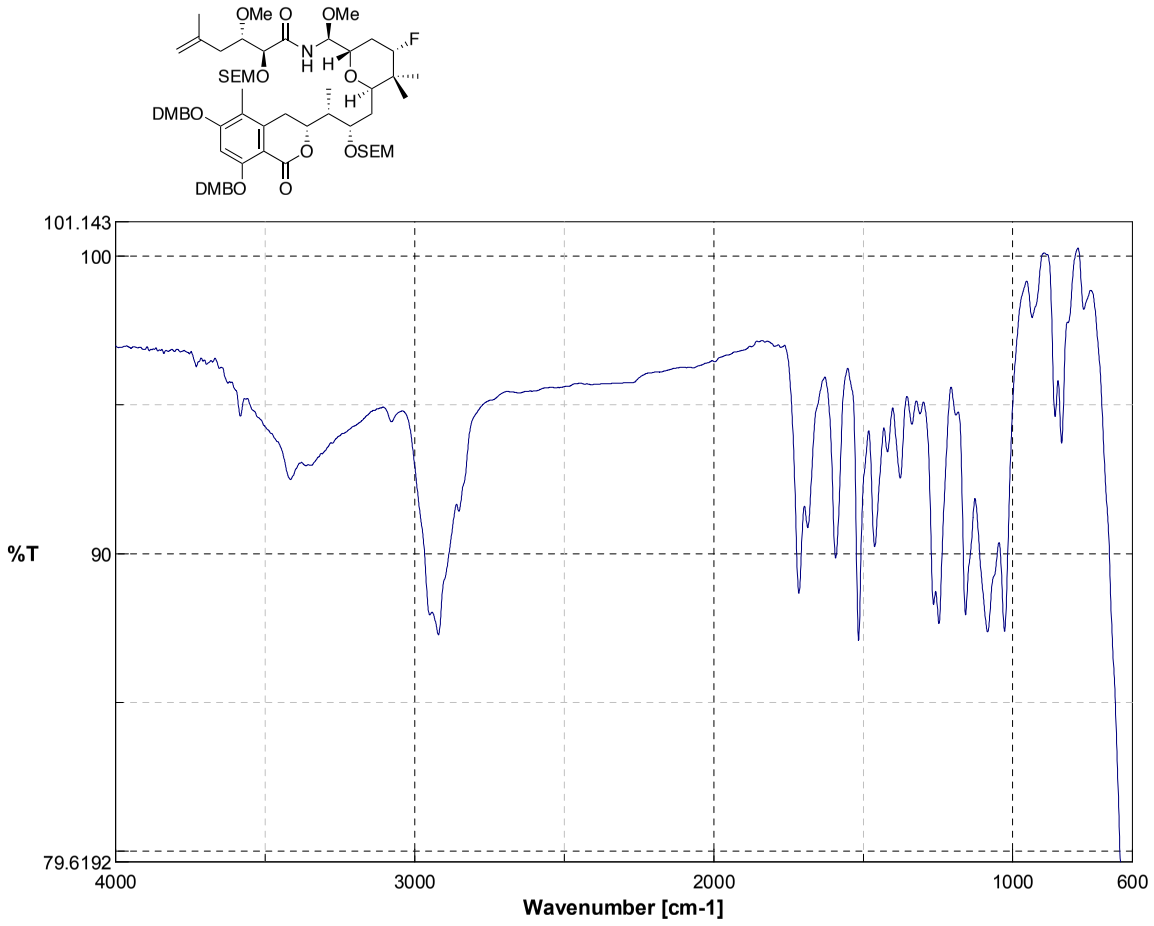

Figure A3.16. Infrared Spectrum of Compound (+)-**S4**

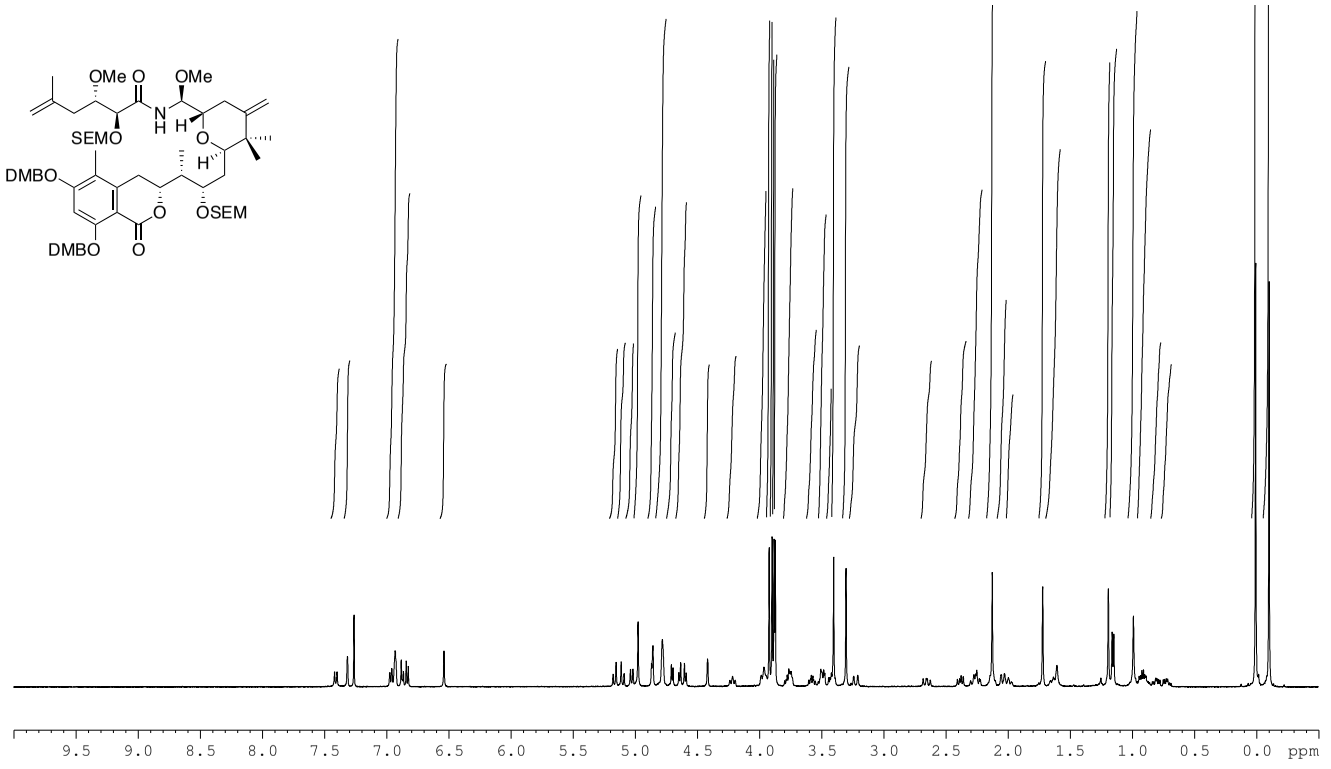

Figure A3.17. ^{1}H NMR Spectrum (500 MHz) of Compound (–)-**S5** in $CDCl_3$

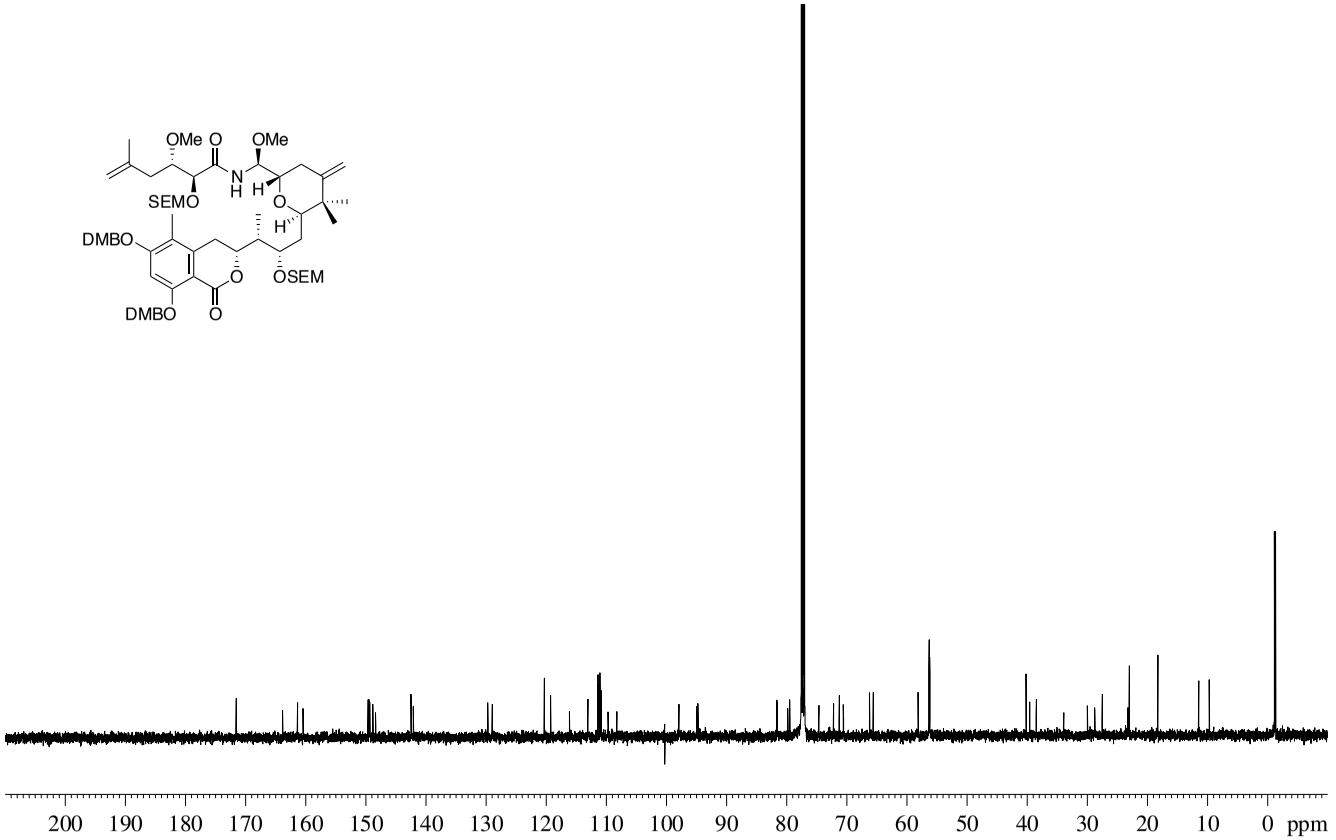

Figure A3.18. ^{13}C NMR Spectrum (125 MHz) of Compound (–)-**S5** in $CDCl_3$

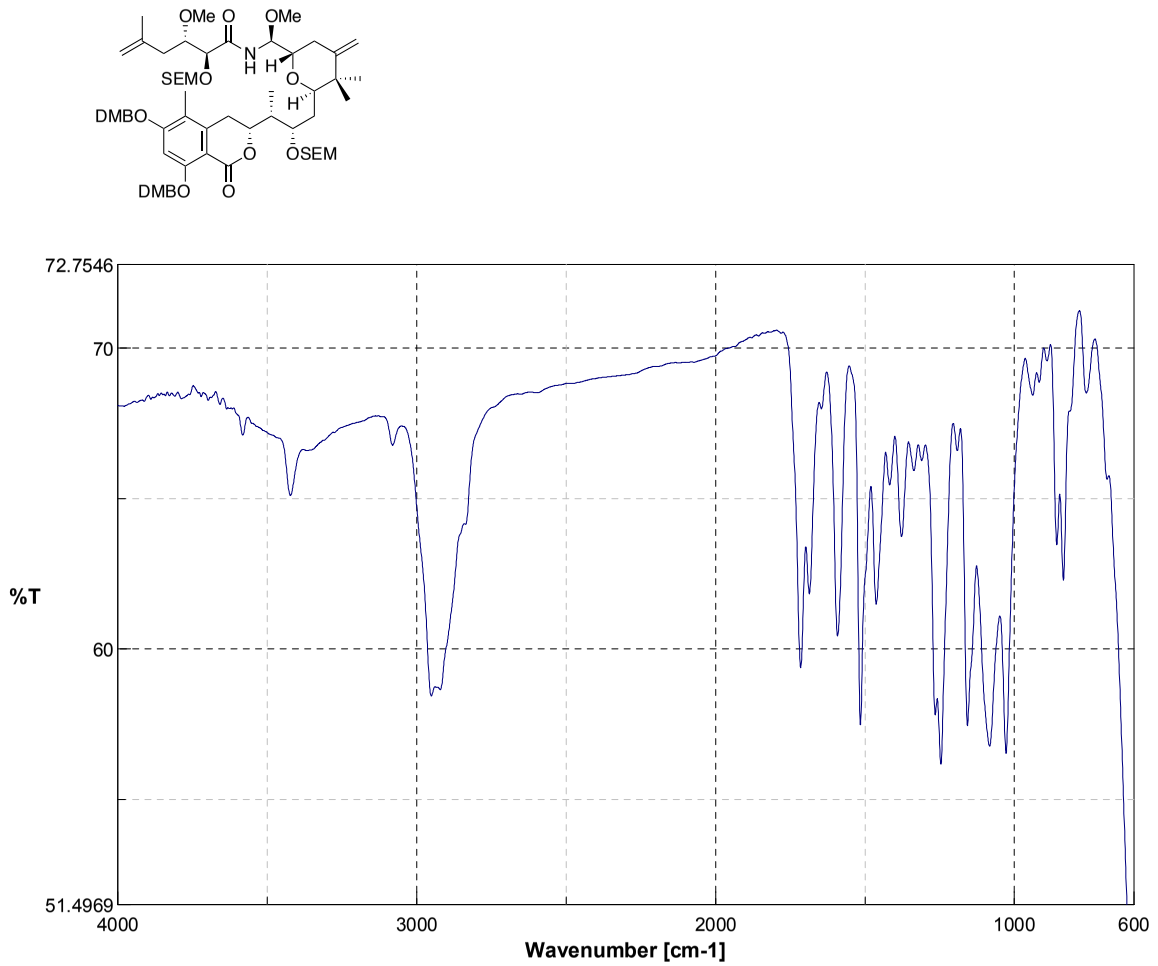

Figure A3.19. Infrared Spectrum of Compound (–)-**S5**

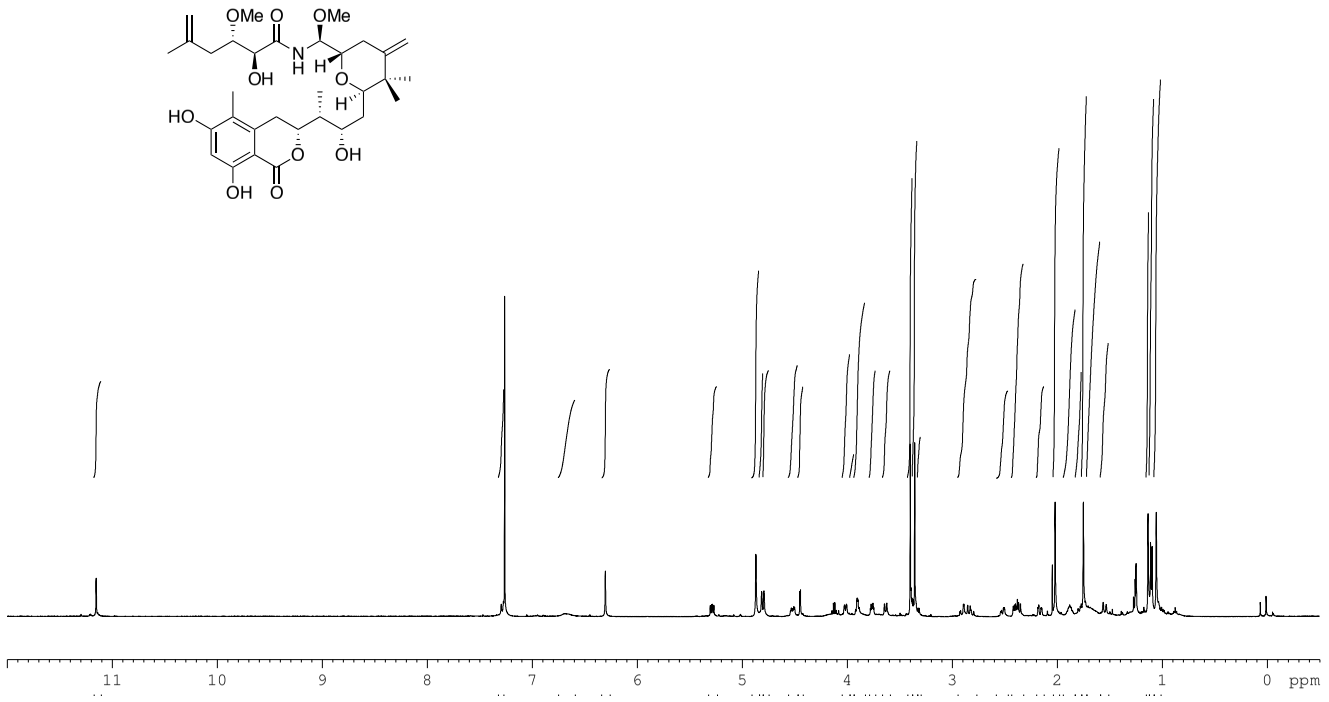

Figure A3.20. ^{1}H NMR Spectrum (500 MHz) of Compound (+)-**3.9** in $CDCl_3$

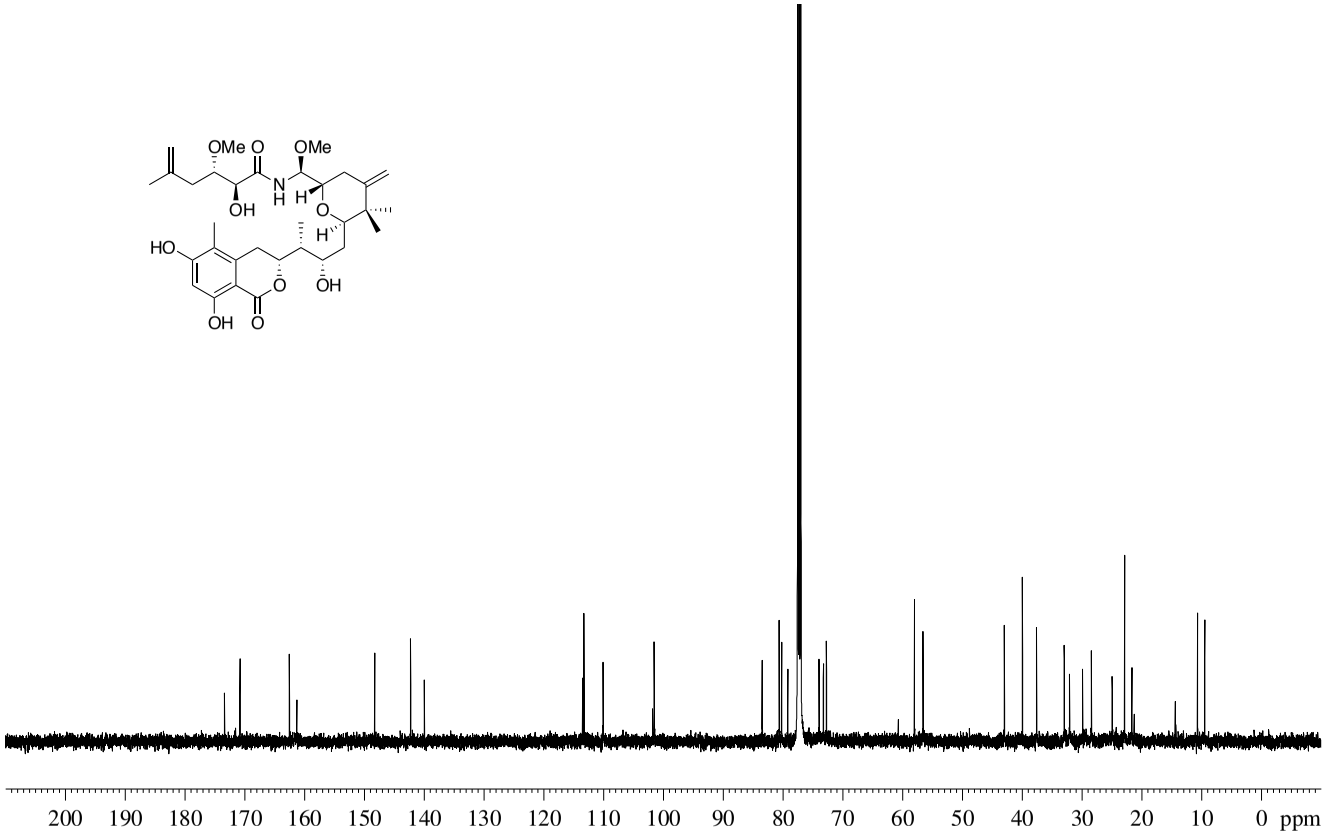

Figure A3.21. ^{13}C NMR Spectrum (125 MHz) of Compound (+)-**3.9** in $CDCl_3$

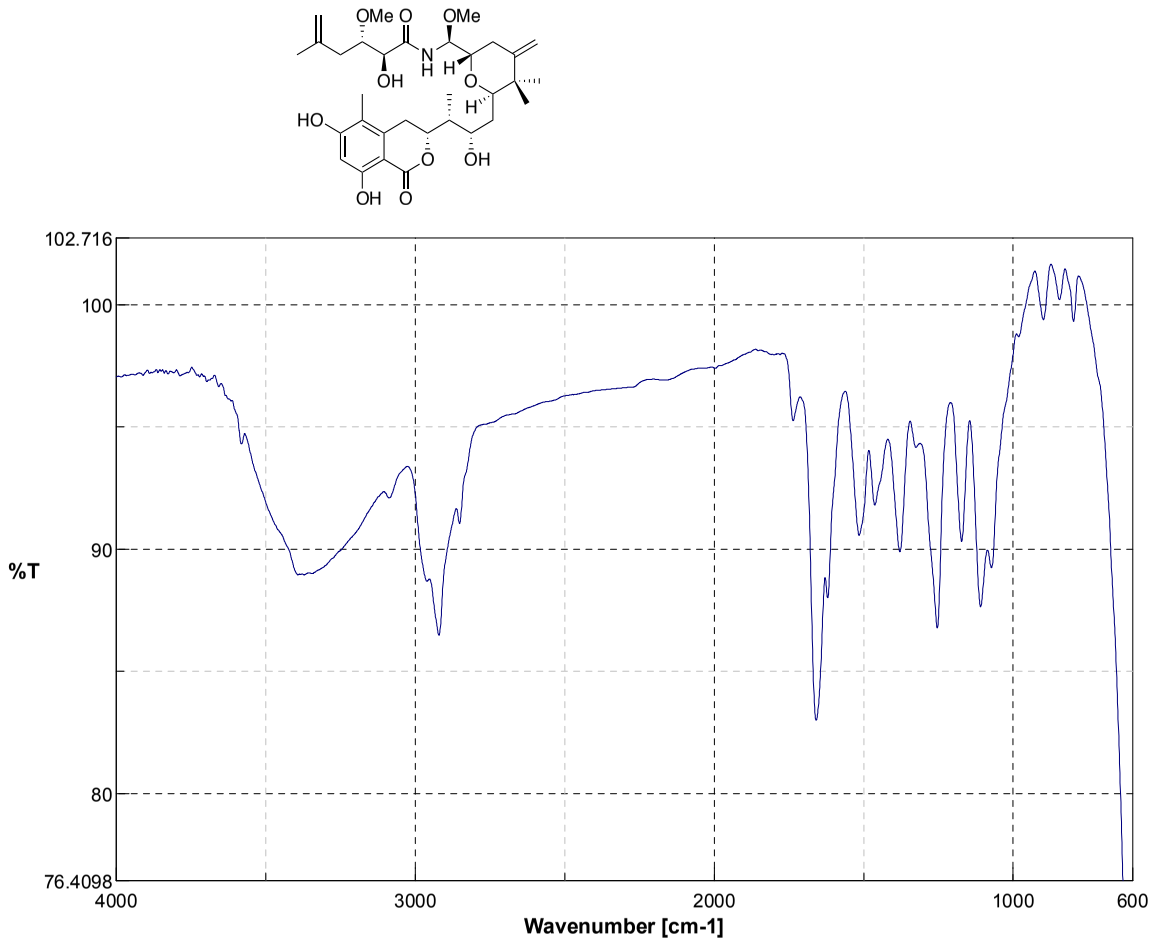

Figure A3.22. Infrared Spectrum of Compound (+)-**3.9**

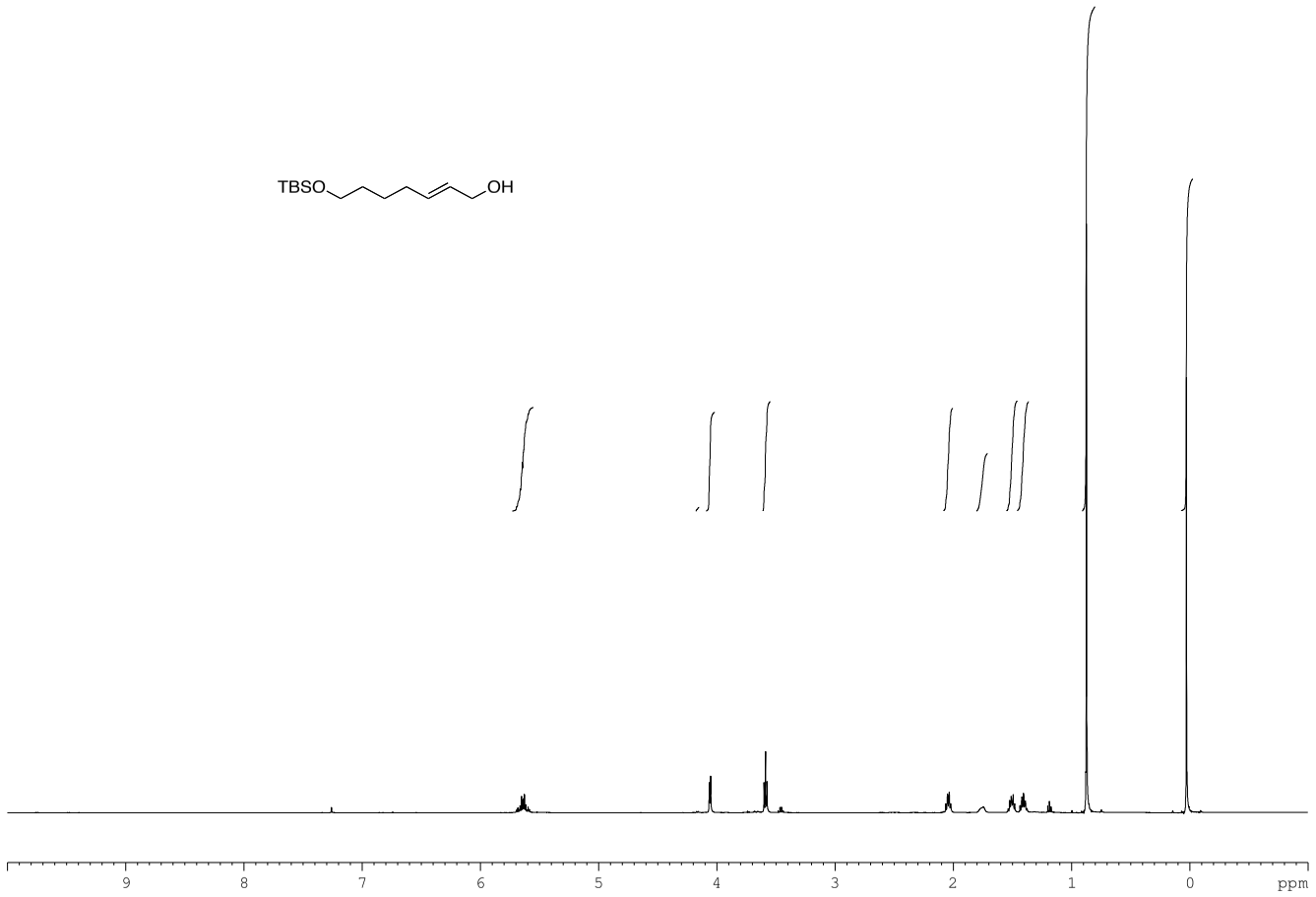

Figure A3.23. ^{1}H NMR Spectrum (500 MHz) of Compound **3.15** in $CDCl_3$

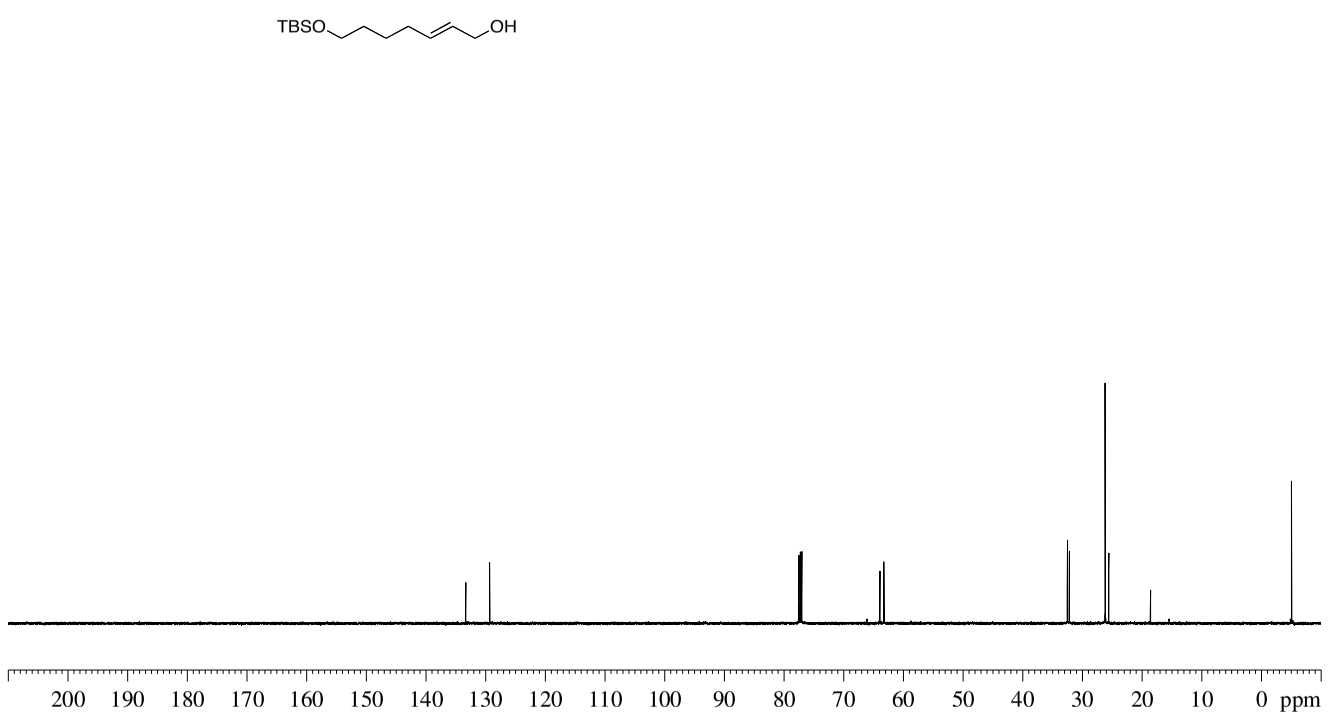

Figure A3.24. ^{13}C NMR Spectrum (125 MHz) of Compound **3.15** in $CDCl_3$

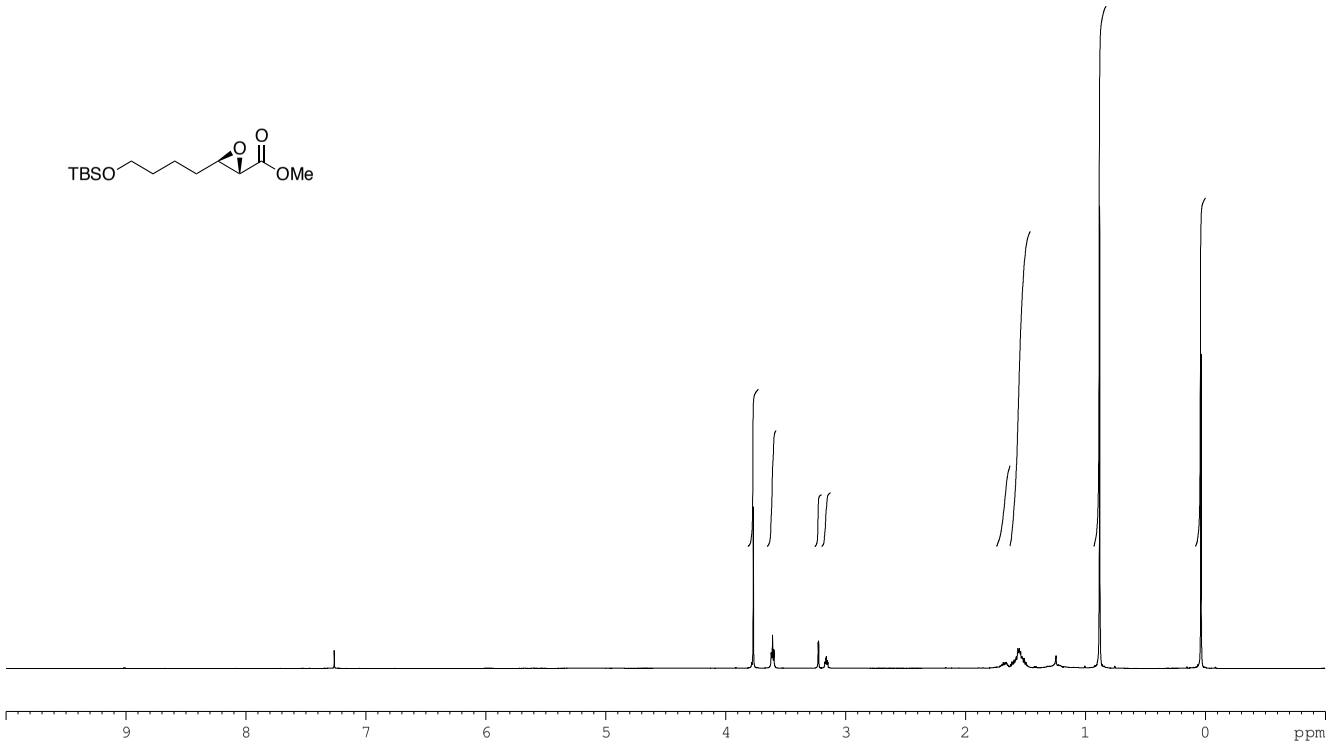

Figure A3.25. ^{1}H NMR Spectrum (500 MHz) of Compound (+)-**3.17** in $CDCl_3$

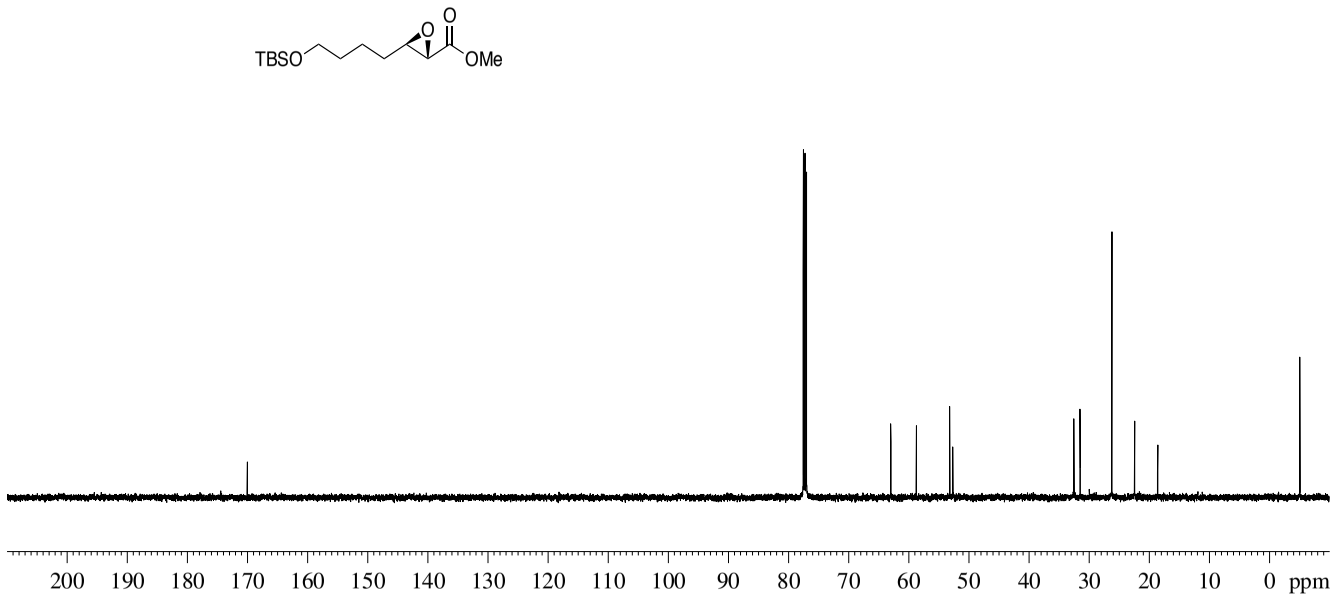

Figure A3.26. ^{13}C NMR Spectrum (125 MHz) of Compound (+)-**3.17** in $CDCl_3$

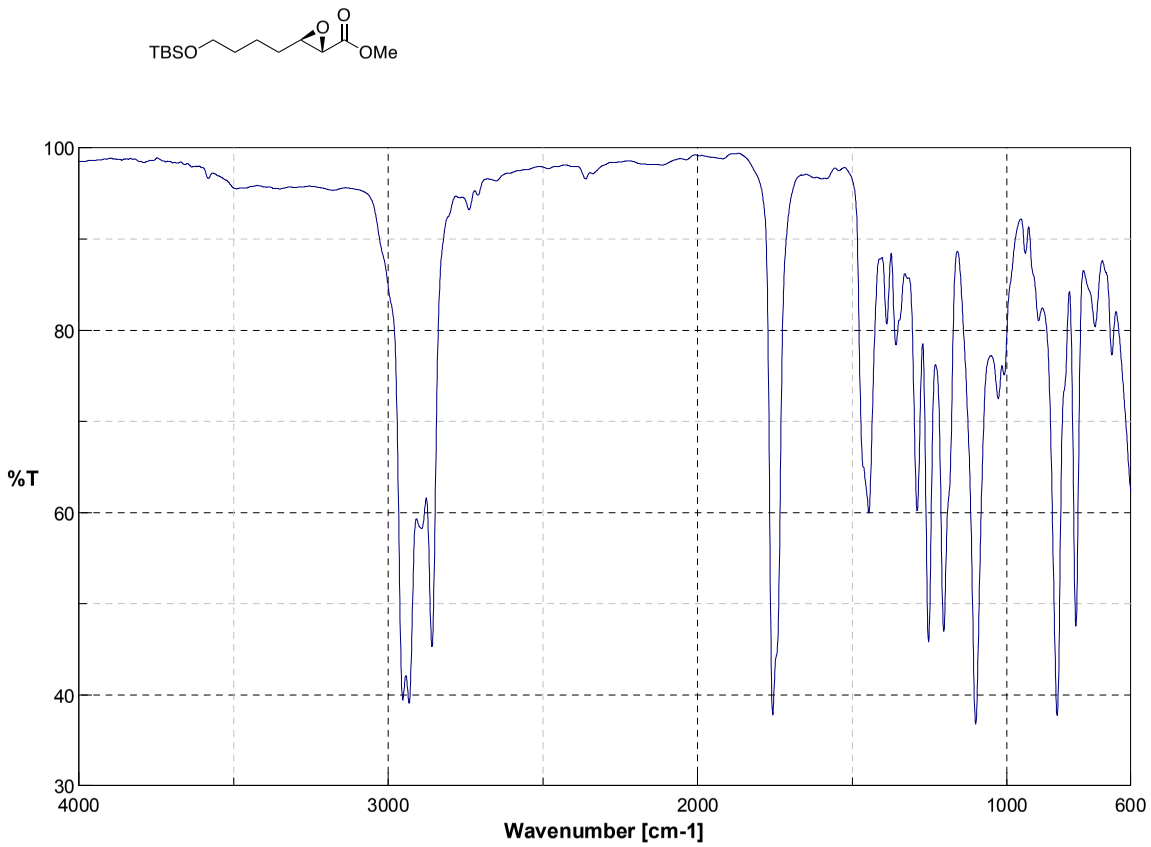

Figure A3.27. Infrared Spectrum of Compound (+)-**3.17**

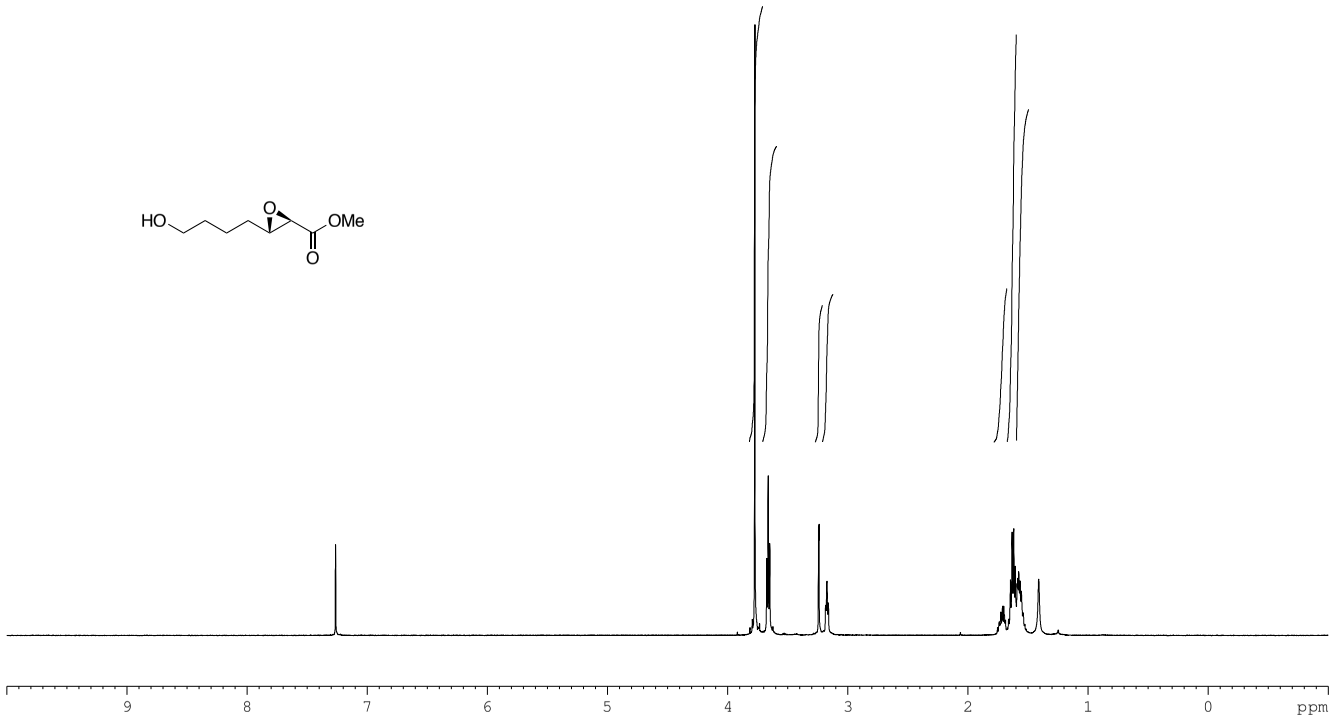

Figure A3.28. ^{1}H NMR Spectrum (500 MHz) of Compound (+)-**3.18** in $CDCl_3$

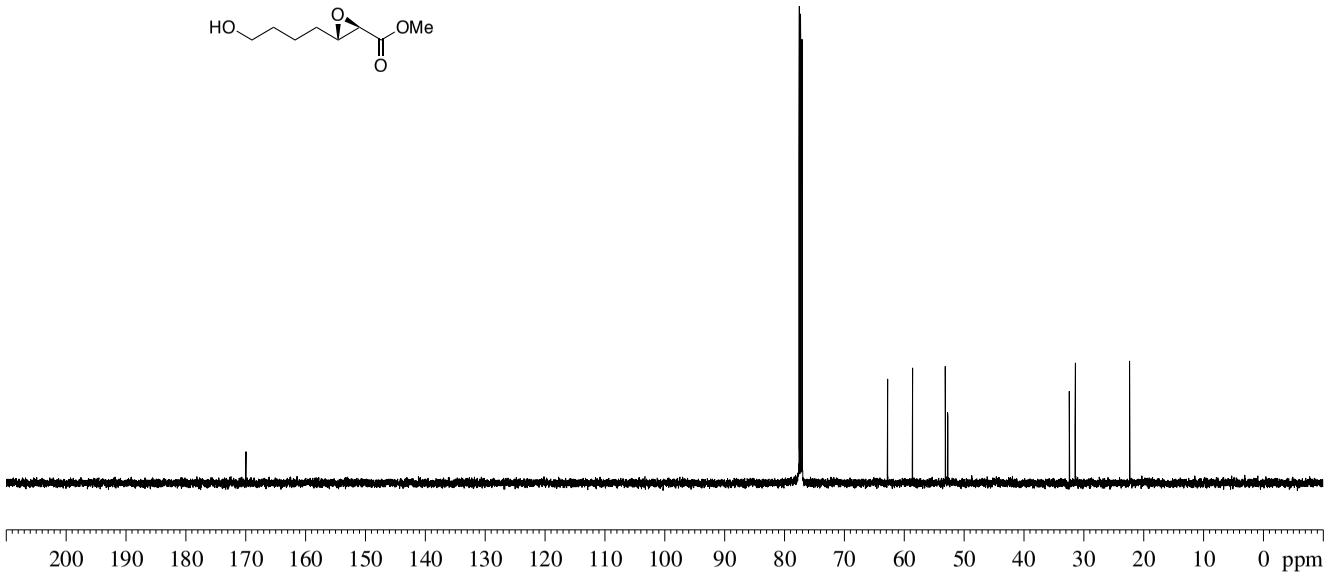

Figure A3.29. ^{13}C NMR Spectrum (125 MHz) of Compound (+)-**3.18** in $CDCl_3$

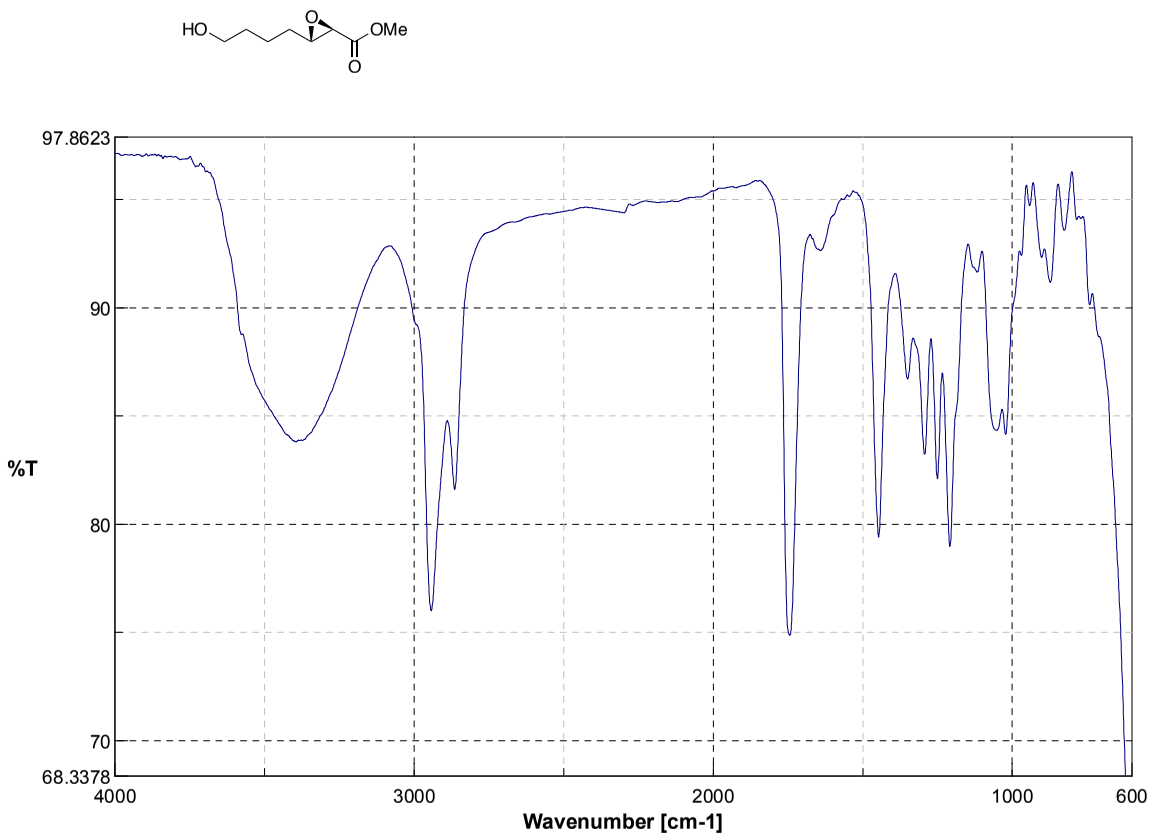

Figure A3.30. Infrared Spectrum of Compound (+)-**3.18**

BIBLIOGRAPHY

Allevi, P.; Anastasia, M.; Ciuffreda, P.; Fiecchi, A.; Scala, A. *J. Chem. Soc., Perkin Trans. 1* **1989**, 1275-1280.

An, C.; Hoye, A. T.; Smith, A. B. *Org. Lett.* **2012**, *14*, 4350-4353.

An, C.; Jurica, J. A.; Walsh, S. P.; Hoye, A. T.; Smith, A. B. *J. Org. Chem.* **2013***, 78*, 4278-4296.

Ayala, L.; Lucero, C. G.; Romero, J. A. C.; Tabacco, S. A.; Woerpel, K. A. *J. Am. Chem. Soc.* **2003**, *125*, 15521-15528.

Bal, B. S.; Childers Jr, W. E.; Pinnick, H. W. *Tetrahedron* 1981, *37*, 2091-2096.

Baldwin, J. E. *J. Chem. Soc., Chem. Commun.* **1976**, 734-736.

Burres, N. S.; Clement, J. J. *Cancer Res.* **1989**, *49*, 2935-2940.

Byeon, S. R.; Park, H.; Kim, H.; Hong, J. *Org. Lett.* **2011**, *13*, 5816-5819.

Byrson, T. A.; Dolak, T. M. *Org. Synth.* **1977**, *57*, 62.

Cardani, C.; Ghiringhelli, D.; Mondelli, R.; Quilico, A. *Tetrahedron Lett.* **1965**, *6*, 2537-2545.

Chen, K.-M.; Hardtmann, G. E.; Prasad, K.; Repič, O.; Shapiro, M. J. *Tetrahedron Lett.* **1987**, *28*, 155-158.

Chinen, T.; Nagumo, Y.; Watanabe, T.; Imaizumi, T.; Shibuya, M.; Kataoka, T.; Kanoh, N.; Iwabuchi, Y.; Usui, T. *Toxicol. Lett.* **2010**, *199*, 341-346.

Cichewicz, R. H.; Valeriote, F. A.; Crews, P. *Org. Lett.* **2004**, *6*, 1951-1954.

Corey, E. J.; Helal, C. J. *Angew. Chem. Int. Ed.* **1998**, *37*, 1986-2012.

Crimmins, M. T.; Stevens, J. M.; Schaaf, G. M. *Org. Lett.* **2009**, *11*, 3990-3993.

Denmark, S. E.; Kobayashi, T.; Regens, C. S. *Tetrahedron* **2010**, *66*, 4745-4759.

Dess, D. B.; Martin, J. C. *J. Org. Chem.* **1983**, *48*, 4155-4156.

Dieckmann, M.; Menche, D. *Org. Lett.* **2012**, *15*, 228-231.

Erker, G.; Frömberg, W.; Atwood, J. L.; Hunter, W. E. *Angew. Chemie. Int. Ed.* **1984**, *23*, 68-69.

Evans, D. A.; Calter, M. A. *Tetrahedron Lett.* **1993**, *34*, 6871-6874.

Evans, D. A.; Hoveyda, A. H. *J. Org. Chem.* **1990**, *55*, 5190-5192.

Feng, Y.; Jiang, X.; De Brabander, J. K. *J. Am. Chem. Soc.* **2012**, *134*, 17083-17093.

Fukui, H.; Tsuchiya, Y.; Fujita, K.; Nakagawa, T.; Koshino, H.; Nakata, T. *Bioorg. Med. Chem. Lett.* **1997**, *7*, 2081-2086.

Fusetani, N.; Sugawara, T.; Matsunaga, S. *J. Org. Chem.* **1992**, *57*, 3828-3832.

Ghaffar, T.; Parkins, A. W. *Tetrahedron Lett.* **1995**, *36*, 8657-8660.

Grieco, P. A.; Takigawa, T.; Schillinger, W. J. *J. Org. Chem.* **1980**, *45*, 2247-2251.

Hamana, H.; Sasakura, K.; Sugasawa, T. *Chem. Lett.* **1984**, *13*, 1729-1732.

Hoye, T. R.; Jeffrey, C. S.; Shao, F. *Nat. Protoc.* **2007**, *2*, 2451-2458.

Huang, X.; Shao, N.; Huryk, R.; Palani, A.; Aslanian, R.; Seidel-Dugan, C. *Org. Lett.* **2009**, *11*, 867-870.

Huang, X.; Shao, N.; Palani, A.; Aslanian, R. *Tetrahedron Lett.* **2007**, *48*, 1967-1971.

Huang, X.; Shao, N.; Palani, A.; Aslanian, R.; Buevich, A. *Org. Lett.* **2007**, *9*, 2597-2600.

Jiang, L.; Job, G. E.; Klapars, A.; Buchwald, S. L. *Org. Lett.* **2003**, *5*, 3667-3669.

Jiang, X.; Garcia-Fortanet, J.; De Brabander, J. K. *J. Am. Chem. Soc.* **2005**, *127*, 11254-11255.

Jiang, X.; Williams, N.; De Brabander, J. K. *Org. Lett.* **2007**, *9*, 227-230.

Jung, M. E.; Berliner, J. A.; Koroniak, L.; Gugiu, B. G.; Watson, A. D. *Org. Lett.* **2008**, *10*, 4207-4209.

Katsuki, T.; Sharpless, K. B. *J. Am. Chem. Soc.* **1980**, *102*, 5974-5976.

Katsuki, T.; Sharpless, K. B. *J. Am. Chem. Soc.* **1980**, *102*, 5974-5976.

Langer, P.; Kracke, B. *Tetrahedron Lett.* **2000**, *41*, 4545-4547.

Lee, K.-H.; Nishimura, S.; Matsunaga, S.; Fusetani, N.; Horinouchi, S.; Yoshida, M. *Cancer Sci.* **2005**, *96*, 357-364.

Li, P.; Li, J.; Arikan, F.; Ahlbrecht, W.; Dieckmann, M.; Menche, D. *J. Org. Chem.* **2010**, *75*, 2429-2444.

Maraval, A.; Igau, A.; Donnadieu, B.; Majoral, J.-P. *Eur. J. Org. Chem.* **2003**, *2003*, 385-394.

Mori, M.; Uozumi, Y.; Ban, Y. *J. Chem. Soc., Chem. Commun.* **1986**, 841-842.

Mosey, R. A.; Floreancig, P. E. *Nat. Prod. Rep.* **2012**, *29*, 980-995.

Müller, K.; Faeh, C.; Diederich, F. o. *Science* 2007, *317*, 1881-1886.

Noyori, R.; Nishida, I.; Sakata, J.; Nishizawa, M. *J. Am. Chem. Soc.* **1980**, *102*, 1223-1225.

Noyori, R.; Nishida, I.; Sakata, J.; Nishizawa, M. *J. Am. Chem. Soc.* **1980**, *102*, 1223-1225.

Ohtani, I.; Kusumi, T.; Kashman, Y.; Kakisawa, H. *J. Am. Chem. Soc.* **1991**, *113*, 4092-4096.

Parikh, J. R.; Doering, W. v. E. *J. Am. Chem. Soc.* **1967**, *89*, 5505-5507.

Paterson, I.; Goodman, J. M. *Tetrahedron Lett.* **1989**, *30*, 997-1000.

Paterson, I.; Goodman, J. M.; Anne Lister, M.; Schumann, R. C.; McClure, C. K.; Norcross, R. D. *Tetrahedron* **1990**, *46*, 4663-4684.

Pavan, M.; Bo, M. *Mem. Soc. Entom. It.* **1952**, *31*, 67.

Perry, N. B.; Blunt, J. W.; Munro, M. H. G.; Pannell, L. K. *J. Am. Chem. Soc.* **1988**, *110*, 4850-4851.

Pettit, G. R.; Xu, J.-P.; Chapuis, J.-C.; Pettit, R. K.; Tackett, L. P.; Doubek, D. L.; Hooper, J. N. A.; Schmidt, J. M. *J. Med. Chem.* **2004**, *47*, 1149-1152.

Private Conversation to Amos B. Smith III from Ralph Hirschmann.

Richter, A.; Kocienski, P.; Raubo, P.; Davies, D. *Anti-Cancer Drug Des.* **1997**, *12*, 217-227.

Rostovtsev, V. V.; Green, L. G.; Fokin, V. V.; Sharpless, K. B. *Angew. Chem. Int. Ed.* **2002**, *41*, 2596-2599.

Roth, G. P.; Marshall, D. R.; Chen, S.-H. *Tetrahedron Lett.* 1995, *36*, 1609-1612.

Scheidt, K. A.; Chen, H.; Follows, B. C.; Chemler, S. R.; Coffey, D. S.; Roush, W. R. *J. Org. Chem.* **1998**, *63*, 6436-6437.

Shao, N.; Huang, X.; Palani, A.; Aslanian, R.; Buevich, A.; Piwinski, J.; Huryk, R.; Seidel-Dugan, C. *Synthesis* **2009**, *2009*, 2855-2872.

Shibuya, M.; Tomizawa, M.; Suzuki, I.; Iwabuchi, Y. *J. Am. Chem. Soc.* **2006**, *128*, 8412-8413.

Simsek, S.; Horzella, M.; Kalesse, M. *Org. Lett.* **2007**, *9*, 5637-5639.

Smith, A. B.; Jurica, J. A.; Walsh, S. P. *Org. Lett.* **2008**, *10*, 5625-5628.

Smith, A. B.; Safonov, I. G.; Corbett, R. M. *J. Am. Chem. Soc.* **2002**, *124*, 11102-11113.

Takai, K.; Nitta, K.; Utimoto, K. *J. Am. Chem. Soc.* **1986**, *108*, 7408-7410.

Vakalopoulos, A.; Hoffmann, H. M. R. *Org. Lett.* **2000**, *2*, 1447-1450.

Wan, S.; Green, M. E.; Park, J.-H.; Floreancig, P. E. *Org. Lett.* **2007**, *9*, 5385-5388.

Wan, S.; Wu, F.; Rech, J. C.; Green, M. E.; Balachandran, R.; Horne, W. S.; Day, B. W.; Floreancig, P. E. *J. Am. Chem. Soc.* **2011**, *133*, 16668-16679.

Watanabe, T.; Imaizumi, T.; Chinen, T.; Nagumo, Y.; Shibuya, M.; Usui, T.; Kanoh, N.; Iwabuchi, Y. *Org. Lett.* **2010**, *12*, 1040-1043.

Weinstock, J. *J. Org. Chem.* **1961**, *26*, 3511-3511.

Wittig, G.; Schöllkopf, U. *Chem. Ber.* 1954, *87*, 1318-1330.

Wu, C.-Y.; Feng, Y.; Cardenas, E. R.; Williams, N.; Floreancig, P. E.; De Brabander, J. K.; Roth, M. G. *J. Am. Chem. Soc.* **2012**, *134*, 18998-19003.

Xiao, Q.; Floreancig, P. E. *Org. Lett.* **2008**, *10*, 1139-1142.

Yamamoto, K.; Suzuki, S.; Tsuji, J. *Chem. Lett.* **1978**, *7*, 649-652.

Zeng, W.; Chemler, S. R. *J. Org. Chem.* **2008**, *73*, 6045.

Zhao, M. M.; Li, J.; E, M.; Song, Z. J.; Taschaen, D. M. *Org. Synth.* **2005**, 195.

ABOUT THE AUTHOR

Chihui An was born to Haoyun An and Zhengming Yan in Zhengzhou, China in 1985. He immigrated to the United States with his family at the age of three. In the U.S, he lived in both Provo, Utah and Charlottesville, Virginia before moving to San Diego California where his family now lives.

After graduating from San Dieguito High School Academy in 2004, Chihui moved from sunny San Diego to begin his undergraduate studies at the University of California, Berkeley. Initially unsure what to major in, after completing first semester organic chemistry, he decided to join the College of Chemistry where he changed his major to Chemical Biology. Chihui was an active member of Alpha Chi Sigma, Professional Chemistry Fraternity at UC Berkeley, where he held many positions including president. While an undergraduate, he had the great opportunity to work as a Graduate Student Instructor for both organic chemistry laboratory and general chemistry laboratory courses. Additionally, he conducted undergraduate research under the supervision of Professor Jonathan Ellman. During this time, he worked on the development and optimization of a diastereoselective method for the synthesis of serine proteasome inhibitors. This was accomplished by the use of (*R*)-*tert*-butane sulfinamide as a chiral auxiliary to direct the stereoselective addition of a boronic ester group into sulfinylimines stereoselectively. In May 2008, Chihui was awarded a B.S. degree in Chemical Biology from the University of California, Berkeley, graduating with honors in the College of Chemistry.

In the summer of 2008, Chihui moved to Philadelphia where he began his graduate work under the supervision of Professor Amos B. Smith III at the University of

Pennsylvania. After getting accustomed to living in a city with four seasons, he successfully designed and implemented a synthetic strategy to achieve the first total synthesis of (–)-irciniastatin B. He has also contributed to the design and synthesis of novel irciniastatin analogues. After defending his dissertation in May 2013, Chihui will be awarded a Ph.D. in Chemistry in August 2013.

After becoming proficient in organic synthetic chemistry, Chihui decided to change his research direction and broaden his skill set. In the summer of 2013, Chihui will begin a postdoctoral fellowship with Professor David Liu at Harvard University. Professor Liu's diverse research program includes directed evolution of biomolecules and DNA-templated synthesis. Chihui looks forward to learning the latest methods in molecular cloning, protein engineering, and gene sequencing.